Production of Renewable Fuels from Bio-Based Feedstocks: A Viable Path to Enhance Value Chain and Sustainability

by

Kodanda Phani Raj Dandamudi

A Dissertation Presented in Partial Fulfillment
of the Requirements for the Degree
Doctor of Philosophy

Approved November 2020 by the
Graduate Supervisory Committee:

Shuguang Deng, Chair
Peter J. Lammers
Elham H. Fini
Marylaura Lind Thomas
Arul M. Varman

ARIZONA STATE UNIVERSITY

December 2020

ABSTRACT

The continued reliance on fossil fuel for energy resources has proven to be unsustainable, leading to depletion of world reserves and emission of greenhouse gases during their combustion. Therefore, research initiatives to develop potentially carbon-neutral biofuels were given the highest importance. Hydrothermal liquefaction (HTL, a thermochemical conversion process) of microalgae is recognized as a favorable and efficient technique to produce liquid biofuels from wet feedstocks. In this work, three different microalgae (Kirchneriella sp., Galdieria sulphuraria, Micractinium sp.) grown and harvested at Arizona State University were hydrothermally liquefied to optimize their process conditions under different temperatures (200-375 Â°C), residence times (15-60 min), solids loadings (10-20 wt.%), and process pressures (9-24 MPa). A one-factor-at-a-time approach was employed, and comprehensive experiments were conducted at 10 % solid loadings and a residence time of 30 min. Co-liquefaction of Salicornia bigelovii Torr. (SL), Swine manure (SM) with Cyanidioschyzon merolae (CM) was tested for the presence of synergy. A positive synergistic effect was observed during the co-liquefaction of biomasses, where the experimental yield (32.95 wt.%) of biocrude oil was higher than the expected value (29.23 wt.%). Co-liquefaction also led to an increase in the energy content of the co-liquefied biocrude oil and a higher energy recovery rate (88.55 %). The HTL biocrude was measured for energy content, elemental, and chemical composition using GC-MS. HTL aqueous phase was analyzed for potential co-products by spectrophotometric techniques and is rich in soluble carbohydrates, dissolved ammoniacal nitrogen, and phosphates. HTL biochar was studied for its nutrient content (nitrogen and

phosphorous) and viability of its recovery to cultivate algae without any inhibition using the nutrient leaching. HTL biochar was also studied to produce hydrogen via pyrolysis using a membrane reactor at 500 Â°C, 1 atm, for 24 h to produce 5.93 wt.% gas. The gaseous product contains 45.7 mol % H2, 44.05 ml % CH4, and 10.25 mol % of CO. The versatile applications of HTL biochar were proposed from a detailed physicochemical characterization. The metal impurities in the algae, bio-oil, and biochar were quantified by ICP-OES where algae and biochar contain a large proportion of phosphorous and magnesium.

DEDICATION

I dedicate this dissertation in memory of my loving uncle & Godfather, Samba Siva Rao Vadlamudi for his love, inspiration, and encouragement throughout my life.

I also want to dedicate this dissertation to all the families that have lost their loved ones due to the COVID-19 virus. The dedication also goes to the front-line medical professional for their immense services during the global pandemic.

ACKNOWLEDGMENTS

I would like to sincerely thank my advisor, Dr. Shuguang Deng, for his constant support and supervision which has been solely and mainly responsible for doing this work. His expert guidance, prompt inspirations, timely guidance, and continual advice in every step until now and in the future will be a positive influence in my life.

I owe a deep sense of gratitude to Dr. Peter J. Lammers for sharing his knowledge and extended guidance in the field of algal biology and upstream processes. I would like to greatly thank Dr. Elham H. Fini for her expertise and guidance in the applications to improve biomass value chain. I would also like to thank Dr. Mary Laura Lind Thomas and Dr. Arul M. Varman for serving in my dissertation committee. I am grateful for the supervision of Dr. Jerry Y. S. Lin on the conversion of HTL biochar to hydrogen in the membrane reactor. This effort was mainly carried out by Dr. Amr F. Ibrahim and I, in Dr. Lin's lab. I am also very thankful to Dr. Lenore Dai for her support and encouragement through the School for Engineering of Matter, Transport, and Energy. I would like to thank Dr. David Nielsen, Mr. Fred Peña for their support during my teaching in summer semesters and for lab safety inspections. I thank all the faculty and staff of SEMTE profusely, for their kind help and co-operation throughout my research and administrative work until the current day. I am also greatly appreciative of the support and friendship my teammates Dr. Tapaswy Muppaneni, Dr. John McGowen, Dr. Mark Seger, Dr. Thinesh Selvaratnam, Dr. Mai Xu, Dr. Amr F. Ibrahim, Dr. Harvind Kumar Reddy, Dr. Sundarvadivelnathan Ponnusamy, Dr. Taylor L. Weiss, Yixin Liu, Tessa Murdock, Kato Muhammad Luboowa, Maymary Liadeson, Melvin Matthew, Connor Copp, Nicholas Csakan, and Chengxi Lu have provided me.

I owe a deep sense of gratitude for the support and trust of me from my family members Sumathi Lakshmi Dandamudi, Ravi Sujith Dandamudi, Edna Pires Dandamudi, Gireesha

Dandamudi, Venkat Rao Vadlamudi, Siva Kumari, Dhana Lakshmi, Aasrith, and Maanas Pranay. I am incredibly indebted to Amith Bharadwaj Banduvula for his constant motivation, genuine support, advice, and assistance in enabling me to reach to this point in my personal and professional life. I would also extend my deepest gratitude and support received from Manoj Mannava, Dr. Alwin D'Souza, Gopi Tripuraneni, Avinash Manchikalapudi, Kranthi Uppuluri, Bus No: 13 family, Biran Singh Atwal, Dr. Jyothi Prakash, and the ASU polytechnic family. I am extremely grateful to everyone that has inspired me in every way and tapped my shoulder during my high and low's; there is no such word to truly describe my appreciation and there is not enough space in this document to name them all.

The co-liquefaction study was supported in part by the U.S. Department of Energy under award #DE-EE0007562 for A Novel Platform for Algal Biomass Production Using Cellulosic Mixotrophy. The characterization of biochar study was sponsored by the National Science Foundation (Award Numbers 1928807) and the ASU LightWorks Sustainable Fuels and Products Seed Grants Initiative. I would also like to extend my gratitude to the Graduate College at Arizona State University and the Associated Students of Arizona State University (ASASU/GPSA) for their valuable financial support for conference travel while presenting this work.

TABLE OF CONTENTS

Page

LIST OF TABLES xiii

LIST OF FIGURES xv

CHAPTER

1 INTRODUCTION……1

Background……..1

Alternative Resources: Biofuels……...3

Microalgae……...5

Problem Statement and Hypothesis……..8

Research Objectives, Significance, and Impact……..12

Dissertation Organization……...13

References……..15

2 HYDROTHERMAL LIQUEFACTION OF MICROALGAE UNDER SUB- AND SUPER-CRITICAL WATER CONDITIONS……..24

Introduction……24

Materials and Methods……...27

Biomass Sources……27

CHAPTER Page

Proximate Analysis……30

Ultimate Analysis……...31

Biochemical Analysis ……32

Heavy Metal Analysis……34

Hydrothermal Processing and Liquefaction……...35

Catalytic Upgrading of Biocrude Oil……..38

Results and Discussion……...39

Analysis of Biomass……...40

Optimization of HTL Conditions to Maximize the Biocrude Oil Yield……...42

Analysis of Liquefaction Products…….50

Catalytic Upgrading of Biocrude Oil Using Heterogeneous Catalysts…….56

Conclusions……60

References……62

CHAPTER Page

3 HYDROTHERMAL LIQUEFACTION OF CYANIDIOSCHYZON MEROLAE WITH SALICORNIA BIGELOVII TORR. AND SWINE MANURE: THE SYNERGISTIC EFFECT ON PRODUCT DISTRIBUTION AND CHEMISTRY……70

Introduction……70

Materials and Methods……...75

Materials…… 75

HTL Experimental Procedure and Product Separation……..76

Analytical Analysis……77

Results and discussion……79

Analysis of Biomass Feedstock……..79

HTL Product Distribution……..82

Elemental Analysis and Energy Recovery…….95

Nutrient Analysis of the HTL Water Phase……99

Gas Chromatography-Mass Spectrometry Analysis of Biocrude.101

Heavy Metal Analysis by ICP-OES……..103

Conclusions……..112

CHAPTER Page

References……114

4 PHYSICOCHEMICAL CHARACTERIZATION OF HYDROTHERMALLY PRODUCED BIOCHARS FROM CYANIDIOSCHYZON MEROLAE AND SWINE MANURE……...124

Introduction……..124

Materials and Methods…….128

Proximate and Ultimate Analysis…….129

Scanning Electron Microscopy (SEM) and Surface Properties…129

Results and Discussion…….131

Analysis of the Biochars……...131

Thermogravimetric Analysis of the Biochars……...135

Surface Properties and Metal Composition……..137

Functional Groups of the Biochars……...143

Crystalline Structures of the Biochar……145

Applications of Biochar……149

Conclusions……..157

References……159

CHAPTER Page

5 RECYCLE OF NITROGEN AND PHOSPHORUS IN HYDROTHERMAL LIQUEFACTION BIOCHAR FROM GALDIERIA SULPHURARIA TO CULTIVATE MICROALGAE……172

Introduction……..172

Materials and Methods…….176

Algae Strain Collection and Maintenance……177

Hydrothermal Liquefaction of GS and Biochar Collection……...178

Analytical Analysis of Biomass and HTL Products……..179

Biochar Leaching Experiments……179

Growth Study with Leached Nutrients…….181

Results and Discussion…….182

Analysis of Biomass and HTL Products……...182

Effect of pH on the Leaching of Nutrients from the Biochar…….188

Comparative Growth of G. sulphuraria in Standard Media Compared to Leached Media……195

Conclusions……..198

References…….200

CHAPTER Page

6 PYROLYSIS OF HYDROTHERMAL LIQUEFACTION PRODUCED ALGAL BIOCHAR FOR HYDROGEN PRODUCTION USING A MEMBRANE REACTOR……...207

Introduction……..207

Materials and Methods…….211

Algae Production and Harvesting…….211

Hydrothermal Liquefaction Experiments and Product Recovery.212

TGA Characterization and Fixed Bed Pyrolysis……...212

Batch Membrane Reactor Experiments……214

Chemical Analysis and Material Characterization……...215

Results and Discussion…….216

Analysis of Feedstock and Biochar……...216

TGA and Fixed Bed Pyrolysis Characteristics……..218

Biochar Batch Reactor Experiments…….223

Membrane Characteristics……229

Conclusions……..234

CHAPTER Page

References……235

7 CONCLUSIONS AND RECOMMENDATION FOR FUTURE WORK …..243

Hydrothermal Liquefaction of Microalgae Under Sub- and Super-Critical Water Conditions……243

Hydrothermal Liquefaction of Cyanidioschyzon Merolae with Salicornia Bigelovii Torr. and Swine Manure: The Synergistic Effect on Product Distribution and Chemistry……..246

Physicochemical Characterization of Hydrothermally Produced Biochars from Cyanidioschyzon Merolae and Swine Manure…….247

Applications of Biochar……249

Recommendations……250

REFERENCES……253

APPENDIX A……..283

APPENDIX B……..289

APPENDIX C……..294

BIOGRAPHICAL SKETCH…….....303

LIST OF TABLES

Table Page

1.1: Comparison of Various Sources of Biodiesel..……. 6

2.1: Name, Source, Strain Code, Growth Media, and Growth Season of the Microalgae Investigated in the Study…….31

2.2: Proximate and Biochemical Composition of the Biomass Under Study…… 40

2.3: Ultimate Analysis of the Biomass Under Study……. 41

2.4: Metal Impurities in the Biomass Under Study Using ICP-OES……. 42

2.5: Elemental Composition of *Kirchneriella sp*. Biomass, Bio-oils, and Biochar Obtained at 300 ˚C, 30 mins, 9 MPa and 10 % Solid Loading.…….52

2.6: Elemental Composition of *Micractinium* & *Galdieria sp.* Biocrude Oils Obtained at 350 ˚C, 30 mins, 9 MPa, and 10 % Solid Loading..……53

2.7: Analysis of HTL Water Phase Obtained at 300 ˚C, 30 mins, 9 MPa, and 10 % Solid Loading..…….54

2.8: Analysis of HTL Biocrude, Biochar Obtained at 300 ˚C, 30 mins, 9 MPa.……... 55

2.9: Elemental Composition of Biocrude Oil vs. Upgraded Biocrude Oil of Micractinium sp. produced at 350 ˚C.……58

3.1: Proximate and Ultimate Analysis of Biomass Under Study…… 79

3.2: Ultimate Analysis of the Biomass and HTL Products.……... 92

3.3: Nutrient Analysis of the HTL Water-Soluble Compound (WSC) Phase…….. 101

3.4**:** Major Compounds Identified in Different Biocrude Oils by GC-MS…….. 104

Table Page

3.5: Metal Concentrations in Biomass, Biocrude, and Biochar Obtained at 300 °C..... 109

4.1: Proximate and Ultimate Analysis of the Biochars Produced at 330 ℃…… 132

4.2: Atomic Ratios for Biomasses and Biochars.……. 135

4.3: Pore Textural Property Analysis of Biochars.……... 139

4.4: Metal Concentrations in Biomasses, Biocrudes, and Biochars by ICP-OES..…….. 141

4.5: Overview of Biochar Applications……... 152

5.1: Analysis of the Feedstock...…….. 182

5.2: Product Yields from Hydrothermal Liquefaction of GS at 300 ºC, 30 min Residence Time, and 20 wt. % Solid Loading……184

5.3**:** Inorganic Metal and Elemental Analysis of the Microalgae, HTL Biocrude, and HTL Biochar...……...186

5.4: Mass Balance and Elemental Recovery from the Hydrothermal Liquefaction Process……..193

6.1: Biochemical and Proximate Analysis of Algal Biomass, *G. sulphuraria*.…..…….... 216

6.2:Ultimate Analysis of Algal Biomass, *G. sulphuraria* Biomass and HTL Products……216

6.3: Ultimate Analysis of the Solids Remaining After Batch Reactor Pyrolysis Tests.… 225

6.4: Hydrogen Balance and Membrane Performance for Pyrolysis of 0.4 g HTL Biochar Samples...……..227

LIST OF FIGURES

Figure Page

1.1: US EIA, International Energy Outlook 2016: World Energy Consumption by Transportation Fuel Source……..2

1.2: Advantages of Algae Biofuels..…… 8

2.1: Experimental Plan of the Study...…… 27

2.2: The Illustrative Layout of 100 ml Parr Reactor…….. 38

2.3: Effect of Reaction Temperature on the Product Distribution at 10 % Solid Loading and 30 min Residence Time.……. 46

2.4: HTL Biocrude Yield Distribution of *Kirchneriella sp.* with Solid Loading at 300 ˚C, 30 min, and 9 MPa Initial Pressure...…….. 47

2.5: HTL Biocrude Yield Distribution of *Kirchneriella sp.* with Pressure at 300 ˚C, 30 min, and 10% Solid Loading.……..49

2.6: HTL Biocrude Yield Distribution of *Kirchneriella sp.* with Time at 300 ˚C, 10 % Solid Loading, and 9 MPa Initial Pressure..……..50

2.7: Upgraded Oil Yields of Algae Biocrude at 350 and 400 ˚C…….. 57

3.1: Schematic of the Experimental Plan...…… 74

3.2: HTL Product Distribution of Individual Liquefaction of SL Biomass.……... 85

3.3: Co-liquefaction Product Distribution of CM/SL Biomass (A) at 250 °C...…… 87

3.4: Co-liquefaction Product Distribution of CM to SM Biomass at 300 °C...…….. 88

Figure Page

3.5: Biocrude Oil Yields from the Experimental vs. Expected Yields at Different CM-SL Biomass Ratios (300 °C, 30 mins and 10 wt. % Solid Loading)……..90

3.6: Biocrude Oil Yields from the Experimental vs. Expected Yields at Different CM-SM Biomass Ratios (330 °C, 30 mins and 20 wt. % solid loading)..…… 91

3.7: Thermal Degradation Behavior of the Raw Biomass (A); Biocrudes Produced at 300 °C, 10 % Solid Loading, and 30 min Residence Time (B)…….....96

3.8: Comparison of the Energy Recovery (ER, %) Over Different HTL Reaction Conditions; (A) CM-SL; (B) CM-SM…….97

4.1: Experimental Plan of the Study……. 127

4.2: TGA Analysis of the Biochars Produced at 330 °C……. 136

4.3: SEM Images of the Biochars Produced from HTL at 330 °C…….. 138

4.4: FT-IR Analysis of the Biochars Produced at 330 °C……... 144

4.5: XRD Analysis of the Biochars Produced at 330 °C…….. 146

4.6: Crystallinity Distribution in Biochars Produced at 330 °C…….. 147

5.1: Experiment Plan of the Study…… 175

5.2: SEM Image of the Produced HTL Biochar from GS Feedstock…….. 185

5.3: Leaching of Phosphates from HTL Biochar Over 7 days……..... 187

Figure Page

5.4: Leaching of Ammoniacal Nitrogen from HTL Biochar Over 7 days……... 191

5.5: Effect of pH on Leaching of Phosphates and Ammoniacal Nitrogen from HTL Biochar……..192

5.6: Growth of GS in (A): 96 Well Microplate Assay and (B): 16 mm Tubular Reactor……..196

6.1: Experimental Plan for This Study……..... 209

6.2: Configuration of the Fixed Bed [A] and Batch [B] Reactors Used for Biochar Pyrolysis……...212

6.3: Thermogravimetric Analysis, TGA, Plot for the *G. sulphuraria* Biomass (A) and a Biochar Sample (B) Remaining after HTL when Heated to a Temperature of 1000 ^{o}C in Nitrogen Atmosphere……219

6.4: Thermogravimetric Analysis, TGA, Plot for the *G. sulphuraria* Biomass…….. 220

6.5: Differential Thermogravimetric, DTG Curves for the HTL Biochar Sample when Heated to a Temperature of 500 ^{o}C in a Nitrogen Atmosphere at Different Heating Rates…….221

6.6: Fixed Bed Pyrolysis of HTL Biochar Gas Distribution as a Function of Pyrolysis Time and Temperature……...222

6.7: Gases Evolved During Batch Pyrolysis of HTL Biochar Samples of Different Weights…….223

Figure Page

6.8: Batch Membrane Reactor Pyrolysis Experiments of 0.3 g and 0.4 g HTL Biochar Samples: Pressure Monitored as a Function of Temperature and Pyrolysis Time with an Impermeable Substrate and with Pd_{77} Ag_{23} Membrane…….225

6.9: Hydrogen Recovered in the Pd_{77} Ag_{23} Membrane Permeate Side as a Function of Pyrolysis Time and Temperature with HTL Biochar Samples of 0.3 and 0.4 g…….226

6.10: SEM Surface Morphology [A-C] and Cross Section [D, E] as Well as EDAX Analysis of the Pd_{77} Ag_{23} Membrane Before and After Pyrolysis Experiments…….229

6.11: XRD Patterns of the Pristine Pd_{77} Ag_{23} Membrane and the Membrane (Face and Back) After Pyrolysis……230

7.1: Possible Reaction Pathways Based on the Characterization by GC-MS.…….246

CHAPTER 1: INTRODUCTION

1.1 Background

At the current rate of increasing global economic development, industrialization, and urbanization the increase in energy consumption by developing countries has pushed the quest for alternatives to fossil fuels sooner than expected (Mercure et al., 2018; Reddy et al., 2014; U.S. EIA and U.S. Energy Information Administration (EIA), 2019). The U.S. EIA has also projected that the current rate of utilization will lead to a total depletion of oil reserves by the year 2052, gas reserves by 2060, and coal by 2088 (Alaswad et al., 2015; Conti et al., 2016). Figure 1.1 illustrates the world energy consumption by transportation fuel source. It has projected that the consumption of energy by jet fuel increased by 10 quadrillion Btu and motor gasoline by 19 quadrillion Btu by 2040 (Conti et al., 2016). According to International Energy Outlook 2018, the world energy consumption of petroleum, and other liquids increased from 172 quadrillion Btu in 2010 to 197 quadrillion Btu in 2018 and is expected to increase to 229 quadrillion Btu in 2040 (U.S. EIA and U.S. Energy Information Administration (EIA), 2019).

In conjunction with the depletion of fossil fuels and energy resource deficit, usage of these non-renewable, limited energy sources has led to an alarming rate of increase in greenhouse gas emissions (GHG) in the atmosphere thereby leading to the increase of global temperatures (Barzagli and Mani, 2019; Hansen et al., 2006; Karl and Trenberth, 2003; Lelieveld et al., 2019). Over the past few decades global emission trends, including

the United States greenhouse gas emissions, increased between 0.5 and 1.0 % per year (Karl and Trenberth, 2003). In the absence of emission control policies, the projected increase in global-mean temperature is around 4.9 °C by the year 2100 leading to an increase in the global sea level (Wigley and Raper, 2001). The rate of climate change cannot be stopped in the current century but can be slowed down, so to keep the global warming temperature well below 2 °C, climate stabilization models suggest the requirement of negative emission technologies (NETs), such as using bioenergy with carbon capture (Creutzig et al., 2019; Hoffert et al., 2002).

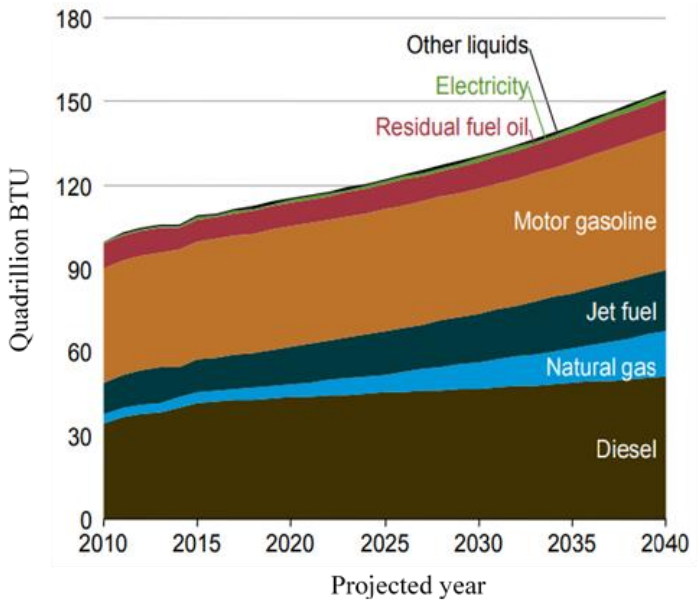

Figure 1.1: US EIA, International Energy Outlook 2016: World energy consumption by transportation fuel source

1.2 Alternative resources: Biofuels

Based on the recent advances in the alternative energy resources, such as electricity in the transportation sector, automobiles have seen good improvement in the recent years, but using electricity for aviation and heavy machinery is still not a viable option. It is primarily due to the range of the vehicles, cost, and safety concerns of the battery-powered engines (Sarmah et al., 2019). The World Economic Outlook (WEO) 2010 predicts that the transport fuel demand will rise by around 40 % by 2035. According to Annual Energy Outlook 2018 (Administration, 2018), the share of renewable energy contributing to the total energy production is projected to increase from 9 quadrillion Btu in 2017 to 15 quadrillion Btu in 2050. A study published in 2009 estimated that the transportation sector was responsible for 23 wt. % of the total CO_2 emitted from fossil fuel combustion (Statistics, 2011). The global jet fuel demand is estimated to increase by 38 % from 2008 to 2025 at a rate of 1.9 % per year, and around 30 % of aviation fuel can be replaced by fuel derived from biomass (ATAG, 2009; Chèze et al., 2011). In conjunction with replacing the aviation fuel with bio-jet fuel, it also has an added advantage of decreasing the greenhouse emissions by 70 % in comparison with petroleum-based jet fuel (Park and Ihm, 2000). Therefore, it is highly crucial that the transportation sector needs a renewable, sustainable, and environmentally benign liquid alternative to reduce CO_2 emissions.

Among the alternatives, biofuels are one of the better choices to create a possible pathway to minimize the GHG emissions as the carbon dioxide emitted during the combustion can be recycled back to the cultivation facilities leading to a reduction in the

net production of the GHG's (Chisti, 2007; Demirbas, 2009; Gnansounou et al., 2009). Biofuels can be a viable solution for the high demand for liquid transportation fuels, especially jet fuel for aviation demands (Hileman and Stratton, 2014; Shonnard et al., 2010).

The history of biofuels dates back centuries, and some early forms include wood and charcoal, which have been used by humanity for centuries for the source of heat, cooking food, and safety. Biofuels and bioproducts are produced from plant biomass and classified into three categories based on the source of origin. First-generation biofuels use raw biomass, the majority of which are edible resources (e.g., corn, rapeseed, sugar cane, sugar beet, and vegetable oils), to produce bioethanol or biodiesel. Carbohydrate-rich sources like sugarcane and corn are fermented to produce bioethanol (Aysu et al., 2015; Demirbas, 2009; Naik et al., 2010). On the other hand, biodiesel is produced by extracting the oils from seeds (sunflower, soybean, etc.) and subjecting them to transesterification using alcohol and an alkali catalyst (Fukuda et al., 2001; Ma and Hanna, 1999; Meher et al., 2006). According to the Renewable Fuel Standard (RFS), the U.S. can produce 15 billion gallons of corn-based bioethanol by 2022 which will meet a part of the 36 billion gallons of liquid transportation fuel requirement (Barry et al., 2016). The second-generation of biofuels are produced from biomass that is usually discarded agricultural or forest waste, such as lignocellulosic materials (stems, twigs, sawdust, switchgrass, and pine). It eliminates the food versus fuel crisis that arises from using first-generation biofuels. Despite having some advantages over the first-generation biofuels, the second-

generation biofuels require a lot of forest land to meet the required demand. This leads to extensive and rapid deforestation that ends up increasing the greenhouse gases in the atmosphere.

Based on the drawbacks of the earlier generation of biofuels, algal biofuels have grown significant importance in the past decade as a potential feedstock to counter the effects of food versus fuel crisis and deforestation.

1.3 Microalgae

Microalgae are diverse organisms that can convert sunlight and carbon dioxide into useful products. Microalgae have shown that it can produce more fuels compared to terrestrial crops in the given area and time. They also have higher biomass productivity in comparison to other terrestrial plants shown in Table 1.1. Chisti et al., (Chisti, 2007) state in their review comparing terrestrial plant oil yields to microalgae (70% or 30% oil) that a potential of 58,700 to 136,900 L/ha could be possible. This is higher than the terrestrial plant's oil yield (e.g., soybean (446 L/ha) and coconut (2689 L/ha)). Algae contain biochemical constituents such as carbohydrates, lipids, and proteins. They also can grow both phototrophically and heterotrophically, and their composition depends greatly on the choice of strain and the geographical conditions (Lowrey et al., 2015; White and Shilo, 1975). Microalgae can be grown and harvested all year round, while the terrestrial plants are grown based on seasonal time phases (Mata et al., 2010; Singh and Olsen, 2011). They have the flexibility to grow in multiple water resources and in non-arable land preventing

further deforestation (Ahmad et al., 2011). Figure 1.2 explains the advantages of algal biofuels regarding its higher oil yields, lesser land requirement, adaptability, and wastewater treatment and carbon dioxide capture.

Table 1.1: Comparison of various sources of biodiesel

Crop	Oil yield (L/ha)	Land area needed (M Ha) [a]	Percent of existing US cropping area
Corn	172	1540	846
Soybean	446	594	326
Canola	1190	223	122
Jatropha	1892	140	77
Coconut	2689	99	54
Oil palm	5950	45	24
Microalgae [b]	136900	2	1.1
Microalgae [c]	58700	4.5	2.5

[a] for meeting 50 % of all transport fuel needs of the United States; [b] 70 wt.% oil in biomass; [c] 30 wt.% oil in biomass

Microalgae can effectively capture carbon from the atmosphere and are estimated to sequester ~1.8 kg of CO_2 for 1 kg of algae grown (Rodolfi et al., 2009). The carbon dioxide in the flue gases can be recycled to supplement algal growth and can be easily integrated with any of the industry involved in flue gas as a by-product (Gnansounou et al., 2009; Lardon et al., 2009) Initial studies of microalgae as fuel investigated the use of lipid in the algae to be converted to biodiesel (Patil et al., 2017; Reddy et al., 2014). In addition to the fuel perspective, microalgae also can produce polyunsaturated fatty acids in the form of EPA (Eicosapentaenoic acid) and DHA (Docosahexaenoic acid). These fatty acids have high economic, commercial value, and add up to the revenue generation of biofuel production (Winwood, 2013). Various nutraceutical industries are already in the market or launching more algae-related products as food supplements due to their high protein content and oils (Chauton et al., 2015). Other valuable products include pigments which are used in the dye and food industries including β-carotene, astaxanthin, and C-phycocyanin (Barba et al., 2015; Brennan et al., 2012; Spolaore et al., 2006). Microalgae has also been proven to clean sewage and wastewater. The US produces 61 trillion L of wastewater in the form of sewage and municipal each year. It is said to contain 0.4 g of C as biological oxygen demand (BOD). The carbon sequestration as CO_2 is equivalent to 25 Billion tons of carbon considering algae could sequester all of it.. This explains the versatility and sequestration capability of microalgae in driving a potential for the implementation of negative emission technologies (NET) and biomass with carbon capture and storage (BECCS).

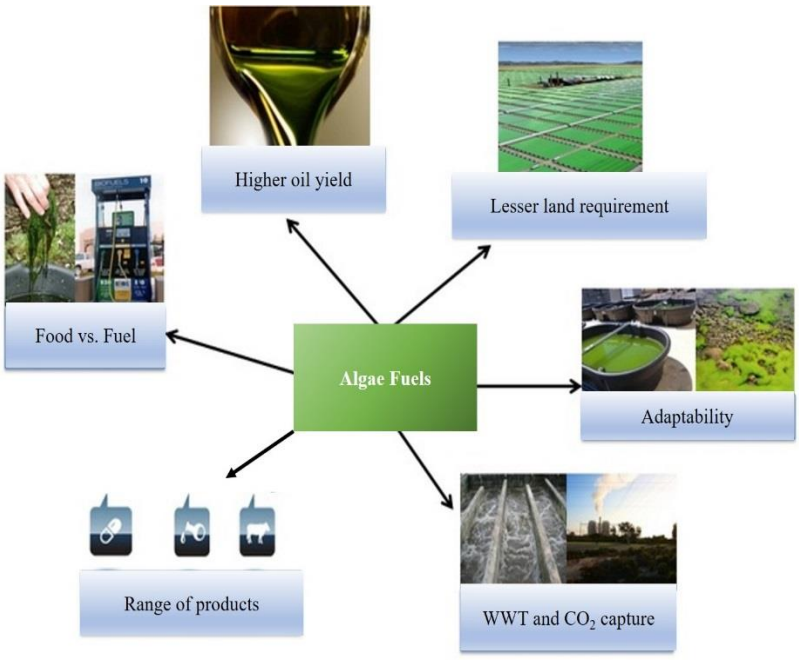

Figure 1.2: Advantages of algal biofuels

1.4 Problem Statement and hypotheses

Various strains of microalgae can be subjected to sub- and /or super-critical conditions of various solvents to produce biofuels (Christensen et al., 2015; Ponnusamy et al., 2014; Reddy et al., 2014). The main target of these solvent extraction processes was to extract and/or to trans-esterify the lipids (triglycerides) present in the biomass to produce fatty acid methyl esters (FAME). It is reported that approximately 15-40 % of all the lipids are triglycerides and only they can be usable in the transesterification process (Kröger and Müller-Langer, 2012). This process does not involve in the conversion of any of the remaining biochemical constituents such as proteins, carbohydrates into biofuel (Elliott,

2016; Kröger and Müller-Langer, 2012). This issue can be addressed by employing thermochemical conversion techniques that can utilize the whole biomass.

Various thermochemical conversion techniques have been reported in the literature to convert either dry or wet whole biomass into fuel components (McKendry, 2002; Patel et al., 2016; Peterson et al., 2008; Verma et al., 2012). Most of these conversion techniques lack the technical feasibility to process high moisture containing feedstocks at a large scale unless by concentrating, dewatering, and drying that adds up to energy expenditure and increases the production costs of the whole process (Toor et al., 2013; Valdez et al., 2012). Therefore, a need has risen to devise a technology that can process wet biomass. Among the available thermochemical conversion techniques, hydrothermal liquefaction (HTL) can use the whole wet biomass to produce liquid biofuels (Elliott et al., 2015; Guo et al., 2015; Tian et al., 2014). Wet conversion techniques like hydrothermal liquefaction (HTL), where biomass is converted to valuable liquid products attracted attention because of its ability to harvest the prominent properties of water as a reaction medium (Tian et al., 2014; Toor et al., 2011). This process eliminates the need for drying the feedstock and can minimize the energy consumption required during the drying process (Chiaramonti et al., 2017). HTL process yields multiple product fractions that involve biocrude oil, biochar, water-soluble, and gaseous fraction. The yield of these product fractions can be influenced by varying the process parameters such as reaction temperature, residence time, pressure, and solid loading (Akhtar and Amin, 2011).

Additionally, the non-gaseous products (biochar, water soluble/aqueous fractions) of HTL are highly abundant in the nutrients containing nitrogen (N) and phosphorous (P). These water-soluble nutrients play an important role in the cultivation of algae and have been investigated for growing algae (Selvaratnam et al., 2015a, 2015b). Therefore, it is crucial to optimize the process parameters and maximize the yield of the product fractions while also recycling the nutrients (N, P) into algae cultivation systems. The biocrude oil produced from HTL has advantages such as higher HHV (31-37 MJ/kg) and lower oxygen content (5-10 wt.%) (Anastasakis and Ross, 2011; Valdez et al., 2012; Wang et al., 2015; Zhou et al., 2010) over the oils produced from other biomass such as pine and other lignocellulosic materials (Mohan et al., 2006; Onwudili et al., 2013). Despite having its advantages, it has some drawbacks such as higher viscosity (40-67 cP), high acidic number (Total Acid Number TAN: 25-118 mg of KOH/g), and high amounts of nitrogen (2-9 wt.%) and sulfur (0.5-1.2 wt.%). These physical and chemical properties make the algae biocrude oil less desirable as a fuel. Although, having the advantages of high calorific value for the biocrude, the applications and/or uses of other by-products such as biochar was never extensively investigated. The attention towards producing biocrude will result in vast quantities of biochar. This creates a potential quantity to be disposed adding more expenditure if no economic viability can be shown. This can also impact the economic sustainability of the algal biofuel and bioproduct industry. Hence, there is a high priority to address the issues mentioned above.

Rationale: Based on the above discussion, other research groups and we have demonstrated that hydrothermal liquefaction (HTL) can process wet microalgae and produce energy-dense products and nutrient-rich aqueous phase.

The product analysis from our HTL experiments has shown the formation of energy-dense biocrude oil, biochar, and water-soluble compound fraction. The HHV of the HTL products biocrude and biochar increased in contrast to the original biomass at the highest HTL biocrude yield conditions. A considerable concentration of nutrients such as organic carbon, ammoniacal nitrogen, phosphates, and dissolved carbohydrates were found in the HTL aqueous phase and biochar. Therefore, these nutrients in the product fraction can be recycled for algae cultivation. Based on the issues mentioned, research hypotheses are stated as follows:

1. HTL can produce energy dense products using the whole biomass.
2. HTL can produce nutrient-rich by-products which can be directly used or recycled into algae cultivation systems.
3. Heteroatoms in the algal biocrude oil can be effectively removed during the heterogeneous catalysis of biocrude oil.
4. HTL biochar can be leached to extract nutrients for cultivating microalgae.
5. HTL biochar can be used to produce energy dense gases via pyrolysis.

These hypotheses are tested further in the next chapters and dissertation organization section will present a detailed explanation.

1.5 Research objectives, significance, and impact

The topic of climate change has been given the highest importance in recent years due to the increase in global mean temperatures and the rise in sea-level around the world. The extensive use of fossil fuel reserves has altered the global carbon cycle by increased emissions of greenhouse gases and thus having a serious impact on climate change. Renewable and carbon-neutral fuels that are also capable of sequestering atmospheric carbon dioxide are required to achieve environmental and economic sustainability. This makes algal biofuels a critical area of research as they can sequester high levels of CO_2 and possibly replace fossil fuels. A lot of success has been seen in recent years by employing different techniques to produce algal biofuels. These methods have shown that algae produce multiple products that have a wide range of potential to be used as fuel, co-fuel, soil amendment, and other products. These products have a higher ratio of nitrogen, phosphorous, sulfur, and oxygen which makes them intermediate product rather than a final product. The presence of these heteroatoms in the fuels will require an entirely new commercial equipment technology, which will increase the production cost of the biofuels.

The comprehensive research objective of this dissertation is

1. To develop a conversion technique that utilizes the whole wet biomass to produce energy-dense product fractions such as biocrude oil and nutrient-rich product fraction such as aqueous phase and biochar.

2. To investigate the influence of heterogeneous catalysts on the upgrading of biocrude oil.
3. To propose multiple potential uses of HTL by-products especially HTL biochar to improve the economic and environmental sustainability of the HTL biofuel process.

1.6 Dissertation organization

This section describes about the organization of the dissertation. All the chapters excluding chapter 1 (introduction) and chapter 7 (conclusions and recommendations) are formatted as a standalone technical paper with correlation to the following chapter. However, each chapter draws its conclusions through hypotheses testing and possesses references of its own.

Chapter 2 discusses testing the hypothesis #1, 2, 3 and the objective #1, 2, of the research study; investigating the optimum conditions to produce HTL products with a range of process parameters and three types of microalgae. All the biomass and HTL products were analyzed for the value and energy content along with any valuable inorganic metals.

Chapter 3 discusses the role of co-liquefying/mixing different biomasses to achieve improved yields. The improved yield happened due to the synergistic effect at a specific biomass co-liquefying ratio. This approach strengthened the applicability of HTL towards the conversion of multiple biomass varieties with positive synergistic affect. The HTL products were analyzed for their energy content and elemental composition.

Chapter 4 focuses on the physicochemical characterization of one of the HTL products, biochar. HTL biochar was analyzed for functional groups, crystalline structures, metal content, elemental analysis, and metal content. The information from these analyzes was used to suggest value-added applications to the improve economic and environmental sustainability of the HTL process.

Chapters 5 & 6 focuses on the applications of HTL biochar to recover nutrients and other valuable gases (H_2 and CO) and testing hypothesis #4 and 5 while following the research objective #3.

Chapter 7 summarizes the research work and provides recommendations for future work

1.7 References

Administration, [USEIA] U S Energy Information, 2018. Annual Energy Outlook 2018 with projections to 2050.

Ahmad, A.L., Yasin, N.H.M., Derek, C.J.C., Lim, J.K., 2011. Microalgae as a sustainable energy source for biodiesel production: a review. Renew. Sustain. Energy Rev. 15, 584–593.

Akhtar, J., Amin, N.A.S., 2011. A review on process conditions for optimum bio-oil yield in hydrothermal liquefaction of biomass. Renew. Sustain. Energy Rev. 15, 1615–1624.

Alaswad, A., Dassisti, M., Prescott, T., Olabi, A.G., 2015. Technologies and developments of third generation biofuel production. Renew. Sustain. Energy Rev. 51, 1446–1460.

Anastasakis, K., Ross, A.B., 2011. Hydrothermal liquefaction of the brown macro-alga Laminaria Saccharina: Effect of reaction conditions on product distribution and composition. Bioresour. Technol. 102, 4876–4883.

ATAG, 2009. Beginners Guide to Aviation Biofuels.

Aysu, T., Demirbaş, A., Bengü, A.Ş., Küçük, M.M., 2015. Evaluation of Eremurus spectabilis for production of bio-oils with supercritical solvents. Process Saf. Environ. Prot. 94, 339–349.

Barba, F.J., Grimi, N., Vorobiev, E., 2015. New approaches for the use of non-conventional cell disruption technologies to extract potential food additives and nutraceuticals from microalgae. Food Eng. Rev. 7, 45–62.

Barry, A., Wolfe, A., English, C., Ruddick, C., Lambert, D., 2016. National algal biofuels technology review. US Dep. Energy, Off. Energy Effic. Renew. Energy, Bioenergy Technol. Off.

Barzagli, F., Mani, F., 2019. The increased anthropogenic gas emissions in the atmosphere and the rising of the Earth's temperature: are there actions to mitigate the global warming? Substantia 3, 101–111.

Brennan, L., Mostaert, A., Murphy, C., Owende, P., 2012. Phytochemicals from algae. Biorefinery Co-Products Phytochem. Prim. Metab. Value-Added Biomass Process. 199–240.

Chauton, M.S., Reitan, K.I., Norsker, N.H., Tveterås, R., Kleivdal, H.T., 2015. A techno-economic analysis of industrial production of marine microalgae as a source of EPA and DHA-rich raw material for aquafeed: research challenges and possibilities. Aquaculture 436, 95–103.

Chèze, B., Gastineau, P., Chevallier, J., 2011. Forecasting world and regional aviation jet fuel demands to the mid-term (2025). Energy Policy 39, 5147–5158.

Chiaramonti, D., Prussi, M., Buffi, M., Rizzo, A.M., Pari, L., 2017. Review and experimental study on pyrolysis and hydrothermal liquefaction of microalgae for

biofuel production. Appl. Energy 185, 963–972.

Chisti, Y., 2007. Biodiesel from microalgae. Biotechnol. Adv. 25, 294–306.

Christensen, E., Sudasinghe, N., Dandamudi, K.P.R., Sebag, R., Schaub, T., Laurens, L.M.L., 2015. Rapid Analysis of Microalgal Triacylglycerols with Direct-Infusion Mass Spectrometry. Energy and Fuels 29. https://doi.org/10.1021/acs.energyfuels.5b01205

Conti, J., Holtberg, P., Diefenderfer, J., LaRose, A., Turnure, J.T., Westfall, L., 2016. International energy outlook 2016 with projections to 2040. USDOE Energy Information Administration (EIA), Washington, DC (United States ….

Creutzig, F., Breyer, C., Hilaire, J., Minx, J., Peters, G.P., Socolow, R., 2019. The mutual dependence of negative emission technologies and energy systems. Energy Environ. Sci. 12, 1805–1817.

Demirbas, A., 2009. Political, economic and environmental impacts of biofuels: A review. Appl. Energy 86, S108–S117.

Elliott, D.C., 2016. Review of recent reports on process technology for thermochemical conversion of whole algae to liquid fuels. Algal Res. 13, 255–263.

Elliott, D.C., Biller, P., Ross, A.B., Schmidt, A.J., Jones, S.B., 2015. Hydrothermal liquefaction of biomass: developments from batch to continuous process. Bioresour. Technol. 178, 147–156.

Fukuda, H., Kondo, A., Noda, H., 2001. Biodiesel fuel production by transesterification of oils. J. Biosci. Bioeng. 92, 405–416.

Gnansounou, E., Dauriat, A., Villegas, J., Panichelli, L., 2009. Life cycle assessment of biofuels: energy and greenhouse gas balances. Bioresour. Technol. 100, 4919–4930.

Guo, Y., Yeh, T., Song, W., Xu, D., Wang, S., 2015. A review of bio-oil production from hydrothermal liquefaction of algae. Renew. Sustain. Energy Rev. 48, 776–790.

Hansen, J., Sato, M., Ruedy, R., Lo, K., Lea, D.W., Medina-Elizade, M., 2006. Global temperature change. Proc. Natl. Acad. Sci. 103, 14288–14293.

Hileman, J.I., Stratton, R.W., 2014. Alternative jet fuel feasibility. Transp. Policy 34, 52–62.

Hoffert, M.I., Caldeira, K., Benford, G., Criswell, D.R., Green, C., Herzog, H., Jain, A.K., Kheshgi, H.S., Lackner, K.S., Lewis, J.S., 2002. Advanced technology paths to global climate stability: energy for a greenhouse planet. Science (80-.). 298, 981–987.

Karl, T.R., Trenberth, K.E., 2003. Modern global climate change. Science (80-.). 302, 1719–1723.

Kröger, M., Müller-Langer, F., 2012. Review on possible algal-biofuel production processes. Biofuels 3, 333–349.

Lardon, L., Hélias, A., Sialve, B., Steyer, J.-P., Bernard, O., 2009. Life-cycle assessment

of biodiesel production from microalgae.

Lelieveld, J., Klingmüller, K., Pozzer, A., Burnett, R.T., Haines, A., Ramanathan, V., 2019. Effects of fossil fuel and total anthropogenic emission removal on public health and climate. Proc. Natl. Acad. Sci. 116, 7192–7197.

Lowrey, J., Brooks, M.S., McGinn, P.J., 2015. Heterotrophic and mixotrophic cultivation of microalgae for biodiesel production in agricultural wastewaters and associated challenges—a critical review. J. Appl. Phycol. 27, 1485–1498.

Ma, F., Hanna, M.A., 1999. Biodiesel production: a review. Bioresour. Technol. 70, 1–15.

Mata, T.M., Martins, A.A., Caetano, N.S., 2010. Microalgae for biodiesel production and other applications: a review. Renew. Sustain. energy Rev. 14, 217–232.

McKendry, P., 2002. Energy production from biomass (part 2): conversion technologies. Bioresour. Technol. 83, 47–54.

Meher, L.C., Sagar, D.V., Naik, S.N., 2006. Technical aspects of biodiesel production by transesterification—a review. Renew. Sustain. energy Rev. 10, 248–268.

Mercure, J.-F., Pollitt, H., Viñuales, J.E., Edwards, N.R., Holden, P.B., Chewpreecha, U., Salas, P., Sognnaes, I., Lam, A., Knobloch, F., 2018. Macroeconomic impact of stranded fossil fuel assets. Nat. Clim. Chang. 8, 588–593.

Mohan, D., Pittman Jr, C.U., Steele, P.H., 2006. Pyrolysis of wood/biomass for bio-oil: a

critical review. Energy & fuels 20, 848–889.

Naik, S.N., Goud, V. V, Rout, P.K., Dalai, A.K., 2010. Production of first and second generation biofuels: a comprehensive review. Renew. Sustain. energy Rev. 14, 578–597.

Onwudili, J.A., Lea-Langton, A.R., Ross, A.B., Williams, P.T., 2013. Catalytic hydrothermal gasification of algae for hydrogen production: composition of reaction products and potential for nutrient recycling. Bioresour. Technol. 127, 72–80.

Park, K.-C., Ihm, S.-K., 2000. Comparison of Pt/zeolite catalysts for n-hexadecane hydroisomerization. Appl. Catal. A Gen. 203, 201–209.

Patel, M., Zhang, X., Kumar, A., 2016. Techno-economic and life cycle assessment on lignocellulosic biomass thermochemical conversion technologies: A review. Renew. Sustain. Energy Rev. 53, 1486–1499.

Patil, P.D., Reddy, H., Muppaneni, T., Deng, S., 2017. Biodiesel fuel production from algal lipids using supercritical methyl acetate (glycerin-free) technology. Fuel 195, 201–207.

Peterson, A.A., Vogel, F., Lachance, R.P., Fröling, M., Antal Jr, M.J., Tester, J.W., 2008. Thermochemical biofuel production in hydrothermal media: a review of sub-and supercritical water technologies. Energy Environ. Sci. 1, 32–65.

Ponnusamy, S., Reddy, H.K., Muppaneni, T., Downes, C.M., Deng, S., 2014. Life cycle assessment of biodiesel production from algal bio-crude oils extracted under

subcritical water conditions. Bioresour. Technol. 170, 454–461.

Reddy, H.K., Muppaneni, T., Sun, Y., Li, Y., Ponnusamy, S., Patil, P.D., Dailey, P., Schaub, T., Holguin, F.O., Dungan, B., Cooke, P., Lammers, P., Voorhies, W., Lu, X., Deng, S., 2014. Subcritical water extraction of lipids from wet algae for biodiesel production. Fuel 133, 73–81. https://doi.org/https://doi.org/10.1016/j.fuel.2014.04.081

Rodolfi, L., Chini Zittelli, G., Bassi, N., Padovani, G., Biondi, N., Bonini, G., Tredici, M.R., 2009. Microalgae for oil: Strain selection, induction of lipid synthesis and outdoor mass cultivation in a low-cost photobioreactor. Biotechnol. Bioeng. 102, 100–112.

Sarmah, S.B., Kalita, P., Garg, A., Niu, X., Zhang, X.-W., Peng, X., Bhattacharjee, D., 2019. A review of state of health estimation of energy storage systems: challenges and possible solutions for futuristic applications of Li-Ion battery packs in electric vehicles. J. Electrochem. Energy Convers. Storage 16.

Selvaratnam, T., Pegallapati, A.K., Reddy, H., Kanapathipillai, N., Nirmalakhandan, N., Deng, S., Lammers, P.J., 2015a. Algal biofuels from urban wastewaters: Maximizing biomass yield using nutrients recycled from hydrothermal processing of biomass. Bioresour. Technol. 182, 232–238.

Selvaratnam, T., Reddy, H., Muppaneni, T., Holguin, F.O., Nirmalakhandan, N., Lammers, P.J., Deng, S., 2015b. Optimizing energy yields from nutrient recycling

using sequential hydrothermal liquefaction with Galdieria sulphuraria. Algal Res. 12, 74–79.

Shonnard, D.R., Williams, L., Kalnes, T.N., 2010. Camelina-derived jet fuel and diesel: Sustainable advanced biofuels. Environ. Prog. Sustain. Energy 29, 382–392.

Singh, A., Olsen, S.I., 2011. A critical review of biochemical conversion, sustainability and life cycle assessment of algal biofuels. Appl. Energy 88, 3548–3555.

Spolaore, P., Joannis-Cassan, C., Duran, E., Isambert, A., 2006. Commercial applications of microalgae. J. Biosci. Bioeng. 101, 87–96.

Statistics, I.E.A., 2011. CO2 emissions from fuel combustion-highlights. IEA, Paris http//www. iea. org/co2highlights/co2highlights. pdf. Cited July.

Tian, C., Li, B., Liu, Z., Zhang, Y., Lu, H., 2014. Hydrothermal liquefaction for algal biorefinery: a critical review. Renew. Sustain. Energy Rev. 38, 933–950.

Toor, S.S., Reddy, H., Deng, S., Hoffmann, J., Spangsmark, D., Madsen, L.B., Holm-Nielsen, J.B., Rosendahl, L.A., 2013. Hydrothermal liquefaction of Spirulina and Nannochloropsis salina under subcritical and supercritical water conditions. Bioresour. Technol. 131, 413–419.

Toor, S.S., Rosendahl, L., Rudolf, A., 2011. Hydrothermal liquefaction of biomass: a review of subcritical water technologies. Energy 36, 2328–2342.

U.S. EIA, U.S. Energy Information Administration (EIA), 2019. Annual Energy Outlook

2019 with projections to 2050. Annu. Energy Outlook 2019 with Proj. to 2050. https://doi.org/DOE/EIA-0383(2012) U.S.

Valdez, P.J., Nelson, M.C., Wang, H.Y., Lin, X.N., Savage, P.E., 2012. Hydrothermal liquefaction of Nannochloropsis sp.: Systematic study of process variables and analysis of the product fractions. Biomass and Bioenergy 46, 317–331.

Verma, M., Godbout, S., Brar, S.K., Solomatnikova, O., Lemay, S.P., Larouche, J.P., 2012. Biofuels production from biomass by thermochemical conversion technologies. Int. J. Chem. Eng. 2012.

Wang, Z., Adhikari, S., Valdez, P., Shakya, R., 2015. Upgrading of hydrothermal liquefaction biocrude from algae grown in municipal wastewater, in: 2015 ASABE Annual International Meeting. American Society of Agricultural and Biological Engineers, p. 1.

White, A.W., Shilo, M., 1975. Heterotrophic growth of the filamentous blue-green alga Plectonema boryanum. Arch. Microbiol. 102, 123–127.

Wigley, T.M.L., Raper, S.C.B., 2001. Interpretation of high projections for global-mean warming. Science (80-.). 293, 451–454.

Winwood, R.J., 2013. Recent developments in the commercial production of DHA and EPA rich oils from micro-algae. Ocl 20, D604.

Zhou, D., Zhang, L., Zhang, S., Fu, H., Chen, J., 2010. Hydrothermal liquefaction of macroalgae Enteromorpha prolifera to bio-oil. Energy & Fuels 24, 4054–4061.

CHAPTER 2: HYDROTHERMAL LIQUEFACTION OF MICROALGAE UNDER SUB- AND SUPER-CRITICAL WATER CONDITIONS

2.1 Introduction

Biofuels can be a potential solution to address current environmental and economic sustainability of depleting fossil fuel resources and accumulation of greenhouse gases. The reduction of CO_2 emissions by 2050 is considered as an immense global challenge which involves a potential feed source to supply renewable energy as well as work in favor of atmospheric CO_2 sequestration (Pachauri et al., 2014; Schenk et al., 2008). Among such feedstocks, microalgae have been elucidated in the recent years due to its high photosynthetic efficiency, high lipid content, high area-specific yields, and their ability to grow in variety of water sources and ecological conditions (Jin et al., 2017; Sudasinghe et al., 2014). Apart from an extensive research of microalgae in the area of biofuels, microalgae were also studied as important sources of producing commercially high-valued foods, animal feeds, and chemicals such as β-carotenes, phycobiliproteins, fatty acids, and polysaccharides (Borowitzka, 2013; Mendes et al., 2009; Milledge, 2012).

Various thermochemical conversion techniques have been investigated in literature to convert either dry or wet biomass into fuel components. Most of these conversion techniques lack the technical feasibility to process high moisture containing feedstocks at large scale unless by concentrating, dewatering, and drying which adds up to energy

expenditure and increases the production costs of the whole process (Toor et al., 2013; Valdez et al., 2012). Therefore, wet conversion techniques like hydrothermal liquefaction (HTL), where biomass is converted to valuable liquid products attracted attention because of its ability to harvest the prominent properties of water as reaction medium. This eliminates the need for drying the feedstock and can minimize the energy consumption required during other biomass conversion techniques involving drying step. Gai et al.,(Gai et al., 2015a) Toor et al.,(Toor et al., 2011) have mentioned that HTL is a promising technique which involves in breaking complex bio-macromolecules in the biomass via dehydrogenation, hydrolysis, decarboxylation, deamination etc., into smaller energy dense fuel components. The products of hydrothermal liquefaction contain both organic and inorganic components and depending on their physical state can be upgraded with or without using catalysts to produce liquid transportation or industrial fuels (Toor et al., 2013; Z. Wang et al., 2015). Recent studies on liquefaction of algae also involved utilizing algae produced from wastewater treatment system, recycling of HTL's aqueous phase that is rich in macro- and micro-nutrients, and recovering valuable co-products like polysaccharides to achieve and maximize energy output in bio-energy production (Chakraborty et al., 2012; Chen et al., 2014).

The studies in literature (Lombardi et al., 2002; Saeed et al., 2012) investigated the potential of green alga *Kirchneriella* in the abolition and bio-sequestering (Huang et al., 2017) of heavy metals like hexavalent chromium, lead, and copper. Previous studies

(Eustance, 2011; Song et al., 2013) evaluated the biofuel potential, nitrogen utilization of different strains of *Kirchneriella*. However, the effect of hydrothermal liquefaction of fresh water *Kirchneriella* sp. has never been investigated as a source of biofuels. Therefore, in the current study, the effect of process parameters on the sub- and super-critical extraction of green alga, *Kirchneriella* sp. and the qualitative and quantitative performances were reported. Since, this alga has never been evaluated from biofuels perspective, the authors are experimenting with a broad range of hydrothermal conversion techniques involving sub- and super-critical conditions using water as reaction media. This alga was selected as a potential species to be grown during cold/winter months at the algal test facility. The microalgae *Micractinium sp., and Galdieria sp.* were grown during other seasons to maximize the annual biomass productivity through crop-rotation strategies. Three different microalgae were hydrothermally liquefied under a range of processing conditions. It is hypothesized that HTL can produce energy dense and nutrient rich products. It is also hypothesized that heterogenous catalysts can improve the quality of biocrude oil, while heteroatoms in the biocrude oil improve the properties of recycled asphalt when blended. The overall story of this research ultimately connects to the production of liquid renewable fuels and improving value chain of this technology by proposing economical applications. The objectives include:

1. Optimizing the parameters to achieve the highest yield of products
2. Evaluating and measuring the nutrient rich and energy density of products along with other impurities.

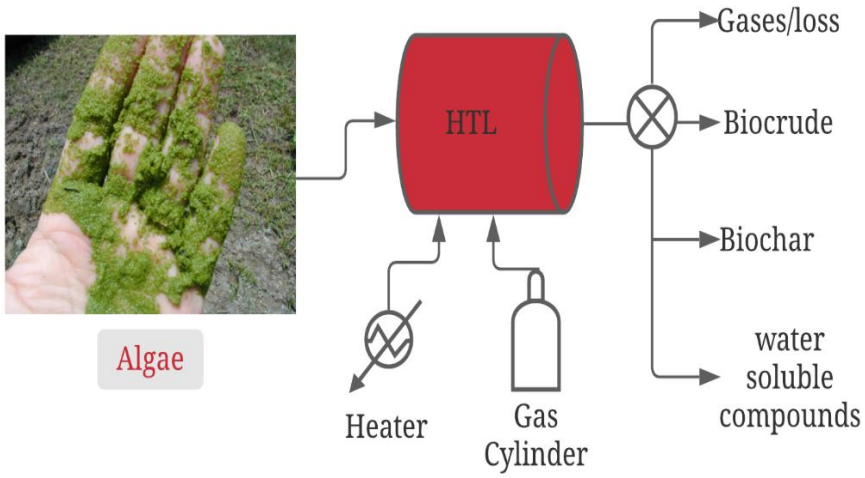

Figure 2.1: Experimental plan of the study

2.2 Materials and methods

This section discusses about the experimental plan implemented in this chapter via figure 2.1. In this section, details of the standard procedure describing how samples have been analyzed and processed are included. Subsequently, a detailed procedure describing the experimental protocol about the hydrothermal liquefaction is included. In this chapter, general techniques which have been used throughout the dissertation are listed.

2.2.1 Biomass sources

The microalgae samples investigated in this course of the study were mainly grown and collected from Arizona Center for Algae Technology and Innovation (AzCATI), Arizona State University and Heliae Development, LLC., Gilbert, Arizona which are summarized

in table 2.1. The source of the algae, strain details and growth media used to these algae are also summarized.

Kirchneriella sp. (26B-AM), a green alga was assessed in the study and grown outdoors (natural\ sunlight) in a standard BG-11 medium in a 50 L flat panel vertical photo-bioreactor. The cultures were grown in the winter season (01/19/2016-02/10/2016) at the test location, and the ambient temperature was recorded in the range of 7–27 °C. The cultures were maintained at a neutral pH (7–8.5) with an average 24-hr temperature of 12.6 °C and an average photoperiod of 10.8 h. The light intensities varied during the day with a maximum of 733 $W.m^{-2}$ and an average of 375.12 $W.m^{-2}$ throughout the whole daylight duration. The cultures were supplemented with 2.5% CO_2 mixed with air and delivered through sparging systems which also assisted in mixing. The biomass growth in the culture was spectrophotometrically monitored daily in terms of optical density (OD) at a wavelength of 750 nm measured with Beckman DU530 spectrophotometer (Beckman Coulter Inc., USA). The samples from each bioreactor were collected daily and centrifuged at 4000 rpm for 10 min, and the aliquot was measured for soluble ammonia-N (Salicylate TNT Method 10031) and P (Phosver 3 Method 8048) using HACH DR6000 spectrophotometer (HACH, Colorado, USA) to evaluate the nutrient uptake of the biomass. The biomass was harvested during the stationary growth phase and concentrated using a centrifuge (AML Industries Lavin, Model: 12-413v). 200 L (4*50 L) of the collected culture was centrifuged continuously at 3000 × g and ambient conditions. The slurry (∼30% solids) was stored at −20 °C before being used in the liquefaction experiments. The

current work on *Kirchneriella sp.* has been recently published and is as cited (Dandamudi et al., 2019).

Galdieria sulphuraria (*G. sulphuraria* CCMEE 5587.1) (Toplin et al., 2008), is a strain of acido-thermophilic unicellular red alga obtained from the Culture Collection of Microorganisms from Extreme Environments (Pacific Northwest National Laboratory, Richland, U.S.A. The cultures were isolated from single colonies to tissue culture flasks and were mixed at 40 °C in a lighted incubator (Percival Scientific, IA, USA). These were supplemented with 2% CO_2 under constant light source (100 µmol photons m^{-2} s^{-1}). A modified cyanidium medium at pH 2.5 (Selvaratnam et al., 2014), was used for verification, scale-up, and experiments. The composition of the medium, per liter, was as follows: $(NH_4)_2SO_4$, 2.64 g; KH_2PO_4, 0.20 g; NaCl, 0.12 g; $MgSO_4 \cdot 7H_2O$, 0.25 g; $CaCl_2 \cdot 2H_2O$, 0.07 g; Nitch's Trace Element Solution, 0.5 ml; $FeCl_3$ (solution = 0.29 g L^{-1}), 1.0 ml. The axenic stock cultures were scaled up indoors from tissue culture flasks to 15 L vertical panels and were supplemented with 2% CO_2 and maintained at 40 °C under a 14/10h light (450 µmol photons m^{-2} s^{-1}) to dark cycle. The 15 L indoor panels were then used to inoculate three 4x4 foot outdoor vertical panels (50 L; 4 cm light path) where the cultures could grow around 2 g/L. These were used to inoculate 48 vertical panels (1200 L; 10 cm light path, starting density: 0.25 g/L). The outdoor vertical systems used air spargers lining at the bottom of the reactors for mixing (0.3 vvm) and CO_2 (2.0%) supplemental. The cultures were harvested at a final density of 3 g/L by centrifugation.

Micractinium sp. was procured from Heliae Development LLC as a thick paste containing 20 % biomass and the rest to be water and or growth media. All the samples were stored under -20 °C before analyzed for biochemical, ultimate analysis and liquefaction experiments.

2.2.2 Proximate analysis

Proximate analysis was carried out on all the microalgal samples to calculate the amount of moisture and ash content. These calculations were crucial to estimate the biomass being used during the liquefaction experiments and therefore to calculate the mass balance and report product yields on a dry weight basis. Approximately, 2.0 g of the wet samples were weighed in a crucible and placed in an oven at 105 °C for 10 h. The weight loss of the samples was constantly recorded until two consecutive readings are similar. The final remaining dry biomass was weighed, and the moisture content was calculated based on the weight from the wet biomass. The ash content was determined by placing around 0.1 g of dry biomass in a muffle furnace at 575 ± 25 °C for 24 ± 6 hours. The samples were then removed and placed in a desiccator to cool down. The ash values were calculated based on the dry biomass used and the amount of ash left at the end of the heating duration (Laurens, 2016).

Table 2.1: Name, source, strain code, growth media, and growth season of the microalgae investigated in the study

Name	**Source**	**Strain**	**Growth Media**	**Growth Season**
Kirchneriella sp.	AzCATI	26B-AM	Standard BG-11	winter
Galdieria sulphuraria	AzCATI	CCMEE 5587.1	modified cyanidium	Summer
Micractinium immerum	Heliae	unknown	(Doucha and Lívanský, 2012)	-

2.2.3 Ultimate Analysis

Ultimate analysis of the samples was performed to analyze the weight percentages of organic (Carbon, Hydrogen) and heteroatoms (Nitrogen, Sulphur). The samples were lyophilized to remove the excess moisture, weighed in triplicates (1-3.0 mg), and sealed in a tin crucible before being analyzed by Perkin Elmer 2400 Series II elemental analyzer. The instrument was initially calibrated using an instrumental standard (Cystine) which contains 29.99 wt.% carbon, 5.03 wt.% hydrogen, 11.67 wt.% nitrogen, 26.69 wt.% sulfur in an oxygen-rich condition (Patil et al., 2018; J. Wang et al., 2015). The analyzer calculates the different atoms based on NOx, CO2, and SO2 gas concentrations in the exhaust gases

passed through a series of pre-packed catalysts to convert them into their respective oxides. The atoms are expressed on a weight basis of the dry sample used in the tin crucible, and the mean values are reported. The values provided an insight into the calorific value (High Heating Value, HHV) of the biomass under the study and were calculated using the Dulong formula (Browne, 1990).

2.2.4 Biochemical analysis

The biochemical analysis of the biomass samples was performed to analyze the amount of carbohydrates, lipids, and protein. The total lipids were expressed as the fatty acid methyl esters (FAME, hereafter) after direct, in situ transesterification of algal biomass with an acid catalyst -hydrochloric acid in methanol, based on the dry weight of the biomass sample (Van Wychen et al., 2016). Following the reaction, the samples were cooled down to room temperature, and the FAME fraction was extracted using hexane, which separates the polar compounds at the bottom phase. The total FAME was quantified using C13:0 ME as an internal standard by a Gas Chromatography-Mass Spectrometer (GC-MS) as mentioned in (Van Wychen et al., 2016).

Carbohydrates were analyzed by using a two-step sulfuric acid hydrolysis to hydrolyze the polymeric forms of complex carbohydrates in the microalgal biomass into their respective monomeric units. The released monosaccharides were quantified using a spectroscopic method set to measure at 620 nm using a range of calibration standards and a calibration curve. This method does not count into account that some of the carbohydrates may not be hydrolyzed. A detailed description of the method and the accuracies were

mentioned in Van Wychen S et al.,(Van Wychen and Laurens, 2016). The amount of protein in the microalgae significantly influences the fuel potential, food value and in the co-product development. Various analytical methods can be employed to estimate the protein content in the biomass involving spectroscopic techniques, UV or IR techniques, hydrolysis methods, and elemental nitrogen analysis (Moore et al., 2010). The earlier mentioned techniques have issues with generating the absolute protein values which are crucial in biochemical component mass balance. The spectroscopic methods rely on the complete solubilization of all the cell-bound proteins to interact with reagents being used. The choice of reagent and standard of proteins play an important role for quantification as the standard should be a representative of solubilized protein. A nitrogen-to-protein conversion factor seems to be a hassle-free solution considering the analytical issues regarding solvent choice, extraction efficiency, interference between analytes (Lourenço et al., 2004, 1998). Based on the literature, a conversion factor of 4.78 (*N%) was chosen to estimate the protein content in the given algal biomass sample. Table 2.2 summarizes the list of carbohydrates, lipids, and protein content of the biomass under the study. *Galdieria sp*. has the highest amount of protein (54.68 %) and the lowest amount of lipid content (5.88 %) based on the dry weight of biomass. *Micractinium sp.* has the highest carbohydrate content (44.02 %) based on the dry weight of biomass while it also has the highest amount of lipids (16.05 %) among the three species under study. The difference in the total mass balance from the ultimate, proximate and biochemical analysis can be accounted for the presence of non-fuel-relevant compounds, such as pigments,

hydrophobic amino acids and incomplete extraction of all the lipids from the algae as FAME.

2.2.5 Heavy metal analysis

The presence of low concentrations of heavy metals in the HTL biocrude and biochar are favorable for enhanced combustion; thereby improving stability during storage and later upgrading processes (Sudasinghe et al., 2014). It is crucial to monitor the concentrations of various metals in the products to reduce the cost of scalability and maintenance in the downstream processing, i.e., catalyst selection, poisoning, and fouling of storage vessels. The results in table 2.4 reveals the presence of barium (Ba), calcium (Ca), chromium (Cr), iron (Fe), potassium (K), sodium (Na), phosphorous (P), zinc (Zn), magnesium (Mg), nickel (Ni) similar to that of (Eboibi et al., 2014; Sudasinghe et al., 2014). The results suggest that among all of the detected metals phosphorus, potassium, sodium, and magnesium were the dominant metals found in biomass as they were the macronutrients essential and were fed through the growth culture medium (Selvaratnam et al., 2015a). The dissolved macronutrients were thus utilized by microalgae for various biological and biochemical pathways. Apart from them, micronutrients such as iron, zinc, copper, and calcium were supplemented during the growth and were also detected in the original biomass. The presence of aluminum can be arising from the salts used to prepare the stock solutions during growth and could be an issue of contamination. Approximately 0.2 g of the algae samples were weighed using a balance and were acid digested as per the protocol adapted from (Chemists and Horwitz, 1975). Following digestion, the samples

were quantified for presence of metals using a ThermoFisher iCAP 6300 ICP-OES (Inductively Coupled Plasma Optical Emission Spectrometry) unit. The instrument was calibrated and optimized to measure the metals of interest based on the instructions from vendors operational wavelength specific to different metals. The wavelength (in nm) set was the following: Al 328.068, 167.079 and 308.215; As 189.042 and 193.759; Ba 455.403; Be 311.107; Ca 393.366; Cd 214.438; Co 228.616; Cr 205.560; Cu 324.754; Fe 259.940; Hg 184.950 and 194.227; K 766.490; Li 670.784; Mg 279.553; Mn 257.610; Mo 202.030; Na 589.592; Ni 231.604; P 177.495 and 213.618; Pb 220.353; S 180.731; Sb 206.833; Se 196.090; Sn 189.989 and 283.999; Sr 407.771; Ti 336.121; Tl 190.856 and 276.787; V 309.311 and Zn 213.856.

2.2.6 Hydrothermal processing and liquefaction

Hydrothermal processing is a promising technique which involves in breaking complex bio-macromolecules in the biomass via dehydrogenation, hydrolysis, decarboxylation, deamination, etc., into smaller energy dense fuel components. The products of hydrothermal liquefaction contain both organic and inorganic components and depending on their physical state can be upgraded with or without using catalysts to produce liquid transportation or industrial fuels (Gai et al., 2015b; Z. Wang et al., 2015). Recent studies on liquefaction of algae also involved utilizing algae produced from wastewater treatment system, recycling of HTL's aqueous phase that is rich in macro- and micro-nutrients, and recovering valuable co-products like polysaccharides to achieve and maximize energy output in bio-energy production (Chakraborty et al., 2012; Chen et al., 2014).

HTL experiments were performed as mentioned in previous work (Muppaneni et al., 2017). In brief, the HTL reactions were performed in a 100-ml stainless steel bench top reactor (Model 4593, Parr Instrument Company, Moline, IL) equipped with a magnetic stirrer, heater, and a 4843-controller unit. The reactor was designed to be operated up to 500 °C and can withhold pressure up to 20 MPa. The reactor was loaded with either 5 or 10 grams of the biomass and the remaining as water to make up 50 grams of slurry. The reactor was then sealed and subsequently purged with nitrogen gas (99.98% pure) at least three times to remove all the residual air on top of the liquid mixture. An initial pressure of 2.3 MPa was maintained in the reactor during all the experiments by adding nitrogen. The reactor was heated using an external heater at a rate of 10 °C/min and maintained at the desired reaction temperature for a specified period. The reactor was then cooled to room temperature by removing the heating jacket and exposing it to ambient air for about 2 hours. Following the system to be at room temperature, the gases are vented, and the reaction vessel was opened. The reaction mixture was added with 25 ml of dichloromethane (DCM), and the contents were mixed. The contents (liquid and solid mixture) were filtered and transferred to a glass separation funnel. The liquid fraction was allowed to phase separate, and the settled bottom fraction of the organic portion was collected. The DCM was removed using a rotary evaporator at 65 °C under vacuum to recover the biocrude. The solid fraction was dried in an oven at 80 °C for >6 h and termed as biochar. The aqueous fraction following removal of biocrude phase from the separatory funnel was also collected and termed as the aqueous fraction. All the product samples were collected and stored at 5

°C for further analysis. Each run was performed in triplicate at similar experimental conditions and mean values were reported. The schematic of the reactor assembly is shown in Figure 3.2. The yields of the products (biocrude, biochar, aqueous phase, and gaseous phase) were calculated based on the equations mentioned below:

$$\text{Biocrude oil yield BC, \%} = \frac{\text{Weight of the biocrude oil}}{\text{dry weight of the biomass loaded}} * 100$$

(2.1)

$$\text{Biochar yield BCH, \%} = \frac{\text{Weight of the biochar}}{\text{dry weight of the biomass loaded}} * 100$$

(2.2)

$$\text{Aqueous phase yield AQ, \%} = \frac{\text{Weight of the water-soluble compounds}}{\text{dry weight of the biomass loaded}} * 100$$

(2.3)

Gas Phase yield GP, %=

$$\frac{(\text{dry weight of the biomass loaded}) - (\text{weight of BC}) - (\text{weight of BCH}) - (\text{weight of AQ})}{\text{dry weight of the biomass loaded}} * 100$$

(2.4)

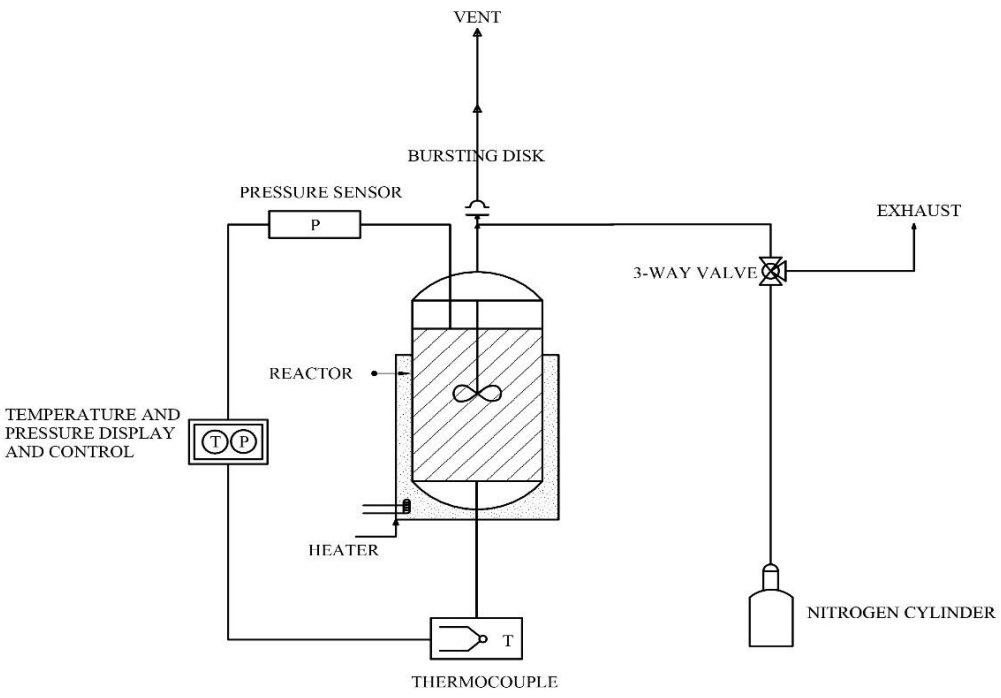

Figure 2.2: The illustrative layout of 100 ml Parr reactor

2.2.7 Catalytic upgrading of biocrude oil

Most of the studies on upgrading biocrude oil were performed in the presence of supercritical water environment. These studies reported that upgrading reaction temperature was the main influential factor among the selected and the selected catalyst choice is responsible for the removal of specific atoms from the biocrude thereby changing its chemical properties. These studies involved in using 3 different catalysts (MO_2C, Pt/C, and HZSM-5), variable temperature (350, 400 °C), residence time (4 h), and catalyst loading (15 wt.%). The catalysts were chosen based on their efficiency in decarboxylation of fatty acids, and hydrotreating in sub-critical water environment.

Hence, the current study was involved in the upgrading of bio-oil produced from the HTL of *Micractinium sp*. and to investigate the influence of temperature, catalyst choice, and water to oil ratio on selective hydrodeoxygenation, hydrodenitrogenation, and hydro desulphurization. These give an idea about which processing conditions are crucial, and the base case was performed using hydrogen with no catalyst used. The catalytic upgrading experiments were performed in a 100 ml stainless steel batch reactor. In a typical run, ~2 g of the bio-oil was used, and 15 wt.% of the catalyst was loaded with 10 grams of water resulting in 1:5 of oil to water. The upgrading experiments were performed after attaining the desired temperature for 4 hours. The assembly was wiped properly and sealed to ensure leak-free environment. The air inside the reactor was purged with nitrogen multiple times to create an inert atmosphere throughout the reaction. It was later flushed with hydrogen to create a hydrogen-rich environment and allowed to reach 1000 psi of hydrogen. The reactor assembly was later checked for any possible leaks, and the heater was attached to initiate the reaction.

2.3 Results and discussion

This section describes the research approaches chosen and the experiments planned to test the hypotheses mentioned in the previous section. As mentioned earlier, the product yields from HTL depends on the reaction temperature, solid loading, residence time, process pressures were varied to optimize the HTL conditions.

2.3.1 Analysis of biomass

Table 2.2 summarizes the ash content and the moisture content of the biomass under study. It is observed among all samples *Kirchneriella sp*. has a higher ash content of around 6 % compared to *Micractinium sp*. and *Galdieria sp.* Among the biomass samples, *Micractinium sp.* tends to have more water content in contrast with the rest; this may be due to the lower efficiency of the harvesting techniques.

Table 2.3 summarizes the elemental composition of the biomass under study. It is observed that with the increase in the amount of oxygen in the sample decreased the HHV value of the sample. Among all the biomass under study Kirchneriella sp. has one of the highest amounts of oxygen content (35.5 wt. %) among all leading to the lowest of HHV. Galdieria sp. has the highest amount of nitrogen atom content (11.14 %) and sulfur content (1.83 %). These analysis results were crucial to analyze and to evaluate the properties of the biomass and quality of products. The analysis of metals in algae under study were tabulated in Table 2.4.

Table 2.2: Proximate and biochemical composition of the biomass under study

	Kirchneriella sp.	*Micractinium sp.*	*Galdieria Sp.*
Moisture content, %	70.21 ± 0.41	79.90 ± 0.15	69.99 ± 0.11
Ash content (dw, %)	6.22 ± 0.89	2.12 ± 0.10	3.14 ± 0.31

Lipid content (FAME) (dw, %)	12.62 ± 0.58	16.05 ± 0.55	5.88 ± 0.21
Carbohydrates (dw, %)	26.47 ± 0.99	44.02 ± 1.10	18.13 ± 0.11
Proteins (dw, %)	28.11 ± 0.61	21.79 ± 0.88	54.68 ± 1.51
Others[a] (dw, %)	26.58	16.02	18.17

dw: based on dry weight calculations; [a]: calculated by difference (100-Sum (ash, lipid, carbohydrate, protein content))

Table 2.3: Ultimate analysis of the biomass under study

Atom, Wt.%	*Kirchneriella sp.*	*Micractinium sp.*	*Galdieria Sp.*
Carbon C, %	51.54	48.56	51.44
Hydrogen H, %	5.96	9.15	7.83
Nitrogen N, %	5.88	4.56	11.14
Sulphur S, %	1.11	0.88	1.83
Oxygen O[a], %	35.5	36.85	27.76
HHV, MJ/kg	19.73	23.07	23.79

[a]: calculated by difference (100-Sum (C, H, N, S content))

Table 2.4: Metal impurities in the biomass under study using ICP-OES

mg/kg	*Kirchneriella sp.*	*Micractinium sp.*	*Galdieria Sp.*
Al	444.05	105.2	234.69
Ca	120.17	1339.4	778.7
Cu	20.94	17.3	40.31
Fe	808.16	81.2	232.52
K	5610.47	1426.6	4458.46
Mg	2035.42	857.7	1694.8
Mn	40.23	15.5	41.42
Na	2741.74	1495.7	5632.14
Ni	94.45	nd	nd
Zn	21.73	31.3	23.3
P	7669.69	998.2	6664.44

nd: not detected

2.3.2 Optimization of HTL conditions to maximize the biocrude oil yield

This section involves in performing the experiments to produce various liquefaction products like biocrude oil, biochar, and aqueous phase that are further used in testing the hypotheses. Recent studies have suggested that process metrics such as reaction temperature, residence time, process pressure, solid/biomass loading were the influential factors on the HTL product distribution. Therefore, the influence of these parameters was investigated during this study under different temperatures (200-375 °C), residence times

(15-60 min), solid loadings (10-20 wt.%), process pressures (9-24 MPa), and solvents (hexane, dichloromethane, acetone). Using our group's previous expertise in the work related to the performance of HTL solvents, dichloromethane was used as the non-polar/working solvent in all the experiments discussed.

2.3.2.1 Effect of reaction temperature on the products

The effect of hydrothermal liquefaction on the wet biomass was studied in the temperature range of 200-375 °C with 30 min of reaction time and solid loadings varying between 10 and 20 wt.%. Figure 4.1 (A) shows the yield of biocrude and other products from the hydrothermal liquefaction of *Kirchneriella sp.* with respect to different reaction temperatures, 30 mins of residence time, 9 MPa initial pressure and 10 % solid loading. The biocrude oil yields ranged from 22.88 % to 45.50 %, where the highest value was achieved at 300 °C and minimum value at 200 °C, suggesting that temperature increase has increased in the degradation of biomass to fuel fraction and therefore considered as a key process parameter. A similar trend was observed during the HTL study (Dandamudi et al., 2019; Gai et al., 2015b; Muppaneni et al., 2017) where an increase in temperature has led to an increase in biocrude oil yield. The minimum yield of biocrude at 200 °C can be understood by the minimum conversion of biomass into the oil components. The biocrude oil formation is a result of various mechanisms which involves degradation of biomacromolecules such as lipids, carbohydrates, and proteins into smaller biomolecules (fatty acids, amino acids, and sugars) via numerous pathways of deamination, decarboxylation, hydrolysis, dehydrogenation, isomerization, and repolymerization (Yang

et al., 2015). These pathways and reactions are highly sensitive to temperature and need certain activation energies to undergo specified reactions and end up into biocrude oil. The higher biochar yields (38.06 %) also suggest that there was a minimum conversion of biomass at 200 °C. This also reinforces the fact that higher temperatures were required to initiate reactions and convert biochemical constituents into product fractions. The yields of biochar product fraction ranged from 38.06 % to 9.8 %, within the temperature range from 200-375 °C suggesting conversion of biomass into different product fractions.

On the other hand, increase in temperature beyond 300 through 375 °C with 25 °C increments led to the drop in the biocrude oil yield from 45.5 to 34.06 % suggests that liquefaction was surpassed by gasification reactions and increase in incondensable gas yields. The results were also supported by the increase in gas yields from 2.75 to 51.81 %. The slight increase in biochar at 375 °C might be due to repolymerization reactions where smaller molecular compounds fuse/repolymerize to re-settle as biochar. The aqueous fraction followed a trend where its yield increased gradually until 300 °C and then finally decreased as the reaction temperature was increased beyond 300 °C.

M*icractinium sp*. has the highest yield of biocrude oil at 300 and 350 °C, 22.57 and 27.95 % (Fig 4.1 B) on a dry weight basis. Almost half of the biomass was left unreacted or counted as biochar at 200 °C, suggesting that the temperature was not enough to lyse the cells and leading to the reaction of intracellular components. This is also explained by the lower biocrude oil yield (9.04 %) at 200 °C suggesting the temperature needs to be increased. The increase in biocrude oil yield is observed when the temperature was

increased to 250 °C (18.18 %), suggesting more amount of biomass is converted into the biocrude phase. The biocrude oil yield continued to increase until 350 °C from 250 °C with a 50 °C increments where the maximum yield was achieved at 350 °C (27.95 %). This result was also supported by the decrease in biochar yield at 250 °C (31.57 %) to 350 °C (14.42 %). A similar trend was also observed during the liquefaction of *Galdieria sp*. (Fig 4.1 C) where the minimum biocrude oil yield (8.15 %) and the maximum biochar yield (50.99 %) was observed at 200 °C, implicating to demonstrate the influence of an increase in temperature. The increase in biocrude and decrease in biochar was observed when the temperature was increased to 350 °C. The aqueous phase increased (22.56 %) until 200 °C leading to more water-soluble components in the aqueous phase and increase in temperature has led to the decrease in the water-soluble components in the aqueous phase to 14.89 % at 350 °C. The maximum biocrude oil yield was reported as 37.51 wt.% at 350 °C and 10 wt. % solid loading.

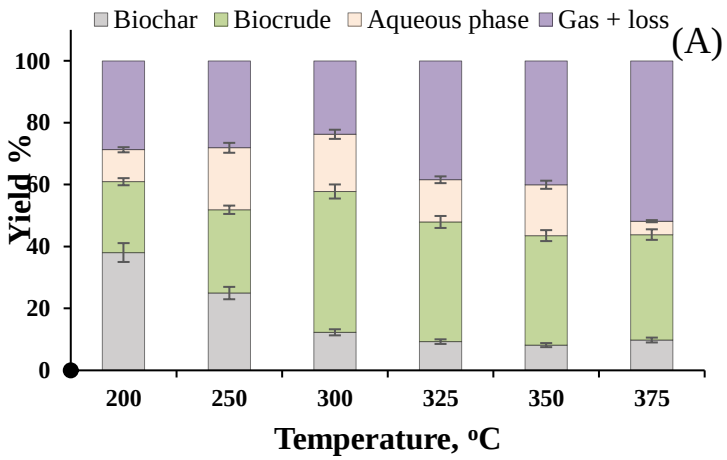

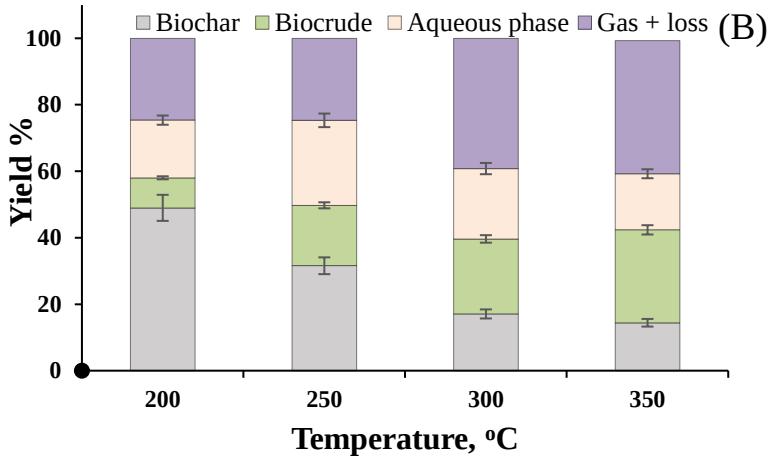

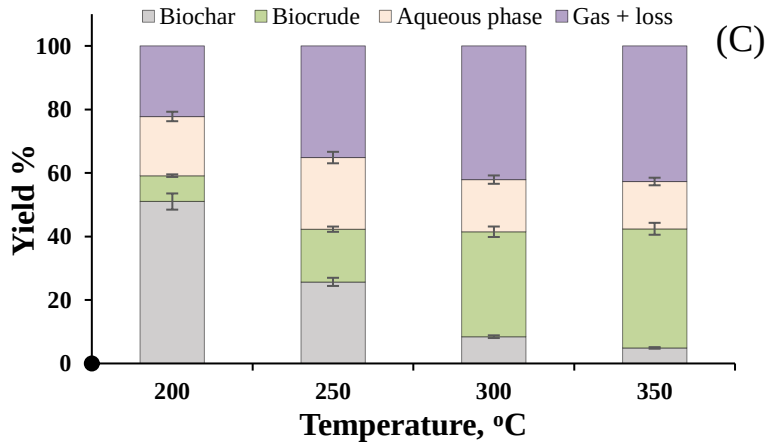

Figure 2.3: Effect of reaction temperature on the product distribution at 10 % solid loading and 30 min residence time: Kirchneriella sp. (A), Micractinium sp.(B), Galdieria sp. (C)

2.3.2.2 Effect of solid loading on the product fractions

Water in the HTL plays multiple roles as a reactant, solvent, and a catalyst. During liquefaction, water has interesting properties such as lower viscosity, lower dielectric

constant and increased ionic product which gives rise to efficient medium, increased the solubility of non-polar compounds and accelerated biomass hydrolysis, respectively (Wang et al., 2019). The solid loading ratio on the yields of product fractions was examined at 300 °C, 30 min, 90 MPa and 10-20 % solid loading for *Kirchneriella sp*. Figure 2.4 shows the experimental results and has been observed that 45.5 % of the product fraction yield was obtained as biocrude oil at 10 % solid loading and it decreased to 41.0 % at 20 % solid loading inferring to more conversion at 10 % solid loading. This could also be inferred that more amount of energy was available per unit mass of biomass in the less solid loading condition relative to a higher solid loading scenario. Therefore, 10 % solid loading was chosen for further experiments.

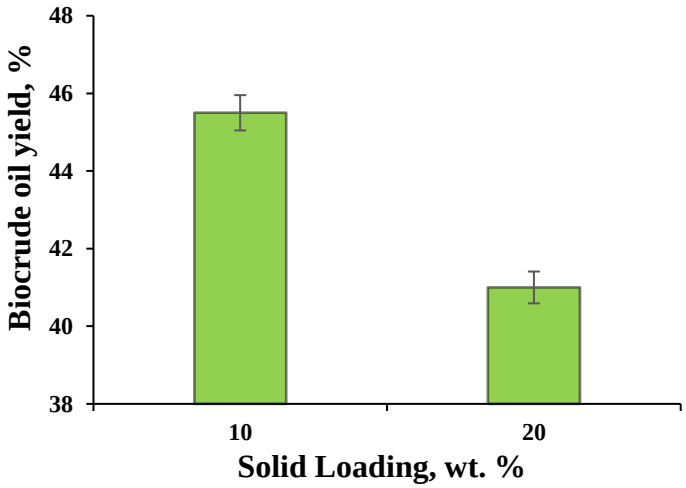

Figure 2.4: HTL biocrude yield distribution of *Kirchneriella sp.* with solid loading at 300 ˚C, 30 min, and 9 MPa initial pressure

2.3.2.3 Effect of process pressure on the product fractions

The influence of pressure on the yields of *Kirchneriella sp*. liquefaction product fractions was investigated in this section. In the current study, the input pressure during the reaction was varied from 9 MPa to 25 MPa. Figure 2.5 shows the experimental results. Compared to the effect of temperature, the increase in pressure slightly decreased the biocrude oil yield. The highest biocrude oil yield (45.5 %) was recorded at 9 MPa, while the lowest yield (43.3 %) was recorded at 25 MPa of initial pressure. This might be due to the higher initial pressures favoring the conversion of biomass into the gaseous fraction. Since lower pressures have favored the formation of higher biocrude oil yields, all the further experiments were performed at conditions supporting liquefaction conditions during the reaction (i.e., 9 MPa). A similar trend was also observed in previous studies where initial pressure over saturation pressure of water had a very small effect on the production of biocrude oil and other HTL product fractions (Chen et al., 2014).

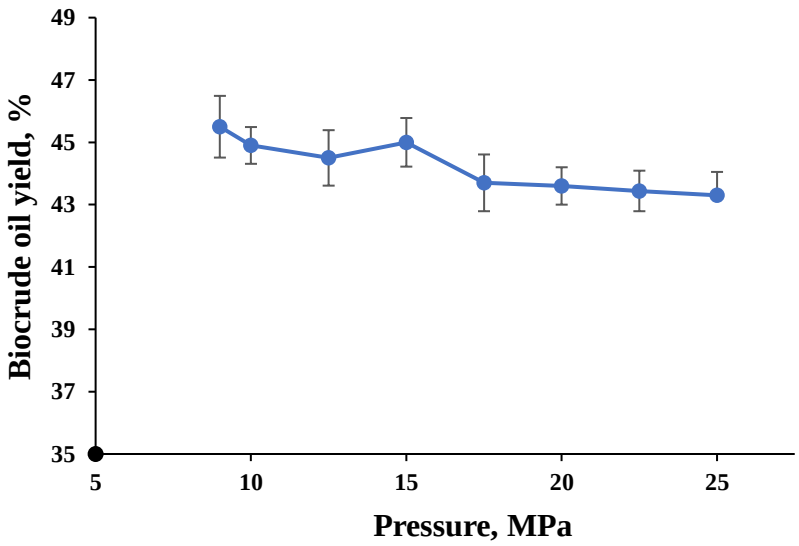

Figure 2.5: HTL biocrude yield distribution of *Kirchneriella sp.* with pressure at 300 ˚C, 30 min, and 10% solid loading

2.3.2.4 Effect of process time on the product fractions

The overall conversion of biomass into products was studied by the influence of duration of residence time. Therefore, the effect of residence time on the yields of product fractions was studied at 300 °C, 9 MPa and 10 % solid loading for 15 to 60 minutes with an interval of 15 minutes. Figure 2.6 shows the experimental results of the change in biocrude oil with respect to the residence time of the HTL reaction. The biocrude oil yields were observed to be increasing with the residence time change from 15 mins to 30 min. The biocrude oil yields increased from 41.63 % to 45.50 %, suggesting more residence time for further degradation of the biomass into the product phase. Therefore, further experiments are performed with 45, 60 min residence time and observed that the biocrude

oil yield has decreased (38.9 %, 38.5 % respectively) owing to subsequent condensation and/or polymerization of energy-dense oil molecules to interact with intermediates resulting in the formation of heavy tar-like substances which ended up in biochar (Jazrawi et al., 2013). The highest biocrude oil yield was obtained at 300 °C, 90 MPa and 10 % solid loading and 30 min residence time.

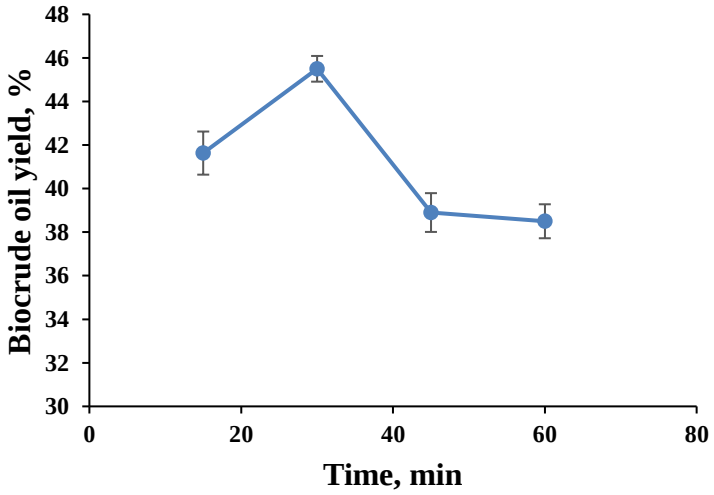

Figure 2.6: HTL biocrude yield distribution of *Kirchneriella sp.* with time at 300 ˚C, 10 % solid loading, and 9 MPa initial pressure

2.3.3 Analysis of liquefaction products

2.3.3.1 Ultimate analysis and energy recovery calculations

Table 2.5 shows the results of elemental analysis and energy values of *Kirchneriella sp*. feedstock and resulting HTL biocrude oil and biochar at 300 °C, 9 MPa, 10 % solid loading and 30 min residence time. It was evident that the elemental composition of carbon

and hydrogen were increased in the products when compared to the raw biomass, suggesting energy densification process. The increase of the carbon and hydrogen content in the products also strengthens the statement of the presence of more energy dense compounds. The presence of oxygen-rich compounds arises during the hydrolysis of carbohydrates and oxygen rich heterocyclic compounds. The decreased oxygen content of biocrude product phase was achieved during the process. The results also showed the nitrogen content in the products inferring to the degradation/ presence of protein fragments originating from the biomass. The presence of hetero-atoms of nitrogen and oxygen can lead to corrosion, fuel instability and storage issues which can be addressed via suitable upgrading techniques (Sudasinghe et al., 2014). The high levels of sulfur and nitrogen lead to the formation of NO_x and SO_x, during the combustion of biofuels. The presence of sulfur compounds can also lead to engine knocking and poisoning the catalyst. The increase in the oxygen content of the biochar suggests that most of the oxygenated compounds ended in the biochar phase. The presence of high oxygen numbers has decreased the calorific value of the product phase. The higher heating values of raw biomass, HTL products biocrude oil and biochar were determined by a bomb calorimeter, and the energy recovery calculations suggest that 95 % of the energy in algae was recovered.

Similar trends have been observed in the case of *Micractinium* and *Galdieria sp*. with the biocrude oil produced at 350 ˚C, 10 % solid loading as summarized in table 2.6. As compared to both raw feedstocks, the carbon and hydrogen numbers have increased signifying the energy densification process. It can be explained by the idea of increased

free fatty acid or hydrocarbons separated into the biocrude phase. The increased nitrogen content can be explained by the presence of non-polar nitrogen compounds soluble in the solvent and ended up in biocrude phase. The oxygen content in both the species' biocrude decreased after the liquefaction experiments. This also explains the fact of increased HHV values in both cases.

Table 2.5: Elemental composition of *Kirchneriella sp*. biomass, bio-oils, and biochar obtained at 300 ˚C, 30 mins, 9 MPa and 10 % solid loading

	Algae	Bio-oil	Biochar
C, %	51.54	76.63	66.01
H, %	5.96	8.95	3.91
N, %	5.88	5.22	4.18
S, %	1.11	1.25	0.65
O[a], %	35.5	7.94	25.24
HHV, $MJ.kg^{-1}$	19.73	37.52	23.48
Energy Recovery (ER), %	94.90		

[a], determined by difference; HHV: Higher Heating Value, $MJ.kg^{-1}$

Table 2.6: Elemental composition of *Micractinium* & *Galdieria sp.* biocrude oils obtained at 350 ˚C, 30 mins, 9 MPa, and 10 % solid loading

	Micractinium sp. Biocrude	*Galdieria sp.* Biocrude
C, %	74.27	75.17
H, %	7.56	8.48
N, %	6.77	7.99
S, %	0.92	2.36
O[a], %	10.47	6.06
HHV, $MJ.kg^{-1}$	34.23	36.80

2.3.3.2 Analysis of HTL aqueous phase

Several studies have suggested the presence of valuable co-products such as carbohydrates, ammoniacal nitrogen, phosphates, the organic carbon in the HTL water phase (Biller et al., 2012; Jena et al., 2011). Table 2.7 **s**hows the analysis results of the HTL water-phase obtained at 300 °C, 90 MPa, 10 % solid loading, and for 30 min. The presence of these compounds might be due to the polar compounds arising during degradation of bio-macromolecules from protein, lipid, and carbohydrates. Selvaratnam et al.,(Selvaratnam et al., 2015b) have shown that these compounds can be recycled back to

the algae ponds under various conditions addressing co-product development. A similar trend has been observed for *Galdieria sp.* where ammoniacal nitrogen was responsible for half of the total nitrogen available (Selvaratnam et al., 2015a).

Table 2.7: Analysis of HTL water phase obtained at 300 ˚C, 30 mins, 9 MPa, and 10 % solid loading

Analyzed component, mg. L^{-1}	*Kirchneriella sp.*	*Galdieria sp.*	*Micractinium sp.*
Ammoniacal Nitrogen, N-NH_3	3033	5797	1933
Total Nitrogen, TN	11130	11000	8867
Phosphates, P-PO_4^{-3}	8652	2196	2934
Carbohydrates	1200	-	-
Total organic carbon, TOC	20666	29000	19500

2.3.3.3 Heavy metal analysis of HTL biocrude by ICP-OES

The analysis results of the metal content in the biocrude oil are tabulated in table 2.8. The results report that the aluminum (Al), copper (Cu), iron (Fe), potassium (K), zinc (Zn),

phosphorous (P) are the detected elements among all the biocrudes. The metals mentioned above were also detected in all the three respective biomasses in different concentrations in table 2.. The metals calcium, magnesium, sodium, and nickel were detected in the dry biomass but were not detected in their respective biocrude oil fraction. Among all the metals detected, potassium is the highest concentrated metal in all the three biocrudes. The metal concentrations of the biocrude look relatively less when compared to the other product fractions. Most of the metals were concentrated into the biochar fraction where phosphorous, magnesium, calcium, and potassium were the leading contributors of metals which is similar to the work published in Anastasakis K. et al., (Anastasakis and Ross, 2011). Phosphorus was the highest concentrated metal detected in the biochar for both *Kirchneriella sp*. and *Galdieria sp*. Iron, manganese, aluminum, and copper were also detected in considerable amounts in the biochar product fraction. These metals can lead to reactor or storage vessel fouling issues, corrosion of equipment, poisoning the catalysts, reducing the heat transfer (Duan and Savage, 2011). Thus, the removal of these metals before upgrading or further processing is crucial before introducing into a refinery (Jarvis et al., 2016).

Table 2.8: Analysis of HTL biocrude, biochar obtained at 300 ˚C, 30 mins, 9 MPa

mg/kg	*Kirchneriella sp.*		*Micractinium sp.*		*Galdieria sp.*	
	Biocrude	Biochar	Biocrude	Biochar	Biocrude	Biochar
Al	32.1	3377.8	17.6	103.8	39.4	745.07

Ca	nd	4906	nd	4832.5	nd	2601.57
Cu	20.37	62.98	nd	21.3	7.15	78.71
Fe	37.22	3831.17	45.6	1310.6	24.49	1055.1
K	373.95	4491.6	356.5	488.3	429.49	869.2
Mg	nd	15277.6	nd	1031.2	nd	4324.2
Mn	1.19	399.1	nd	77.8	1.2	124.4
Na	nd	450.69	nd	nd	nd	nd
Ni	nd	nd	nd	nd	nd	nd
Zn	58.33	343.13	65.1	nd	31.21	152.76
P	34.41	20926	28.8	3065.4	19.02	6607.52

nd: not detected

2.3.4 Catalytic upgrading of biocrude oil using heterogeneous catalysts

This section discusses the results from the upgrading experiments using heterogeneous catalysts. Hypothesis #3 from chapter 1 is tested here.

2.3.4.1 Effect of catalyst and temperature on upgrading yields

The effect of a catalyst on the yields of upgraded biocrude oil while upgrading at 350 and 400 °C is shown in Figure 2.7. The base case is considered here with no catalyst usage and the same pressure of hydrogen used with catalysts. The base case has upgraded

biocrude yield of 70.18 wt.% and 64.15 wt.%, at 350 and 400 °C, respectively. Among all the three different cases with catalysts, HZSM-5 has a higher yield (75.25 wt.%) followed by Pt/C (73.7 wt.%) and MO_2C (67.5 wt.%) at 350 °C. The lower temperature has favored the formation of more upgraded biocrude oil yield compared to the 400 °C. The decrease in the upgraded biocrude oil at higher temperature could be due to coke formation when higher molecular fractions repolymerize and catalyzed reactions towards more gas formation. Among higher temperature (400 °C), the upgraded biocrude yield followed a different trend where Pt/C has a higher yield (71.45 wt.%) followed by HZSM-5 (68 wt.%), and MO_2C (65 wt.%).

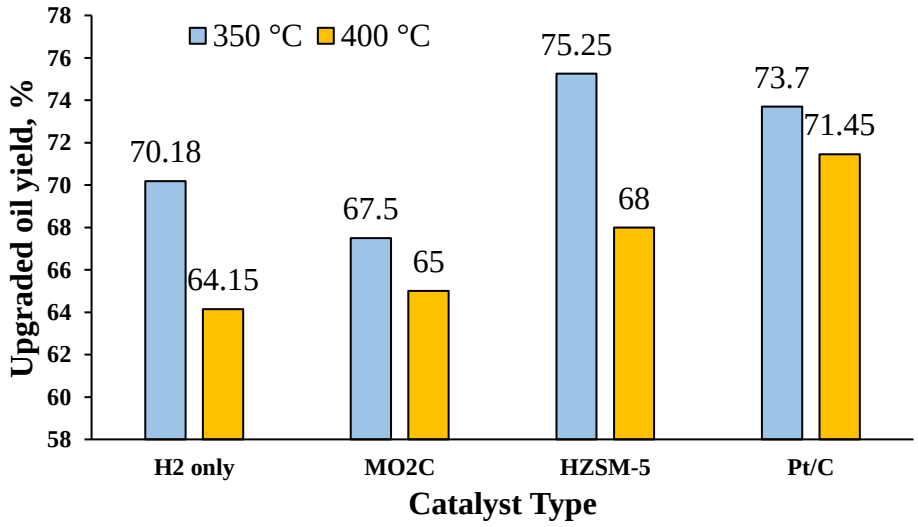

Figure 2.7: Upgraded oil yields of algae biocrude at 350 and 400 °C

Table 2.9: Elemental composition of biocrude oil vs. upgraded biocrude oil of *micractinium sp.* produced at 350 °C

	***Micractinium* Biocrude**	**H_2 only**	**MO_2C**	**HZSM-5**	**Pt/C**	**Petroleum**
C, %	74.27	75.89	81.14	89.85	83.71	83-87
H, %	7.56	10.44	10.72	6.56	10.84	10-14
N, %	6.77	4.80	2.59	2.56	2.59	0.1-2
S, %	0.92	0.48	n.d.	n.d.	n.d.	0.05-6
O, % (by difference)	10.47	8.07	5.31	1.03	2.86	0.05-1.5
TAN (mg KOH/g)	25.67	21.89	19.59	19.12	16.17	-
HHV, MJ/kg	34.26	39.16	41.90	39.55	43.26	45.0-46.4

2.3.4.2 Effect of catalyst on the elemental composition of the upgraded oil

Table 2.9 shows the properties of the upgraded biocrude produced at a temperature of 350 °C. All the reactor walls were properly washed and stirred with dichloromethane to ensure all the oil combination is collected. It is seen that the TAN value of the original

biocrude was decreased in all the cases of the upgrading experiments. The lowest TAN value was observed when Pt/C catalyst (16.17 mg KOH/g) was used as the metal catalyst is known to catalyze or promote decarboxylation and decarbonylation reaction resulting in organic acids converting into alkanes followed by HZSM-5 and MO_2C. The observed decrease might be due to the removal of highly acidic compounds such as phenols and fatty acids present in the bio-oil. The HHV of all the upgraded biocrude oils also increased considerably suggesting cleaner and energy dense fuel. The biocrude oil produced with Pt/C has the highest HHV value almost like that of the petroleum products (diesel: 44.8 MJ/kg). Hydrogen alone experiment also has significant improvement in the case of HHV.

While the nitrogen values decreased in the catalysts of choice in all the upgraded oils, they almost remained same. This suggests that they were not effective in denitrogenation. The nitrogen-containing compounds can cause issues such as catalyst inhibition, acid-base pair-related electron corrosion, storage stability, thermal stability, gum formation, and metal complexation. The denitrogenation can be favored at a higher temperature but that needs to be compensated by the reduction in upgraded oil yield and formation of coke. This suggests that specific denitrogenation selective catalysts needs to be selected that can remove nitrogen from biocrude oils at mild operating conditions.

A different application of these heteroatom rich biocrude oils include blending with recycled asphalt to improve intercalation into oxidized asphaltenes nanoaggregates. These sustainable bio-rejuvenator was produced from blending high-protein algae and high-lipid animal manure. The interaction of these rejuvenators with aged bitumen molecules to

revitalize aged asphalt not only restored chemical balance but also confirmed molecular composition. The blending of the rejuvenators assisted the heteroatoms in the biocrude oil to restore its physicochemical and rheological properties. The comprehensive rejuvenation increased both crossover modulus and crossover frequency and favored in de-agglomeration of self-assembled oxidized asphaltenes. The bio-rejuvenator molecules have peptizing effect on oxidized asphaltene molecules and reduced the intensity of radial distribution function of asphaltenes in heptane (Samieadel et al., 2020).

2.4 Conclusions

Hydrothermal liquefaction has been proven to be one of the attractive technologies on the standpoint of energy utilization and process integration to convert high-moisture algal biomass to liquid phase, renewable bio-oils. HTL product yields depend on the processing conditions such as reaction temperature, residence time and solid loading. The effect of pressure does not seem to have a significant influence on the biocrude oil yield. Three different microalgae (*Kirchneriella sp.*, *Micractinium sp.*, *Galdieria sp.*) were hydrothermally liquefied, and the influence of process parameters on the yield of product fractions was investigated. The process parameters were optimized based on the biocrude oil yield. The maximum biocrude oil yield of 45.5% was obtained at 300 °C, 9 MPa, 10% solid loading, and for a residence time of 30 min. *Micractinium sp*. and *Galdieria sp.* have reported maximum biocrude oil yield (27.95 wt.% and 37.51 wt.%, respectively) at 350 °C. HTL conditions also reduced the oxygen content and led to the formation of energy-dense biocrude oil. The increase in temperature above 300 °C have led to super

critical gasification and decreased the biocrude oil yield. The HHV of the HTL products biocrude and biochar were estimated to be 37.52 and 23.48 MJ kg^{-1} at the highest biocrude yield conditions. The energy recovery of products at highest biocrude yield conditions were calculated to be 94.90%. As hypothesized, HTL of algae produce nutrient-rich and energy dense products. A considerable concentration of nutrients such as organic carbon, ammoniacal nitrogen, phosphates and dissolved carbohydrate were found in the HTL aqueous phase. Metals such as phosphorous, sodium, magnesium, and potassium were detected in both biomass and HTL products. The results suggest that all three catalysts employed were effective in decreasing the heteroatom content in the upgraded biocrude oil. Based on the conclusions from the previous upgrading experiments it is concluded that one specific catalyst material was effective in deoxygenation and the others were effective in decreasing the TAN values.

2.5 References

Anastasakis, K., Ross, A.B., 2011. Hydrothermal liquefaction of the brown macro-alga Laminaria Saccharina: Effect of reaction conditions on product distribution and composition. Bioresour. Technol. 102, 4876–4883.

Biller, P., Ross, A.B., Skill, S.C., Lea-Langton, A., Balasundaram, B., Hall, C., Riley, R., Llewellyn, C.A., 2012. Nutrient recycling of aqueous phase for microalgae cultivation from the hydrothermal liquefaction process. Algal Res. 1, 70–76.

Borowitzka, M.A., 2013. High-value products from microalgae—their development and commercialisation. J. Appl. Phycol. 25, 743–756.

Browne, F.X., 1990. Stormwater management, Standard Handbook of Environmental Engineering, RA Corbitt.

Chakraborty, M., Miao, C., McDonald, A., Chen, S., 2012. Concomitant extraction of bio-oil and value added polysaccharides from Chlorella sorokiniana using a unique sequential hydrothermal extraction technology. Fuel 95, 63–70.

Chemists, A. of O.A., Horwitz, W., 1975. Official methods of analysis. Association of Official Analytical Chemists Washington, DC.

Chen, W.-T., Zhang, Y., Zhang, J., Yu, G., Schideman, L.C., Zhang, P., Minarick, M., 2014. Hydrothermal liquefaction of mixed-culture algal biomass from wastewater treatment system into bio-crude oil. Bioresour. Technol. 152, 130–139.

Dandamudi, K.P.R., Muppaneni, T., Markovski, J.S., Lammers, P., Deng, S., 2019. Hydrothermal liquefaction of green microalga Kirchneriella sp. under sub- and super-critical water conditions. Biomass and Bioenergy 120. https://doi.org/10.1016/j.biombioe.2018.11.021

Doucha, J., Lívanský, K., 2012. Production of high-density Chlorella culture grown in fermenters. J. Appl. Phycol. 24, 35–43.

Duan, P., Savage, P.E., 2011. Upgrading of crude algal bio-oil in supercritical water. Bioresour. Technol. 102, 1899–1906.

Eboibi, B.E.-O., Lewis, D.M., Ashman, P.J., Chinnasamy, S., 2014. Hydrothermal liquefaction of microalgae for biocrude production: Improving the biocrude properties with vacuum distillation. Bioresour. Technol. 174, 212–221.

Eustance, E.O., 2011. Biofuel potential, nitrogen utilization, and growth rates of two green algae isolated from a wastewater treatment facility.

Gai, C., Liu, Z., Han, G., Peng, N., Fan, A., 2015a. Combustion behavior and kinetics of low-lipid microalgae via thermogravimetric analysis. Bioresour. Technol. 181, 148–154.

Gai, C., Zhang, Y., Chen, W.-T., Zhang, P., Dong, Y., 2015b. An investigation of reaction pathways of hydrothermal liquefaction using Chlorella pyrenoidosa and Spirulina platensis. Energy Convers. Manag. 96, 330–339.

Huang, C., Zeng, G., Huang, D., Lai, C., Xu, P., Zhang, C., Cheng, M., Wan, J., Hu, L.,

Zhang, Y., 2017. Effect of Phanerochaete chrysosporium inoculation on bacterial community and metal stabilization in lead-contaminated agricultural waste composting. Bioresour. Technol. 243, 294–303.

Jarvis, J.M., Sudasinghe, N.M., Albrecht, K.O., Schmidt, A.J., Hallen, R.T., Anderson, D.B., Billing, J.M., Schaub, T.M., 2016. Impact of iron porphyrin complexes when hydroprocessing algal HTL biocrude. Fuel 182, 411–418.

Jazrawi, C., Biller, P., Ross, A.B., Montoya, A., Maschmeyer, T., Haynes, B.S., 2013. Pilot plant testing of continuous hydrothermal liquefaction of microalgae. Algal Res. 2, 268–277.

Jena, U., Vaidyanathan, N., Chinnasamy, S., Das, K.C., 2011. Evaluation of microalgae cultivation using recovered aqueous co-product from thermochemical liquefaction of algal biomass. Bioresour. Technol. 102, 3380–3387.

Jin, M., Oh, Y.-K., Chang, Y.K., Choi, M., 2017. Optimum utilization of biochemical components in Chlorella sp. KR1 via subcritical hydrothermal liquefaction. ACS Sustain. Chem. Eng. 5, 7240–7248.

Laurens, L.M.L., 2016. Summative Mass Analysis of Algal Biomass-Integration of Analytical Procedures: Laboratory Analytical Procedure (LAP). National Renewable Energy Lab.(NREL), Golden, CO (United States).

Lombardi, A.T., Vieira, A.A.H., Sartori, L.A., 2002. Mucilaginous capsule adsorption and intracellular uptake of copper by Kirchneriella aperta (Chlorococcales). J.

Phycol. 38, 332–337.

Lourenço, S.O., Barbarino, E., Lavín, P.L., Lanfer Marquez, U.M., Aidar, E., 2004. Distribution of intracellular nitrogen in marine microalgae: calculation of new nitrogen-to-protein conversion factors. Eur. J. Phycol. 39, 17–32.

Lourenço, S.O., Barbarino, E., Marquez, U.M.L., Aidar, E., 1998. Distribution of intracellular nitrogen in marine microalgae: basis for the calculation of specific nitrogen-to-protein conversion factors. J. Phycol. 34, 798–811.

Mendes, A., Reis, A., Vasconcelos, R., Guerra, P., da Silva, T.L., 2009. Crypthecodinium cohnii with emphasis on DHA production: a review. J. Appl. Phycol. 21, 199–214.

Milledge, J.J., 2012. Microalgae-commercial potential for fuel, food and feed. Food Sci. Technol. 26, 28–30.

Moore, J.C., DeVries, J.W., Lipp, M., Griffiths, J.C., Abernethy, D.R., 2010. Total protein methods and their potential utility to reduce the risk of food protein adulteration. Compr. Rev. Food Sci. Food Saf. 9, 330–357.

Muppaneni, T., Reddy, H.K., Selvaratnam, T., Dandamudi, K.P.R., Dungan, B., Nirmalakhandan, N., Schaub, T., Omar Holguin, F., Voorhies, W., Lammers, P., Deng, S., 2017. Hydrothermal liquefaction of Cyanidioschyzon merolae and the influence of catalysts on products. Bioresour. Technol. 223. https://doi.org/10.1016/j.biortech.2016.10.022

Pachauri, R.K., Allen, M.R., Barros, V.R., Broome, J., Cramer, W., Christ, R., Church,

J.A., Clarke, L., Dahe, Q., Dasgupta, P., 2014. Climate change 2014: synthesis report. Contribution of Working Groups I, II and III to the fifth assessment report of the Intergovernmental Panel on Climate Change. Ipcc.

Patil, P.D., Dandamudi, K.P.R., Wang, J., Deng, Q., Deng, S., 2018. Extraction of bio-oils from algae with supercritical carbon dioxide and co-solvents. J. Supercrit. Fluids 135, 60–68. https://doi.org/https://doi.org/10.1016/j.supflu.2017.12.019

Saeed, A., Iqbal, M., Sahibzada, K.I., Parvez, S., 2012. Evaluation of the biosequestering potential of microalga kirchneriella contorta in the removal of hexavalent chromium from aqueous solution: Batch and continuous flow fixed-bed column bioreactor studies. Pak J Bot 44, 989–998.

Schenk, P.M., Thomas-Hall, S.R., Stephens, E., Marx, U.C., Mussgnug, J.H., Posten, C., Kruse, O., Hankamer, B., 2008. Second generation biofuels: high-efficiency microalgae for biodiesel production. Bioenergy Res. 1, 20–43.

Selvaratnam, T., Pegallapati, A.K., Montelya, F., Rodriguez, G., Nirmalakhandan, N., Van Voorhies, W., Lammers, P.J., 2014. Evaluation of a thermo-tolerant acidophilic alga, Galdieria sulphuraria, for nutrient removal from urban wastewaters. Bioresour. Technol. 156, 395–399.

Selvaratnam, T., Pegallapati, A.K., Reddy, H., Kanapathipillai, N., Nirmalakhandan, N., Deng, S., Lammers, P.J., 2015a. Algal biofuels from urban wastewaters: Maximizing biomass yield using nutrients recycled from hydrothermal processing of

biomass. Bioresour. Technol. 182, 232–238.

Selvaratnam, T., Reddy, H., Muppaneni, T., Holguin, F.O., Nirmalakhandan, N., Lammers, P.J., Deng, S., 2015b. Optimizing energy yields from nutrient recycling using sequential hydrothermal liquefaction with Galdieria sulphuraria. Algal Res. 12, 74–79.

Song, M., Pei, H., Hu, W., Ma, G., 2013. Evaluation of the potential of 10 microalgal strains for biodiesel production. Bioresour. Technol. 141, 245–251.

Sudasinghe, N., Dungan, B., Lammers, P., Albrecht, K., Elliott, D., Hallen, R., Schaub, T., 2014. High resolution FT-ICR mass spectral analysis of bio-oil and residual water soluble organics produced by hydrothermal liquefaction of the marine microalga Nannochloropsis salina. Fuel 119, 47–56.

Toor, S.S., Reddy, H., Deng, S., Hoffmann, J., Spangsmark, D., Madsen, L.B., Holm-Nielsen, J.B., Rosendahl, L.A., 2013. Hydrothermal liquefaction of Spirulina and Nannochloropsis salina under subcritical and supercritical water conditions. Bioresour. Technol. 131, 413–419.

Toor, S.S., Rosendahl, L., Rudolf, A., 2011. Hydrothermal liquefaction of biomass: a review of subcritical water technologies. Energy 36, 2328–2342.

Toplin, J.A., Norris, T.B., Lehr, C.R., McDermott, T.R., Castenholz, R.W., 2008. Biogeographic and phylogenetic diversity of thermoacidophilic cyanidiales in Yellowstone National Park, Japan, and New Zealand. Appl. Environ. Microbiol. 74,

2822–2833.

Valdez, P.J., Nelson, M.C., Wang, H.Y., Lin, X.N., Savage, P.E., 2012. Hydrothermal liquefaction of Nannochloropsis sp.: Systematic study of process variables and analysis of the product fractions. Biomass and Bioenergy 46, 317–331.

Van Wychen, S., Laurens, L.M.L., 2016. Determination of total carbohydrates in algal biomass: laboratory analytical procedure (LAP). National Renewable Energy Lab.(NREL), Golden, CO (United States).

Van Wychen, S., Ramirez, K., Laurens, L.M.L., 2016. Determination of total lipids as fatty acid methyl esters (FAME) by in situ transesterification: laboratory analytical procedure (LAP). National Renewable Energy Lab.(NREL), Golden, CO (United States).

Wang, J., Krishna, R., Yang, J., Dandamudi, K.P.R., Deng, S., 2015. Nitrogen-doped porous carbons for highly selective CO<inf>2</inf> capture from flue gases and natural gas upgrading. Mater. Today Commun. 4. https://doi.org/10.1016/j.mtcomm.2015.06.009

Wang, J., Peng, X., Chen, X., Ma, X., 2019. Co-liquefaction of low-lipid microalgae and starch-rich biomass waste: The interaction effect on product distribution and composition. J. Anal. Appl. Pyrolysis 139, 250–257.

Wang, Z., Adhikari, S., Valdez, P., Shakya, R., 2015. Upgrading of hydrothermal liquefaction biocrude from algae grown in municipal wastewater, in: 2015 ASABE

Annual International Meeting. American Society of Agricultural and Biological Engineers, p. 1.

Yang, W., Li, X., Li, Z., Tong, C., Feng, L., 2015. Understanding low-lipid algae hydrothermal liquefaction characteristics and pathways through hydrothermal liquefaction of algal major components: Crude polysaccharides, crude proteins and their binary mixtures. Bioresour. Technol. 196, 99–108.

CHAPTER 3: HYDROTHERMAL LIQUEFACTION OF CYANIDIOSCHYZON MEROLAE WITH SALICORNIA BIGELOVII TORR. AND SWINE MANURE: THE SYNERGISTIC EFFECT ON PRODUCT DISTRIBUTION AND CHEMISTRY

3.1 Introduction

Systems for bioenergy carbon capture and storage (BECCS) are designed with the dual purpose of generating renewable energy in the context of net-negative-emissions of greenhouse gases (Azar et al., 2010; Bui et al., 2018). BECCS systems typically utilize biomass in combined heat and power (CHP) generation followed by recapturing some of the CO_2 using amine-based separations as a prelude to sequestration. A variant on this design called ABECCS displaces soybean fields with a eucalyptus plantation. A portion of the CO_2 derived eucalyptus CHP operations is then captured via algae cultivation on saltwater yielding algae biomass for fishmeal and soybean replacements (Beal et al., 2018).

Given global limitations for freshwater and arable land, we reasoned that replacement of eucalyptus by a saltwater tolerant, oilseed crop like *Salicornia* would expand the potential for ABECCS deployment to undeveloped, arid coastal regions in the Middle East, Africa, Australia and western South America (Glenn et al., 1999; Ventura and Sagi, 2013). *Salicornia bigelovii* Torr. (SL, hereafter) is a forage, terrestrial oilseed halophyte with leafless, green succulent stems that grows in subtropical coastal deserts. It is an annual salt marsh plant that forms terminal fruiting spikes in which seeds are formed.

The biomass yields ranged from 13.6-23.1 t DM ha^{-1} with seed yields ranging from 177-246 g. m^{-2}, of which 28.2 wt. % corresponds to oil weight in the seed. *Salicornia sp*. has a requisite salt tolerance and grows well in a root salinity of 70-75 $g.L^{-1}$, which accounts for high salt content in the biomass (Glenn et al., 1997, 1991). For this study, we assumed that *Salicornia* oilseed could yield triacylglyceride feedstock for biodiesel and a protein-rich meal for soybean and fishmeal replacements. The standard ABECCS option for use of the *Salicornia* stems would be to dry and process via CHP to yield power and CO_2. Here we evaluate an alternative use of *Salicornia* stems as a co-liquefaction feedstock to produce biofuels by hydrothermal liquefaction.

Hydrothermal liquefaction (HTL) has proven to be an efficient conversion technology for converting high moisture content feedstock to biofuel intermediates. HTL has the added advantage of reducing the process energy consumption due to the omitting of the drying step and using water in the biomass as a potent reaction medium at elevated temperatures (180-375 °C) and pressures (4-30 MPa) (Dimitriadis and Bezergianni, 2017). The increased non-polarity of water at elevated temperature and pressure helps the decomposition of biomacromolecules (lipids, carbohydrates, and proteins) in biomass into smaller fragments by various reaction mechanisms (hydrolysis, decarboxylation, denitrogenation, deoxygenation) (Muppaneni et al., 2017) to produce biocrude oil, biochar, water-soluble compounds, and gaseous fraction. The resultant major fuel products (biochar, biocrude) have an energy content higher than that of the original biomass, suggesting HTL to be energy densification process (Dimitriadis and Bezergianni, 2017;

Reddy et al., 2016; Savage and Hestekin, 2013). HTL has an added advantage over other biomass to fuel conversion techniques such as microwave-assisted extraction and enzymatic hydrolysis. In both the cases of microwave irradiation and enzymatic hydrolysis to extract the bio-lipids, energy is invested to lyse the cell membrane and only a fraction of the biochemical constituents (lipids yield, usually) is given a priority. The lipid extracted algae still contains valuable carbohydrates and proteins to be further processed. On the contrary, HTL is a thermochemical technique which converts majority of the biochemical constituents into fuel precursors (Dandamudi et al., 2019; Muppaneni et al., 2017; Reddy et al., 2016). The enzymatic hydrolysis for bio-lipid production has advantages such as lower energy consumption and converting low quality feedstock, however, the main impediments to industrial scaling include high enzyme cost and conversion efficiency (Pourzolfaghar et al., 2016). The microwave assisted bio-lipid production has advantages which include lower energy consumption, substantial reduction in residence times and solvent requirements, enhanced selectivity to minimize the by-product formation. The challenges in microwave assisted technology include its inability to penetrate through large sample volumes and controlled heating (Gude et al., 2013). The conventional sub-critical water extraction was able to extract around 70 % of the lipids from the wet algal biomass (Reddy et al., 2014), while microwave irradiation recovered 38.31 % from *Nannochloropsis* sp. (Wahidin et al., 2014) and enzyme hydrolysis achieved 85.3 % from *Chlorella vulgaris* after 72 h (Cho et al., 2013).

The biochemical characteristics of the biomass play a crucial role in the HTL product yield and composition. Microalgae have attracted interest due to their ability to grow on non-arable land and non-potable water (Henkanatte-Gedera et al., 2017) and high biocrude yields via HTL and HHVs close to that of petroleum crude (42.0 MJ/kg) (Dandamudi et al., 2019). Microalgae also have been studied for the commercial and sustainable production of valuable byproducts like eicosapentaenoic acid (EPA), docosahexaenoic acid (DHA), omega-3 fatty acids, β-carotenes, fatty acids, and polysaccharides (Dandamudi et al., 2019). Extensive research has been conducted on the HTL of microalgae with a varied biochemical composition of high to low lipids, high to low proteins, and it has concluded that the lipids, proteins and carbohydrates play an essential role in the formation of biocrude oil (Biller et al., 2012; Ross et al., 2010; Zhang et al., 2019). Despite microalgae having higher biomass productivity and rate of growth, the low level of cultivation of microalgae and the sensitivity of cultures to environmental factors like temperature, sunlight, and pH make the consistent supply of biomass to biofuel industry a challenge. Therefore, it is extremely important to find biomass alternatives that do not compete with food production as potential sources for co-processing along with microalgae during a shortage.

Co-liquefaction of different biomass would be a promising technique to produce large-scale, continuous production of biocrude oil. Jin et al. (Jin et al., 2013) observed a positive synergistic effect during co-liquefaction of freshwater microalgae, *Spirulina platensis*, and saltwater macroalgae, *Entermorpha prolifera*, leading to increase in

biocrude oil yield, energy recovery, and promoted the in-situ deoxygenation of the biocrude oil. Other studies included co-liquefying two different microalgae (Dandamudi et al., 2017), microalgae with lignocellulosic biomass (Zhang et al., 2019), low-lipid microalgae with starch-rich wastes (Wang et al., 2019), and swine manure with mixed-culture algal biomass (Chen et al., 2014). To strengthen the issue of abundant biomass availability to the biofuel industry, we investigated the co-liquefaction and energy recovery efficiency of SL and CM biomass in this work. Also, to the best of our knowledge, no prior research has been performed to hydrothermally liquefy SL biomass and to study the effect of interaction between the two-biomass feedstock via HTL.

It was hypothesized that there might be a synergistic effect in the product phase during the co-liquefaction of the two biomasses. The objectives were to test the influence of HTL parameters of temperature, solid loading, and biomass mixture ratios. The products were analyzed by elemental analyzer, ICP-OES, GC-MS, and TGA. The research findings from this chapter supports the statement of production of renewable fuels from biomass and connects to the sustainability and improving value chain.

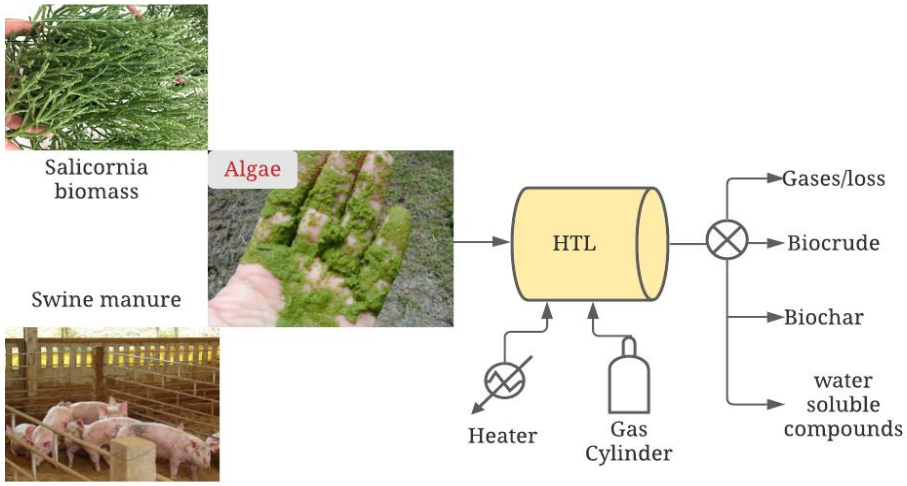

Figure 3.1: Schematic of the experimental plan

3.2 Materials and methods

This section discusses the experimental protocol followed in this chapter. Figure 3.1 discusses the schematic of the experimental plan. The three different biomasses were subjected to HTL and the products were separated. Mass balance calculations were made with the individual and co-liquefied samples. The biomass and products were analyzed by various techniques to characterize the chemistry of the compounds.

3.2.1 Materials

HTL was performed on three different biomasses, *Cyanidioschyzon merolae* (*C. merolae* MS1-YNP) (CM, hereafter) (Dandamudi et al., 2017), a thermo acidophilic red alga was grown outdoors (natural/sunlight) and *Salicornia bigelovii* Torr. (SL, hereafter) understudy at Arizona Center for Algae Technology (AzCATI), Arizona State University.

Swine manure (SM, hereafter) was acquired from a pig farm in Mount Olive, North Carolina. SL biomass was grown in greenhouses simulating high saline water conditions replicating ocean currents. The temperature in the greenhouses ranged from 25-18.5 °C for 24 hours cycle. The plants were watered twice a day, with salinity increasing weekly to 35000 ppm salt using Instant Ocean salt in conjunction with a custom hydroponic fertilizer. The soil media was 2:1 parts of sand to peat moss in 1-gallon pots. The algae slurry (approximately 30 % solids by dry weight) and Salicornia biomass (~14.5 % solids) from post-harvesting were stored at -20 °C and further used in the liquefaction experiments. All other chemicals and solvents used in the study were obtained commercially (analytical grade) and used as received. HTL biocrude oil was separated from the HTL product mixture in the reactor and the glassware using dichloromethane, DCM, as the solvent. This solvent, coupled with the benefit of lower boiling point (~40 °C), has proven to extract the highest amount of biocrude oil with minimal product loss (Valdez et al., 2011). Ultra-high purity gases (>99.999 %) of Helium (GC-MS), Oxygen (GC-MS and elemental analysis), and nitrogen (TGA) were used during the biomass and HTL product analysis.

3.2.2 HTL experimental procedure and product separation

HTL liquefaction experiments (individual and co-liquefaction) were performed in a 4593 Parr Instrument company stainless steel benchtop reactor. The reactor has an inner volume of 100 ml, a magnetic stirrer, and an electric furnace heater controlled by a 4843-controller. In a typical experimental run, 5 grams of equivalent dry biomass (including mixture) and the rest as deionized water were added into the reactor to make a 50 grams

slurry. The reactor was sealed and purged from high purity nitrogen to create an inert environment over the reaction mixture. Following the purging process, 2.9 MPa of initial pressure of nitrogen was maintained before it was heated to the desired temperature, as mentioned by the previous study (Dandamudi et al., 2017). The reaction time begins as soon as the temperature reaches the desired value. The reactor was then left to cool down to room temperature post-reaction, the incondensable gases are vented, and the reactor is opened. The products were separated from the mixture by adding 25-30 ml of dichloromethane. The reactor, stirrer, and glassware were also washed with 15 ml of dichloromethane to avoid product losses. The heating rate plays an important role in the conversion of biomass into products. The heating and cooling rate profile were shown in Appendix A (Figure A-1). The product separation protocol and product yields (biocrude, biochar, and water-soluble compounds) were calculated using equations mentioned in the previous study (Muppaneni et al., 2017). The expected yield of biocrude during co-liquefaction is estimated using the following equation.

Expected biocrude yield, % = (Biocrude oil yield $_{CM}$ *x Weight fraction of CM) + (Biocrude oil yield* $_{SL}$ *x Weight fraction of SL)* ……. (1)

3.2.3 Analytical analysis

The proximate analysis (volatile matter (VM), ash content (AC), and fixed carbon (FC)) of the biomass, biochar, and biocrude were performed according to ASTM D3172 (D3172-07a, 2013) using the thermogravimetric analysis (TGA). The TGA analysis included heating ~10 mg of the dry sample from room temperature to 925 °C (heating rate: 20

K/min) under a nitrogen flow rate of 50 ml/min and a purge flow rate of 30 ml/min using NETZSCH TG 209 Libra thermal analyzer (Germany). Fixed carbon was calculated from equation 2. The elemental analysis of the biocrude, biochar, and biomass was carried out on an elemental analyzer (Perkin Elmer Series II 2400), as mentioned in (Wang et al., 2015). Higher heating value (HHV) was used as a metric to estimate the energy content of the biochar, biocrude, and the dry biomass and was measured using a bomb calorimeter (Parr Model 6725 Semi-micro calorimeter, Moline, IL).

The biocrude oil samples were analyzed for chemical composition using an Agilent 6890N-5973N single quadrupole Mass Spectrometer (GC-MS). The mass spectrometer was equipped with a DB-5 capillary column (30 m x 0.25 mm x 0.25 µm), which is efficient to analyze the volatiles in the biocrude. The samples were dissolved in dichloromethane and filtering through a 0.2 µm PTFE filter. The carrier gas was UHP helium at a flow rate of 1 ml/min, and 1 µL samples were injected in splitless mode. The gas chromatography was programmed to hold at 40 °C for 1 min and then ramp to 300 °C at a rate of 5 °C/min. The inlet temperature was maintained at 280 °C with a transfer line at 250 °C and ion source at 230 °C. The chromatographs were integrated using ChemStation software with a Gaussian smoothened function (15 points), and the chemical compounds were identified using a mass spectral database from NIST (National Institute of Standards and Technology), 2017.

HTL water phase was analyzed for the presence of water-soluble nutrients such as total nitrogen (TN), ammoniacal nitrogen (NH_3-N), Nitrates (NO_3-N), Nitrites (NO_2-N),

Total phosphates (TP, $P\text{-}PO_4^{-3}$), orthophosphates ($P\text{-}PO_4^{-3}$) using a HACH DR6000 spectrophotometer (HACH, Colorado, USA) along with the procedure manual TNT 828, TNT 832, TNT 836, TNT 839, TNT 843, respectively.

$$\textit{Fixed carbon (FC), \%} = \textit{100-VM \%-AC \%} \quad (2)$$

The biomass, biocrude, and the biochar were acid digested in the nitric, sulfuric, and hydrofluoric acid (only for biochar) and the digestion protocol was mentioned in the Appendix A. The digested samples were analyzed for the presence of metals using Thermo Fischer iCAP 6300 ICP-OES (Inductively Coupled Plasma Optical Emission Spectrometry) using a 24 element and a phosphorous calibration standard.

3.3 Results and discussion

3.3.1 Analysis of biomass feedstock

The proximate and ultimate analysis of the two biomass feedstocks were presented in Table 3.1. The results indicate that *Salicornia sp*. (SL) had a very high ash content as expected, 46.27 wt. % on a dry basis compared to that of CM (1.76 wt. %). The high ash content of the SL results from the high salinity of feed water during its growth and accumulation of these salts in the plant tissue. Swine manure (SM) also has a high ash content due to the source it is procured from. The solids content in Table 3.1 represents the amounts of solids presented in the biomass as analyzed post-harvesting (14. 5, 63.79, 30.0 wt. % for SL, SM, and CM, respectively). CM has the highest volatile matter (~80.29 wt. %), fixed carbon (17.95 wt. %) compared to SL (46.27 wt. % and 9.76 wt. %). The SM

biomass also has a higher volatile content (52.05 wt. %) in comparison to SL biomass. In comparison with all the biomasses under study, CM also has higher fixed carbon value (17.95 wt. %) than SM (12.2 wt. %) and SL (9.76 wt. %). The calorific value of the microalgae, CM (16.52 MJ/kg), was comparable to that of a similar strain of algae (18.11 MJ/kg) in the previous study (Dandamudi et al., 2017) and is higher than SL (5.43 MJ/kg) and SM (12.15 MJ/kg). The C, H, N, S, and O content of the SL biomass was 19.99±0.62, 3.13±0.32, 2.70±0.20, 0.99±0.04, and 73.19±0.98 wt. % and for CM biomass was 48.93±0.43, 7.31±0.03, 9.38±0.29, 1.24±0.09, and 33.14±0.11 wt. %, respectively. The higher oxygen and ash content of the SL biomass resulted in a lower HHV value. The SM biomass also has a lower HHV than CM biomass. The CM biomass has higher carbon and hydrogen relative to SL and lower oxygen content (33.14 ±0.11 wt. %). This results in a higher calorific value compared to the rest of the biomass.

Table 3.1: Proximate and ultimate analysis of biomass under study

	Salicornia sp. **(SL)**	**Swine manure** ***(SM)***	***C. merolae*** **(CM)**
Proximate (wt. %)			
Solids content	14.5	63.79	30.0
Ash	46.27	35.75	1.76
Volatile matter content	43.96	52.05	80.29
Fixed carbon content	9.76	12.2	17.95

Ultimate (wt. %)			
Elemental Composition (wt. %)			
C	19.99±0.62	33.54±0.08	48.93±0.43
H	3.13±0.32	4.99±0.15	7.31±0.03
N	2.70±0.20	3.73±0.18	9.38±0.29
S	0.99±0.04	-	1.24±0.09
O[a]	73.19±0.98	57.74±0.98	33.14±0.11
Calorific value, HHV (MJ/kg)			
Calorific value	5.43	12.15	16.52

[a]: Calculated by difference O, %=100- Sum (C, H, N, S)

Thermogravimetric analysis (TGA) is a valuable technique to understand the thermal degradation and/or stability mechanisms of the material (Cantero-Tubilla et al., 2018; Carrier et al., 2011; Sanchez-Silva et al., 2012). The CM biomass degradation was observed in three different stages. The first weight-loss stage was observed between 85-105 °C and was associated with the loss of water as free moisture and water loosely bound to bio-macromolecules, which leads to the destruction of cell structure with a change in lipid structures and protein thermal unfolding (Marcilla et al., 2009). The second stage between 200-400 °C associated with the degradation of volatile compounds such as triglycerides, proteins, and carbohydrates. A rapid weight loss of volatile matter was observed in the region, suggesting the presence of organic matter (Marcilla et al., 2009;

Peng et al., 2001). The last stage took place over 450 °C, associated with the decomposition/oxidation of remaining organic matter. The CM biomass had a less residue yield compared with the SL indicating the presence of higher organic/volatile matter. On the other hand, SL biomass has four weight-loss stages and was observed between 80-150 °C, 200- 350 °C, 400-500 °C, and over 640 °C associated with moisture and lower molecular weight volatile compounds, devolatilization of proteins, carbohydrates, extracts, hemicellulose, cellulose and lignin, and complete oxidation of organic matter resulting in ash matter, respectively. Hydrogen (H_2), carbon dioxide, light hydrocarbons, and moisture were the main gaseous products observed during the TGA (Bui et al., 2015; Miranda et al., 2009; Yang et al., 2019).

3.3.2 HTL product distribution

The crucial factors for the HTL include the choice and chemical composition of the feedstock, operational parameters like solid loading, reaction temperature, reaction time, and the type of catalysts (Tian et al., 2014). This section discusses about the influence of various process parameters on the direct and co-liquefaction of the biomasses under study.

3.3.2.1 Direct HTL

The influence of the HTL process temperature on the product distribution was studied in the temperature range of 250-350 °C with a 50 °C interval. From Figure 3.2 (A), the highest yield (7.65 wt. %) of biocrude oil from SL biomass was obtained at 300 °C compared to the lowest yield (1.97 wt. %) at 250 °C. The increase in temperature from 250

to 300 °C increased the biocrude oil yield due to the hydrolysis of biomass and favors the cleavage of peptide bonds in proteins and C-C and C-O-C bonds in carbohydrates and lipids (Barreiro et al., 2013; Jiang and Savage, 2017; Muppaneni et al., 2017). On the contrary, increasing temperature from 300 to 350 °C decreased the biocrude oil due to the onset of gasification reactions (Kruse et al., 2010). A similar decrease in the biocrude oil yield effect was observed in the HTL of *Kirchneriella sp*. biomass from 300 to 375 °C due to the increase of incondensable gases (Dandamudi et al., 2019). This suggests that the reactions favoring the formation of biocrude oil from SL biomass were predominant and maximum at 300 °C resulting in the cell lysis. An increase in biocrude yield from 5.26 wt. % to 6.27 wt. % was observed in the case of SM biomass. This suggests that SM biomass needs higher temperature to degrade and form biocrude oil. A similar trend has been observed in the case of biochar from SL biomass. The biochar yield was the highest at 250 °C at around 20.65 wt. % and decreasing to 11.64 wt. % when the temperature was increased to 300 °C. The decrease in biochar yields was due to the increased hydrolysis of the biomass and thereby resulted in the formation of higher biocrude yield. The biochar yields increased slightly when the temperature was increased to 350 °C due to the re-polymerization of lighter molecules to form tar-like compounds and settle down as biochar. In the case of Sm biomass, the biochar yield increased with increase of temperature heavier compounds accumulating into the biochar phase. The water-soluble compound fraction (WSC) for CM also followed a similar trend with a yield of 5.95 wt. % at 250 °C. The high yield of WSC at lower temperatures was due to the formation of polysaccharide-rich water

extract as performed in (Chakraborty et al., 2012; Miao et al., 2012). The WSC yield decreased as the temperature was increased to 300 °C resulting in the formation of more biocrude oil components. Similar results were obtained in the studies where water-soluble compounds were converted into biocrude oil at higher temperatures (Garcia Alba et al., 2011; Zhou et al., 2010). It was also evident from the color of the HTL water-soluble compound phase, as it was browner in all the temperature (>250 °C) cases, indicating the presence of Maillard reaction products like melanoidins (Miao et al., 2012; Minowa et al., 2004). In the case of SM biomass, the WSC yields for increased with increase in temperature from 300 to 330 °C. This suggests that high temperatures have favored in the formation of more water-soluble fraction compounds.

In the case of CM, the biocrude yields were higher compared to the HTL of SL biomass. This was due to the higher volatile matter content and fixed carbon content in the biomass and lower ash content. These facilitate the conversion of more organic matter in the biomass from various HTL products. From Figure 3.2 (B), CM biocrude yield also followed a similar trend to that of SL biomass, where the biocrude oil increased from 28.64 to 34.63 wt. % when the temperature was increased from 250 to 300 °C. Due to the decrease in the dielectric constant of the water with an increase in temperature, water behaves more like an organic solvent and catalyzes a higher number of non-polar reactions resulting in the extraction of highly non-polar and mildly polar compounds from the biomass. Further increase in temperature to 350 °C decreased the biocrude oil yield to 29.46 wt. %. The decrease in biocrude oil yield occurs because of the intensification of gaseous reactions at

higher temperatures, and similar results were observed in earlier studies [26,27]. The yield of biochar also decreased from 8.29 to 3.88 wt. % when the reaction temperature was increased from 250 to 300 °C. Further increase in reaction temperature to 350 °C decreased the biochar yields, suggesting gasification and conversion of biomass into gaseous phase products. The WSC yields at all the temperatures were considerably lower than the SL biomass scenarios suggesting the dominant conversion of biomass into the biocrude oil. Similar trends in the yields of HTL products were achieved in previous studies (Anastasakis and Ross, 2011; Aresta et al., 2005; Reddy et al., 2016).

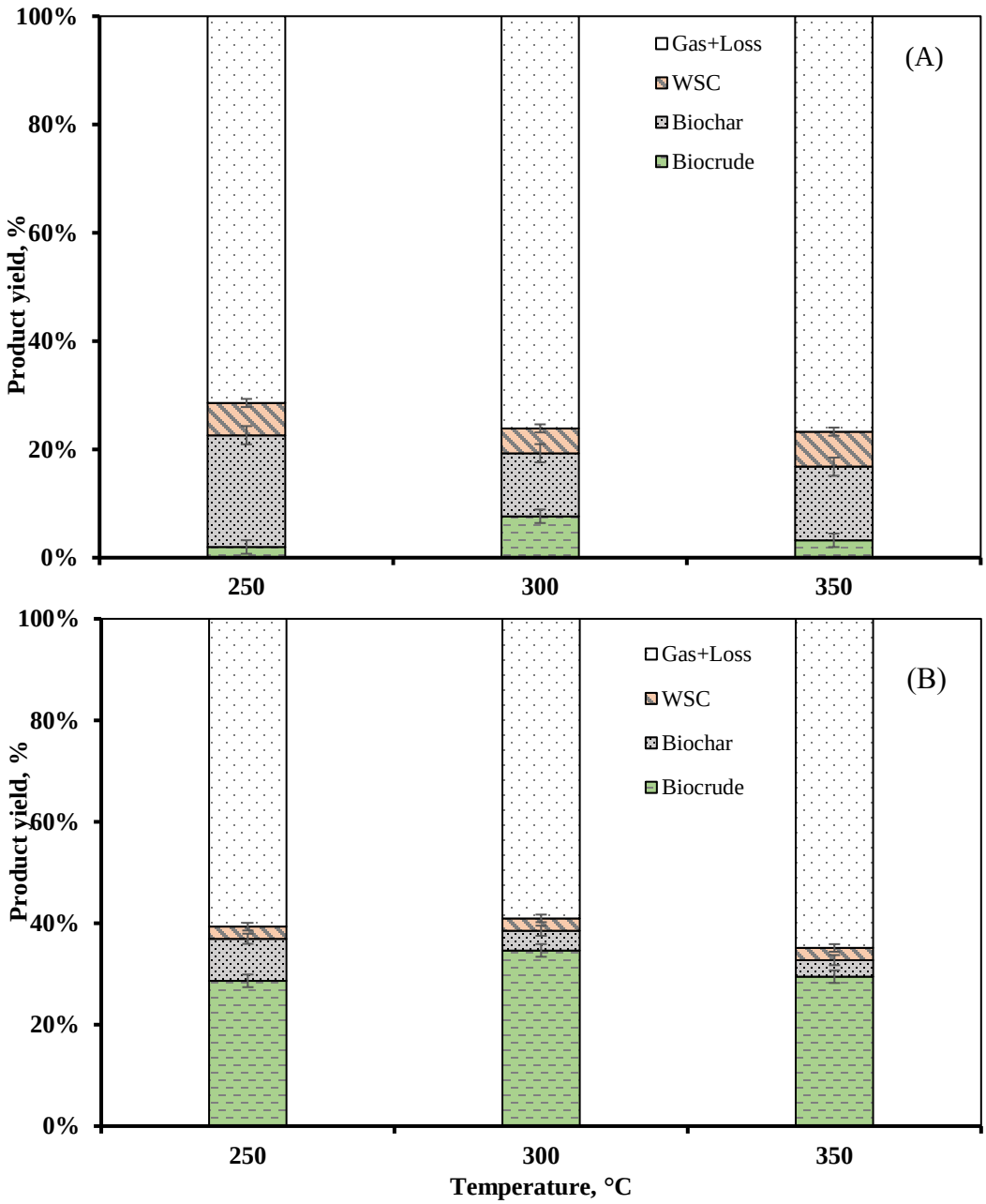

Figure 3.2: HTL product distribution of individual liquefaction of SL biomass (A); CM biomass (B); w.r.t. the temperature at 10 wt. % solid loading and 30 min residence time.

3.3.2.2 Co-liquefaction of CM with SL and SM

The biomasses were liquefied in various CM to SL and CM to SM mass ratios (80/20, 50/50, 20/80) to see the influence of co-liquefaction. Based on the results from individual liquefaction, 300 °C (maximum biocrude yield) and 250 °C were chosen as the temperatures to be studied. The product distribution from different ratios was presented in figures 3.3 & 3.4, respectively. The lower temperature, 250 °C, was chosen based on the idea that positive synergy during co-liquefaction might shift the decomposition temperature required to achieve the same or higher biocrude yield produced at 300 °C. On the contrary, in the case of co-liquefaction at 250 °C, the experimental results of biocrude yield were slightly lower than that of calculated expected yield results in all the three blending ratios. As mentioned earlier, the expected yield of biocrude oil was calculated from equation 1. The expected and experimental biocrude yields at the reaction temperature of 300 °C, 30 min, and 10 wt. % were compared in figures 3.5 & 3.6. In both the ratios of 50/50 and 20/80 of CM-SL biomass, the calculated yields were less than the experimental results. However, in the case of the 80/20 mass ratio (CS^*, hereafter) of CM-SL biomass, the experimental biocrude yield (32.95 wt. %) was higher than the calculated value (29.23 wt. %). Similar effect was observed in the case of CM-SM and CM-SL biomass mixture. This suggests a positive synergistic effect during the co-liquefaction at this specific CM-SL biomass ratio. This further investigates the variations in the quality of the products which will be discussed in further sections.

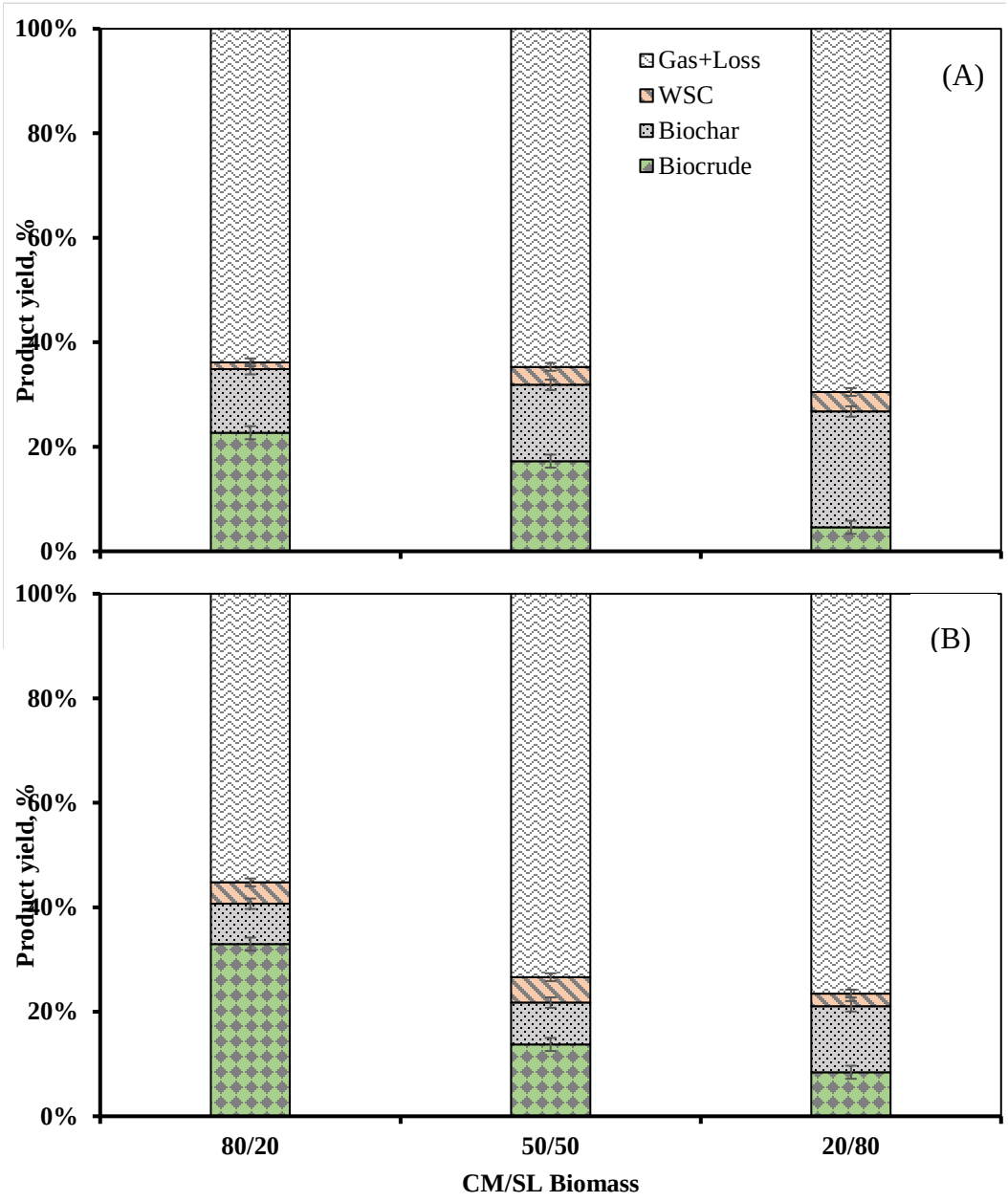

Figure 3.3: Co-liquefaction product distribution of CM/SL biomass (A) at 250 °C; CM-SL biomass at 300 °C (B); w.r.t. to biomass loading ratio at 10 wt. % solid loading and 30 min residence time.

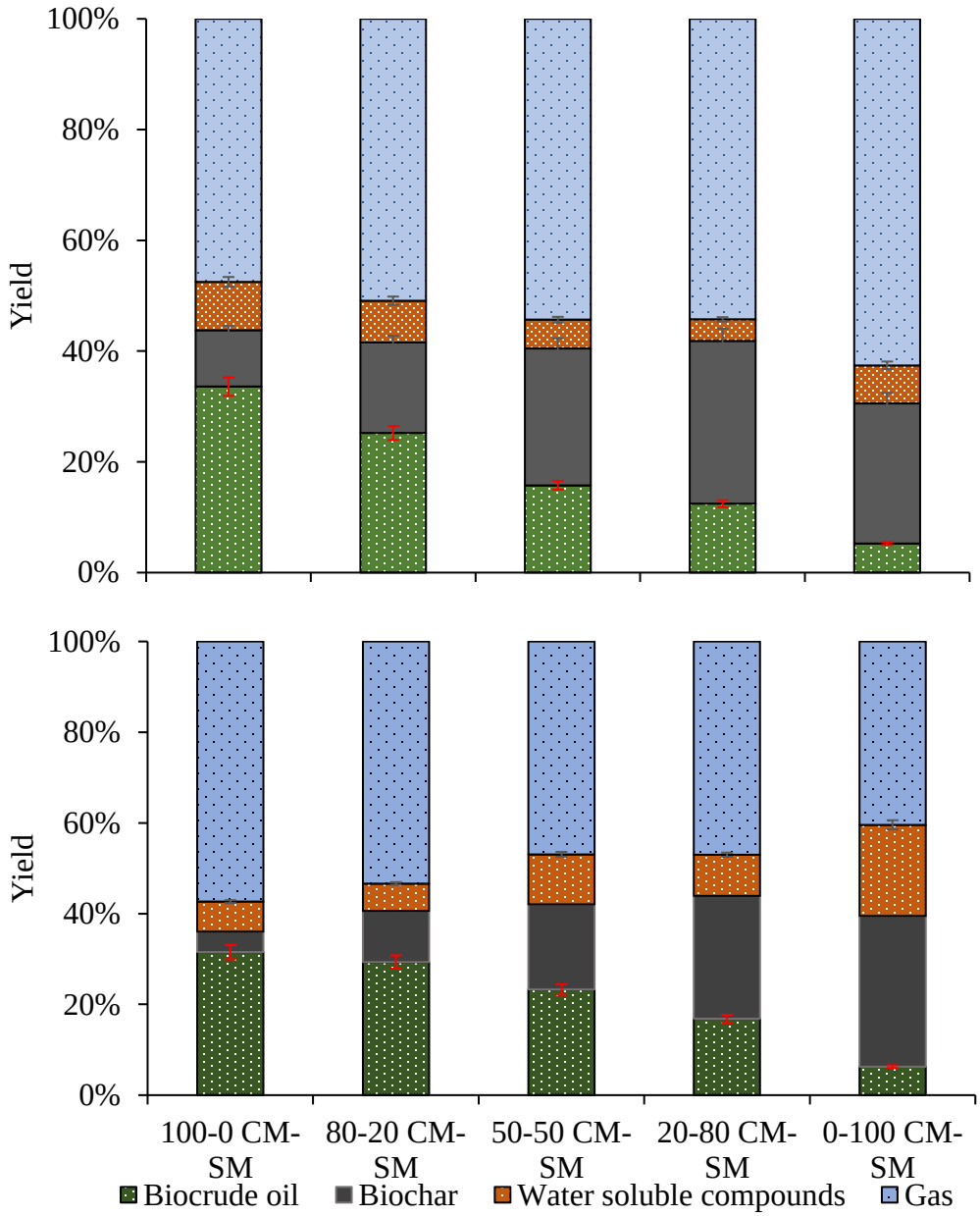

Figure 3.4: Co-liquefaction product distribution of CM to SM biomass at 300 °C (A); CM-SM biomass at 330 °C (B); w.r.t. to biomass loading ratio at 20 wt. % solid loading and 30 min residence time.

It is hypothesized that the interaction of inorganic salts may initiate a catalytic activity from the SL and free fatty acids derived from the CM biomass, leading to greater degradation of the biomass. Dandamudi et. al., (Dandamudi et al., 2017) showed the presence of positive synergy and mutually enhancing effect during the co-liquefaction of two microalgae, *Cyanidioschyzon merolae* and *Galdieria sulphuraria* at a temperature of 300 °C, 10 wt. % solid loading, and 30 min residence time. During co-liquefaction, a higher biocrude oil yield (25.88 wt. %) was reported compared to the individual liquefaction yields (18.9 and 14.0 wt. % for *C. merolae* and *G. sulphuraria*, respectively). The compositional comparison of the individual and co-liquefied oils using FT-ICR MS indicated the presence of similar heteroatom classes with similar carbon number and DBE distributions. Similar catalytic activity and positive synergistic effect were observed during the co-liquefaction of microalgae and macro-algae (Jin et al., 2013) in subcritical water conditions where the fatty acids derived from the microalgae showed the catalytic effect to the hydrolysis of protein and carbohydrates in the macro-algae. The catalytic activity was highly temperature sensitive and elemental analysis also showed the in-situ deoxygenation of the biocrude oil. Thus, reporting an improvement in the quantity and quality of the produced biocrude oil during co-liquefaction.

In both temperature scenarios, the 20/80 CM-SL co-liquefaction condition yielded the highest biochar among all the co-liquefaction scenarios. This may be due to the high ash content of the SL biomass and accumulation of the ash in the biochar phase during separation. The thermal degradation behaviors of both biomass samples and their

corresponding HTL biocrude oil products are shown in figure 3.7. The TGA curve of the CS* is very similar to that of CM biocrude because of the higher percentage of the CM in the feedstock mixture. The CM and CS* biocrudes showed the presence of chemical compounds with boiling point ranging in between 200-500 °C. On the other hand, SL biocrude showed compounds decomposed between 130-500 °C. All the three biocrudes did not show a change in weight loss beyond 500 °C suggesting that majority of the volatile compounds were decomposed. The ultimate/ash analysis of all the biocrudes concluded that they have less than 0.1 % of dissolved ash.

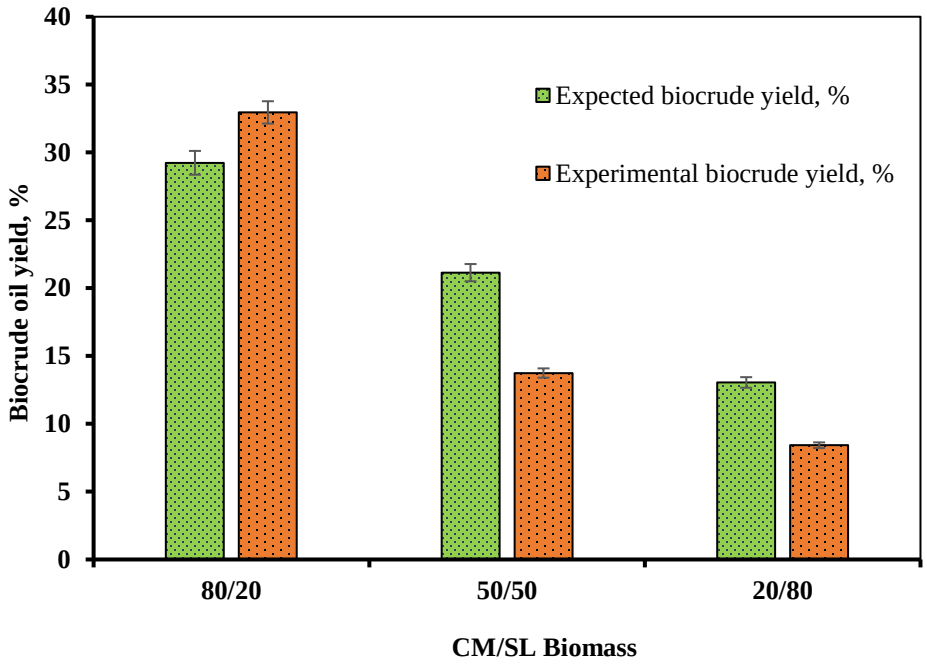

Figure 3.5: Biocrude oil yields from the experimental vs. expected yields at different CM-SL biomass ratios (300 °C, 30 mins and 10 wt. % solid loading)

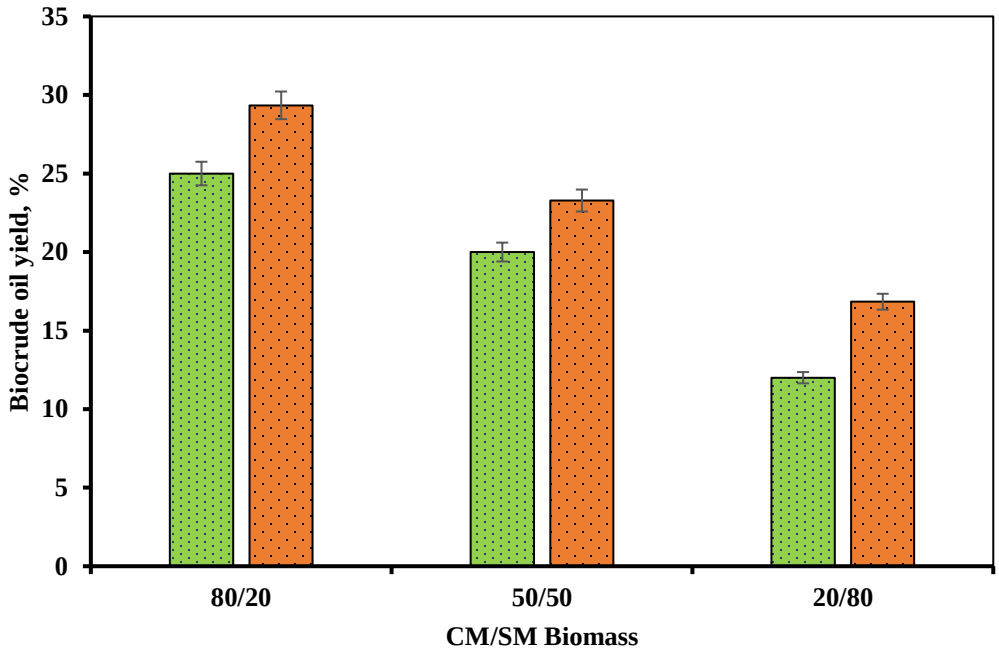

Figure 3.6: Biocrude oil yields from the experimental vs. expected yields at different CM-SM biomass ratios (330 °C, 30 mins and 20 wt. % solid loading)

Table 3.2: Ultimate analysis of the biomass and HTL products (biocrude and biochar)

		Elemental analysis, wt. %				Atomic Ratio			
		C	H	N	O	H/C	O/C	N/C	HHV, MJ/kg
SL	Biomass	19.99±0.62	3.13±0.32	2.70±0.20	74.195±0.98	1.87	2.79	0.11	5.43
	300 biocrude	74.43±0.27	8.38±0.71	5.49±0.52	11.7±0.08	1.34	0.12	0.06	26.4
	350 biocrude	70.27±2.68	7.76±0.52	4.38±0.39	17.6±3.58	1.32	0.19	0.05	28.29
	300 biochar	42.09±0.69	3.63±0.18	2.81±0.18	51.47±1.23	1.03	0.92	0.06	12.12
	350 biochar	47.52±0.55	3.87±0.15	3.17±0.11	45.44±0.99	0.97	0.72	0.06	14.44
CM	Biomass	48.93±0.43	7.31±0.03	9.38±0.29	34.39±0.11	1.78	0.53	0.16	16.52
	250 biocrude	69.6±0.11	8.48±0.61	5.98±0.45	15.94±0.55	1.51	0.17	0.07	31.99
	300 biocrude	72.41±0.16	8.64±0.04	6.02±0.13	12.93±0.33	1.42	0.13	0.07	32.5

	350 biocrude	74.55±0.11	8.5±0.66	6.14±0.09	10.81±0.15	1.36	0.11	0.07	33.12
	250 biochar	61.24±0.13	7.69±0.4	7.55±0.12	23.52±0.86	1.5	0.29	0.11	25.32
	300 biochar	43.47±0.79	3.81±0.35	3.54±0.23	49.18±1.11	1.04	0.85	0.07	14.48
	350 biochar	41.5±0.41	3.99±0.14	4.18±0.19	50.33±1.14	1.15	0.91	0.09	13.9

CS*: 80-20 % of CM-SL HTL experiment; [a]: Calculated by difference O, %=100- Sum (C, H, N, S)

3.3.3 Elemental analysis and energy recovery

Table 3.2 lists the elemental composition, atomic ratios, and measured higher heating value (HHV) of all the biomass and HTL products (biocrude and biochar). It is evident that both product fractions (biocrude and biochar), irrespective of their reaction temperature, have a higher carbon content, suggesting energy densification during the HTL process. The carbon content of the SL, CM, CS*, and SM followed the trend of biocrude> biochar> biomass. Among all the products, biocrude has a higher content of carbon and hydrogen compared to biomass, signifying the presence of hydrocarbon and aromatic compounds. The carbon content of all the biochar samples in this study was over 40 wt. %, which is greater than SL biomass. The oxygen content of the products was lower than that of original biomass in both cases, suggesting deoxygenation. The high nitrogen (N) content of CM biomass (9.38 wt. %) was due to the presence of high protein content (~44.83 wt. %) (Templeton and Laurens, 2015) in the algae biomass.

The HHV values of biocrude oils obtained from SL were in the range of 26.4-28.3 MJ/kg, while the oils obtained from CM exceeded 30 MJ/kg. These values were considerably greater than their respective biomass feedstock's. The highest HHV (33.12 MJ/kg) during individual HTL was obtained for biocrude oil produced at 350 °C from CM biomass and the lowest (26.4 MJ/kg) biocrude produced at 300 °C for SL biomass. The co-liquefied sample with the highest biocrude oil yield at 300 °C also had the highest HHV (34.33±0.24 MJ/kg). The H/C, O/C, and N/C ratios of the HTL products were lower than

that of their feedstock. Overall, the H/C was reduced from 1.78-1.87 to the least of 0.97-1.04 and with a decline of O/C from 2.79 to 0.11, suggesting a major pathway to be dehydration. The decrease in the O/C was mainly due to the decarboxylation and dehydration reactions (Balat, 2008). The N/C was also considerably reduced from the highest of 0.16 and has stayed constant at around 0.06 for products. All the crudes from either individual liquefaction or co-liquefaction have reduced O/C and N/C, but these values are still higher than petroleum (<0.05 mol/mol) and hence need to be upgraded (Sudasinghe et al., 2014a). The energy recovery from various conditions of HTL was presented in Figure 3.8. For example, SL 300 represents the energy recovery from HTL of SL biomass at 300 °C factoring the HHV of biocrude, biochar, and feedstock. The lowest energy recovery (~53 %) was observed in the HTL of SL biomass at 350 °C. The highest energy recovery (~71.5 %) among individual HTL was observed in the case of CM biomass at 300 °C. The highest energy recovery (88.55 %) was observed for the co-liquefaction of CM-SL 80-20 (CS^{*}) biomass at 300 °C. This suggests that co-liquefaction has increased energy recovery, thus showing a synergistic effect.

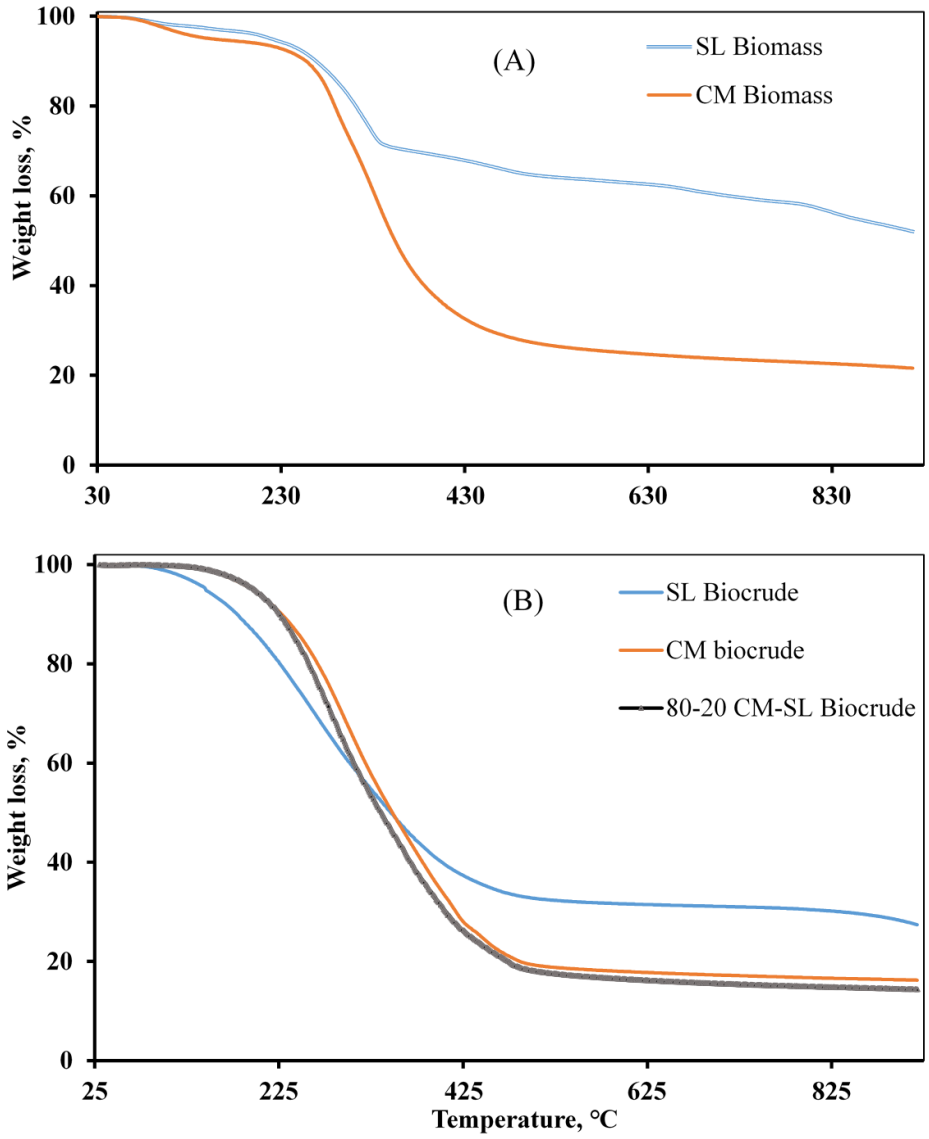

Figure 3.7: Thermal degradation behavior of the raw biomass (A); biocrudes produced at 300 °C, 10 % solid loading, and 30 min residence time (B).

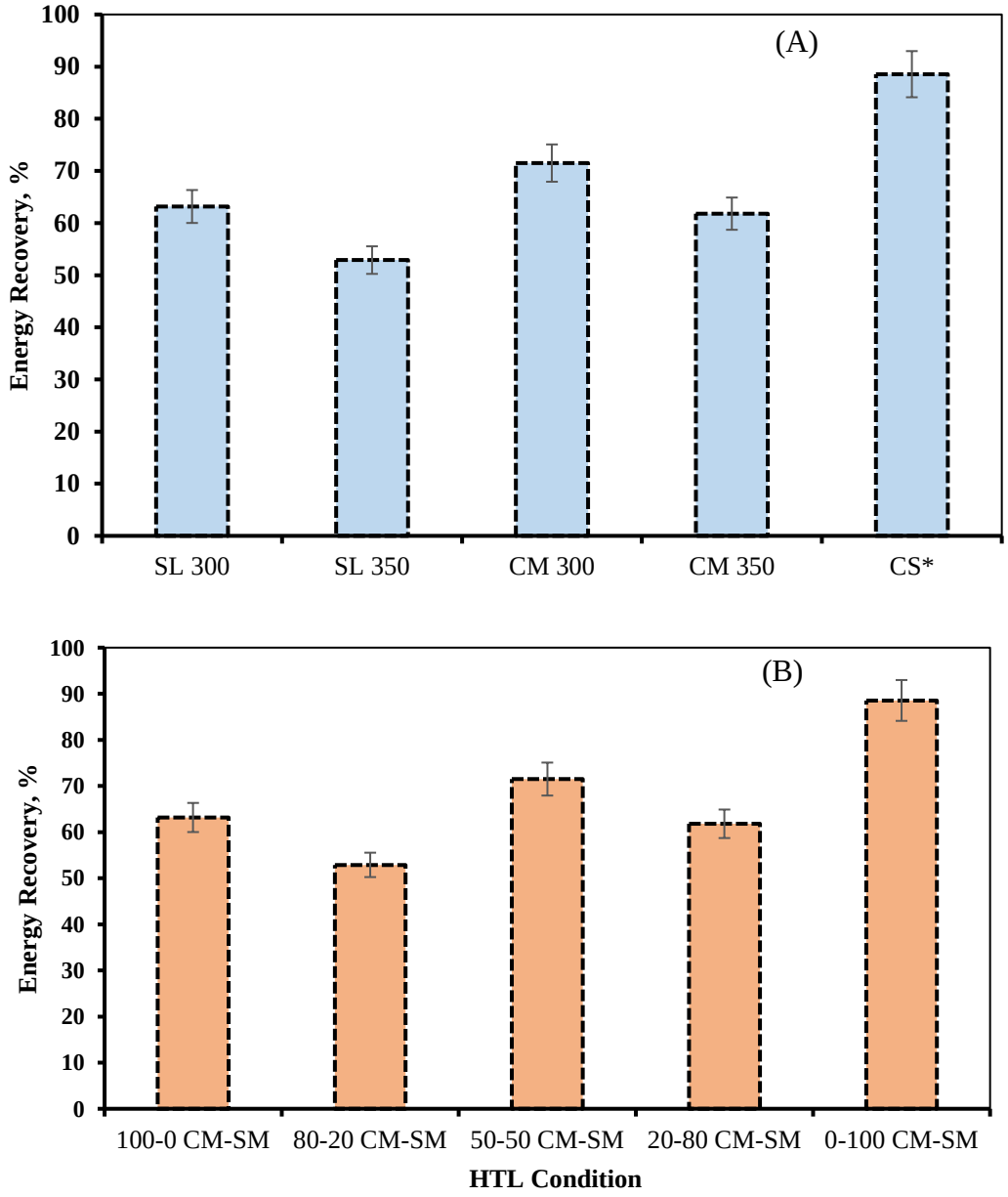

Figure 3.8: Comparison of the energy recovery (ER, %) over different HTL reaction conditions; (A) CM-SL; (B) CM-SM

3.3.4 Nutrient analysis of the HTL water phase

Algal biomass can contain up to 10 wt. % of nitrogen and 1 wt. % of phosphorus in its dry form (Jena et al., 2011). Nitrogen and phosphorous in their various forms are used by microalgae for its growth, and many researchers have shown that the water phase can be recycled back to re-grow microalgae (Biller et al., 2012; Selvaratnam et al., 2015). The water-soluble compounds in the HTL water phase recovered from different temperatures were measured (mg/L) and presented in Table 3.3. The water phase contained a large amount of total nitrogen (TN) dissolved in it. The major portion of the TN was arising from the dissolved ammoniacal nitrogen (NH_3-N) and nitrates (NO_3-N). The nitrites in the HTL water soluble phase were present in a small range (0.27-1.14 mg/L). The TN value for direct HTL of SL biomass and CS^* decreased with the increase in temperature, suggesting that lower temperatures favor dissolving nitrogen-based compounds into the water phase. In contrast, the ammoniacal nitrogen value increased with an increase in temperature. The total nitrogen values of the CM biomass were always higher than that of SL biomass or the co-liquefied sample suggesting the presence of higher value of proteins in the biomass. The nitrogen in the water phase is due to the degradation of proteins in the biomass and conversion of nitrogen in the biomass to form ammonia, nitrogen heterocyclic compounds (pyrroles, indoles, nitriles, imines, and carbazole derivatives) (Ross et al., 2010) and remain dissolved in the water phase (Jena et al., 2011; Minowa and Sawayama, 1999). A wide variety of basic N_2, N_1, N_3 compounds were identified in the analysis of the HTL water

phase by FT-ICR MS (Sudasinghe et al., 2014b). The presence of ammoniacal nitrogen and TN in higher values were also reported in the HTL of *Kirchneriella sp*. (3033±49, 11130±100 mg/L) (Dandamudi et al., 2019) and *Cyanidioschyzon merolae* (3833, 6703 mg/L) (Muppaneni et al., 2017). A slightly lower concentration of ammoniacal nitrogen (2260 mg/L) and TN (5320 mg/L) was reported in this current study for CM in comparison with the previous study (Muppaneni et al., 2017) at similar HTL conditions.

The water samples were also analyzed for total phosphates (TP) and orthophosphates. The TP (both bound and free orthophosphates) from SL biomass decreased with an increase in temperature from 250 to 350 °C. The TP value for direct HTL of CM biomass was constant with a change in the temperature and was higher than of the direct HTL of SL biomass and CS*. A similar trend in the decrease of orthophosphates was observed for all the different HTL samples. The majority of the total phosphates were primarily orthophosphates in the case of CM biomass. It suggests that HTL may be efficient in converting the majority of phosphorous in the biomass into free phosphates. The HTL water samples can be diluted and then used in the cultivation of algae biomass (Henkanatte-Gedera et al., 2017). Among other potential applications, HTL water can be used to produce methane via anaerobic digestion (AD) and/or hydrothermal gasification.

3.3.5 Gas chromatography-mass spectrometry analysis of biocrude

The chemical composition of the biocrude oils obtained from direct HTL (300 °C) of SL, CM biomass, and co-liquefaction (300 °C) of CM-SL at 80-20 mass ratio were presented in Table 3.4. The analysis of the spectra against the NIST database helped in identifying over 40 different compounds in each biocrude sample. This does not assure the identification of all the compounds as the GC instrument method has a limitation of reaching a maximum temperature of 300 °C. Any compounds with a boiling point over the maximum threshold temperature were unable to be identified. The method also has a solvent delay of up to 3 minutes, resulting in the loss of lower molecular weight compounds. Oleic acid and n-hexadecanoic acid were the predominant compounds present in the biocrude oil from SL biomass. N-hexadecanoic acid and phenol were the predominant compounds present in the biocrude oil from CM biomass.

Pyrrolo [1, 2-a] pyrazine-1, 4-dione, hexahydro-3-(2-methylpropyl)- was also a dominant peak in the analysis of biocrude oil from CM. This results from the degradation of proteins and carbohydrates in the raw feedstock. Apart from it, amides and other cyclic compounds were identified in both direct HTL biocrude oils and co-liquefied biocrude oil sample. During HTL, the long-chain fatty acids were formed by the hydrolysis of lipids in the biomass. The hydrolysis and degradation of triacylglycerides (TAG's) result in the formation of these long-chain free fatty acids. Phenol arises during the degradation of carbohydrates and protein fraction in the biomass under high temperatures and pressure in

the reactor. The degradation of lignin during HTL also identified the similar composition of phenols from the presence of large quantities of carbohydrates (Singh et al., 2014). In the case of co-liquefied biocrude oil, oleic acid, n-hexadecanoic acid, phenol, pyrrolo [1, 2-a] pyrazine-1, 4-dione, hexahydro-3-(2-methylpropyl)-, and arachidamide, N-methyl- were the dominant compounds identified. All of these were also identified in their individual, direct HTL steps, suggesting that co-liquefaction still produced similar compounds qualitatively but varied in composition. The composition of the chemical compounds in the biocrude oil varies with the composition of the biomass blend. The relative abundance of the major compounds identified in the three biocrude oils was presented in table 3.4. The chromatograms of the individual spectra are available in Appendix A.

Table 3.3: Nutrient analysis of the HTL water-soluble compound (WSC) phase

	HTL Temperature, °C	Total Nitrogen, TN (mg/L)	Ammoniacal Nitrogen, NH_3-N (mg/L)	Nitrates, NO_3-N (mg/L)	Nitrites, NO_2-N (mg/L)	Total Phosphates, PO_4^{-3}-P (mg/L)	Orthophosphates, PO_4^{-3}-P (mg/L)
SL	250	2620	335	625	0.38	210	141.5
CM	250	5240	1456	93.8	1.14	1076	980
CS*	250	3500	766	300	1	206	80

SL	300	2245	710	33.5	0.53	30.55	9.06
CM	300	5320	2260	34.7	0.44	916	892
CS*	300	2460	1900	59.4	0.51	18.7	7.59
SL	350	1365	720	22.4	0.35	23.7	6.7
CM	350	4345	3240	17.8	0.29	1032	928
CS*	350	2165	1475	26.7	0.27	68.5	27.4

CS*: 80-20 % of CM-SL HTL experiment

3.3.6 Heavy metal analysis by ICP-OES

The heavy metal composition of the biomass and their HTL products (biocrude and biochar) were presented in Table 3.5. SL biomass contained large concentrations of metals relative to the microalgae. Sodium (Na) was the abundant element (49502.8 $mg.kg^{-1}$) identified in the SL biomass followed by calcium (Ca), potassium (K), magnesium (Mg). This corresponds to the growth conditions of the biomass in high saline conditions and the accumulation of the salts in the plant tissue. In terms of their measured abundance, the order of the elements in SL biomass was Na>Ca>K>Mg>P>Al>Ni>Sr≅Fe>Mn>Zn>Cu>Cr>Mo. To the best of our knowledge, SL biomass has never been analyzed for heavy metal content. In the case of CM biomass, phosphorous, potassium, magnesium were the abundant elements found. Some previous research studies (Dandamudi et al., 2019; Sudasinghe et al., 2014b) also observed similar

results with the presence of heavy metals in the biomass. The presence of these metals and some additional micronutrients (Cu, Fe, Al, and Na) arise from the salts used during algal growth and subsequent use by the microalgae via various biological pathways. In terms of their measured abundance, the order of the elements in CM biomass was P>K>Mg>Fe>Al>Ca>Cu>Na>Mn>Zn>Cr>Ni>Mo.

In the case of biocrude oil produced at 300 °C from the HTL of CM, SL, and CS*, the common metals found were Fe, Cu, Mn, Mo, Na, Ni, Zn. The presence of Fe and Ni can be explained due to the presence of porphyrin structures in the biocrude oil similar to that of petroleum-based oils. These metal-containing species lead to the catalyst deactivation, pore plugging, coke formation, and increase the stability of water-in-oil emulsions (Jarvis et al., 2016). The Na content of the HTL biocrude produced from SL biomass and CS* is higher than the biocrude oil from CM biomass. This can be removed by a prewashing water step adapted to treat high salinity petroleum crudes (McKechnie and Thompson, 1987). In all the cases, biochar contained the highest concentration of Ca, Fe, K, Mg, Na, and P. Phosphorous was the leading contributor of metal in all the three-biochar analyzed. The lower concentration of these heavy metals in the biocrude favors cleaner combustion and plays a major factor in storage stability and further hydro-treating during the upgrading process. This also plays a crucial role in the technical and economic feasibility of this process in selecting the choice of catalyst, reactor design, environmental pollution, unpleasant odors in the processing plants.

Table 3.4**:** Major compounds identified in different biocrude oils by GC-MS

Chemical Compound	RT, min	Relative Abundance, %		
		SL biocrude	CM biocrude	CS* biocrude
Oleic Acid	22.7	5.25	4.7	8.5
n-Hexadecanoic acid	21.025	5.07	9.7	7.75
Phenol	7.90	1.91	5.2	1.13
Pyrrolo[1,2-a]pyrazine-1,4-dione, hexahydro-3-(2-methylpropyl)-	20.861	3.15	5.2	3.24
Arachidamide, N-methyl-	23.413	1.51	1.7	2.12
p-Cresol	11.786	-	3.4	2.0
2,6-Dimethyl-4,4-pentamethylene-1,4-dihydropyridine-3,5-dicarbonitrile	17.862	3.23	-	-

Acetic acid, 3,7,11,15-tetramethyl-hexadecyl ester	19.796	3.15	-	-
13-Heptadecyn-1-ol	20.172	3.48	-	-
3-Buten-2-ol,3-methyl-4-(2,6,6-trimethyl-2-cyclohexen-1-yl)-	15.393	2.16	-	-
Oxiraneundecanoic acid, 3-pentyl-, methyl ester, cis-	22.36	2.14	-	-
9H-Pyrido[3,4-b]indole, 1-methyl-	21.179	2.13	-	-
1H-Indole, 5,7-dimethyl-	15.775	2.12	-	-
Hexadecanoic acid, methyl ester	20.643	1.93	-	-
Acetic acid, 3,7,11,15-tetramethyl-hexadecyl ester	19.658	1.48	-	-

1-Naphthalenecarbonitrile, 8-amino-	21.324	1.24	-	-
Dodecanamide, N-butyl-	24.991	1.13	-	1.04
(3-Methoxyphenyl)ethanolamine	14.267	1.11	-	-
Tetrazol-5-amine,N-(3,4-dimethoxybenzyl)-	17.98	1.10	-	-
2-Cyclopenten-1-one, 2,3-dimethyl-	8.892	1.02	-	-
Heptane, 2,4-dimethyl-	4.718	-	6.7	1.5
Undecane, 3,7-dimethyl-	12.616	-	6.3	-
Octane, 4-methyl-	5.715	-	6.1	1.37
1-Undecene	12.389	-	5.3	1.62
2-Pentanol, 4-methyl-	4.507	-	4.6	-
Undecane, 4,7-dimethyl-	11.245	-	4.5	3.15
9,12-Octadecadienoic acid (Z,Z)-	27.943	-	4.3	3.37
Undecane, 5-methyl-	12.791	-	3.4	2.48

Pyrazine, 2,5-dimethyl-	7.035	-	3.3	-
Indole	18.601	-	3.3	2.16
Pyrazine, methyl-	4.841	-	3.2	2.15
2-Cyclopenten-1-one, 2-methyl-	6.794	-	3.0	2.14
Cyclo(L-prolyl-L-valine)	33.37	-	2.6	2.13
N,3-Diethyl-3-octanamine	30.981	-	2.5	2.12
2-Butylamine, N-nonyl-	30.949	-	2.5	1.93
Cyclo(L-prolyl-L-valine)	30.319	-	2.3	1.50
Pentanamide	30.872	-	2.0	1.48
Dodecane, 1-iodo-	19.028	-	2.0	1.23
Pyrazine, trimethyl-	9.62	-	1.9	1.23
Pyrazine, ethyl-	7.126	-	1.7	1.13
3-Ethyl-3-methylheptane	17.733	-	1.7	1.11

Pentane, 3-ethyl-3-methyl-	11.415	-	1.6	1.10

Table 3.5: Metal concentrations in biomass, biocrude, and biochar obtained at 300 °C

Element	CM biomass	CM 300 biocrude	CM 300 biochar	SL biomass	SL 300 biocrude	SL 300 biochar	CS* biocrude	CS* biochar
	$mg.kg^{-1}$	$mg.kg^{-1}$	$mg.kg^{-1}$	$mg.kg^{-1}$	$mg.kg^{-1}$	$mg.kg^{-1}$	$mg.kg^{-1}$	$mg.kg^{-1}$
Al	428.3	n.d.	7437.5	151.1	n.d.	655.8	n.d.	7021.4
Ca	365.4	n.d.	24124.8	8965	767.4	11788.2	n.d.	49605.8
Cr	11.4	n.d.	898.4	1.3	n.d.	85.2	20	125
Cu	338.5	131.6	236.2	4.5	32.7	114.7	50.5	381.6
Fe	760.7	2214.3	16140.2	80.1	97.4	2078.4	1019.8	9266.2
K	5818.6	n.d.	19387.1	4380	400.1	4764	n.d.	1378.7

Mg	1781.3	n.d.	54926.3	3356.5	n.d.	5578.2	n.d.	46270
Mn	30.3	2.0	1686.9	61.5	8.6	513	9.4	1152.3
Mo	3.3	15.8	159.5	1.3	9.6	17.5	11	48.3
Na	225.0	489.5	6048.5	49502.8	3520.1	8000.2	7556	18013.3
Ni	6.7	54.3	252.4	89.9	7.1	58.4	14.8	2253.7
P	7090.7	n.d.	86053.6	1469.6	41.3	13135.1	65.5	89985.2
Sr	n.d.	n.d.	n.d.	80.3	7.8	320.4	n.d.	896.3
Zn	27.7	66.5	1141.6	31.2	33	302.1	73.9	557.6

n.d.: not detected

3.4 Conclusions

Hydrothermal liquefaction is effective for producing high quality renewable biocrude oil from different wet feedstocks including the salt-tolerant *Salicornia bigelovii* Torr. It was found that the HTL biocrude oil yield strongly depends on the composition and the organic contents of the biomass feedstock. The CM biomass has a higher organic content compared to that of SL biomass. The maximum direct HTL biocrude yield of 7.65 wt. % and 34.63 wt. % was obtained at 300 °C, 10 wt. % solid loading, and 30 min of reaction time for SL and CM biomass, respectively. Co-liquefaction of both biomasses increased the biocrude oil yield, and the maximum yield (32.95 wt. %) of biocrude oil was obtained at 80-20 mass ratio of CM-SL at 300 °C and 30 minutes, which suggests that *Salicornia bigelovii Torr*. can be used as viable biomass feedstock in co-liquefaction with algae to produce renewable biofuels. The HTL products (biocrude, biochar) had higher energy content (HHV) than that of the original biomass, suggesting energy densification during the HTL process. The HHV of the biocrude oil produced from HTL of SL biomass was measured to be 28.29 MJ/kg, while that of CM biomass was around 32.5 MJ/kg. The co-liquefaction has led to the positive synergistic effect and maximum energy recovery (88.55 %) compared to individual liquefaction conditions. HTL water phase analysis showed the presence of water-soluble nutrients, which can be recycled to re-grow algae. The biomass,

biocrude, and biochar were analyzed by ICP-OES for heavy metals, and the biochar contained the highest concentration of metals accumulated in the product phase. The biocrude oil from SL biomass needs to undergo a prewashing step to remove the salts before entering a refinery. The GC-MS showed the presence of similar compounds in the co-liquefied oils compared to that of individual HTL oils. Although, HTL seems to be an effective technique, it should still address the limitations and challenges for the scalability of the current research such as feedstock preparation, continuous year-round supply of feedstock, scale-up of HTL units, nutrient recycle, by-product handling and commercialization, and process integration.

3.5 References

Anastasakis, K., Ross, A.B., 2011. Hydrothermal liquefaction of the brown macro-alga Laminaria saccharina: effect of reaction conditions on product distribution and composition. Bioresour. Technol. 102, 4876–4883.

Aresta, M., Dibenedetto, A., Carone, M., Colonna, T., Fragale, C., 2005. Production of biodiesel from macroalgae by supercritical CO 2 extraction and thermochemical liquefaction. Environ. Chem. Lett. 3, 136–139.

Azar, C., Lindgren, K., Obersteiner, M., Riahi, K., van Vuuren, D.P., den Elzen, K.M.G.J., Möllersten, K., Larson, E.D., 2010. The feasibility of low CO 2 concentration targets and the role of bio-energy with carbon capture and storage (BECCS). Clim. Change 100, 195–202.

Balat, M., 2008. Mechanisms of thermochemical biomass conversion processes. Part 1: reactions of pyrolysis. Energy Sources, Part A 30, 620–635.

Barreiro, D.L., Prins, W., Ronsse, F., Brilman, W., 2013. Hydrothermal liquefaction (HTL) of microalgae for biofuel production: state of the art review and future prospects. Biomass and Bioenergy 53, 113–127.

Beal, C.M., Archibald, I., Huntley, M.E., Greene, C.H., Johnson, Z.I., 2018. Integrating algae with bioenergy carbon capture and storage (ABECCS) increases sustainability.

Earth's Futur. 6, 524–542.

Biller, P., Ross, A.B., Skill, S.C., Lea-Langton, A., Balasundaram, B., Hall, C., Riley, R., Llewellyn, C.A., 2012. Nutrient recycling of aqueous phase for microalgae cultivation from the hydrothermal liquefaction process. Algal Res. 1, 70–76.

Brown, T.M., Duan, P., Savage, P.E., 2010. Hydrothermal liquefaction and gasification of Nannochloropsis sp. Energy & Fuels 24, 3639–3646.

Bui, H.H., Tran, K.Q., Chen, W.H., 2015. Pyrolysis of microalgae residues - A Kinetic study. Bioresour. Technol. https://doi.org/10.1016/j.biortech.2015.08.069

Bui, M., Adjiman, C.S., Bardow, A., Anthony, E.J., Boston, A., Brown, S., Fennell, P.S., Fuss, S., Galindo, A., Hackett, L.A., 2018. Carbon capture and storage (CCS): the way forward. Energy Environ. Sci. 11, 1062–1176.

Cantero-Tubilla, B., Cantero, D.A., Martinez, C.M., Tester, J.W., Walker, L.P., Posmanik, R., 2018. Characterization of the solid products from hydrothermal liquefaction of waste feedstocks from food and agricultural industries. J. Supercrit. Fluids. https://doi.org/10.1016/j.supflu.2017.07.009

Carrier, M., Loppinet-Serani, A., Denux, D., Lasnier, J.M., Ham-Pichavant, F., Cansell, F., Aymonier, C., 2011. Thermogravimetric analysis as a new method to determine the lignocellulosic composition of biomass. Biomass and Bioenergy.

https://doi.org/10.1016/j.biombioe.2010.08.067

Chakraborty, M., Miao, C., McDonald, A., Chen, S., 2012. Concomitant extraction of bio-oil and value added polysaccharides from Chlorella sorokiniana using a unique sequential hydrothermal extraction technology. Fuel 95, 63–70.

Chen, W.T., Zhang, Y., Zhang, J., Schideman, L., Yu, G., Zhang, P., Minarick, M., 2014. Co-liquefaction of swine manure and mixed-culture algal biomass from a wastewater treatment system to produce bio-crude oil. Appl. Energy. https://doi.org/10.1016/j.apenergy.2014.04.068

Cho, H.-S., Oh, Y.-K., Park, S.-C., Lee, J.-W., Park, J.-Y., 2013. Effects of enzymatic hydrolysis on lipid extraction from Chlorella vulgaris. Renew. Energy 54, 156–160. https://doi.org/https://doi.org/10.1016/j.renene.2012.08.031

D3172-07a, A., 2013. Standard Practice for Proximate Analysis of Coal and Coke.

Dandamudi, K.P.R., Muppaneni, T., Markovski, J.S., Lammers, P., Deng, S., 2019. Hydrothermal liquefaction of green microalga Kirchneriella sp. under sub-and super-critical water conditions. Biomass and bioenergy 120, 224–228.

Dandamudi, K.P.R., Muppaneni, T., Sudasinghe, N., Schaub, T., Holguin, F.O., Lammers, P.J., Deng, S., 2017. Co-liquefaction of mixed culture microalgal strains under sub-critical water conditions. Bioresour. Technol. 236.

https://doi.org/10.1016/j.biortech.2017.03.165

Dimitriadis, A., Bezergianni, S., 2017. Hydrothermal liquefaction of various biomass and waste feedstocks for biocrude production: A state of the art review. Renew. Sustain. Energy Rev. 68, 113–125.

Garcia Alba, L., Torri, C., Samorì, C., van der Spek, J., Fabbri, D., Kersten, S.R.A., Brilman, D.W.F., 2011. Hydrothermal treatment (HTT) of microalgae: evaluation of the process as conversion method in an algae biorefinery concept. Energy & fuels 26, 642–657.

Glenn, E., Miyamoto, S., Moore, D., Brown, J.J., Thompson, T.L., Brown, P., 1997. Water requirements for cultivatingSalicornia bigeloviiTorr. with seawater on sand in a coastal desert environment. J. Arid Environ. 36, 711–730.

Glenn, E.P., Brown, J.J., Blumwald, E., 1999. Salt tolerance and crop potential of halophytes. CRC. Crit. Rev. Plant Sci. 18, 227–255.

Glenn, E.P., O'LEARY, J.W., Watson, M.C., Thompson, T.L., Kuehl, R.O., 1991. Salicornia bigelovii Torr.: an oilseed halophyte for seawater irrigation. Science (80-.). 251, 1065–1067.

Gude, V.G., Patil, P., Martinez-Guerra, E., Deng, S., Nirmalakhandan, N., 2013. Microwave energy potential for biodiesel production. Sustain. Chem. Process. 1, 5.

Henkanatte-Gedera, S.M., Selvaratnam, T., Karbakhshravari, M., Myint, M., Nirmalakhandan, N., Van Voorhies, W., Lammers, P.J., 2017. Removal of dissolved organic carbon and nutrients from urban wastewaters by Galdieria sulphuraria: laboratory to field scale demonstration. Algal Res. 24, 450–456.

Jarvis, J.M., Sudasinghe, N.M., Albrecht, K.O., Schmidt, A.J., Hallen, R.T., Anderson, D.B., Billing, J.M., Schaub, T.M., 2016. Impact of iron porphyrin complexes when hydroprocessing algal HTL biocrude. Fuel 182, 411–418. https://doi.org/https://doi.org/10.1016/j.fuel.2016.05.107

Jena, U., Vaidyanathan, N., Chinnasamy, S., Das, K.C., 2011. Evaluation of microalgae cultivation using recovered aqueous co-product from thermochemical liquefaction of algal biomass. Bioresour. Technol. 102, 3380–3387.

Jiang, J., Savage, P.E., 2017. Influence of process conditions and interventions on metals content in biocrude from hydrothermal liquefaction of microalgae. Algal Res. 26, 131–134.

Jin, B., Duan, P., Xu, Y., Wang, F., Fan, Y., 2013. Co-liquefaction of micro- and macroalgae in subcritical water. Bioresour. Technol. https://doi.org/10.1016/j.biortech.2013.09.045

Kruse, A., Bernolle, P., Dahmen, N., Dinjus, E., Maniam, P., 2010. Hydrothermal

gasification of biomass: consecutive reactions to long-living intermediates. Energy Environ. Sci. 3, 136–143.

Marcilla, A., Gómez-Siurana, A., Gomis, C., Chápuli, E., Catalá, M.C., Valdés, F.J., 2009. Characterization of microalgal species through TGA/FTIR analysis: Application to nannochloropsis sp. Thermochim. Acta 484, 41–47.

McKechnie, M.T., Thompson, D.G., 1987. Method for desalting crude oil.

Miao, C., Chakraborty, M., Chen, S., 2012. Impact of reaction conditions on the simultaneous production of polysaccharides and bio-oil from heterotrophically grown Chlorella sorokiniana by a unique sequential hydrothermal liquefaction process. Bioresour. Technol. 110, 617–627.

Minowa, T., Inoue, S., Hanaoka, T., MATSUMURA, Y., 2004. Hydrothermal reaction of glucose and glycine as model compounds of biomass. J. Japan Inst. Energy 83, 794–798.

Minowa, T., Sawayama, S., 1999. A novel microalgal system for energy production with nitrogen cycling. Fuel 78, 1213–1215.

Miranda, R., Bustos-Martinez, D., Blanco, C.S., Villarreal, M.H.G., Cantú, M.E.R., 2009. Pyrolysis of sweet orange (Citrus sinensis) dry peel. J. Anal. Appl. Pyrolysis. https://doi.org/10.1016/j.jaap.2009.06.001

Muppaneni, T., Reddy, H.K., Selvaratnam, T., Dandamudi, K.P.R., Dungan, B., Nirmalakhandan, N., Schaub, T., Omar Holguin, F., Voorhies, W., Lammers, P., Deng, S., 2017. Hydrothermal liquefaction of Cyanidioschyzon merolae and the influence of catalysts on products. Bioresour. Technol. 223. https://doi.org/10.1016/j.biortech.2016.10.022

Peng, W., Wu, Q., Tu, P., Zhao, N., 2001. Pyrolytic characteristics of microalgae as renewable energy source determined by thermogravimetric analysis. Bioresour. Technol. https://doi.org/10.1016/S0960-8524(01)00072-4

Pourzolfaghar, H., Abnisa, F., Daud, W.M.A.W., Aroua, M.K., 2016. A review of the enzymatic hydroesterification process for biodiesel production. Renew. Sustain. Energy Rev. 61, 245–257. https://doi.org/https://doi.org/10.1016/j.rser.2016.03.048

Reddy, H.K., Muppaneni, T., Ponnusamy, S., Sudasinghe, N., Pegallapati, A., Selvaratnam, T., Seger, M., Dungan, B., Nirmalakhandan, N., Schaub, T., 2016. Temperature effect on hydrothermal liquefaction of Nannochloropsis gaditana and Chlorella sp. Appl. Energy 165, 943–951.

Reddy, H.K., Muppaneni, T., Sun, Y., Li, Y., Ponnusamy, S., Patil, P.D., Dailey, P., Schaub, T., Holguin, F.O., Dungan, B., Cooke, P., Lammers, P., Voorhies, W., Lu, X., Deng, S., 2014. Subcritical water extraction of lipids from wet algae for

biodiesel production. Fuel 133, 73–81. https://doi.org/https://doi.org/10.1016/j.fuel.2014.04.081

Ross, A.B., Biller, P., Kubacki, M.L., Li, H., Lea-Langton, A., Jones, J.M., 2010. Hydrothermal processing of microalgae using alkali and organic acids. Fuel 89, 2234–2243.

Sanchez-Silva, L., López-González, D., Villaseñor, J., Sánchez, P., Valverde, J.L., 2012. Thermogravimetric–mass spectrometric analysis of lignocellulosic and marine biomass pyrolysis. Bioresour. Technol. 109, 163–172.

Savage, P.E., Hestekin, J.A., 2013. A perspective on algae, the environment, and energy. Environ. Prog. Sustain. Energy 32, 877–883.

Selvaratnam, T., Reddy, H., Muppaneni, T., Holguin, F.O., Nirmalakhandan, N., Lammers, P.J., Deng, S., 2015. Optimizing energy yields from nutrient recycling using sequential hydrothermal liquefaction with Galdieria sulphuraria. Algal Res. 12, 74–79.

Singh, R., Prakash, A., Dhiman, S.K., Balagurumurthy, B., Arora, A.K., Puri, S.K., Bhaskar, T., 2014. Hydrothermal conversion of lignin to substituted phenols and aromatic ethers. Bioresour. Technol. 165, 319–322.

Sudasinghe, N., Cort, J.R., Hallen, R., Olarte, M., Schmidt, A., Schaub, T., 2014a.

Hydrothermal liquefaction oil and hydrotreated product from pine feedstock characterized by heteronuclear two-dimensional NMR spectroscopy and FT-ICR mass spectrometry. Fuel 137, 60–69.

Sudasinghe, N., Dungan, B., Lammers, P., Albrecht, K., Elliott, D., Hallen, R., Schaub, T., 2014b. High resolution FT-ICR mass spectral analysis of bio-oil and residual water soluble organics produced by hydrothermal liquefaction of the marine microalga Nannochloropsis salina. Fuel 119, 47–56.

Templeton, D.W., Laurens, L.M.L., 2015. Nitrogen-to-protein conversion factors revisited for applications of microalgal biomass conversion to food, feed and fuel. Algal Res. 11, 359–367.

Tian, C., Li, B., Liu, Z., Zhang, Y., Lu, H., 2014. Hydrothermal liquefaction for algal biorefinery: A critical review. Renew. Sustain. Energy Rev. 38, 933–950. https://doi.org/https://doi.org/10.1016/j.rser.2014.07.030

Valdez, P.J., Dickinson, J.G., Savage, P.E., 2011. Characterization of product fractions from hydrothermal liquefaction of Nannochloropsis sp. and the influence of solvents. Energy & Fuels 25, 3235–3243.

Ventura, Y., Sagi, M., 2013. Halophyte crop cultivation: the case for Salicornia and Sarcocornia. Environ. Exp. Bot. 92, 144–153.

Wahidin, S., Idris, A., Shaleh, S.R.M., 2014. Rapid biodiesel production using wet microalgae via microwave irradiation. Energy Convers. Manag. 84, 227–233. https://doi.org/https://doi.org/10.1016/j.enconman.2014.04.034

Wang, J., Krishna, R., Yang, J., Dandamudi, K.P.R., Deng, S., 2015. Nitrogen-doped porous carbons for highly selective CO 2 capture from flue gases and natural gas upgrading. Mater. Today Commun. 4, 156–165.

Wang, J., Peng, X., Chen, X., Ma, X., 2019. Co-liquefaction of low-lipid microalgae and starch-rich biomass waste: The interaction effect on product distribution and composition. J. Anal. Appl. Pyrolysis 139, 250–257.

Yang, C., Li, R., Zhang, B., Qiu, Q., Wang, B., Yang, H., Ding, Y., Wang, C., 2019. Pyrolysis of microalgae: A critical review. Fuel Process. Technol. https://doi.org/10.1016/j.fuproc.2018.12.012

Zhang, B., Chen, J., He, Z., Chen, H., Kandasamy, S., 2019. Hydrothermal liquefaction of fresh lemon-peel: Parameter optimisation and product chemistry. Renew. Energy 143, 512–519.

Zhou, D., Zhang, L., Zhang, S., Fu, H., Chen, J., 2010. Hydrothermal liquefaction of macroalgae Enteromorpha prolifera to bio-oil. Energy & Fuels 24, 4054–4061.

CHAPTER 4: PHYSICOCHEMICAL CHARACTERIZATION OF HYDROTHERMALLY PRODUCED BIOCHARS FROM *CYANIDIOSCHYZON MEROLAE* AND SWINE MANURE

4.1 Introduction

Energy security, economic development, increasing energy demand, and mitigation of anthropogenic emissions of greenhouse gases have made renewable energy feedstocks more attractive in recent years (Christensen et al., 2015; Dandamudi et al., 2017; Muppaneni et al., 2012). Energy security has been addressed by advances in the conversion of renewable feedstocks into energy-dense fuels. This in turn helps decrease the use of fossil fuel reserves, reduce fluctuations in fuel prices, offset emissions of greenhouse gases, and significantly boost economic development by increasing employment (Sues et al., 2010). The effective deployment of renewable energy strategies not only needs candidates with high energy density, but also requires value-added applications of side products to promote the overall life cycle and technoeconomic of the entire biomass supply chain (Mohanty et al., 2013). Among candidate applications, renewable feedstocks of waste-derived biochar have gained attention due to versatile physical and chemical properties, negative surface charge, higher charge density, and resistance to microbial breakdown.

They also have multiple applications: improving soil fertility and crop productivity, carbon storage and sequestration, and removal of dissolved pollutants (Lehmann and Joseph, 2015; Mohanty et al., 2013; Tsai et al., 2012). Ibrahim *et al.*, 2020 investigated the production of hydrogen using a hydrogen-selective membrane reactor from the hydrothermal liquefaction of algal biochar.

Among multiple thermochemical conversion pathways to produce biochar, hydrothermal liquefaction (HTL) has attracted interest over the past decade due to its ability to use wet feedstock, its high carbon recovery, and energy recovery. This gives HTL a lead over conversion methods like gasification and pyrolysis that require costly drying of the feedstock (Dandamudi et al., 2019; Muppaneni et al., 2017). During the HTL process, the feedstock is treated under high pressure (5-20 MPa) and temperature (180-374 °C). Under these conditions, the biomacromolecules (carbohydrates, proteins, and lipids) in the feedstock undergo a variety of depolymerization reaction such as hydrolysis, dehydration, deoxygenation, decarboxylation, and dealkylation to produce a solid residue (biochar), an oil phase (biocrude), a water-soluble nutrient phase, and a gaseous phase with low-carbon compounds (Toor et al., 2013, 2011). The yield and composition of the products from HTL are greatly influenced by the composition of feedstock and the reaction operation parameters (Hosseinnezhad et al., 2016).

Microalgae as a feedstock have gained interest in the past decade due to its faster growth rate, higher photosynthetic efficiency, and higher oil yield compared to conventional crops (Chisti, 2007). Microalgae have the potential to be integrated with wastewater treatment, thereby reducing the cost of cultivation which in turn improves the economic feasibility of the entire process. However, the process of HTL of algae biomass has yet to reach the level of the traditional fuel industry due to potential energy bottlenecks: cultivation, concentration, and extraction (Chisti, 2007).

Another feedstock that has gained attention due to their abundance of carbon is biowaste. Among renewable wastes, swine manure is a carbon-rich candidate which can be converted to energy-rich fuel and bioproducts (Fini et al., 2011; Walter et al., 2014; Xiu et al., 2012). The porous and functionalized surfaces of its resulting biochar make it a potential candidate for construction and agriculture applications, with carbon credits derived from carbon sequestration (Meng et al., 2013; Tsai et al., 2012).

Until now, HTL has been investigated as a thermochemical conversion technique only to produce biocrude and bio-products. Researchers have reported optimized conditions for the HTL of multiple strains of microalgae (Patil et al., 2018; Peng et al., 2001; Ross et al., 2010; Savage and Hestekin, 2013), lignocellulosic feedstock (Sudasinghe et al., 2014), agricultural residues, and municipal/sewage sludge (Cantero-Tubilla et al.,

2018; Vardon et al., 2011). In addition to the optimization of HTL for specific strains, the co-liquefaction of two strains of microalgae (Dandamudi et al., 2017) and of microalgae and macroalgae (Jin et al., 2013) have resulted in a synergistic effect on the increase in biocrude oil. However, the abovementioned research focused on biocrude and dealt with the biochar as a byproduct or a so-called waste of the HTL process, with minimal information on the yield and elemental composition of the biochar. The recent reports have shown that the HTL technology produced final fuel (gasoline equivalents) has a minimum fuel selling price of 0.6-1.3 USD/L. Therefore, it is crucial to investigate the technologies for co-product development and applications to increase the commercial value of the capital-intensive process and minimize waste generation (Lozano et al., 2020). Accordingly, the literature has limited information about the physicochemical characterization of the biochar produced in the HTL process, including volatiles, fixed carbon, ash, heavy metals content, quality of the functional groups, and crystallinity. This chapter proposes various application of biochar suggesting and improving the biomass value chain. These applications can add credits for techno-economical analysis and improving the economics of the technology. These always support the carbon sequestration by employing carbon capture and storage.

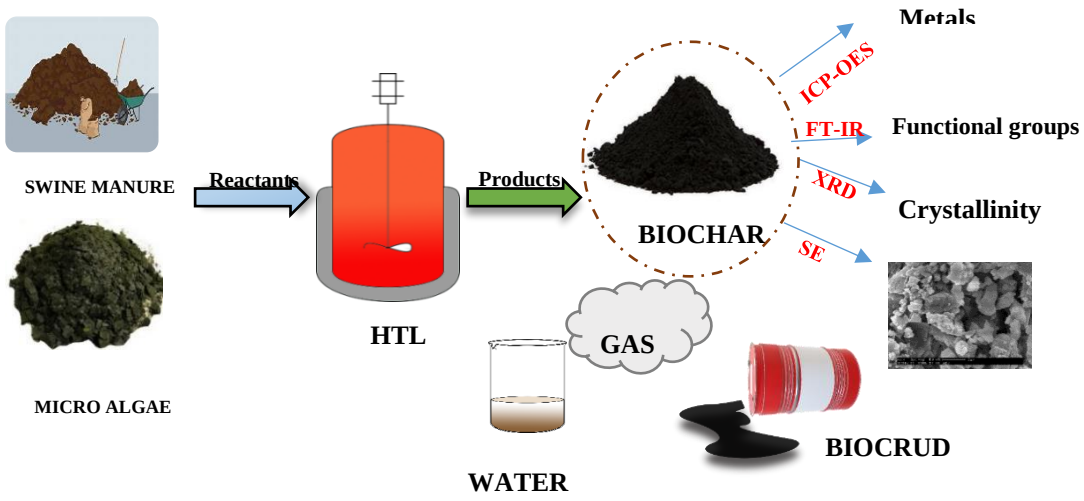

Figure 4.1: Experimental plan of this study

4.2 Materials and Methods

Figure 4.1 elaborates the experimental plan of the study. The objective of this paper is to investigate the physicochemical properties of the biochars produced from the direct liquefaction and co-liquefaction of microalgae and swine manure at different blending ratios. The biochars were characterized by HHV (higher heating value), surface area, porosity, elemental analysis using a CHN/O elemental analyzer, thermal behavior and stability using TGA (thermogravimetric analyzer), metals and heavy metals content by ICP-OES (inductively coupled plasma optical emission spectroscopy), functional groups

by FT-IR (Fourier transform infrared) spectroscopy, and crystallinity using X-ray diffraction (XRD). The description of both the biomasses, the HTL procedure details, and ICP-OES protocol was mentioned in Chapter 3.

4.2.1 Proximate and ultimate analysis

The biomasses and products produced from the liquefaction experiments were analyzed by proximate analysis. Thermogravimetric Analysis (TGA) was performed using a NETZSCH TG 209 Libra thermal analyzer (Germany). The tests that were performed using the thermal analyzer were tests for volatile matter content (VM), ash content (AC), and fixed carbon content (FC). A bomb calorimeter (Parr Model 6725 Semi-micro calorimeter, Moline, IL) was used to estimate the higher heating value (HHV) in MJ/kg. The ultimate analysis of the products was analyzed using a Thermo Series II CHNS/O elemental analyzer. Approximately 3-5 mg of the sample is used in the analyzer to measure the carbon (C), hydrogen (H), nitrogen (N), and oxygen (O). Ultra-high-purity gases (nitrogen, oxygen) were used during the operation of the TGA, the bomb calorimeter, and the CHNS/O elemental analyzer.

4.2.2 Scanning electron microscopy (SEM) and surface properties

The surface morphology of the biochar samples was analyzed by a XL30 Environmental SEM with an accelerated voltage of 30kV, resolution of 3 nm, and a field-

emission source. The beam current was 21pA and the probe diameter was 0.4 nm. The biochar samples were sputter-coated with gold (Au) particles for 100 seconds to reach a coating thickness of 8 nm. The porosity and the Brunauer-Emmett-Teller (BET) surface area were measured by a 3Flex surface analyzer. To measure the BET surface area, approximately 0.1 g of the sample was degassed at 80 °C for 6 h under vacuum to ensure all the moisture and the adsorbed gases were removed. The functional groups on the surface of the biochar samples were analyzed by Fourier transform infrared (FT-IR) spectroscopy. The samples were scanned for an average of 96 scans from 200-4000 cm^{-1} at 2 cm^{-1} resolution. X-ray diffraction (XRD) analysis of the biochar samples was performed using a PANalytical Aeris powder X-ray diffractometer. The diffractometer was equipped to use CuKα radiation at 40 kV, 15.0 mA and with a scanning angle (2θ) of 10-60° using a step size of 0.0109° per step, a scan speed of 0.2173 °/s, and a scan step time of 12.75 s. The soller slits were maintained at 0.04 rad and a $^1/_4$° divergence slit was used to collect the spectra. The detector was a PIXcel3D-Medipix 1x1 with a scanning line detector mode and an active length of 5.542° (2θ). The spectra were processed, and the peaks/phases were identified using high-score software and referenced with the International Center for Diffraction Data (ICDD).

4.3 Results and Discussion

4.3.1 Analysis of the biochars

The analyses determining the organic and mineral composition of the feedstocks and the products are crucial to evaluate the effectiveness of the conversion process (Dandamudi et al., 2020; Naik et al., 2010). The elemental analyses of the biomasses were performed, and the CM biomass has a higher carbon, hydrogen, and nitrogen content compared to the SM biomass. The higher concentration of nitrogen (9.38 wt. %) in CM indicates a higher concentration of proteins in the CM biomass. The SM biomass has a higher oxygen content compared to that of the CM biomass. Also, the SM's ash content and calcite and quartz are higher than CM biomass (Tsai et al., 2012). The higher heating value (HHV) of the CM biomass is 16.52 MJ/kg; for the SM biomass, HHV is 12.15 MJ/kg. The proximate and ultimate analyses of the biochars produced are shown in Table 4.1. It can be seen all the biochars have very low moisture content (<1.5 %). Among all the biochar blends produced, the CM biochar has the highest volatile matter (59.27 %), while 20-80 CM-SM has the lowest volatile matter (27.79%). The carbon content in the biochar follows the trend of 100-0 CM-SM > 80-20 CM-SM > 50-50 CM-SM > 0-100 CM-SM > 20-80 CM-SM. The biochar derived from 100-0 CM-SM has the highest energy content (13.9 MJ/kg). Among the blended feedstock scenarios, 80-20 CM-SM has the highest energy content (10.87 MJ/kg). The swine-manure-derived biochar 0-100 CM-SM has a HHV of 6.69 MJ/kg.

Cantrell *et al.*, 2012 reported that the swine solids biochar at 350 °C has an HHV value of 21.12 MJ/kg. The lower HHV of swine-manure biochar in the current study can be attributed to a higher percentage of ash in the raw feedstock. In line with prior research, the application of the HTL biochar toward a fuel perspective crucially depends on the quality and type of biomass (Tsai et al., 2012).

Table 4.1: Proximate and ultimate analysis of the biochars produced at 330 °C

Biochar	Proximate analysis (wt. %)				Ultimate analysis (wt. %)				HHV (MJ/kg)
	Moisture	Ash	Fixed carbon[b]	Volatile matter	C	H	N	O[a]	
100-0 CM-SM	1.64	0.05	13.07	85.24	74.55±0.11	8.5±0.66	6.14±0.09	10.81±0.15	34.909
80-20 CM-SM	2.49	0.1	9.72	87.69	74.85	9.61	6.37	9.17	34.58
50-50 CM-SM	1.77	0.5	11.73	86.0	75.00	8.77	5.19	11.04	34.11
20-80 CM-SM	4.15	0.1	8.08	87.67	75.33	8.00	4.0	12.67	34.16
0-100 CM-SM	1.22	0.5	8.96	89.32	76.33	8.52	3.66	11.49	36.23

[a]: Calculated by difference O, %=100- Sum (C, H, N); [b]: Fixed carbon, % = 100-volatile matter-ash-moisture

The aromaticity and the degree of carbonation have important roles in the product quality, and they were evaluated by atomic H/C and O/C. The varying extent of aromaticity and the degree of carbonization is believed to substantially affect the stability and resistance of the char against degradation in the ambient environment. The aromaticity and degree of carbonation also influence biochar's sequestration potential and the duration, which can benefit the medium to which it is introduced (Wiedemeier et al., 2015). Table 4.2 gives the atomic ratios of the biomasses and biochars produced in this work. Based on the elemental information, the empirical formula for the CM biomass was established as $CH_{1.78}N_{0.16}O_{0.53}$ and for the SM biomass as $CH_{1.77}N_{0.09}O_{1.30}$. In comparison with the raw biomasses, the O/C of the biochars increased, and the H/C decreased. This suggests a possible demethanation reaction resulting in the lower energy densities of the biochars relative to the biomasses. Wang *et al.*, 2019 also reported a similar demethanation reaction and lower energy densities during the co-liquefaction of low-lipid microalgae and starch-rich biomass waste. Among all the biochars, 80-20 CM-SM biochar exhibited a larger extent of demethanation and decarboxylation.

4.3.2 Thermogravimetric analysis of the biochars

Thermogravimetric analysis (TGA) is an analysis technique to characterize a material based on measuring the physico-chemical properties as a function of variable temperature (Coats and Redfern, 1963; Dandamudi et al., 2020; Ibrahim et al., 2020; Zhang et al., 2019).

Figure 2 represents the weight-loss properties of the CM and SM biochars with different mixture ratios as a function of temperature. In the case of 0-100 CM-SM, three major weight-loss stages were observed; the last two stages overlapped with the rest of the mixtures (20-80, 50-50, and 80-20 CM-SM, respectively). Among the three major stages, the first stage (70-110 °C) corresponds to the loss of moisture and lower volatile compounds. The next two weight-loss stages (180-300 °C, 400-900 °C) corresponds to the loss and/or degradation of extracts, proteins, hemicellulose, cellulose, lignin, and higher-molecular-weight compounds (Miranda et al., 2009; Zhang et al., 2019). In the case of 100-0 CM-SM, most of the weight loss was observed in the range of 80-150 °C, signifying moisture loss.

Table 4.2: Atomic ratios for biomasses and biochars

Sample	O/C	H/C	N/C	Empirical formula
Biochar @80-20 CM-SM, 330 °C	2.25	1.12	0.07	$CH_{1.12}N_{0.07}O_{2.25}$
Biochar @50-50 CM-SM, 330 °C	1.89	1.28	0.07	$CH_{1.28}N_{0.07}O_{1.89}$
Biochar @20-80 CM-SM, 330 °C	1.63	1.14	0.06	$CH_{1.14}N_{0.06}O_{1.63}$
Biochar @100-0 CM-SM, 330 °C	0.91	1.15	0.086	$CH_{1.15}N_{0.086}O_{0.91}$
Biochar @0-100 CM-SM, 330 °C	1.99	1.00	0.04	$CH_{1.00}N_{0.04}O_{1.99}$
SM biomass	1.30	1.77	0.09	$CH_{1.77}N_{0.09}O_{1.30}$
CM biomass	0.53	1.78	0.16	$CH_{1.78}N_{0.16}O_{0.53}$

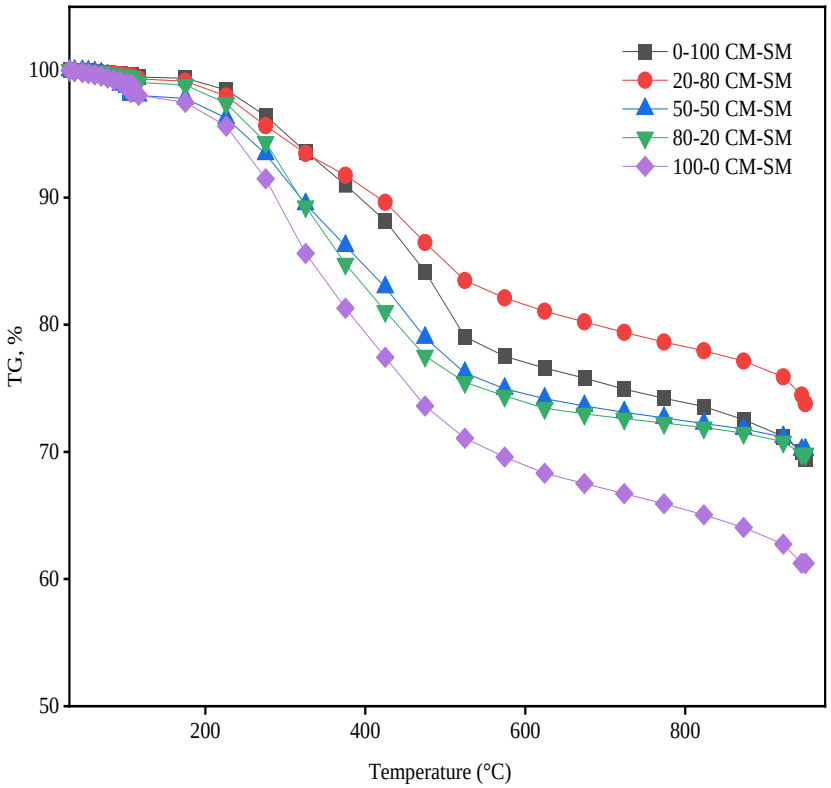

Figure 4.2: TGA analysis of the biochars produced at 330 °C; CM-SM (*C. merolae*- Swine manure)

4.3.3 Surface properties and metal composition

The surface morphologies of biochars produced at individual and blended HTL conditions of CM and SM can be compared from the SEM images. The SEM images were

taken considering a representative microparticle or a group of microparticles. Figure 3 (A) represents the HTL biochar produced from the pure CM biomass and confirms the amorphous and heterogeneous structure of the biochar. The visible holes represent the formation of channels for the volatile content to exit the biochar particles during the reaction. As shown in Figure 3 (E), several small granules were dispersed on the surface of the biochar produced from HTL of pure SM, which could possibly be the accumulation of inorganics and metal complexes. Steinmetz et al. reported that Co, Cr, Fe, Mg, and P were found in the swine-manure samples measured using ICP-OES (Radis Steinmetz et al., 2009). The metal and inorganic content from Table 4.4 also strengthen the statement of the accumulation of inorganic metal complexes. In the case of biochars from Figure 3 (B-D), the surface of the biochars tends to be more heterogeneous and resemble the dominant type of biomass present. For example, Figure 3 (B) looks very similar to the original biochar produced from the CM biomass, as it contains 80 % of the CM biomass. The larger particles are attributed to the formation of phenolic compounds from the hydrolysis and carbonization of lignin particles. These phenolic compounds further decompose and repolymerize into phenolic biochar (Wang et al., 2019). In the case of Figure 3 (C-D), the smaller microstructures were formed by hydrolysis of carbohydrates from the SM biomass to form reducing sugars, then re-fused into larger structures.

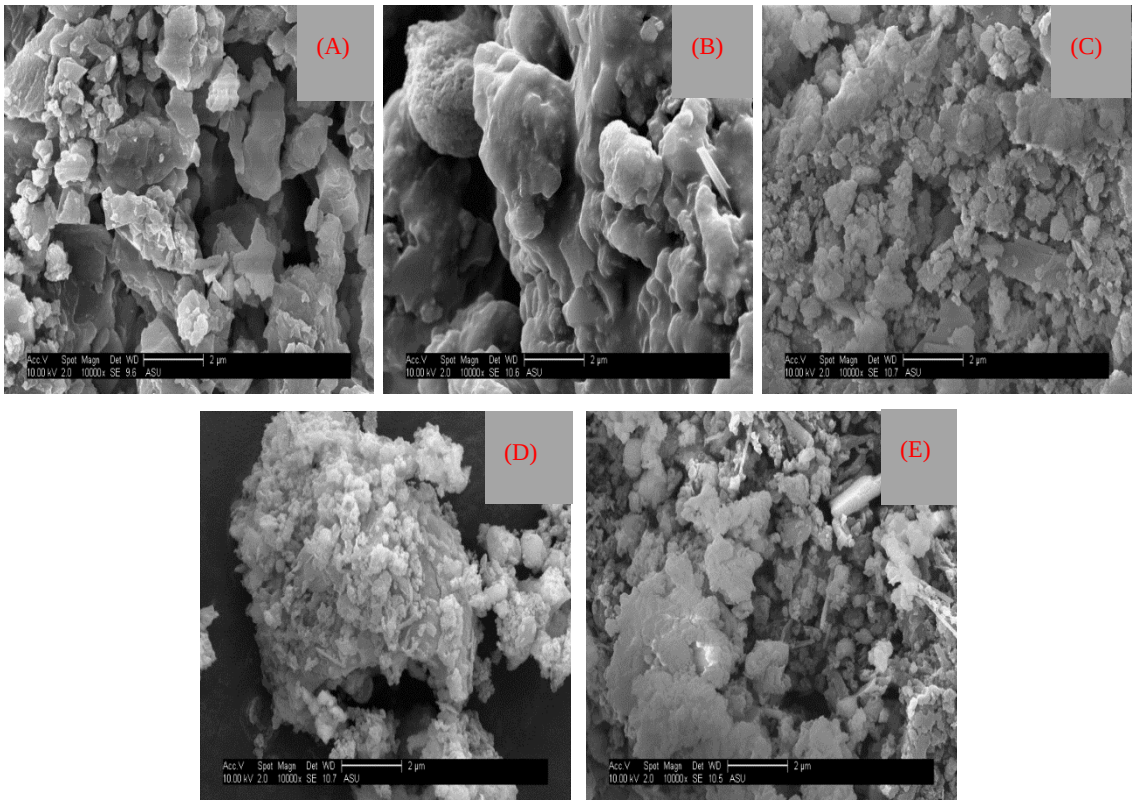

Figure 4.3: SEM images of the biochars produced from HTL at 330 °C; (A): 100 -0 CM-SM (*C. merolae*- Swine manure) biochar, (B): 80 -20 CM-SM biochar, (C): 50 -50 CM-SM biochar, (D): 20 -80 CM-SM biochar, (E): 0 -100 CM-SM biochar

Among the physical properties of the biochar, porosity (surface area, total volume, and average pore size) has a crucial role in the commercialization of biochar. Porosity of biochar plays a major role in the removal of contaminants such as hydrogen sulfide, formaldehyde as well as certain heavy metals; in fact, porosity combined with alkalinity

was shown to be the key for effective removal of formaldehyde (Suresh et al., 2019). The results of the porosity analyses of the biochars are shown in Table 4.3. The results suggest that the surface area of the biochars ranges from 1-5.8 m^2/g, total volume from 0.019-0.045 cm^3/g, and the average pore diameter ranges from 250-360 A°. Based on the studies of average pore size, most of the biochar pores are in the mesoporous range, and hence it can be concluded that the current HTL biochar under study is a mesoporous substance. This also explains the lower surface area. Recent studies (Leng et al., 2015; Ponnusamy et al., 2020; Wang et al., 2015) on the porosity analyses of HTL biochars of different feedstock origins have also shown lower surface area, such as sewage sludge (7.95 m^2/g), spirulina microalgae (1.56 m^2/g), and rice straw (2.72 m^2/g), in comparison to activated carbon (2146 m^2/g).

Table 4.3: Pore textural property analysis of biochars

Biochar	Surface Area$_{Total}$ (m^2/g)	Volume$_{Total}$ (cm^3/g)	Average Pore size (Å)
80-20 CM-SM	1.5	0.019	274.9
50-50 CM-SM	3.7	0.041	250.0
20-80 CM-SM	5.5	0.036	273.1
100-0 CM-SM	3.3	0.029	360.5

0-100 CM-SM	5.8	0.045	300.5

The high ash content of the SM biomass suggests the presence of metal oxides and alkali salts in the biochar. The heavy metals content of the HTL biochar must be carefully monitored prior to using biochar as a soil amendment and further in agricultural and/or animal feed facilities (Dandamudi et al., 2019; Leng et al., 2015; Muppaneni et al., 2017). A detailed list of the content of heavy metals in HTL biochar provides insight into the type of material for storage, thereby factoring the cost of scalability and fouling of the storage vessels. The results in Table 4.4 show the presence of Al, Ca, Cr, Cu, Fe, K, Mg, Mn, Mo, Na, Ni, P, and Zn in the case of CM biomass and biochar. The dominant metals in the CM biomass are P>K>Mg>Fe>Al>Ca. Similar metals are found in the CM biochar, and P is still the dominant inorganic metal. Most of the metals in the CM biomass arise from the cultures and nutrient salts in which they were grown. In the case of SM, the metal content was relatively higher than that of CM biomass. Ca, Fe, P, Al, Cu, Zn are the dominant metals in the SM biomass. It is evident that the high ash content of SM biomass can be related to the dominant alkali and alkaline earth metals. The SM biochar and the rest of the biochar blends also show the presence of the major metals observed in the SM biomass. The high content of the P, Mg, K, and Ca metals in the biochar suggests a possible way of blending with soil to reduce the acidity and can focus on improving the quality of agricultural soil (Fan et al., 2018b, 2018a; Ibrahim et al., 2020). This suggests that majority

of the metals in the biomass are concentrated into the biochar through both direct and co-liquefied HTL.

Table 4.4: Metal concentrations in biomasses, biocrudes, and biochars by ICP-OES

Element	CM biomass	SM biomass	CM 330 biochar	SM 330 biochar	80-20 CM-SM biochar	50-50 CM-SM biochar	20-80 CM-SM biochar
	$mg.kg^{-1}$	$mg.kg^{-1}$	$mg.kg^{-1}$	$mg.kg^{-1}$	$mg.kg^{-1}$	$mg.kg^{-1}$	$mg.kg^{-1}$
Al	428.3	3538	9000.8	18750	7021.0	2340	3847
Ca	365.4	2388	29145.9	13261	49606	11361	18221
Cr	11.4	56	300	128	125	146	222
Cu	338.5	2370	425.3	3940	382	3300	4913
Fe	760.7	12640	20015	16902	9266	20449	21830
K	5818.6	3980.39	12590	4050	1379	6177	5179
Mg	1781.3	19945.43	2000.89	13980	46270	15013	21717

Mn	30.3	1257.56	1289	2145	1152	2180	2060
Mo	3.3	37.30	200.9	47.0	48	40	43
Na	225.0	1150.63	4826	1757	18013	1885	2049
Ni	6.7	29.37	189.21	64	2254	73	118
P	7090.7	19810	80569.36	30000	89985	37298	41593
Sr	n.d.	246.27	n.d.	207	896	211	241
Zn	27.7	1977	899.91	2930	558	2688	3454

n.d.: not detected

4.3.4 Functional groups of the biochars

FT-IR analysis was performed to reveal the functional group characteristics of the individual and blended biochars. Functional group assignments and interpretations were based on the literature from previous studies (Cheng et al., 2017; Nam et al., 2016; Tsai et al., 2012; Vardon et al., 2011). The FT-IR spectra of the biochars are shown in Figure 4. The absorption peaks at 3500-3600 cm^{-1} indicate the -OH stretching from the alcohols. (Leng et al., 2015) reported the presence of oxygen-containing functional groups such as phenols, hydroxyl, carboxyl, and carbonyl. The bands between 2800-3000 cm^{-1} represent the presence of a strong alkane peak with CH_3, CH_2, and CH assignments from the free

fatty acids and/or cellulose, hemicellulose, and lignin. This specific peak was stronger in the 100-0 CM-SM and 80-20 CM-SM biochar. The 1900-2000 bands represent a strong C=C asymmetric stretch from alkenes. The small peaks between 2100-2270 cm^{-1} represents peaks from diimides, azides, and ketenes. These might be arising from the biocrude oil left over in the pores of the biochar after the product separation. The bands between 1600-1670 represent an N-H stretching peak, indicating the presence of cyclic amides in the sample. The peak between 970-1250 cm^{-1} represents a strong C-O bond, showing the presence of carbohydrate derivatives, fatty acid/esters. The absorption band from 550-700 cm^{-1} is an indicative of a strong C-H deformation bond arising from the alkynes.

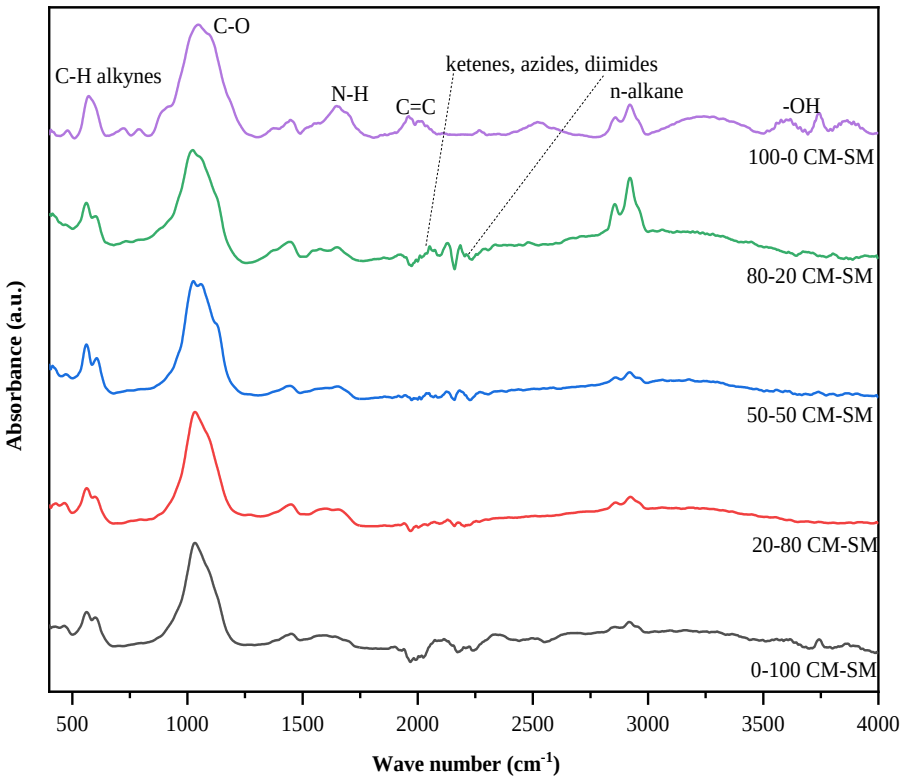

Figure 4.4: FT-IR analysis of the biochars produced at 330 °C; CM-SM (*C. merolae*- Swine manure)

4.3.5 Crystalline structures of the biochar

The biochar samples were analyzed close to the XRD detection limits, and the results in Figure 5 suggest that the presence of various crystalline and semi-crystalline phases

mainly made up of minerals: Si, Al, C, P, O, Ca, Fe, and K. The peaks identified in biochar produced from 0-100 CM-SM suggest that peaks at 26.501° and 20.640° (2θ) belong to quartz (SiO_2; Si on the graph) formed during high-pressure reactions. It is evident that the biochar produced in this work was produced from high-temperature and high-pressure HTL reactions. In the case of 100-0 CM-SM, the peaks at 26.426° and 43.019° (2θ) belong to carbon-graphite (G on the graph), which can be seen from the elemental analysis in Table 4.1. The peaks at 26.492°, 20.801°, and 49.822° (2θ) represent $AlPO_4$ (A on the graph) in its hexagonal form. The $AlPO_4$ seems to be arising from the salts used in the algae cultivation and entering the biochar during the product separation. The rest of the blended biochars also consist of peaks from both quartz (SiO_2) and$AlPO_4$. The Ca in all the biochars was present mostly as $CaCO_3$ and P as $Ca_2P_2O_7$ (Ca on the graph). The presence of quartz and $AlPO_4$ explains the crystalline structure of the biochar; Figure 6 shows the extent of crystallinity in different biochar samples produced. Figure 6 shows that among all the biochars, 100-0 CM-SM (pure algae biochar) has the least crystallinity, followed by the 0-100 CM-SM biochar (pure swine manure biochar). All the biochar samples from the co-liquefaction experiments exhibited higher crystallinity.

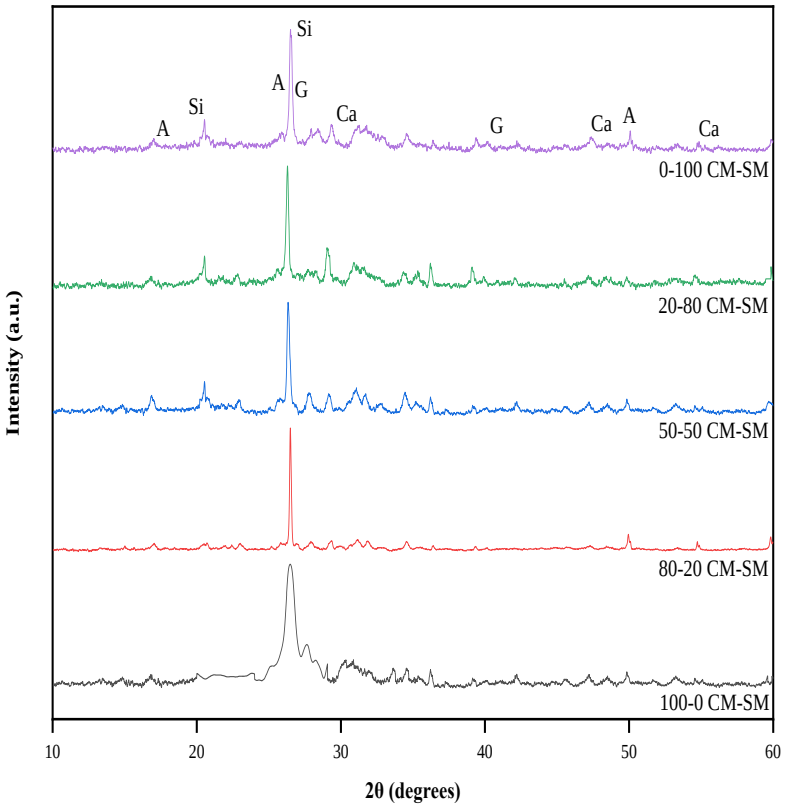

Figure 4.5: XRD analysis of the biochars produced at 330 °C; CM-SM (*C. merolae*- Swine manure)

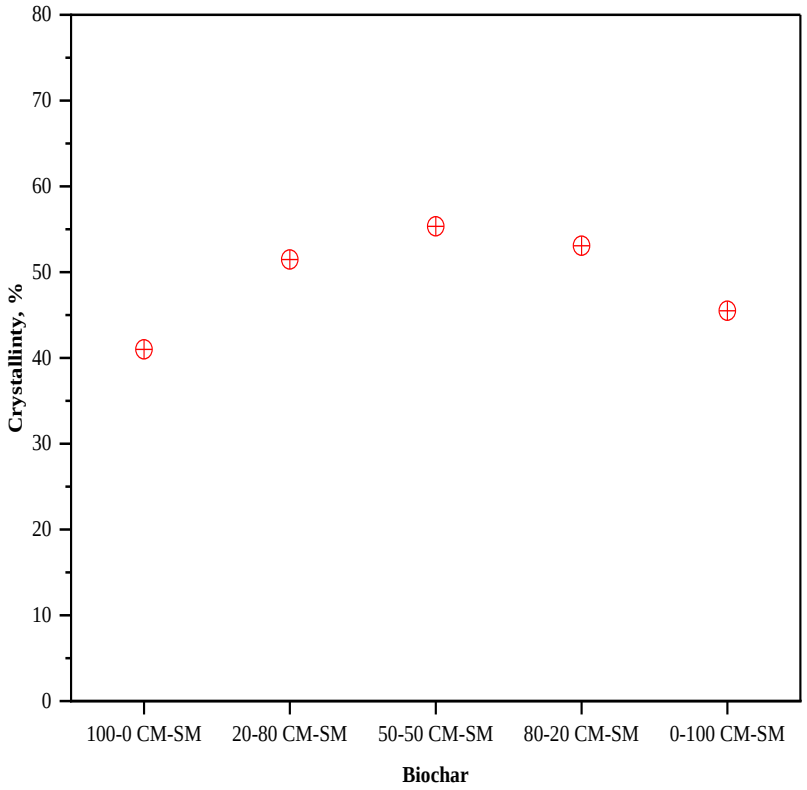

Figure 4.6: Crystallinity distribution in biochars produced at 330 °C; CM-SM (*C. merolae*-Swine manure)

4.4 Applications of biochar

It should be noted that in terms of source dependency of the resulting biochar, even though swine manure composition changes to some extent based on the animal feed, most confined facilities have a relatively consistent diet. In addition, the conversion process reduces the variation by breaking down biomass structures to mostly hydrocarbons. Studies have shown that bio-oils and biochars made from various swine manure sources are quite similar in physicochemical and mechanical properties targeted for construction applications (Fini et al., 2011). The concept of optimizing the biomass value chain rather than maximizing a single product and generating few by-products as waste is the main motivation behind this paper; this is a novel approach to promote the economic viability of the biofuel industry via a multi-product process. For instance, it has been shown that a balanced feedstock of high protein and high lipid from a combination of algae and swine manure can lead to an effective and sustainable hybrid rejuvenator for asphalt application (Pahlavan et al., 2020). Therefore, developing a parallel application for the respective biochar made from swine manure and algae blend would promote biomass value chain and resource conservation.

Based on the analysis results from the physicochemical characterization of the hydrothermally produced biochar, we have identified following plausible applications for

resulting biochar. The high carbon and nitrogen content in conjunction with inorganic metals like P, K, Mg, Ca facilitates the biochar to be added to as an amendment for the soil in agricultural practices (Cao and Harris, 2010; Liang et al., 2014). (Masto et al., 2013) have shown that addition of biochar to soil helps improve the overall health of the soil enzyme activity, seed germination, and soil respiration. Considering the high metal content of biochar, the leachate needs to be evaluated before most biochar applications are suggested. The leachate type and content are highly dependent on the type and method of application. It should be noted that in some cases, construction applications are used to sequester such contaminants due to the confinement capacity of construction materials such as bricks, asphalt concrete, and cement concrete. EPA's Toxicity Characteristic Leaching Procedure (TCLP) is commonly used for novel construction applications to ensure the safety of such usage. In the case of biochar made from swine manure and algae, its porous and inherently functionalized surface can contribute to enhanced interaction with various matrices including but not limited to thermoplastics to reduce the chance of leachate. Our prior studies of biochar in a bituminous matrix showed biochar not only enhanced bitumen properties but also showed high potential to remove select contaminants that encountered. No leachate from biochar itself was detected (Wallace et al., 2017; Walters et al., 2015).

The presence of surface active moieties allows the biochar to be a good adsorbent for removing pollutants and heavy metals from waste waters. (Hu et al., 2019) showed the

adsorption of Cr (VI) and Cu (II) from aqueous solutions by biochar. Biochar can also be co-fed as fuel sources with coal and biomass due to its calorific value and energy recovery (Liu et al., 2013; Waqas et al., 2018) and as a material to produce hydrogen using a membrane reactor (Ibrahim et al., 2020). The presence of various functional groups on biochar makes it promising for the construction application due to the significant potential of biochar to delay aging of bituminous composites via UV blockage and free radical scavenger pathways (Gupta and Kua, 2017; Liu et al., 2015; Walters et al., 2015). It should be noted that for the biochar to work as a free radical scavenger, few functional groups and/or a monolayer covering carbon particles can suffice. It has been documented that the presence of specific functional groups can change the surface properties of biochar from hydrophobic to hydrophilic (Reddy Karnati et al., 2020). The presence of amide functional groups is specially known to interact with free radicals, which in turn can delay their diffusion deep into bitumen to cause further aging (Hung and Fini, 2020; Hung et al., 2019). It has been documented that diffusion of aging products in bituminous composite can be delayed when biochar containing active functional groups is introduced to bitumen (Rajib and Fini, 2020). Biochar is expected to impart some flame-retardant capability. The observed presence of amide functional groups on the surface of our hydrothermally produced biochar may promote as a flame retardant. However, on the other hand, the oxygen content of biochar may negatively affect the latter ability (Nosaka et al., 2020;

Reddy Karnati et al., 2020). The quantification of such capacity is part of the application characterization to be conducted in our follow-up study.

In terms of concrete/construction applications, biochar can reduce shrinkage cracking and assists in improving the durability (Fini, 2019; Ofori-Boadu et al., 2018). Biochar has also been used as a cement replacement for internal curing in ultra-high performance concrete and also used as carbon sequestering and green additive in cement mortar and cement-based composites (Dixit et al., 2019; Gupta et al., 2018; Wang et al., 2020). The use of biochar in the thermoplastic composite as reinforcement and filler could be another novel application. The prior study used coal as filler in high-density polyethylene (HDPE) composites (Phillips et al., 2019); the performance of such composites depends not only on surface functional groups of biochar but also on the polymer matrix. Interaction between the two can be promoted using compatibilizer to avoid loss of mechanical properties; in our prior study, we applied bio-compatibilizer to enhance the interaction of montmorillonite clay with Linear Low-density polyethylene (LLDPE) (Fini et al., 2017; Høgsaa et al., 2018). Use of biochar as a filler and reinforcement could render new applications for biochar to promote resource conservation and bio-mass value chain.

Table 4.5: Overview of Biochar Applications

Applications of biochar	Findings	References
Soil Amendment or conditioner	Abundant in P, K, Ca, Mg; improved particle size distribution, pore size, swelling-shrinking dynamics, permeability, density, packing, soil health, and fertility; sequestrating atmospheric carbon into the soil	(Downie et al., 2009; Lehmann and Joseph, 2015; Masto et al., 2013; Verheijen et al., 2010)
Energy or Fuel	Hydrogen production, high energy density to be used in coal-fired broilers or as a co-feed with biomass	(Ibrahim et al., 2020; Liu et al., 2013; Waqas et al., 2018)

Water Treatment	Removal of micropollutants, organic, and inorganic pollutants; improved turbidity removal in aquaponics	(Khiari et al., 2020; Qambrani et al., 2017; Thompson et al., 2016)
Construction	Improved shrinkage of cracks and assists in improving the durability by UV blockage and free radical scavenger pathways; cement replacement for internal curing in ultra-high-performance concrete, used as carbon sequestering and green additive in cement mortar and cement-based composites	(Dixit et al., 2019; Gupta et al., 2018; Gupta and Kua, 2017; Ofori-Boadu et al., 2018)

Energy storage and conversion	Hydrogen storage and production, oxygen electrocatalysts, fuel cell technology, super capacitors, and lithium ion batteries. Used in the production of performing cathode electrodes.	(Bartoli et al., 2020; Liu et al., 2019; Rahman et al., 2020)
Composites	Improves strength and water tightness, mitigating autogenous shrinkage of cement materials, improved sound absorption	(Bartoli et al., 2020; Cuthbertson et al., 2019; Oancea et al., 2018)
Adsorptive materials	Involved in electron-donor for the reduction of Cr(VI) to Cr(III) by adsorbing onto a carbonaceous structure,	(Brum et al., 2010; Rengaraj et al., 2001)

	copper adsorption, adsorption of neat biochar particles was also used to clean Cd(III), Pb(II), Cu(II), Zn(II), Sm(III)

4.5 Conclusions

This paper presents a comprehensive physicochemical and surface characterization of biochar obtained from hydrothermal liquefaction of microalgae *Cyanidioschyzon merolae* and swine manure. While due to the presence of heavy metals and the lower higher heating value (HHV), biochar may not qualify as fuel (Baxter et al., 1998), biochar's applications may present new opportunities to enhance sustainability in the construction industry (Walter et al., 2012). Specifically, our study outcome shows that due to the presence of diverse surface functional groups, the high volatile matter, and the abundance of redox moieties on the surface of biochar, the biochar made from algae and swine manure has a great potential for use as a free-radical scavenger in asphalt roads and roofing shingles. The following specific conclusions were drawn from this study:

- Hydrothermal liquefaction of algae and swine manure blend at 330 °C yielded biochars in the range of 4.5-33.2 wt. % and biocrude in the range of 31.5-6.27 wt. %.
- The biochars from the individual liquefaction and those from the co-liquefaction exhibited a similar thermal degradation behavior under the presence of nitrogen (N_2), with 100-0 CM-SM biochar having the highest volatile content (59.27 %).

- The elemental and ultimate analysis of the co-liquefied biochars found that 80-20 CM-SM has a carbon content of 29.97 wt. % and the highest HHV of 10.87 MJ/kg compared with other scenarios.
- In the case of blended feedstocks, the O/C and H/C are indicative of demethanation. HTL biochar has a surface area of up to 5.8 m^2/g and is considered as a mesoporous substance (50nm > pores > 2nm). Among nutrients, P, Mg, and K were found to be dominant in all studied biochar.
- The functional group analysis using FT-IR revealed the presence of oxygen-containing groups, alkenes, diimides, azides, and ketenes, cyclic amides, and carbohydrate derivatives.
- XRD analysis showed the presence of quartz (SiO_2), graphitic carbon, and hexagonal $AlPO_4$ with trace amounts of $CaCO_3$, and $Ca_2P_2O_7$.

4.6 References

Bartoli, M., Giorcelli, M., Jagdale, P., Rovere, M., Tagliaferro, A., 2020. A review of non-soil biochar applications. Materials (Basel). 13, 261.

Baxter, L.L., Miles, T.R., Miles Jr, T.R., Jenkins, B.M., Milne, T., Dayton, D., Bryers, R.W., Oden, L.L., 1998. The behavior of inorganic material in biomass-fired power boilers: field and laboratory experiences. Fuel Process. Technol. 54, 47–78.

Brum, M.C., Capitaneo, J.L., Oliveira, J.F., 2010. Removal of hexavalent chromium from water by adsorption onto surfactant modified montmorillonite. Miner. Eng. 23, 270–272.

Cantero-Tubilla, B., Cantero, D.A., Martinez, C.M., Tester, J.W., Walker, L.P., Posmanik, R., 2018. Characterization of the solid products from hydrothermal liquefaction of waste feedstocks from food and agricultural industries. J. Supercrit. Fluids. https://doi.org/10.1016/j.supflu.2017.07.009

Cantrell, K.B., Hunt, P.G., Uchimiya, M., Novak, J.M., Ro, K.S., 2012. Impact of pyrolysis temperature and manure source on physicochemical characteristics of biochar. Bioresour. Technol. 107, 419–428.

Cao, X., Harris, W., 2010. Properties of dairy-manure-derived biochar pertinent to its potential use in remediation. Bioresour. Technol. 101, 5222–5228.

Cheng, F., Cui, Z., Chen, L., Jarvis, J., Paz, N., Schaub, T., Nirmalakhandan, N., Brewer,

C.E., 2017. Hydrothermal liquefaction of high-and low-lipid algae: Bio-crude oil chemistry. Appl. Energy 206, 278–292.

Chisti, Y., 2007. Biodiesel from microalgae. Biotechnol. Adv. 25, 294–306.

Christensen, E., Sudasinghe, N., Dandamudi, K.P.R., Sebag, R., Schaub, T., Laurens, L.M.L., 2015. Rapid Analysis of Microalgal Triacylglycerols with Direct-Infusion Mass Spectrometry. Energy and Fuels 29. https://doi.org/10.1021/acs.energyfuels.5b01205

Coats, A.W., Redfern, J.P., 1963. Thermogravimetric analysis. A review. Analyst 88, 906–924.

Cuthbertson, D., Berardi, U., Briens, C., Berruti, F., 2019. Biochar from residual biomass as a concrete filler for improved thermal and acoustic properties. Biomass and Bioenergy 120, 77–83.

Dandamudi, K.P.R., Muhammed Luboowa, K., Laideson, M., Murdock, T., Seger, M., McGowen, J., Lammers, P.J., Deng, S., 2020. Hydrothermal Liquefaction of Cyanidioschyzon merolae and Salicornia bigelovii Torr.: The interaction effect on product distribution and chemistry. Fuel 277. https://doi.org/10.1016/j.fuel.2020.118146

Dandamudi, K.P.R., Muppaneni, T., Markovski, J.S., Lammers, P., Deng, S., 2019. Hydrothermal liquefaction of green microalga Kirchneriella sp. under sub-and

super-critical water conditions. Biomass and bioenergy 120, 224–228.

Dandamudi, K.P.R., Muppaneni, T., Sudasinghe, N., Schaub, T., Holguin, F.O., Lammers, P.J., Deng, S., 2017. Co-liquefaction of mixed culture microalgal strains under sub-critical water conditions. Bioresour. Technol. 236. https://doi.org/10.1016/j.biortech.2017.03.165

Dixit, A., Gupta, S., Dai Pang, S., Kua, H.W., 2019. Waste Valorisation using biochar for cement replacement and internal curing in ultra-high performance concrete. J. Clean. Prod. 238, 117876.

Downie, A., Crosky, A., Munroe, P., 2009. Physical properties of biochar. Biochar Environ. Manag. Sci. Technol. 1.

Fan, W., Bryant, L., Srisupan, M., Trembly, J., 2018a. An assessment of hydrothermal treatment of dairy waste as a tool for a sustainable phosphorus supply chain in comparison with commercial phosphatic fertilizers. Clean Technol. Environ. Policy 20, 1467–1478.

Fan, W., Srisupan, M., Bryant, L., Trembly, J.P., 2018b. Utilization of fly ash as pH adjustment for efficient immobilization and reutilization of nutrients from swine manure using hydrothermal treatment. Waste Manag. 79, 709–716.

Fini, E.H., 2019. Preparation and uses of bio-adhesives.

Fini, E.H., Høgsaa, B., Christiansen, J.D.C., Sanporean, C.-G., Jensen, E.A., Mousavi,

M., Pahlavan, F., 2017. Multiscale investigation of a bioresidue as a novel intercalant for sodium montmorillonite. J. Phys. Chem. C 121, 1794–1802.

Fini, E.H., Kalberer, E.W., Shahbazi, A., Basti, M., You, Z., Ozer, H., Aurangzeb, Q., 2011. Chemical characterization of biobinder from swine manure: Sustainable modifier for asphalt binder. J. Mater. Civ. Eng. 23, 1506–1513.

Gupta, S., Kua, H.W., 2017. Factors determining the potential of biochar as a carbon capturing and sequestering construction material: critical review. J. Mater. Civ. Eng. 29, 4017086.

Gupta, S., Kua, H.W., Low, C.Y., 2018. Use of biochar as carbon sequestering additive in cement mortar. Cem. Concr. Compos. 87, 110–129.

Høgsaa, B., Fini, E.H., Christiansen, J. de C., Hung, A., Mousavi, M., Jensen, E.A., Pahlavan, F., Pedersen, T.H., Sanporean, C.-G., 2018. A novel bioresidue to compatibilize sodium montmorillonite and linear low density polyethylene. Ind. Eng. Chem. Res. 57, 1213–1224.

Hu, X., Song, J., Wang, H., Zhang, W., Wang, B., Lyu, W., Wang, Q., Liu, P., Chen, L., Xing, J., 2019. Adsorption of Cr (VI) and Cu (II) from aqueous solutions by biochar derived from Chaenomeles sinensis seed. Water Sci. Technol. 80, 2260–2272.

Hung, A., Fini, E.H., 2020. Surface Morphology and Chemical Mapping of UV-Aged Thin Films of Bitumen. ACS Sustain. Chem. Eng. 8, 11764–11771.

Hung, A.M., Kazembeyki, M., Hoover, C.G., Fini, E.H., 2019. Evolution of Morphological and Nanomechanical Properties of Bitumen Thin Films as a Result of Compositional Changes Due to Ultraviolet Radiation. ACS Sustain. Chem. Eng. 7, 18005–18014.

Ibrahim, A.F.M., Dandamudi, K.P.R., Deng, S., Lin, J.Y.S., 2020. Pyrolysis of hydrothermal liquefaction algal biochar for hydrogen production in a membrane reactor. Fuel 265, 116935. https://doi.org/https://doi.org/10.1016/j.fuel.2019.116935

Jin, B., Duan, P., Xu, Y., Wang, F., Fan, Y., 2013. Co-liquefaction of micro- and macroalgae in subcritical water. Bioresour. Technol. https://doi.org/10.1016/j.biortech.2013.09.045

Khiari, Z., Alka, K., Kelloway, S., Mason, B., Savidov, N., 2020. Integration of Biochar Filtration into Aquaponics: Effects on Particle Size Distribution and Turbidity Removal. Agric. Water Manag. 229, 105874.

Lehmann, J., Joseph, S., 2015. Biochar for environmental management: an introduction, in: Biochar for Environmental Management. Routledge, pp. 33–46.

Leng, L., Yuan, X., Huang, H., Wang, H., Wu, Z., Fu, L., Peng, X., Chen, X., Zeng, G., 2015. Characterization and application of bio-chars from liquefaction of microalgae, lignocellulosic biomass and sewage sludge. Fuel Process. Technol. 129, 8–14.

Liang, Y., Cao, X., Zhao, L., Xu, X., Harris, W., 2014. Phosphorus release from dairy

manure, the manure-derived biochar, and their amended soil: Effects of phosphorus nature and soil property. J. Environ. Qual. 43, 1504–1509.

Liu, W.-J., Jiang, H., Yu, H.-Q., 2019. Emerging applications of biochar-based materials for energy storage and conversion. Energy Environ. Sci. 12, 1751–1779.

Liu, W.-J., Jiang, H., Yu, H.-Q., 2015. Development of biochar-based functional materials: toward a sustainable platform carbon material. Chem. Rev. 115, 12251–12285.

Liu, Z., Quek, A., Hoekman, S.K., Balasubramanian, R., 2013. Production of solid biochar fuel from waste biomass by hydrothermal carbonization. Fuel 103, 943–949.

Lozano, E.M., Pedersen, T.H., Rosendahl, L.A., 2020. Integration of hydrothermal liquefaction and carbon capture and storage for the production of advanced liquid biofuels with negative CO2 emissions. Appl. Energy 279, 115753.

Masto, R.E., Kumar, S., Rout, T.K., Sarkar, P., George, J., Ram, L.C., 2013. Biochar from water hyacinth (Eichornia crassipes) and its impact on soil biological activity. Catena 111, 64–71.

Meng, J., Wang, L., Liu, X., Wu, J., Brookes, P.C., Xu, J., 2013. Physicochemical properties of biochar produced from aerobically composted swine manure and its potential use as an environmental amendment. Bioresour. Technol. 142, 641–646.

Miranda, R., Bustos-Martinez, D., Blanco, C.S., Villarreal, M.H.G., Cantú, M.E.R., 2009.

Pyrolysis of sweet orange (Citrus sinensis) dry peel. J. Anal. Appl. Pyrolysis. https://doi.org/10.1016/j.jaap.2009.06.001

Mohanty, P., Nanda, S., Pant, K.K., Naik, S., Kozinski, J.A., Dalai, A.K., 2013. Evaluation of the physiochemical development of biochars obtained from pyrolysis of wheat straw, timothy grass and pinewood: effects of heating rate. J. Anal. Appl. Pyrolysis 104, 485–493.

Muppaneni, T., Reddy, H.K., Patil, P.D., Dailey, P., Aday, C., Deng, S., 2012. Ethanolysis of camelina oil under supercritical condition with hexane as a co-solvent. Appl. Energy 94, 84–88.

Muppaneni, T., Reddy, H.K., Selvaratnam, T., Dandamudi, K.P.R., Dungan, B., Nirmalakhandan, N., Schaub, T., Omar Holguin, F., Voorhies, W., Lammers, P., Deng, S., 2017. Hydrothermal liquefaction of Cyanidioschyzon merolae and the influence of catalysts on products. Bioresour. Technol. 223. https://doi.org/10.1016/j.biortech.2016.10.022

Naik, S., Goud, V. V, Rout, P.K., Jacobson, K., Dalai, A.K., 2010. Characterization of Canadian biomass for alternative renewable biofuel. Renew. energy 35, 1624–1631.

Nam, H., Choi, J., Capareda, S.C., 2016. Comparative study of vacuum and fractional distillation using pyrolytic microalgae (Nannochloropsis oculata) bio-oil. Algal Res. 17, 87–96.

Nosaka, T., Lankone, R., Westerhoff, P., Herckes, P., 2020. Flame retardant performance of carbonaceous nanomaterials on polyester fabric. Polym. Test. 106497.

Oancea, I., Bujoreanu, C., Budescu, M., Benchea, M., Grădinaru, C.M., 2018. Considerations on sound absorption coefficient of sustainable concrete with different waste replacements. J. Clean. Prod. 203, 301–312.

Ofori-Boadu, A.N., Abrokwah, R.Y., Gbewonyo, S., Fini, E., 2018. Effect of swine-waste bio-char on the water absorption characteristics of cement pastes. Int. J. Build. Pathol. Adapt.

Pahlavan, F., Rajib, A., Deng, S., Lammers, P., Fini, E.H., 2020. Investigation of Balanced Feedstocks of Lipids and Proteins To Synthesize Highly Effective Rejuvenators for Oxidized Asphalt. ACS Sustain. Chem. Eng.

Patil, P.D., Dandamudi, K.P.R., Wang, J., Deng, Q., Deng, S., 2018. Extraction of bio-oils from algae with supercritical carbon dioxide and co-solvents. J. Supercrit. Fluids 135, 60–68. https://doi.org/https://doi.org/10.1016/j.supflu.2017.12.019

Peng, W., Wu, Q., Tu, P., Zhao, N., 2001. Pyrolytic characteristics of microalgae as renewable energy source determined by thermogravimetric analysis. Bioresour. Technol. https://doi.org/10.1016/S0960-8524(01)00072-4

Phillips, L.N., Kappagantula, K.S., Trembly, J.P., 2019. Mechanical performance of thermoplastic composites using bituminous coal as filler: Study of a potentially

sustainable end-use application for Appalachian coal. Polym. Compos. 40, 591–599.

Ponnusamy, V.K., Nagappan, S., Bhosale, R.R., Lay, C.-H., Nguyen, D.D., Pugazhendhi, A., Woong, C.S., Kumar, G., 2020. Review on sustainable production of biochar through hydrothermal liquefaction: Physico-chemical properties and applications. Bioresour. Technol. 123414.

Qambrani, N.A., Rahman, M.M., Won, S., Shim, S., Ra, C., 2017. Biochar properties and eco-friendly applications for climate change mitigation, waste management, and wastewater treatment: A review. Renew. Sustain. Energy Rev. 79, 255–273.

Radis Steinmetz, R.L., Kunz, A., Dressler, V.L., de Moraes Flores, É.M., Figueiredo Martins, A., 2009. Study of metal distribution in raw and screened swine manure. CLEAN–Soil, Air, Water 37, 239–244.

Rahman, M.Z., Edvinsson, T., Kwong, P., 2020. Biochar for Electrochemical Applications. Curr. Opin. Green Sustain. Chem.

Rajib, A., Fini, E.H., 2020. Inherently Functionalized Carbon from Lipid and Protein-Rich Biomass to Reduce Ultraviolet-Induced Damages in Bituminous Materials. ACS Omega. https://doi.org/10.1021/acsomega.0c03514

Reddy Karnati, S., Høgsaa, B., Zhang, L., Fini, E.H., 2020. Developing carbon nanoparticles with tunable morphology and surface chemistry for use in construction. Constr. Build. Mater. 262, 120780.

https://doi.org/https://doi.org/10.1016/j.conbuildmat.2020.120780

Rengaraj, S., Yeon, K.-H., Moon, S.-H., 2001. Removal of chromium from water and wastewater by ion exchange resins. J. Hazard. Mater. 87, 273–287.

Ross, A.B., Biller, P., Kubacki, M.L., Li, H., Lea-Langton, A., Jones, J.M., 2010. Hydrothermal processing of microalgae using alkali and organic acids. Fuel 89, 2234–2243.

Savage, P.E., Hestekin, J.A., 2013. A perspective on algae, the environment, and energy. Environ. Prog. Sustain. Energy 32, 877–883.

Sudasinghe, N., Cort, J.R., Hallen, R., Olarte, M., Schmidt, A., Schaub, T., 2014. Hydrothermal liquefaction oil and hydrotreated product from pine feedstock characterized by heteronuclear two-dimensional NMR spectroscopy and FT-ICR mass spectrometry. Fuel 137, 60–69.

Sues, A., Juraščík, M., Ptasinski, K., 2010. Exergetic evaluation of 5 biowastes-to-biofuels routes via gasification. Energy 35, 996–1007.

Suresh, S., Kante, K., Fini, E.H., Bandosz, T.J., 2019. Combination of alkalinity and porosity enhances formaldehyde adsorption on pig manure-derived composite adsorbents. Microporous Mesoporous Mater. 286, 155–162.

Thompson, K.A., Shimabuku, K.K., Kearns, J.P., Knappe, D.R.U., Summers, R.S., Cook, S.M., 2016. Environmental comparison of biochar and activated carbon for tertiary

wastewater treatment. Environ. Sci. Technol. 50, 11253–11262.

Toor, S.S., Reddy, H., Deng, S., Hoffmann, J., Spangsmark, D., Madsen, L.B., Holm-Nielsen, J.B., Rosendahl, L.A., 2013. Hydrothermal liquefaction of Spirulina and Nannochloropsis salina under subcritical and supercritical water conditions. Bioresour. Technol. 131, 413–419.

Toor, S.S., Rosendahl, L., Rudolf, A., 2011. Hydrothermal liquefaction of biomass: a review of subcritical water technologies. Energy 36, 2328–2342.

Tsai, W.-T., Liu, S.-C., Chen, H.-R., Chang, Y.-M., Tsai, Y.-L., 2012. Textural and chemical properties of swine-manure-derived biochar pertinent to its potential use as a soil amendment. Chemosphere 89, 198–203.

Vardon, D.R., Sharma, B.K., Scott, J., Yu, G., Wang, Z., Schideman, L., Zhang, Y., Strathmann, T.J., 2011. Chemical properties of biocrude oil from the hydrothermal liquefaction of Spirulina algae, swine manure, and digested anaerobic sludge. Bioresour. Technol. 102, 8295–8303.

Verheijen, F., Jeffery, S., Bastos, A.C., Van der Velde, M., Diafas, I., 2010. Biochar application to soils. A Crit. Sci. Rev. Eff. soil Prop. Process. Funct. EUR 24099, 162.

Wallace, R., Suresh, S., Fini, E.H., Bandosz, T.J., 2017. Efficient Air Desulfurization Catalysts Derived from Pig Manure Liquefaction Char. C—Journal Carbon Res. 3,

37.

Walters, R., Begum, S.A., Fini, E.H., Abu-Lebdeh, T.M., 2015. Investigating bio-char as flow modifier and water treatment agent for sustainable pavement design. Am. J. Eng. Appl. Sci. 8, 138–146.

Wang, J., Krishna, R., Yang, J., Dandamudi, K.P.R., Deng, S., 2015. Nitrogen-doped porous carbons for highly selective CO<inf>2</inf> capture from flue gases and natural gas upgrading. Mater. Today Commun. 4. https://doi.org/10.1016/j.mtcomm.2015.06.009

Wang, J., Peng, X., Chen, X., Ma, X., 2019. Co-liquefaction of low-lipid microalgae and starch-rich biomass waste: The interaction effect on product distribution and composition. J. Anal. Appl. Pyrolysis 139, 250–257.

Wang, L., Chen, L., Tsang, D.C.W., Guo, B., Yang, J., Shen, Z., Hou, D., Ok, Y.S., Poon, C.S., 2020. Biochar as green additives in cement-based composites with carbon dioxide curing. J. Clean. Prod. 258, 120678.

Waqas, M., Aburiazaiza, A.S., Miandad, R., Rehan, M., Barakat, M.A., Nizami, A.S., 2018. Development of biochar as fuel and catalyst in energy recovery technologies. J. Clean. Prod. 188, 477–488.

Wiedemeier, D.B., Abiven, S., Hockaday, W.C., Keiluweit, M., Kleber, M., Masiello, C.A., McBeath, A. V, Nico, P.S., Pyle, L.A., Schneider, M.P.W., 2015. Aromaticity

and degree of aromatic condensation of char. Org. Geochem. 78, 135–143.

Zhang, B., Chen, J., He, Z., Chen, H., Kandasamy, S., 2019. Hydrothermal liquefaction of fresh lemon-peel: Parameter optimisation and product chemistry. Renew. Energy 143, 512–519.

CHAPTER 5: RECYCLE OF NITROGEN AND PHOSPHORUS IN HYDROTHERMAL LIQUEFACTION BIOCHAR FROM *GALDIERIA SULPHURARIA* TO CULTIVATE MICROALGAE

5.1 Introduction

Meeting an increasing energy demand of an ever-growing population is a prominent obstacle in the way of modernization. Bioenergy is considered a vital component in creating a possible pathway to minimize greenhouse gas (GHG) emissions. The carbon dioxide emitted during the combustion can be recycled back to the cultivation facilities leading to a reduction in the net production of GHG (Dandamudi et al., 2020; Demirbas, 2009). The recent steps taken in bioenergy made algal sources of fuels at the forefront due to its potential as a feedstock to counter the effects of food versus fuel crisis and deforestation (Aysu et al., 2015; Chisti, 2007). Microalgae can be grown in multiple water resources and are shown to capture carbon from the atmosphere effectively and are estimated to sequester ~1.8 kg of CO_2 for 1 kg of algae grown (Dandamudi et al., 2019; Lammers et al., 2017; Selvaratnam et al., 2015b).

The United States annual energy demand was at 101.3 quadrillions BTU in 2019 (U.S. EIA and U.S. Energy Information Administration (EIA), 2019). If at least 10 % of the demand were met using bioenergy from algae, the phosphorous requirement would be 294-

kilotonnes**.** The agriculture sector uses the majority (~90 %) of the global extracted phosphorous for fertilizing the crops (Cisse and Mrabet, 2004; Karbakhshravari et al., 2020). Bouwman et al. (Bouwman et al., 2013) projected that the worldwide demand for phosphorous in 2050 would be 24 million tons per year. Phosphorous being a major mined element, this demand alone would spike the prices of the mineral and hence, warranting the need for the recycle step in a bio-refinery plant.

The thermochemical generation of usable energy products from algae has been proven possible by pyrolysis (Bridgwater, 2012; Collard and Blin, 2014), hydrothermal liquefaction (HTL) (Dandamudi et al., 2019), gasification (Zhan et al., 2020), and combustion (Gai et al., 2015; Toor et al., 2013). Among the available thermochemical conversion techniques, HTL has gained a lot of prominence due to its ability to use wet biomass (Muppaneni et al., 2017; Reddy et al., 2014). Hydrothermal liquefaction (HTL) is a thermochemical process employing an elevated temperature and pressure to convert wet biomass into energy-intensive liquid fuel feedstock (biocrude), a carbon-rich water phase, and solid biochar under subcritical water condition (Dandamudi et al., 2020; Muppaneni et al., 2017). When water is heated under pressure its dielectric constant and density change, resulting in a change in its solvent and reactant properties to promote chemical deconstruction of biomass (Kruse and Dinjus, 2007). Recent studies have shown the production of HTL products (biocrude, biochar, water-soluble compounds, and gaseous phase) from an individual-, co-liquefaction of algae species (Ikenaga et al., 2001; Wang et

al., 2019) with or without using homogeneous catalysts (Muppaneni et al., 2017). Earlier, a lot of emphases was given to the production, characterization, and energy content of biocrude oil. The analyzed biocrude oil was upgraded into final fuel using hydrogen (Xu et al., 2018) and/or blended with recycled asphalt as a sustainable hybrid rejuvenator (Samieadel et al., 2020). Lately, it has been realized that the economic value of other by-products, such as biochar and water-soluble compounds, plays a vital role in the circular economy of the whole biofuel industry (Beal et al., 2018). This also improved the recycling of nutrients into the algal cultivation network. One of the first-ever reported works on aqueous phase recycle from liquefaction was in 2013 by *Alba et al.* (Alba et al., 2013). The recycling of the HTL aqueous phase in the growth of algal species was discussed by Selvaratnam et al. on *G. sulphuraria* (Selvaratnam et al., 2015a, 2015b). Further, a study of polycultures for HTL aqueous phase recycle was reported by Godwin et al. (Godwin et al., 2017) used a polyculture consisting of *Ankistrodesmus falcatus, Chlorella sorokiniana, Pediastrum duplex, Scenedesmus acuminatus, Scenedesmus ecornis,* and *Selenastrum capricornutum*. As mentioned, extensive research works have been published on the HTL product applications of the biocrude and aqueous phase. The applications of HTL biochar has been vastly limited to the application in agriculture as a soil amendment (Ibrahim et al., 2020) and water treatment (Son et al., 2018). Despite possessing high phosphorous (1.7-16.1 wt. %) and nitrogen (1.1-4.0 wt.%) content, HTL biochar was never investigated for recovering and re-using nutrients from it to grow microalgae.

Herein, we present work to study the nutrient content and the viability of its recovery from the HTL biochar. It is hypothesized that nutrients from the HTL biochar can be leached and re-used to cultivate microalgae. The direct utilization reduces the number of steps within the plant and overhead costs for incorporating such a recycle step in the process. Further, a low energy recycling step would reduce the energy demand for mining and processing these nutrients. The possibility of nutrient recovery prior to many of these proven uses improves revenue generation from HTL. This, in turn, is expected to reduce the cost to produce a gallon of biofuel. The implemenation of this technology credits for techno-economic analysis by minimizing waste byproduct and phosphorous fertilizer saving. This improves the value chain of the biomass conversion and product technology

The objectives of the study include:

1. Testing the leaching characteristic of algal biochar with multiple pH values of media ranging from 0.5-7.0 (0.5, 1.0, 2.5, 7.0) and controls of water at pH of 2.5 and 7.0
2. The growth experiments of GS in 96 well plate and 16 mm tubular reactor to monitor growth differences
3. Evaluating the ultimate and metal content of the product stream to find a mass balance

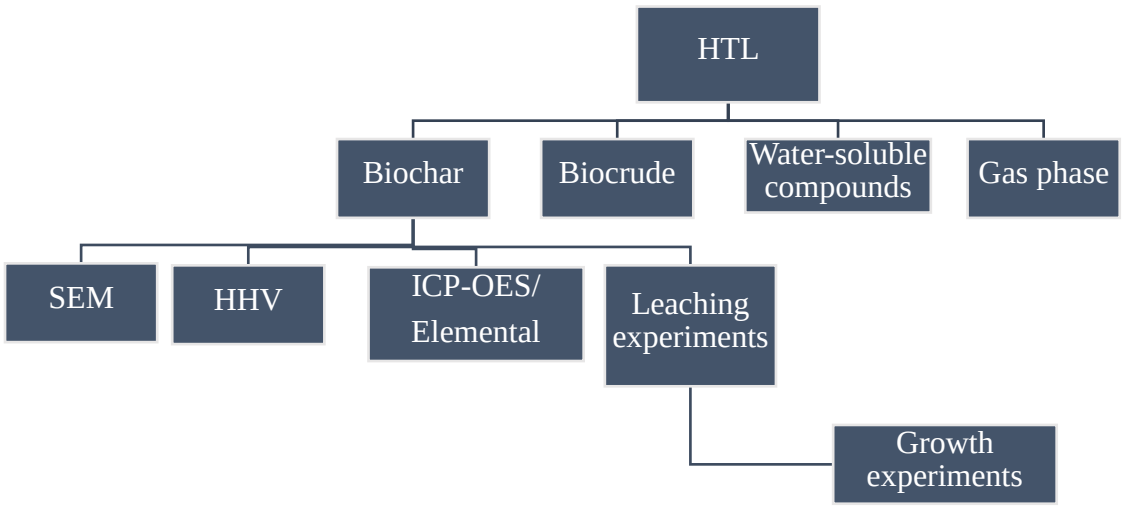

Figure 5.1: Experiment Plan of the Study

5.2 Materials and Methods

Figure 5.1 shows the detailed experiment plan including different tests performed on biochar including SEM, HHV by bomb calorimeter, and elemental analysis and metal content by CHN/O analyzer and ICP-OES, respectively. The specific leaching and regrowth methods are described in later sections.

5.2.1 Algae Strain collection and maintenance

The experiments in this study were performed with the red algae GS (*G. sulphuraria*; CCMEE 5587.1) (Dandamudi et al., 2017). The algae cultures were scaled up from single colonies to tissue culture flasks, and axenic *G. sulphuraria* (5587.1) cultures were verified by sequencing regions of the 18S rRNA and RuBisCo LSU genes (Gross et al., 2001; Lammers et al., 2017). A cleaved amplified polymorphic sequence (CAPS) method was developed for *G. sulphuraria* (5587.1) using these markers as a diagnostic tool to ensure cultures were not compromised throughout the scale-up process and during experiments (data not shown). The axenic stock cultures were maintained, as mentioned in a previous study (Dandamudi et al., 2017). A modified Cyanidium medium (CM) (Andersen, 2005) at pH 2.5 was used for verification, scale-up, and experiments.

For each experiment, axenic stock cultures were scaled up indoors from the tissue culture flasks to 15 L vertical panels. The cultures were supplemented with 2 % CO_2 and maintained at 40 ºC under a 14/10 h light (450 μmol photons m^{-2} s^{-1})/dark cycle. Fifteen-liter indoor panels were then used to inoculate three 4x4' outdoor vertical panels (50L; 4cm light path), which were then allowed to grow to ~2 g/L. These cultures were pooled and used to inoculate 48' vertical panels (1200 L; 10 cm light path; starting density: 0.25 g L^{-1}). This culture grew 0.08 g L^{-1} d^{-1}, and the slurry was harvested at a final density of 3 g L^{-1}. The slurry was concentrated using a centrifuge, as mentioned in (Dandamudi et al.,

2020). The concentrated biomass (~30 % solids) was stored at -20 ºC to be used for further analysis and to produce HTL products.

5.2.2 Hydrothermal liquefaction of GS and biochar collection

HTL reaction conditions such as temperature, pressure, and residence time play a crucial role in the conversion of biomass into products (Dandamudi et al., 2020; Muppaneni et al., 2017). The optimum temperature for liquefaction of *G. sulphuraria* to produce maximum bio-crude was reported to be between 300 and 350 °C (Dandamudi et al., 2017; Selvaratnam et al., 2015a). The percentage of solid residues produced from the process informed to decrease with temperature and reported lowest at operational conditions above 300 °C (Toor et al., 2013). GS was subjected to HTL at 300 °C, 30 min residence time, and 20 wt. % solid loading. The reactants were stirred continuously in a 250 ml Parr Instrument company 4576A stainless steel benchtop reactor with a 4843-controller. The detailed procedure about the experimentation, ramp rate, and product separation and product storage was mentioned in a previous study (Dandamudi et al., 2020). The gaseous products from HTL were not collected due to a limitation in the experimental setup. The gaseous yield and losses were measured as the difference of other significant products from the weight of dried microalgae used in each run. The HTL experiments were done in replicates (n=5), and the mean values for the product yields were reported. Following the separation protocol, the biochar was collected and stored in glass vials for leaching experiments.

5.2.3 Analytical analysis of biomass and HTL products

The proximate and biochemical analysis of the biomass (GS) were performed based on the methods mentioned elsewhere (Dandamudi et al., 2020; Muppaneni et al., 2017). The ultimate study including elemental composition (C, H, N, S, and O) and calorific value (Higher Heating Value, HHV (MJ/kg)) were measured based on methods mentioned in (Patil et al., 2018; Wang et al., 2015). Microalgae, HTL biocrude, and biochar were digested in a CEM Mars 6 microwave digestor (CEM Corporation, Matthews, North Carolina, USA). The digested samples were analyzed for the presence of inorganic trace metals using Thermo Fischer iCAP 6300 ICP-OES (Inductively Coupled Plasma Optical Emission Spectrometry), as mentioned in (Dandamudi et al., 2020). The operational wavelength for detecting metallic ions in the biomass samples was set according to the vendor's operational manual in axial mode mentioned in the supplementary information. In the case of multiple wavelengths, the average concentration of the metal was used to ascertain the amount of the metal present. The surface morphology of the biochar understudy was analyzed by an XL30 Environmental Scanning Electron Microscope (SEM).

5.2.4 Biochar leaching experiments

In order to test the hypothesis and the objective #1, a series of experiments were performed to evaluate the feasibility of leaching phosphates and ammoniacal nitrogen from the HTL biochar obtained from the conditions mentioned in section 2.2. For leaching

experiments, 30 mg of biochar were weighed out and added to thirty 50 ml polypropylene (PP) centrifugal tubular reactors. Leaching of nutrients using the reactor was completed in tubular reactor added with 40 ml of: (i) CM with no initial phosphates and ammoniacal nitrogen at pH 0.5 corrected using sulfuric acid (five replicates, n = 5), (ii) CM with no initial phosphates and ammoniacal nitrogen at pH 1.0 corrected using sulfuric acid (n = 5), (iii) CM with no initial phosphates and ammoniacal nitrogen at pH 2.5 corrected using sulfuric acid (n = 5), (iv) CM with no initial phosphates and ammoniacal nitrogen at pH 7.0 (n = 5), (v) Deionized water at pH 2.5 corrected using sulfuric acid (n = 5) and (vi) Deionized water at pH 7.0 (n = 5). All leaching experiments were done for seven days, with five replicates for each leachate. The leaching of phosphate and ammoniacal nitrogen in each reactor was measured every alternate day in triplicates. The change in the fraction of phosphate and ammonia leached from the biochar over time was measured using a HACH DR5000 spectrometer (HACH Company, Colorado, USA) during leaching studies, and at the initiation and completion of the growth studies. The media removed were replenished with DI water before resuming the growth studies. The amount of N and P were found in terms of ammoniacal nitrogen (NH_3-N) and phosphates (PO_4^{3-}) using the Salicylate TNT Method 10031 and Phosver 3 Method 8048, respectively. The pH levels in all reactors remained the same during the experimental period.

5.2.5 Growth study with leached nutrients

In this section objective #2 was implemented to see if the leached nutrient can be released into the media and can be used during the growth. The leached nutrient-rich medium prepared from the methods mentioned in section 2.4 was autoclaved (at 121 °C) and stored at 4 °C for further usage. At the beginning of each cultivation test, the inoculum was centrifuged using a Beckman Coulter Allegra X-15R Centrifuge (Beckman Coulter Inc., California USA), and the algae pellets were suspended in the control set medium. The biomass growth was quantified periodically, in terms of the optical density (OD) measured with a HACH DR5000 UV-Vis spectrophotometer at a wavelength of 750 nm. The biomass density was found in terms of ash-free dry weight (AFDW) in g/L that was related to the OD at 750 nm using the relation:

$$\text{AFDW } (\text{g L}^{-1}) = 0.54*(\text{OD@750 nm}) + 0.023$$

5.2.5.1 Experimental conditions for the growth studies

Initial growth studies were conducted in a 250 µL microplate assay to study the influence of leached nutrients compared to the standard growth media. A total of 10 reactors of each condition were used in this study. The optical density throughout the growth experiments was tested using a HACH DR5000 Spectrometer. The microplate was housed in an incubator (Percival Company, IA, USA), where the CO_2 level was maintained at 2-3% (vol. / vol.) throughout the experiments.

A volumetric scale-up was done to study the possible effects on the growth that could change the growth rate. The cultures were grown in 16 mm borosilicate glass tubes, capped with plastic caps, and sealed with parafilm to reduce evaporative losses. Each tube was inoculated with 6 mL of culture and placed in the outer rim of a roller drum (New Brunswick Scientific Company, Eppendorf, CT, USA) rotating at 16 rpm. The roller drum was housed in the same incubator (where the CO_2 level was maintained at 2-3 %) throughout the experiments.

5.3 Results and Discussion

5.3.1 Analysis of biomass and HTL products

Table 5.1 presents the proximate and biochemical composition of the GS feedstock. As shown, GS represents a high-protein microalga with 53.25 wt. % measured as proteins and lipids calculated as Fatty Acid Methyl Esters (FAME) at 8.85 wt. %. A previous study (Dandamudi et al., 2017) of similar algae (GS) also reported protein content of 45.1 wt.% suggesting GS to be a high protein alga. The HHV of the current algae under study (15.80 MJ/kg) and the published research (16.4 MJ/kg) mentioned earlier were comparable. This strain also reports a low ash value (2.41 wt. %) relative to the published study corresponding to differences in cultivation setups. The carbohydrates were around 35.49 wt. % and were comparable to the published data.

Table 5.1: Analysis of the feedstock

Species	current study GS	previous study (Dandamudi et al., 2017)
Proximate (wt. %)		
Ash content	2.41	9.4
Moisture	70.00	67.35
Biochemical (wt. %)		
Lipids	8.85	3.21
Proteins	53.25	45.1
Carbohydrates [a]	35.49	42.29
HHV, MJ/kg	15.80	16.4

[a]: Carbohydrates=100-Sum (Lipids+Proteins+Ash); HHV: High Heating Value in MJ/kg

The biocrude oil yield at 300 °C was measured to be 32.12 wt.%, biochar yield at 2.74 wt.%, and water-soluble compounds (WSC) at 6.84 wt. %. From current work, it is evident that the reported bio-crude yield (32.12 wt.%), as seen in Table 5.2, was more than the initial lipid content (8.85 wt.%), proving the conversion of other major biochemical components in the biomass like proteins and carbohydrates into bio-crude. Dandamudi et al. and Muppaneni et al. (Dandamudi et al., 2019; Muppaneni et al., 2017) has also reported similar results where the biocrude yield was higher than that of the lipid content of algae

suggesting other biochemical constituents (proteins and carbohydrates) hydrolyzing during the HTL reaction and contributing to various compounds in the product fraction. Table 5.3 reports the elemental analysis and inorganic metal content of the GS, HTL biocrude, and HTL biochar. The biomass has at least half of its weight as carbon (51.44 wt. %) with oxygen (20.45 wt. %) and nitrogen (11.14 wt. %) as the other major components. The HTL biocrude on the product fraction has reported an increase in carbon and hydrogen content owing to the removal of heteroatoms during the liquefaction process. HTL also helped in the deoxygenation process and led to a decrease in the oxygen content of biocrude to 5.26 wt. % in comparison with the biomass oxygen content of 20.45 wt. %. A similar effect was also observed in the case of biochar, where the measured oxygen content was reduced to 1.86 wt. %. (Dandamudi et al., 2019; He et al., 2020) also reports a similar trend in the increase of carbon and hydrogen content and a decrease in the oxygen content. To correlate the quality of bio-crude produced during the process, the H/C and O/C ratio was also reported. H/C and O/C decreased in both the cases suggesting cleaner fuel properties. The decrease in the heteroatom content also correlates with the increase in the energy content of the products. The rise in HHV in the product fraction indicates energy densification during the liquefaction process. The high heating values of the feedstock and HTL products were comparable to a study published by Dandamudi et al. (Dandamudi et al., 2017).

Table 5.2**:** Product yields from hydrothermal liquefaction of GS at 300 ºC, 30 min residence time, and 20 wt. % solid loading

Product	Yield, %
Biocrude	32.12 ± 3.73
Biochar	2.74 ± 0.37
Water-soluble compounds	6.87 ± 2.42
Gas phase and loss*	58.27 + 6.35

*: Gas phase and loss=100-Sum (biocrude+biochar+ Water-soluble compounds)

Table 5.3 also reports the presence of inorganic metals such as phosphorous (P), calcium (Ca), Iron (Fe), Magnesium (Mg), Molybdenum (Mo), Nickel (Ni), Potassium (K), Sodium (Na), and Zinc (Zn). Phosphorous and sodium were the dominant inorganic metals present in the biomass. These metals enter the biomass through the salts used during cultivation and play a vital role in cell metabolism during growth. In the case of HTL biocrude, a very low concentration of metals has been reported. However, a large concentration of metals has been reported in the HTL biochar. This explains the fact that most of the metals are insoluble in the non-polar solvent or the water-soluble compound phase. Among the metals reported, phosphorous was the dominant metal found in the biochar, followed by sodium, zinc, nickel, molybdenum, and magnesium. Karbakhshravari

et al. (Karbakhshravari et al., 2020) has shown a weak correlation between the solid content of the HTL biomass and the phosphorous levels in the water-soluble compound phase. They have suggested that the biochar tends to accumulate a major share of phosphorous (>90 %) among the HTL products. A considerable fraction of nitrogen (5.27 wt. %) was also reported to fraction into biochar. The leaching of phosphorous and nitrogen accumulated in the biochar will be explained in the next sections. Figure 5.2 shows the SEM image of the HTL biochar particles under the study. The results indicated that biochar particle sizes varied from 2 – 300 µm.

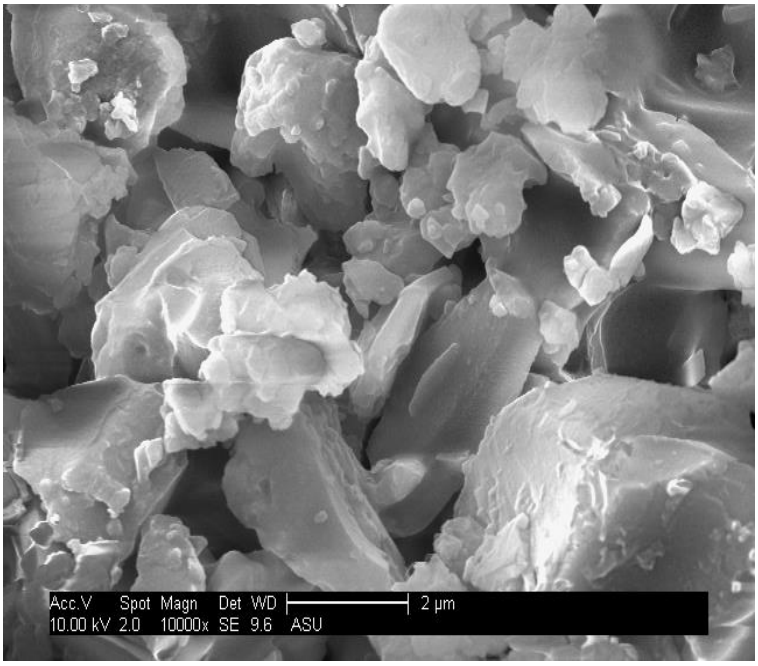

Figure 5.2: SEM image of the produced HTL biochar from GS feedstock

Table 5.3**:** Inorganic metal and elemental analysis of the microalgae, HTL biocrude, and HTL biochar

Element	**Unit**	**GS**	**Bio-crude**	**Biochar**
Phosphorous	Wt.%	1.45	0.01	15.98
Carbon	Wt. %	51.44	73.89	42.90
Hydrogen	Wt.%	7.83	9.13	4.67
Nitrogen	Wt.%	11.14	7.25	5.27
Sulfur	Wt. %	1.83	2.31	0.74
Calcium	Wt.%	0.15	0.05	0.36
Iron	Wt. %	0.04	0.06	0.19
Magnesium	Wt.%	0.08	0.00	1.30
Molybdenum	Wt.%	1.51	0.45	1.53
Nickel	Wt. %	0.27	0.18	2.49
Potassium	Wt.%	0.24	0.00	0.01
Sodium	Wt. %	1.68	0.49	3.73
Zinc	Wt.%	0.44	0.91	2.99
Oxygen*	Wt. %	20.45	5.26	1.86
O/C	mol/mol	0.29	0.05	0.03
H/C	mol/mol	1.81	1.47	1.29
HHV	MJ/kg	15.80	36.42	24.51

*Oxygen content, Wt. %= 100- (Sum of all the elements); HHV: Higher Heating Value (MJ/kg)

5.3.2 Effect of pH on the leaching of nutrients from the biochar

From the ICP-OES result, it can be observed that 15.98 wt.% of phosphorous from the dried algae was present in the biochar. The acidity or basicity of a media aids leaching of nutrients from materials like biochar. An increased presence of H^+ or OH^- in the media is reported to have denaturing effects on the biochar surface, much like the activation of carbonaceous compounds (Lammers et al., 2017). Similar results were considered to cause leaching in this study.

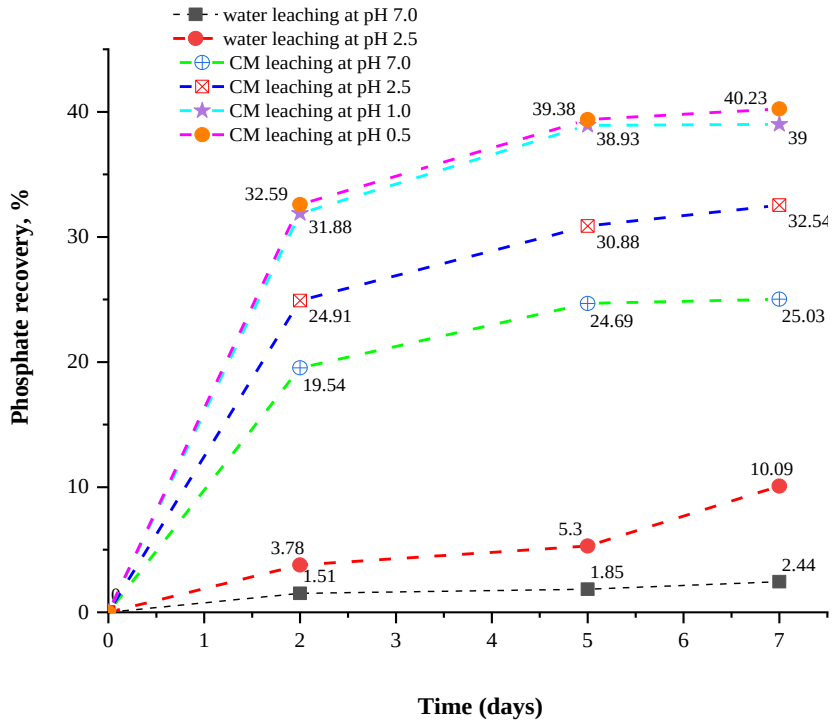

Figure 5.3: Leaching of Phosphates from HTL biochar over 7 days

The pK_a value for phosphoric acid is 2.16 (Selvaratnam et al., 2014); this and the speciation data for phosphoric acid suggest optimal leaching at a pH lesser than 1.5. The choice of a lower pH range for this study stems from the speciation data (Jiang et al., 2016) and reported optimum growth conditions for *G. sulphuraria* (Selvaratnam et al., 2015b, 2015a). The acidic range would ensure that leaching can be done both before and during the growth of *G. sulphuraria* in a reactor. This range of pH in this study was chosen to optimize the application of the process in the industry with low or no operational costs. A higher pH would call for an extra step before growth to reduce the medium pH lower than 4.0. From Figure 5.3, the leaching of phosphates from biochar varied greatly with pH. At CM media pH values lower than 7.0, the percentage of leached phosphates into the media from biochar was seen to increase with a decrease in pH.

The recorded phosphate recovery at pH 7.0 with CM as media was 25.03 % while at the pH of 2.5 reported a recovery of 32.54 %. The increase in pH was also observed with a decrease in pH from 2.5 to 1.0 and 0.5 yielded a recovery of 32.54 and 40.23 %, respectively. These results were compared with a control step of phosphates leaching into the water at a pH of 2.5 and 7.0, where phosphates recovery as 10.09 and 2.44 %, respectively. This almost four-fold increase in leachability can be attributed to the differing acidity. Similar results proving that phosphorus leaching into the water-soluble phase was higher by orders of magnitude in lower pH (<2.5) compared to neutral pH (Yang et al., 2017). Yang et al. suggested that the hydrolysis and solubility of phosphates ions increased

with a decrease in pH and therefore reported a higher recovery at a lower pH (Yang et al., 2017). The phosphate leaching at a pH of 1.0 gave a percentage recovery of 40.23 % while that at a lower pH of 0.5 gave a lower 32.54 % recovery. With consideration of the standard deviation of leaching at pH of 1.0 and 2.5 over seven days, we see that these cases are approximately similar in efficiency. Since pH 2.5 provides considerable leaching at the lower input of sulfuric acid, we chose 2.5 to be an economically feasible option. The feasibility was based on a lower number of steps needed and decreased overhead operational costs for incorporating such a process. The nutrients leached at pH 2.5 (39% efficient) into the media can grow *G. sulphuraria* as optimum growth pH for the strain of microalgae was in the acidic range.

Based on the leaching of ammoniacal nitrogen from biochar (Figure 5.4), it could be concluded that the effect of pH was negligible. At a lower pH of 2.5, ammoniacal nitrogen leached into the CM amounted to 61.00 % of the initial nitrogen present in biochar compared to 53.94 % recovery at neutral pH. The swing in the pH has an insignificant influence to improve the leaching of nitrogen into the growth media as usable ammoniacal nitrogen; similar trends can be observed in the control conditions using water at a similar pH. In the case of controls (Figure 5.4), leaching was found to be negligible. This difference may be due to the possible interactions of the media with the biochar surface and potential ionic strength in the media. The maximum recovery (i.e., 70.01 %) of ammoniacal nitrogen from biochar was observed at a pH of 1.0. Again, economic considerations (described in

phosphate leaching) vouched for utilizing a pH of 2.5 in the leaching step. The initial amount of phosphorous and nitrogen in the biochar was reported to be 15.98 wt. % and 5.27 wt. %, respectively. The best leaching of phosphorous and nitrogen from HTL biochar is observed at pH 0.5 (Figure 5.5), but the associated cost of reducing pH to 0.5 is not justifiable by the slight increase of about 9 % in recovery. Employing the above-mentioned acidic leaching process at pH 2.5, leaching of phosphorous as phosphates were 32.54 % (i.e., 4.95 wt. % leached) efficient and 61 % (i.e., 3.21 wt. % leached) for leaching of nitrogen as ammoniacal nitrogen.

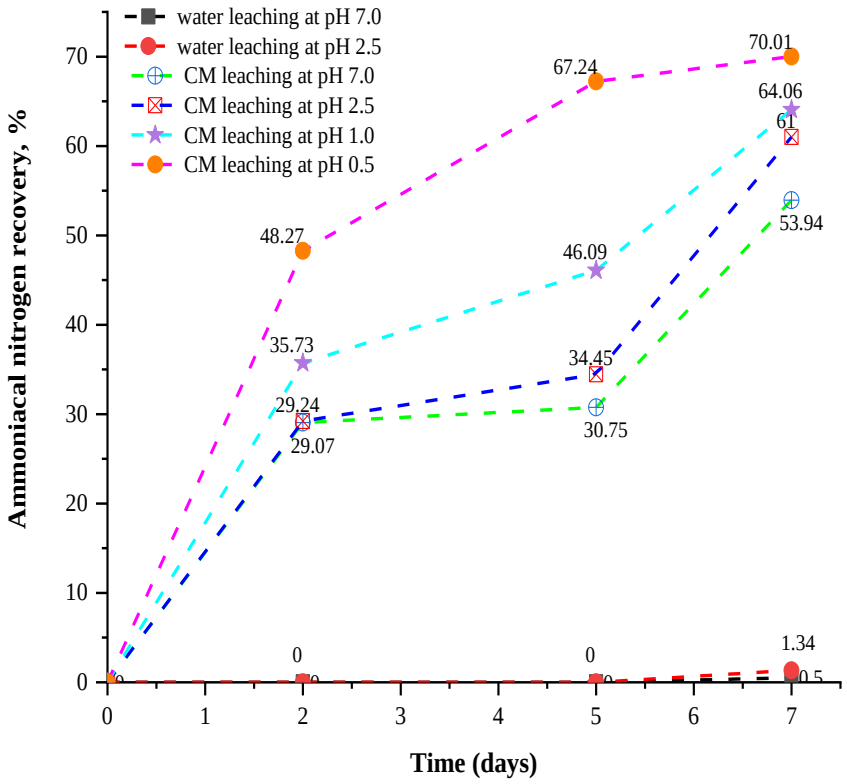

Figure 5.4: Leaching of Ammoniacal nitrogen from HTL biochar over 7 days

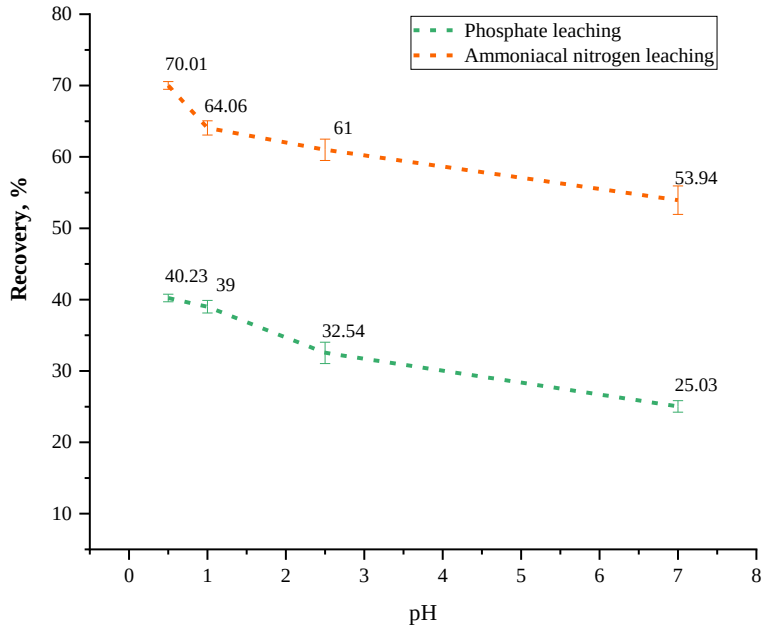

Figure 5.5: Effect of pH on leaching of phosphates and ammoniacal nitrogen from HTL biochar

5.3.2.1 Mass balance of products from HTL and leaching studies

The objective #3 was evaluated in this section. The products from HTL were analyzed for carbon, hydrogen, nitrogen, sulfur, and oxygen by CHNS/O and phosphorous using ICP-OES. Table 5.4 shows the mass balance and concludes with the recovery percentage based on product composition. It can be observed that the recovery of carbon

was at 52.27 wt.%. It can be assumed that the remaining 47.73 wt.% carbon was a part of the gaseous products of liquefaction, which were not studied as a part of this work. A previous review on the composition of the gases from HTL reported the gases mainly constituted of CO_2, CO, CH_4, H_2, C_2 light gases, and H_2O (Barreiro et al., 2013; Xu and Savage, 2017). In the case of hydrogen mass balance, around 45 wt.% of the initial hydrogen was recovered in the overall process. The nitrogen and sulfur recovery were around 31.33 and 44.91 wt.%, respectively. The recovery percentage of oxygen is about 20 wt.% suggesting that more than 75 wt. % of the initial oxygen was lost in the gas phase.

In the case of phosphorous, the majority was found in biochar, and a recovery of 88.29 % was reported, also, at 1.19 wt. % of initial nitrogen in the dry biomass was reported in the biochar fraction. These nutrients in the biochar were leached using above mentioned acidic leaching method at pH 2.5. By this process, about 49.49 % of the phosphorous was recovered as orthophosphates at a pH of 2.5. Approximately, 95.21 % of the initial nitrogen was recovered as ammoniacal nitrogen at the same pH.

Table 5.4: Mass Balance and elemental recovery from the hydrothermal liquefaction process

	Dry Algae		Biocrude		Biochar		WSC		Recovery**
Element	%	g	%	g	%	g	%	g	%
Carbon	51.44	15.57	73.89	7.16	42.90	0.36	29.82	0.62	52.27

Hydrogen	7.83	2.37	9.13	0.88	4.67	0.04	6.80	0.14	44.95
Nitrogen	11.14	3.37	7.25	0.70	5.27	0.04	14.88	0.31	31.33
Sulfur	1.83	0.55	2.31	0.22	0.74	0.01	0.90	0.02	44.91
Phosphorous	1.45	0.44	0.01	0.01	15.98	0.13	11.74	0.24	88.29
Oxygen*	26.31	7.89	7.41	0.59	30.44	0.37	35.86	0.99	24.67

*Oxygen content= 100- Sum (C, H, N, S, P)

**Recovery $_i$ =

$$\frac{\{(\text{mass of 'i' in biocrude})+(\text{mass of 'i' in biochar})+(\text{mass of 'i' in WSC})\}}{\text{mass of 'i' in dry algae}} *100$$

5.3.3 Comparative growth of G. sulphuraria in standard media compared to leached media

The growth in terms of ash-free dry weight (g. L^{-1}) was shown in Figure 5.6. The initial study was completed in a 96 well plate microplate assay (Figure 5.6 (A)) and then scaled up to a 16-mm tubular reactor placed in a roller drum reactor (Figure 5.6 (B)). This study attempted to prove that the leached nutrients from biochar produced after HTL could be successfully employed to grow *G. sulphuraria* at rates comparable with standard CM. This work would serve as a basis for future studies to study the viability and economics of such a recycling step in a microalgae-based bio-refinery. The composition of leached media

was normalized to match ammoniacal nitrogen levels to 360 mg. L^{-1} and phosphates at 170 mg. L^{-1}. This eliminated nitrogen availability as a possible limiting variable in the growth experiments to evaluate *G. sulphuraria* growth in CM media in both leached and standard.

Growth curves of *G. sulphuraria* cultivated in a microplate assay were summarized in Figure 5.6 (A). This initial study warranted that the growth of *G. sulphuraria* in leached CM was comparable to that in standard media. It can be ascertained that there was no toxic effect on the biomass growth by the leached nutrients comparing the similarity in the growth curve slope. The almost identical growth rates prove that the use of leached media to grow microalgae is feasible. Also, it may be ascertained that there are no visible growth inhibitions due to the leaching process.

A secondary confirmation using a tubular photobioreactor showed similar results (Figure 5.6 (B)) as in the microplate assay. This study was a volumetric scale-up from the 250 μL reactor size to 6 ml. This scale-up (~24 fold) did not show a significant difference in the results. The ash-free dry weight increased from 0.128 g/L to 0.613 g/L in the leached media compared to 0.539 g/L in standard media. Further, the growth rates were comparable with those observed in the microplate assay studies (Figure 5.6 (A)), and other reported works on the same strain. These results confirm that *G. sulphuraria* can be successfully grown using recycled biochar from hydrothermal liquefaction.

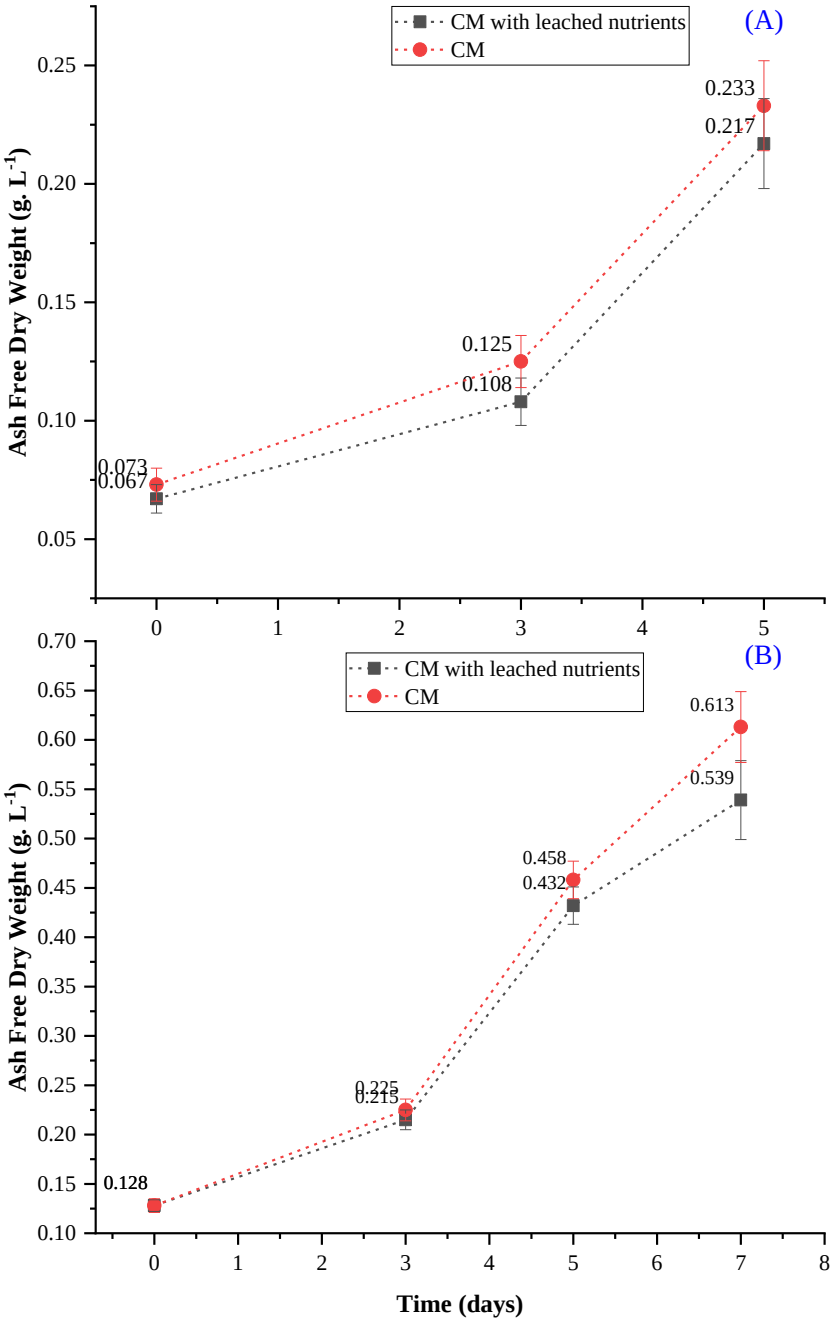
CM with leached nutrients
CM
(A)
Ash Free Dry Weight (g. L-1)
0.25
0.20
0.15
0.10
0.05
0.233
0.217
0.125
0.108
0.073
0.067
0
1
2
3
4
5
CM with leached nutrients
CM
(B)
Ash Free Dry Weight (g. L-1)
0.70
0.65
0.60
0.55
0.50
0.45
0.40
0.35
0.30
0.25
0.20
0.15
0.10
0.613
0.539
0.458
0.432
0.225
0.215
0.128
0
1
2
3
4
5
6
7
8
Time (days)

Figure 5.6: Growth of GS in (A): 96 well microplate assay and (B): 16 mm tubular reactor

5.4 Conclusions

The proposed approach of recovering useful phosphorous and nitrogen from biochar, a by-product of the hydrothermal liquefaction process, was shown to cultivate *G. sulphuraria* without any inhibition. The main hypothesis of this study was tested and proved that algal HTL biochar can be leached under different conditions for nutrients and these nutrients can further be used to regrow algae. The biochar produced at 300 °C and 30 minutes contain 15.98 wt.% of phosphorous and 5.27 wt.% of nitrogen. By the proposed method, 32.54 % of the phosphorus may be recovered as phosphates; and 61 % of the nitrogen as ammoniacal nitrogen at a pH of 2.5 in 7 days of leaching experiments. It can be concluded that *G. sulphuraria* can be cultivated successfully in media leached from the HTL biochar. The rates of growth are comparable to those with the standard CM media. The results of growth experiments in this study showed that *G. sulphuraria* grew better in leached media when compared to a similar standard media. Further, a scale-up investigation has reported similar growth rates.

The mass balance calculations showed that 52.27 %, 44.95 %, 31.33 %, and 88.29 % of C, H, N, and P were recovered in the combined HTL products, including biocrude, biochar, and the water-soluble phase, respectively. The SEM analysis of the HTL biochar measured particles ranging from 2 – 300 μm. In addition to phosphorous (P), the ICP-OES

revealed the presence of sodium (Na), zinc (Zn), and nickel (Ni) as dominant elements. The energy content of the biomass was measured as 15.80 MJ/kg, and that of biochar was measured as 24.51 MJ/kg.

The optimum utilization of HTL by-products improves the economics of the process and makes biofuels viable. HTL is a promising technique for converting wet algae into liquid biofuels because it offers the opportunity of extracting biocrude oil from biomass while recycling nutrients from both the water-soluble compounds and biochar to regrow algae.

5.5 References

Alba, L.G., Torri, C., Fabbri, D., Kersten, S.R.A., Brilman, D.W.F.W., 2013. Microalgae growth on the aqueous phase from hydrothermal liquefaction of the same microalgae. Chem. Eng. J. 228, 214–223.

Andersen, R.A., 2005. Algal culturing techniques. Elsevier.

Aysu, T., Demirbaş, A., Bengü, A.Ş., Küçük, M.M., 2015. Evaluation of Eremurus spectabilis for production of bio-oils with supercritical solvents. Process Saf. Environ. Prot. 94, 339–349.

Barreiro, D.L., Prins, W., Ronsse, F., Brilman, W., 2013. Hydrothermal liquefaction (HTL) of microalgae for biofuel production: state of the art review and future prospects. Biomass and Bioenergy 53, 113–127.

Beal, C.M., Archibald, I., Huntley, M.E., Greene, C.H., Johnson, Z.I., 2018. Integrating algae with bioenergy carbon capture and storage (ABECCS) increases sustainability. Earth's Futur. 6, 524–542.

Bouwman, L., Goldewijk, K.K., Van Der Hoek, K.W., Beusen, A.H.W., Van Vuuren, D.P., Willems, J., Rufino, M.C., Stehfest, E., 2013. Exploring global changes in nitrogen and phosphorus cycles in agriculture induced by livestock production over the 1900–2050 period. Proc. Natl. Acad. Sci. 110, 20882–20887.

Bridgwater, A. V, 2012. Review of fast pyrolysis of biomass and product upgrading.

Biomass and bioenergy 38, 68–94.

Chisti, Y., 2007. Biodiesel from microalgae. Biotechnol. Adv. 25, 294–306.

Cisse, L., Mrabet, T., 2004. World phosphate production: overview and prospects. Phosphorus Res. Bull. 15, 21–25.

Collard, F.-X., Blin, J., 2014. A review on pyrolysis of biomass constituents: Mechanisms and composition of the products obtained from the conversion of cellulose, hemicelluloses and lignin. Renew. Sustain. Energy Rev. 38, 594–608.

Dandamudi, K.P.R., Muhammed Luboowa, K., Laideson, M., Murdock, T., Seger, M., McGowen, J., Lammers, P.J., Deng, S., 2020. Hydrothermal liquefaction of Cyanidioschyzon merolae and Salicornia bigelovii Torr.: The interaction effect on product distribution and chemistry. Fuel 277. https://doi.org/10.1016/j.fuel.2020.118146

Dandamudi, K.P.R., Muppaneni, T., Markovski, J.S., Lammers, P., Deng, S., 2019. Hydrothermal liquefaction of green microalga Kirchneriella sp. under sub-and super-critical water conditions. Biomass and bioenergy 120, 224–228.

Dandamudi, K.P.R., Muppaneni, T., Sudasinghe, N., Schaub, T., Holguin, F.O., Lammers, P.J., Deng, S., 2017. Co-liquefaction of mixed culture microalgal strains under sub-critical water conditions. Bioresour. Technol. 236. https://doi.org/10.1016/j.biortech.2017.03.165

Demirbas, A., 2009. Political, economic and environmental impacts of biofuels: A review. Appl. Energy 86, S108–S117.

Gai, C., Liu, Z., Han, G., Peng, N., Fan, A., 2015. Combustion behavior and kinetics of low-lipid microalgae via thermogravimetric analysis. Bioresour. Technol. 181, 148–154.

Godwin, C.M., Hietala, D.C., Lashaway, A.R., Narwani, A., Savage, P.E., Cardinale, B.J., 2017. Algal polycultures enhance coproduct recycling from hydrothermal liquefaction. Bioresour. Technol. 224, 630–638.

Gross, J.D., Matsuo, H., Fletcher, M., Sachs, A.B., Wagner, G., 2001. Interactions of the eukaryotic translation initiation factor eIF4E, in: Cold Spring Harbor Symposia on Quantitative Biology. Cold Spring Harbor Laboratory Press, pp. 397–402.

He, S., Zhao, M., Wang, J., Cheng, Z., Yan, B., Chen, G., 2020. Hydrothermal liquefaction of low-lipid algae Nannochloropsis sp. and Sargassum sp.: Effect of feedstock composition and temperature. Sci. Total Environ. 712, 135677.

Ibrahim, A.F.M., Dandamudi, K.P.R., Deng, S., Lin, J.Y.S., 2020. Pyrolysis of hydrothermal liquefaction algal biochar for hydrogen production in a membrane reactor. Fuel 265, 116935. https://doi.org/https://doi.org/10.1016/j.fuel.2019.116935

Ikenaga, N., Ueda, C., Matsui, T., Ohtsuki, M., Suzuki, T., 2001. Co-liquefaction of micro algae with coal using coal liquefaction catalysts. Energy and Fuels.

https://doi.org/10.1021/ef000129u

Jiang, L., Liang, B., Xue, Q., Yin, C., 2016. Characterization of phosphorus leaching from phosphate waste rock in the Xiangxi River watershed, Three Gorges Reservoir, China. Chemosphere 150, 130–138.

Karbakhshravari, M., Abeysiriwardana-Arachchige, I.S.A., Henkanatte-Gedera, S.M., Cheng, F., Papelis, C., Brewer, C.E., Nirmalakhandan, N., 2020. Recovery of struvite from hydrothermally processed algal biomass cultivated in urban wastewaters. Resour. Conserv. Recycl. 163, 105089.

Kruse, A., Dinjus, E., 2007. Hot compressed water as reaction medium and reactant: properties and synthesis reactions. J. Supercrit. Fluids 39, 362–380.

Lammers, P.J., Huesemann, M., Boeing, W., Anderson, D.B., Arnold, R.G., Bai, X., Bhole, M., Brhanavan, Y., Brown, L., Brown, J., 2017. Review of the cultivation program within the National Alliance for Advanced Biofuels and Bioproducts. Algal Res. 22, 166–186.

Muppaneni, T., Reddy, H.K., Selvaratnam, T., Dandamudi, K.P.R., Dungan, B., Nirmalakhandan, N., Schaub, T., Omar Holguin, F., Voorhies, W., Lammers, P., Deng, S., 2017. Hydrothermal liquefaction of Cyanidioschyzon merolae and the influence of catalysts on products. Bioresour. Technol. 223. https://doi.org/10.1016/j.biortech.2016.10.022

Patil, P.D., Dandamudi, K.P.R., Wang, J., Deng, Q., Deng, S., 2018. Extraction of bio-oils from algae with supercritical carbon dioxide and co-solvents. J. Supercrit. Fluids 135, 60–68. https://doi.org/https://doi.org/10.1016/j.supflu.2017.12.019

Reddy, H.K., Muppaneni, T., Sun, Y., Li, Y., Ponnusamy, S., Patil, P.D., Dailey, P., Schaub, T., Holguin, F.O., Dungan, B., Cooke, P., Lammers, P., Voorhies, W., Lu, X., Deng, S., 2014. Subcritical water extraction of lipids from wet algae for biodiesel production. Fuel 133, 73–81. https://doi.org/https://doi.org/10.1016/j.fuel.2014.04.081

Samieadel, A., Rajib, A.I., Dandamudi, K.P.R., Deng, S., Fini, E.H., 2020. Improving recycled asphalt using sustainable hybrid rejuvenators with enhanced intercalation into oxidized asphaltenes nanoaggregates. Constr. Build. Mater. 262, 120090.

Selvaratnam, T., Pegallapati, A.K., Montelya, F., Rodriguez, G., Nirmalakhandan, N., Van Voorhies, W., Lammers, P.J., 2014. Evaluation of a thermo-tolerant acidophilic alga, Galdieria sulphuraria, for nutrient removal from urban wastewaters. Bioresour. Technol. 156, 395–399.

Selvaratnam, T., Pegallapati, A.K., Reddy, H., Kanapathipillai, N., Nirmalakhandan, N., Deng, S., Lammers, P.J., 2015a. Algal biofuels from urban wastewaters: Maximizing biomass yield using nutrients recycled from hydrothermal processing of biomass. Bioresour. Technol. 182, 232–238.

Selvaratnam, T., Reddy, H., Muppaneni, T., Holguin, F.O., Nirmalakhandan, N., Lammers, P.J., Deng, S., 2015b. Optimizing energy yields from nutrient recycling using sequential hydrothermal liquefaction with Galdieria sulphuraria. Algal Res. 12, 74–79.

Son, E.-B., Poo, K.-M., Chang, J.-S., Chae, K.-J., 2018. Heavy metal removal from aqueous solutions using engineered magnetic biochars derived from waste marine macro-algal biomass. Sci. Total Environ. 615, 161–168.

Toor, S.S., Reddy, H., Deng, S., Hoffmann, J., Spangsmark, D., Madsen, L.B., Holm-Nielsen, J.B., Rosendahl, L.A., 2013. Hydrothermal liquefaction of Spirulina and Nannochloropsis salina under subcritical and supercritical water conditions. Bioresour. Technol. 131, 413–419.

U.S. EIA, U.S. Energy Information Administration (EIA), 2019. Annual Energy Outlook 2019 with projections to 2050. Annu. Energy Outlook 2019 with Proj. to 2050. https://doi.org/DOE/EIA-0383(2012) U.S.

Wang, J., Krishna, R., Yang, J., Dandamudi, K.P.R., Deng, S., 2015. Nitrogen-doped porous carbons for highly selective CO<inf>2</inf> capture from flue gases and natural gas upgrading. Mater. Today Commun. 4. https://doi.org/10.1016/j.mtcomm.2015.06.009

Wang, J., Peng, X., Chen, X., Ma, X., 2019. Co-liquefaction of low-lipid microalgae and

starch-rich biomass waste: The interaction effect on product distribution and composition. J. Anal. Appl. Pyrolysis 139, 250–257.

Xu, D., Lin, G., Guo, S., Wang, S., Guo, Y., Jing, Z., 2018. Catalytic hydrothermal liquefaction of algae and upgrading of biocrude: a critical review. Renew. Sustain. Energy Rev. 97, 103–118.

Xu, D., Savage, P.E., 2017. Effect of temperature, water loading, and Ru/C catalyst on water-insoluble and water-soluble biocrude fractions from hydrothermal liquefaction of algae. Bioresour. Technol. 239, 1–6.

Yang, C.-M., Lee, C.-G., Won, J.-I., 2017. Improvement of Bio-crude Oil Yield and Phosphorus Content by Hydrothermal Liquefaction Using Microalgae. Chem. Eng. Technol. 40, 2188–2196.

Zhan, L., Jiang, L., Zhang, Y., Gao, B., Xu, Z., 2020. Reduction, detoxification and recycling of solid waste by hydrothermal technology: A review. Chem. Eng. J. 124651.

CHAPTER 6: PYROLYSIS OF HYDROTHERMAL LIQUEFACTION PRODUCED ALGAL BIOCHAR FOR HYDROGEN PRODUCTION USING A MEMBRANE REACTOR

6.1 Introduction

Microalgae hereafter, referred to as ‘algae’ represent a sustainable biomass feedstock that can be converted into a variety of fuels (Brennan and Owende, 2010), which will decrease the dependency on fossil fuels and mitigate environmental problems such as greenhouse gas emissions (GHG) (Kumar et al., 2010; Patil et al., 2018). Among various thermochemical conversion techniques, hydrothermal liquefaction (HTL) is considered as one of the best conversion methods, particularly for low-lipid microalgae. HTL conversion technology has the benefit of utilizing the whole algae components and avoids the costly dewatering and drying steps (example like pyrolysis) of the feedstock, which consumes less process energy (Chen et al., 2015). During HTL, high temperature (573–623 K) and elevated pressure (5-20 MPa) develops a very reactive aqueous medium that decomposes, and reforms biomass macromolecules into energy-dense products (Guo et al., 2015). Following the liquefaction, algae are eventually converted into four products: biocrude oil, aqueous product, gaseous product, and a solid residue known as biochar (Yu et al., 2011).

A crucial challenge surrounding the use of HTL for algae conversion faces with respect to identifying practical applications for the products, bio-crude oil and the solid phase, biochar. While HTL bio-crude oil can be processed and upgraded to liquid transportation fuels and other biobinder applications (Li and Savage, 2013), significant uncertainty remains regarding the solid phase, biochar, which could create a burden on HTL economics, this in turn makes the conversion process less attractive especially with low lipid/high ash algae. The inclining interest in algal biofuels (HTL bio-oil), produces large amounts of biochar, which makes finding an efficient use of biochar more critical to improving the economic viability and environmental sustainability of biomass via HTL conversion technology.

Lately, a lot of research work has been published on algal-based biochar for use in several applications of agriculture and environmental applications (Yu et al., 2017). Algal biochar can be used to balance acidified soils due to its alkaline properties and as a soil fertilizer due to its higher content of nitrogen and phosphorous (Bird et al., 2012, 2011; Cole et al., 2017). Biochar can also be used as a bio-adsorbent in water treatment to remediate inorganic and organic contaminants (Bordoloi et al., 2017; Johansson et al., 2016; Liu and Zhang, 2009; Son et al., 2018; Zheng et al., 2017) and showed good potential in energy storage materials and catalytic applications (Salimi et al., 2019b, 2019a; Taghavi et al., 2018). Hydrothermal conversion of biomass into biofuel could produce a special type of biochar as a byproduct which is quite different from biochar derived from other high-

temperature pyrolysis processes. In spite of containing a significant energy content (9.1-20 MJ/kg) (Yu et al., 2017), no applications were found to recover or make use of this significant energy unless as direct burning for heating.

In the current study, we report on the conversion of HTL biochar to hydrogen under pyrolysis conditions in a hydrogen-selective membrane reactor capable of separating hydrogen from the reaction zone. The specific choice of H_2 as the product for biomass conversion was motivated by three factors: (a) H_2 is a clean fuel for direct burning or electricity generation in fuel cells (Staffell et al., 2019); (b) H_2 is an important raw material for synthesis of a large number of chemicals and fertilizers (Elsherif et al., 2015) and (c) H_2 will be needed for reducing CO_2 into energy-dense hydrocarbon fuels as an effective way of carbon capture, utilization and recycling in the near future (Daiyan et al., 2017; Xiong et al., 2019). An efficient and cost-effective pure H_2 production can be attained by integrating H_2-selective membranes in algae pyrolysis reactors. Various membrane types have been researched for high-temperature H_2 separation, such as microporous silica, zeolite and carbon membranes, and dense mixed-proton-and-electronic conducting oxide and metallic alloy membranes (Ockwig and Nenoff, 2007). Pd-Ag alloy membranes with the composition of 77% Pd and 23% Ag (refered to as $Pd_{77}Ag_{23}$), have high hydrogen permeability and selectivity (Paglieri and Way, 2002; Uemiya et al., 1991), and show the capability to separate H_2 from coal gasification and steam reforming product streams (Kikuchi, 2000; Uemiya et al., 1990).

Based on the literature, the following hypotheses were developed:

- HTL algal biochar can be pyrolyzed to produce renewable gases at controlled conditions.
- A hydrogen selective membrane separate the hydrogen at the pyrolysis reaction conditions of HTL biochar.

The objective of this project is to demonstrate the feasibility of converting HTL biochar into hydrogen in a Pd-Ag alloy membrane reactor under controlled pyrolysis conditions.

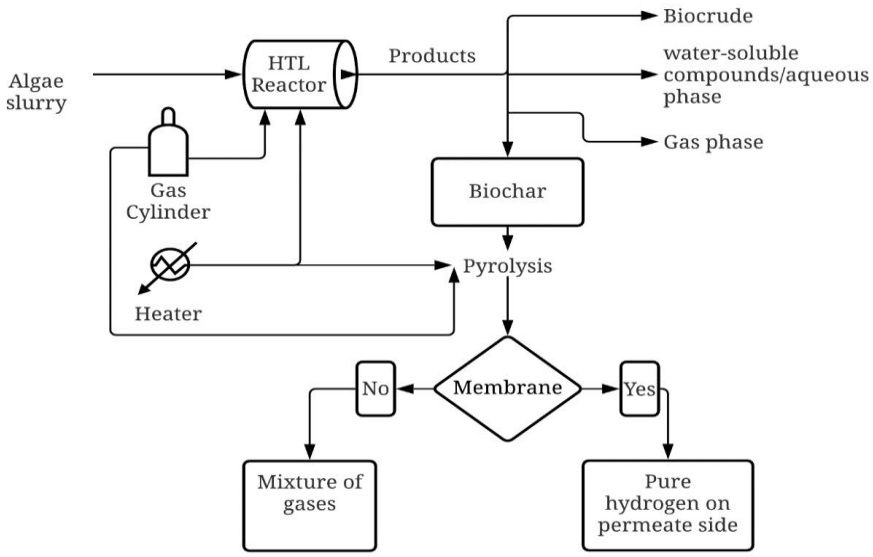

Figure 6.1: Experimental plan for this study

6.2 Materials and Methods

The experimental plan for the study in shown in figure 6.1. The HTL product biochar is pyrolized under various conditions. Pyrolysis was performed with or without a membrane to see the gases on both sides of permeate and retentate. The gas phase was quantified using Gas Chromatography technique while biomass and biochar was analyzed by CHNS/O analyzer, SEM-EDAX, and TGA.

6.2.1 Algae production and harvesting

Galdieria sulphuraria (Culture Collection of Microorganisms from Extreme Environments, CCMEE 5587.1) (Dandamudi et al., 2017; Toplin et al., 2008), an independent isolate of the unicellular thermo-acidophilic red algae was assessed in this study. The biomass used in the hydrothermal liquefaction (HTL) to produce biochar was grown outdoors in a modified cyanidium medium at pH 2.5 in a 50 L flat panel vertical photo-bioreactor at Arizona Center for Algae Technology and Innovation (AzCATI), Arizona State University. The cultures were sparged and maintained at 2-3 % (vol/vol) CO_2 mixed with air. The growth of the biomass in the culture was monitored daily in terms of optical density (OD) at a wavelength of 750 nm measured with Beckman DU530 spectrophotometer. The biomass and the aliquot of the media were harvested and stored, as mentioned in (Dandamudi et al., 2019).

6.2.2 Hydrothermal liquefaction experiments and product recovery

HTL procedure has been explained in Chapter 2 and 3 and follows the same protocol is used in this chapter for experimentation and product separation (Dandamudi et al., 2019; Muppaneni et al., 2017).

6.2.3 TGA characterization and fixed bed pyrolysis

Thermogravimetric analysis (TGA) experiments were performed using SDT-Q-600/TA instruments under nitrogen atmosphere. The TGA chamber was purged using nitrogen before the test at a flow rate of 100 mL/min for 30 min and 30 mL/min during the experiment to displace the chamber air and prevent unwanted oxidation reactions. Approximately, 20 mg biomass and HTL biochar samples were heated from ambient temperature to 1000 ^{o}C at a heating rate of 1^{o}C/min. Also, the biochar samples were heated to 500 ^{o}C at ramping rates of 1, 3 and 5 ^{o}C/min and held at this temperature for 24 h.

Biochar pyrolysis tests were performed using a fixed-bed reactor configuration to identify and measure the composition of the gases and condensable vapors (oil/water) fractions evolved during pyrolysis. A schematic drawing of the used setup is shown in Figure 6.2 (A). The reactor contained a homemade stainless-steel membrane permeation cell (without a membrane). Around 1.5 g biochar sample was purged with 100 mL/min nitrogen for 30 min to maintain inert pyrolysis conditions. The reactor is then heated inside a box furnace at a ramping rate of 3 ^{o} C/min to 500 ^{o}C and held at this temperature for 24 h to compare with TGA results. A low nitrogen flow of 5 ml/min was maintained

throughout the experiments to deliver the pyrolysis gaseous products for composition analysis using online injection gas chromatography (Agilent Technologies, 6890 N equipped with thermal conductivity detector). A cold trap in an ice bath (~ 4 ^{o}C) was installed before gas chromatography at the downstream to condense and collect the water and other condensable volatile products. The weight of bio-liquid (bio-oil+ water) and remaining solids were weighted directly at the ambient temperature (25 ^{o}C). The yield of light gases was determined based on the carrier gas flow rate and the composition as a function of pyrolysis time. The composition of the liquid product mixture was not provided since it is outside the scope of the current study.

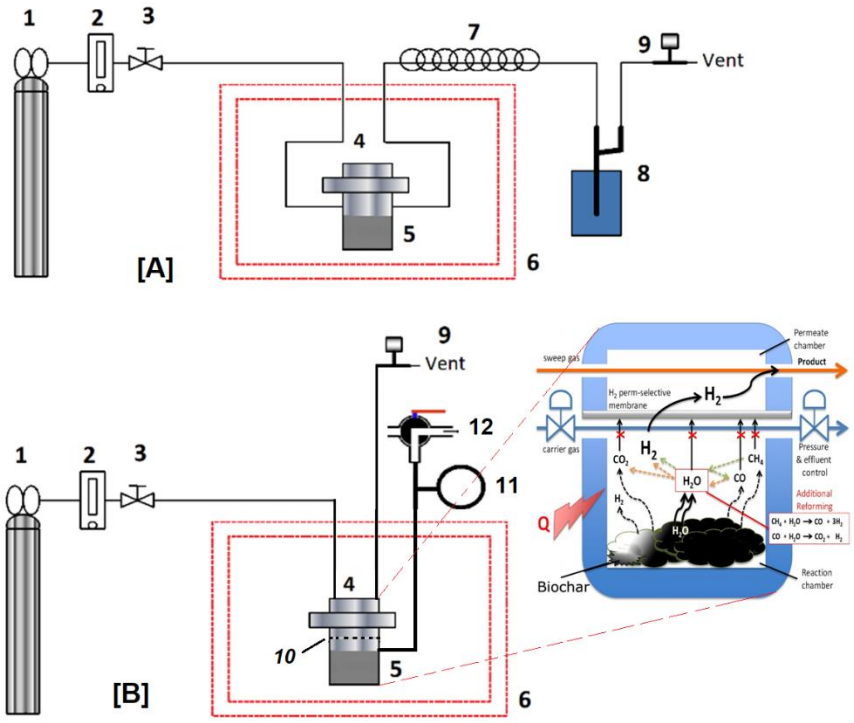

Figure 6.2: Configuration of the fixed bed [A] and batch [B] reactors used for biochar pyrolysis: 1) gas cylinder, 2) mass flow controller, 3) valve, 4) permeation cell, 5) biochar sample, 6) box furnace, 7) heating tape, 8) cold trap and 9) GC online injection,10) hydrogen selective membrane (Pd77Ag23) or impermeable substrate, 11) pressure gage and 12) 3-way valve.

6.2.4 Batch membrane reactor experiments

Biochar pyrolysis tests were also carried out with and without a membrane using a setup given in Figure 6.2 (B), which represents the modified form of the fixed-bed reactor. Initially, pyrolysis experiments were conducted in the absence of a membrane. This was done with the lower part of the reactor chamber of about ~16 mL in volume sealed with an impermeable stainless-steel disk. The biochar samples (0.2, 0.3 or 0.4 g) in the reactor chamber were purged with 100 mL/min nitrogen for 30 min and then the reactor was evacuated for 5 min to ensure inert atmosphere in the reactor. Pyrolysis tests were carried out in a box furnace using a heating rate of 5 ^{o}/min to reach the target temperature of 500 ^{o}C and the system was held at this temperature for 3 h. During the pyrolysis process, the pressure inside the reactor was monitored as a function of pyrolysis time and temperature. The gaseous products were analyzed for composition at the end of the experiment by taking samples at the 3-way valve manually to gas chromatography (GC).

To study the potential of hydrogen separation on the permeate side during pyrolysis of biochar, the impermeable disk was replaced by the metal membrane cut from a commercial

Pd_{77} Ag_{23} foil (Alfa Aesar, 25μm thick, 99.9% metals basis) and sealed with graphite O-rings to provide an effective permeation area of ~$6x10^{-5}$ m^2. A macroporous stainless steel disk was used as support to provide mechanical strength with negligible mass transfer resistance. After biochar sample purging and reactor evacuation, pyrolysis tests were performed at conditions like the conditions above with the impermeable substrate. Ultra-high pure N_2 (~5 mL/min) was introduced in the sweep side (permeate side) of the membrane to purge the gases permeating through the membrane for composition analysis using online injection gas chromatography. The hydrogen permeance was calculated by dividing the hydrogen flux by the hydrogen partial pressure difference over the membrane.

6.2.5 Chemical analysis and material characterization

An elemental analyzer (PE 2400 Series II CHNS/O Analyzer) was used to analyze the elemental composition (C, H, N, S content) of the algae biomass, biocrude oil and biochar samples (Wang et al., 2015). The $Pd_{77}Ag_{23}$ membrane was characterized before and after pyrolysis experiments using XRD for phase structure and crystallinity (Bruker D8ADVANCE X-ray diffractometer; Cu Kα radiation (λ = 1.542 Å) at 40 kV and 40 mA, scan step of 0.05º). The images of membrane surface and cross-section before and after the reaction, as well as EDAX analysis were obtained using a scanning electron microscope, (SEM, Amray 1910). The biochemical composition (lipid, carbohydrate, protein, and ash) of the algae biomass were measured by the standard methods developed by the National Renewable Energy Laboratory (Dandamudi et al., 2019).

6.3 Results and discussion

6.3.1 Analysis of feedstock and biochar

The feedstock's biochemical composition and other characteristics for *G. sulphuraria* are provided in Table 6.1. The biomass shows an ash content of ~10 % post-harvesting and contains a relatively high content of proteins, lesser carbohydrates and lipid content with very little variations from previous reports (Cheng et al., 2017). Ultimate analysis (CHNS/O) of the biomass and HTL biochar are provided in Table 6.2. The low carbon and high nitrogen, as well as the relatively high oxygen of the feedstock, are attributed respectively to low lipid, high protein and relatively high carbohydrate content of *G. sulphuraria* (Dandamudi et al., 2017). The HTL process at 300 °C, 9 MPa, and 30 residence time yielded 32.02 wt. % of biocrude, 12.84 wt. % of biochar, 7.07 wt. % of aqueous phase products. HTL biochar can be a mixture of unreacted biomass, ash, high molecular weight re-polymerized fuel molecules. Table 6.2 shows the CHNS/O elemental content of the biomass and HTL biochar. This correlates with the increased carbon content (57.79 wt. %) compared to that of original biomass (49.71 wt.%) which is similar our previous work (Dandamudi et al., 2017). These results suggest that aliphatic compounds were enriched, and biomass was deoxygenated and denitrogenated during HTL.

Table 6.1: Biochemical and proximate analysis of algal biomass, *G. sulphuraria*

Proximate analysis (wt.%)	
Ash	9.22 ± 0.89%
Moisture	69.99 ± 0.41%
Biochemical content (wt. %)	
Lipid (FAME)	6.25 ± 0.58 %
Carbohydrates	21.4 ± 0.99%
Proteins	52.48 ± 0.61%

Table 6.2: Ultimate analysis of algal biomass, *G. sulphuraria* biomass and HTL products

Element	*G. sulphuraria*	Biochar	Biocrude
C, wt. %	49.71±0.05	57.79±0.97	73.55±1.71
H, wt. %	7.73±0.17	6.36±0.24	9.21±0.04
N, wt. %	10.55±0.41	7.40±0.42	7.05±0.34
S, wt. %	1.83 ±0.07	0.64±0.02	0.99±0.08
O*, wt. %	30.18	27.54	9.2

* wt. %: 100-Sum (C, H, N, S wt. %)

6.3.2 TGA and fixed bed pyrolysis characteristics

The TGA curves of both the biomass and the HTL biochar samples in the nitrogen atmosphere can be separated as three stages as presented in Figure 6.3. The majority of the organic materials decompose during the second stage. The first stage (25 to ~150 °C) shows a minimal weight loss, that represents the loss of moisture. The weight loss at this stage was about 6.0 % for the biomass and 2.8% for the biochar sample. For the biomass, the second stage (150–580 °C) shows a steep weight loss at 150–320 °C (42.8 wt. %) due to the decomposition of the high content of protein, and a less steep decomposition (24.6 wt. %) from 320 to 580 °C due to the decomposition of the lipids and carbohydrates (Cheng et al., 2018; Dandamudi et al., 2020a). The reverse is true for the biochar samples, which shows (13.3 wt.%) weight loss from 150 to 320 °C and (24.6 wt. %) from 320 to 580 °C. The third stage for the biomass and biochar samples (>580 °C) corresponds to the slow degradation of carbonaceous material (Dandamudi et al., 2020b).

The biochar sample resulted in a weight loss of 70.81% (Figure 6.3 (B)) when heated to 1000 ^{o}C. This high temperature, can not be reached during membrane reactor operation due to the sensitivity of membrane to heat. Therefore, isothermal TGA runs were performed using three ramping rates to a holding temperature of 500 ^{o}C. The biochar samples were kept at this temperature for 24 h (Figure 6.4). A slight variation in the final weight loss of biochar samples (56.4-58.7 %) was noticed as a function of the ramping rate

and is presented in Appendix B. The differential thermogravimetric (DTG) curves of the biochar in Figure 6.5, mainly shows two degradation peaks at a temperature of about ~250 and 430 ^{o}C. A change in the rate of degradation curve (first peak) was noticed as the heating rate increased towards the higher temperature. This shift could be due to the temperature gradient inside the biochar sample, the low thermal conductivity of biochar, at higher heating rates (Thangalazhy-Gopakumar et al., 2012).

Fixed bed reactor pyrolysis was performed at similar conditions applied in TGA pyrolysis. The test is first conducted with no biochar sample to bake the carbon O-rings since we found that they emit some gases that could interfere with the test results. As given in Appendix B, when heating the reactor with no sample, H_2, CH_4, and CO_2 gases were identified. H_2, CH_4 reach a minimal value after 10 h of heating at 500 ^{o}C, while CO_2 was almost constant, probably due to the ppm level of oxygen in the used industrial nitrogen. These gases could come from the decomposition of the binding material in the graphite O-ring. TGA tests for graphite O-ring showed a weight loss of 0.94 % when heated in nitrogen stream to 500 ^{o}C and kept at this temperature for 6 h (Appendix B).

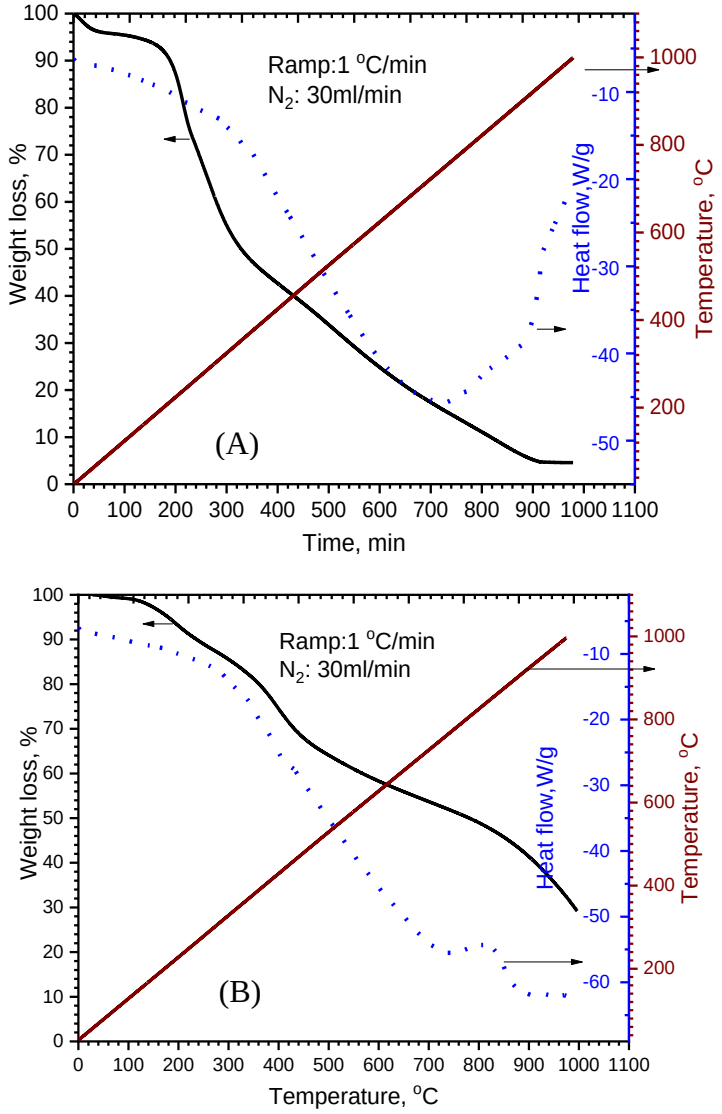

Figure 6.3: Thermogravimetric analysis, TGA, plot for the *G. sulphuraria* biomass (A) and a biochar sample (B) remaining after HTL when heated to a temperature of 1000 °C in nitrogen atmosphere.

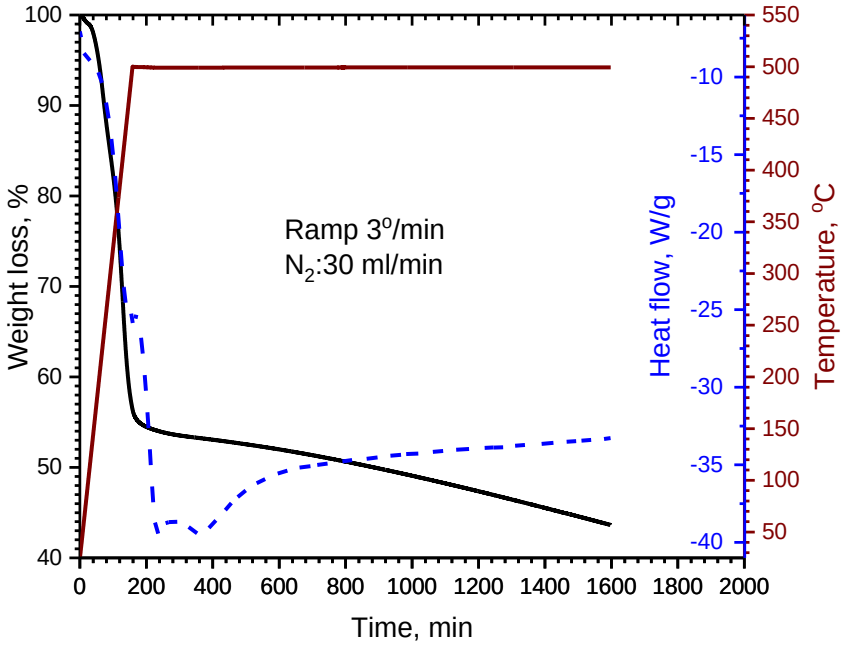

Figure 6.4: Thermogravimetric analysis, TGA, plot for the *G. sulphuraria* biomass

After the reactor cools down to room temperature, the reactor is opened from its bottom and the sample is inserted. The reactor is checked for leakage before conducting the pyrolysis experiment. The distribution of gases during fixed bed pyrolysis experiment are presented as a function of time in Figure 6.6. The gases start to evolve at about 250-300 ^{o} C, go through a maximum at 500 ^{o}C then start to decrease during the isothermal period, which matches the data obtained by TGA. Carbon monoxide (CO) was the first gas to evolve during pyrolysis and was not detected after about 7 h. Fixed bed pyrolysis at these conditions yielded 46.68 wt.% liquid (oil and water), 44.67 wt.% residual ash and 5.93 wt.

% of gases. The evolved gases have the composition of (45.7 H_2, 44.05 CH_4 and 10.25 CO vol. %). Other C_2, C_3 compounds, NOx and H_2S gases were not determined.

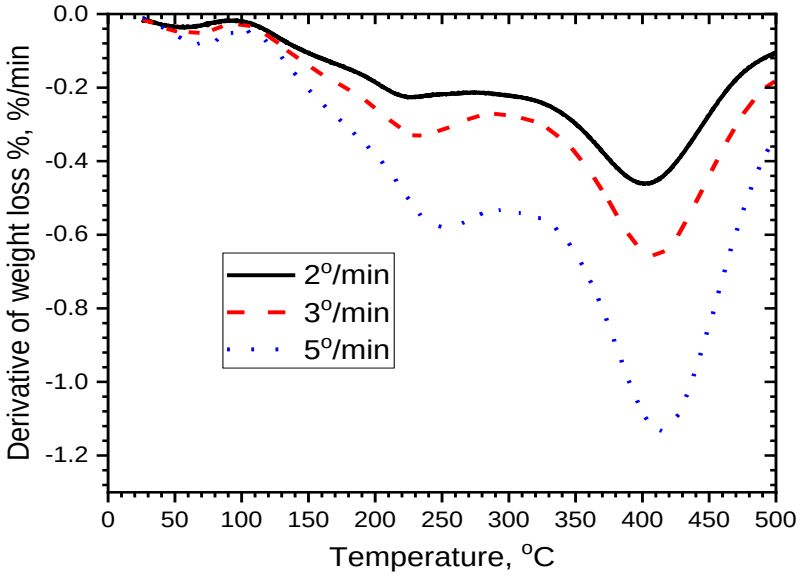

Figure 6.5: Differential thermogravimetric, DTG curves for the HTL biochar sample when heated to a temperature of 500 °C in a nitrogen atmosphere at different heating rates.

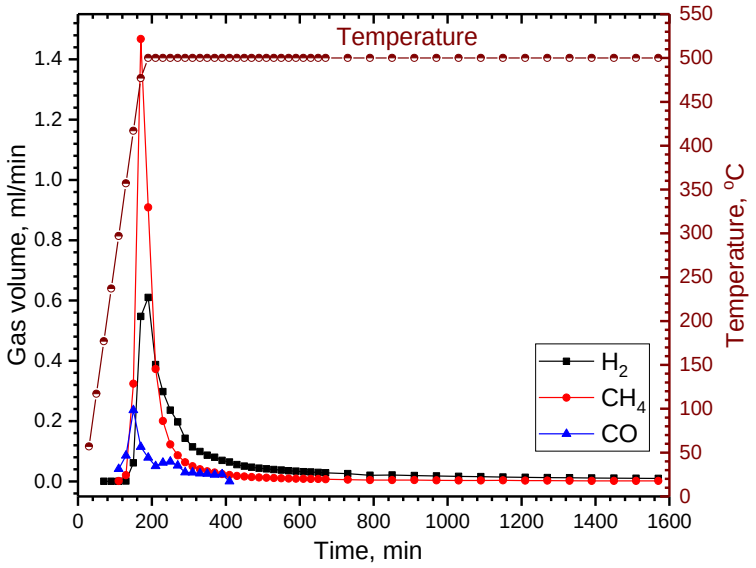

Figure 6.6: Fixed bed pyrolysis of HTL biochar gas distribution as a function of pyrolysis time and temperature.

6.3.3 Biochar batch reactor experiments

Following the fixed bed and TGA experiments, pyrolysis experiments were also performed in a batch closed reactor equipped with/without a membrane. The reactor was heated in an electric furnace for 10 h at 500 ^{o}C to bake the O-rings and reach a minimum level of emitted gases before conducting experiments with biochar samples. For experiments an impermeable disk, the gases evolved and pressure accumulation inside the reactor (gage pressure) increases by increasing the biochar sample as shown in Figure 6.7. Also, the gases evolved per grams sample (Figure 6.7 (B)) were found to increase, which suggests decomposition of part of the produced oil upon increasing the pressure inside the reactor (Maliutina et al., 2018) and the evolution of CO2 is attributed to thermal

decomposition of major amino acids in protein structure) Maliutina et al., 2017(. The remaining ash was found to increases with increasing reactor pressure as given in Table 6.3 since high pressure favors the release of heavy tar components from biochar (Maliutina et al., 2018). The pyrolysis of biochar at high pressure resulted in a lower carbon content in ash, while the hydrogen, nitrogen and oxygen retention in ash increased.

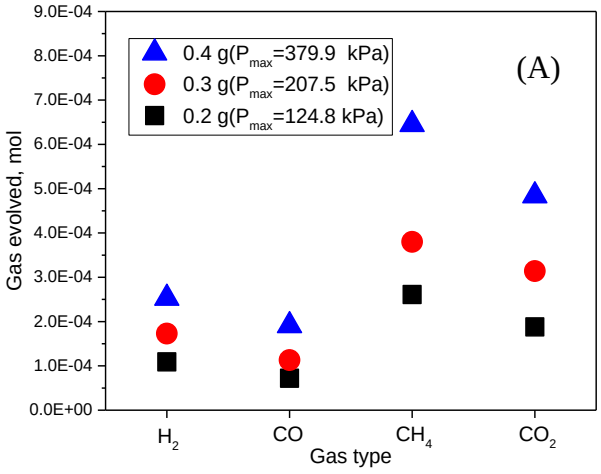

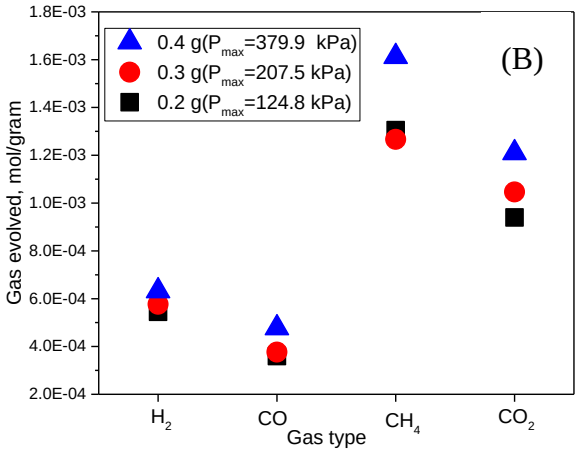

Figure 6.7: Gases evolved during batch pyrolysis of HTL biochar samples of different weights.

Membrane reactor experiments were conducted using the samples 0.3 and 0.4 g since the accumulated pressure inside the reactor is good enough to provide a driving force for hydrogen permeation. The pressure in the reactor as a function of furnace temperature and pyrolysis time for HTL biochar samples with the impermeable disk and Pd_{77} Ag_{23} membrane are given in figure 6.8. As noticed, the pressure inside the reactor is smaller in the case of a Pd_{77} Ag_{23} membrane due to gases, mainly hydrogen, permeating through the membrane. Figure 6.9 shows the hydrogen recovered in the permeate side of the Pd_{77} Ag_{23} membrane as a function of pyrolysis time and temperature. Other gases detected such as CH_4 and CO_2 was less than their level coming out of the baked graphite O-rings. H_2 starts to permeate through the membrane when the pressure inside the reactor builds up to about 100 kPa (gauge pressure) and then shows a peak when the pressure reaches a maximum value in the reactor and then decreases as a function of time although the pressure inside the reactor does not change, which also confirms no leakage through the membrane. This decrease of H_2 through the membrane can be attributed to lower hydrogen partial pressure, driving force, inside the reactor as a function of time.

Table 6.3: Ultimate analysis of the solids remaining after batch reactor pyrolysis tests

Case	Biochar Sample	Remaining solids (%)	C	H	N	S	O *
Impermeable disk	0.2 g	(51.61)	81.36±1.85	2.85±0.25	7.68±0.38	0.18±0.04	7.93
	0.3 g	(51.73)	80.89±0.21	3.13±0.19	7.85±0.27	0.13±0.07	8.0
	0.4 g	(51.90)	80.03±3.21	3.3±0.27	7.87±0.13	0.17±0.02	8.93
d_{77} g_{23} membrane	0.3 g	(51.35)	81.39±0.19	2.96±0.18	7.77±0.15	0.12±0.03	7.76
	0.4 g	(51.64)	80.68±0.28	3.06±0.4	7.91±0.2	0.14±0.04	8.21

* Calculated by difference

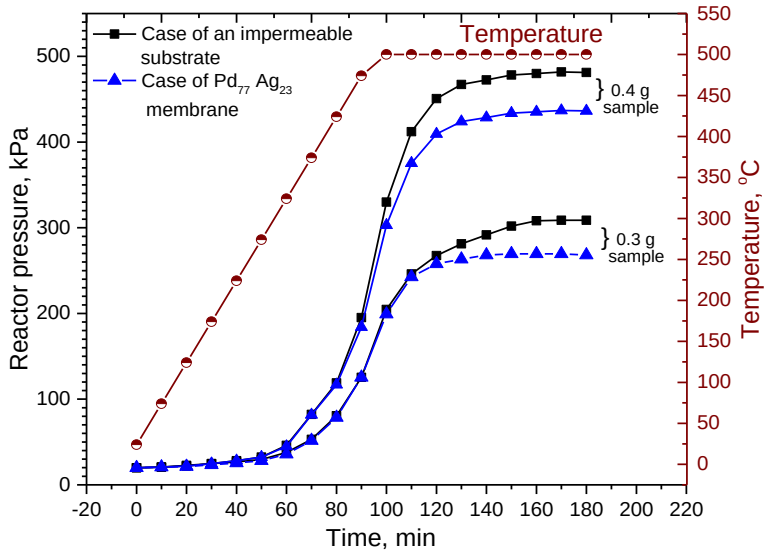

Figure 6.8: Batch membrane reactor pyrolysis experiments of 0.3 g and 0.4 g HTL biochar samples: pressure monitored as a function of temperature and pyrolysis time with an impermeable substrate and with Pd_{77} Ag_{23} membrane.

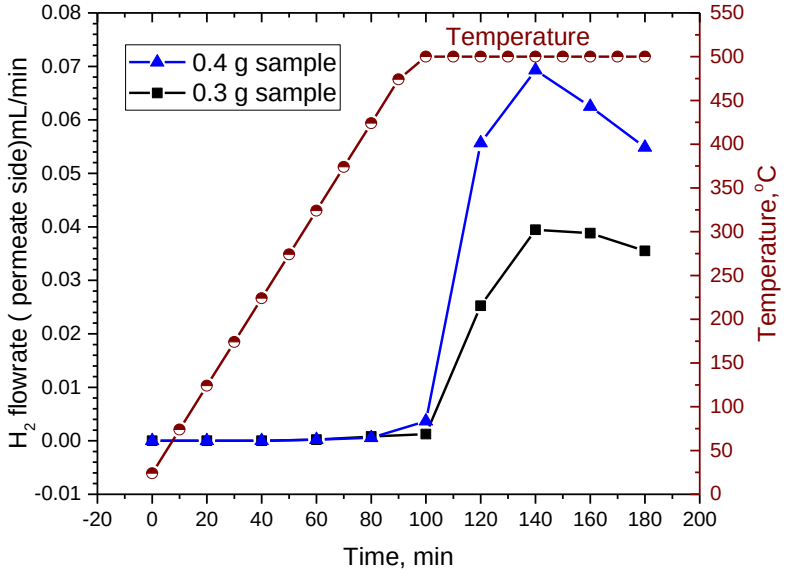

Figure 6.9: Hydrogen recovered in the $Pd_{77}Ag_{23}$ membrane permeate side as a function of pyrolysis time and temperature with HTL biochar samples of 0.3 and 0.4 g

The composition of the gases remaining inside the reactor (retentate stream), with the impermeable disk and $Pd_{77}Ag_{23}$ membrane, as well as the hydrogen permeating through the membrane was determined for the 0.4 g sample test and the data are collected in Table 6.4 expressed as a wt. % of the original biochar sample. The data shows a reduction in the content of H_2, CO and CO_2 in the reactor when the $Pd_{77}Ag_{23}$ membrane is used and there is a significant increase in the content of CH_4. The decrease in H_2 content in the reactor is clearly a result of hydrogen permeation through the membrane. This could also be the reason for more hydrogen to be produced from the biochar sample leading to an increase of the total hydrogen produced when the membrane was used. The hydrogen permeating through the membrane is 2.08 times the hydrogen remaining in the reactor (retentate

stream). The decrease in the content of CO and CO_2 and the increase in the content of CH_4 in the reactor can be only explained by the methanation reaction for CO and CO_2 to CH_4 facilitated at the presence of the palladium membrane (Park and McFarland, 2009). In comparison to the fixed bed pyrolysis experiment the decrease in H_2, CO and CH_4 and the increase in CO_2 are attributed to the buildup of pressure inside the reactor and thermal cracking of the oil coming out of the biochar sample (Maliutina et al., 2018).

Table 6.4: Hydrogen balance and membrane performance for pyrolysis of 0.4 g HTL biochar samples

Case & sample wt.	(Gas /biochar sample) Wt.%						
	Reactor Side				H_2 in Permeate	Total H_2	All gases produced
	H_2	CO	CH_4	CO_2			
Impermeable disk (0.4g)	0.127	1.34	2.39	5.322	/	0.127	9.18
$Pd_{77}Ag_{23}$ membrane (0.4g)	0.047	1.19	2.78	5.10	0.098	0.145	9.22
Fixed bed (1.5g)	0.417	1.536	3.723	/	/	0.417	5.67

6.3.4 Membrane characteristics

The $Pd_{77}Ag_{23}$ membrane before and after pyrolysis experiments was characterized using SEM, EDAX and XRD. The as-received $Pd_{77}Ag_{23}$ membrane exhibits a relatively flat and smooth surface, with no surface defects as imaged by SEM (Figure 6.10 (A)). Post pyrolysis, the membrane surface (feed side) loses its luster and shows a noticeable etching or pitting and particle-like substances (nodules: micron-scale features protruding from the surface) on the membrane surface as presented in Figure 6.10 (B&C). It seems that the etching is not very uniform as shown in the low magnification SEM image (Figure 6.10 (C)). These microstructure changes are only on the membrane surfaces and do not create transmembrane defects that would allow permeation for gas species other than H_2 (Figure 6.10 (E)). This surface roughening could be attributed to sulfide formation on the membrane feed surface (Antoniazzi et al., 1989; Kulprathipanja et al., 2005). It was clearly given that sulfur content of the fresh biochar samples reduced from 0.64 to about ~0.15 after batch reactor pyrolysis tests as given in Tables 6.2 and 6.3.

The surface composition, as determined by EDAX, of the as received $Pd_{77}Ag_{23}$ alloy membrane is approximately equal to its ratio expected. The feed side of the membrane shows a sulfur concentration of ~2.36 and 4.05 wt. % for the membrane whole area, and the large nodules seen on the membrane surface. The small decrease in the Pd/Ag ratio noticed by EDAX analysis indicates that silver segregation from the bulk to the top surface has occurred. This observation was previously reported for a Pd–23%Ag exposed to trace

amounts of H_2S and can be confirmed using X-ray photoelectron spectroscopy, XPS (Peters et al., 2016) technique but this is beyond the focus of our study.

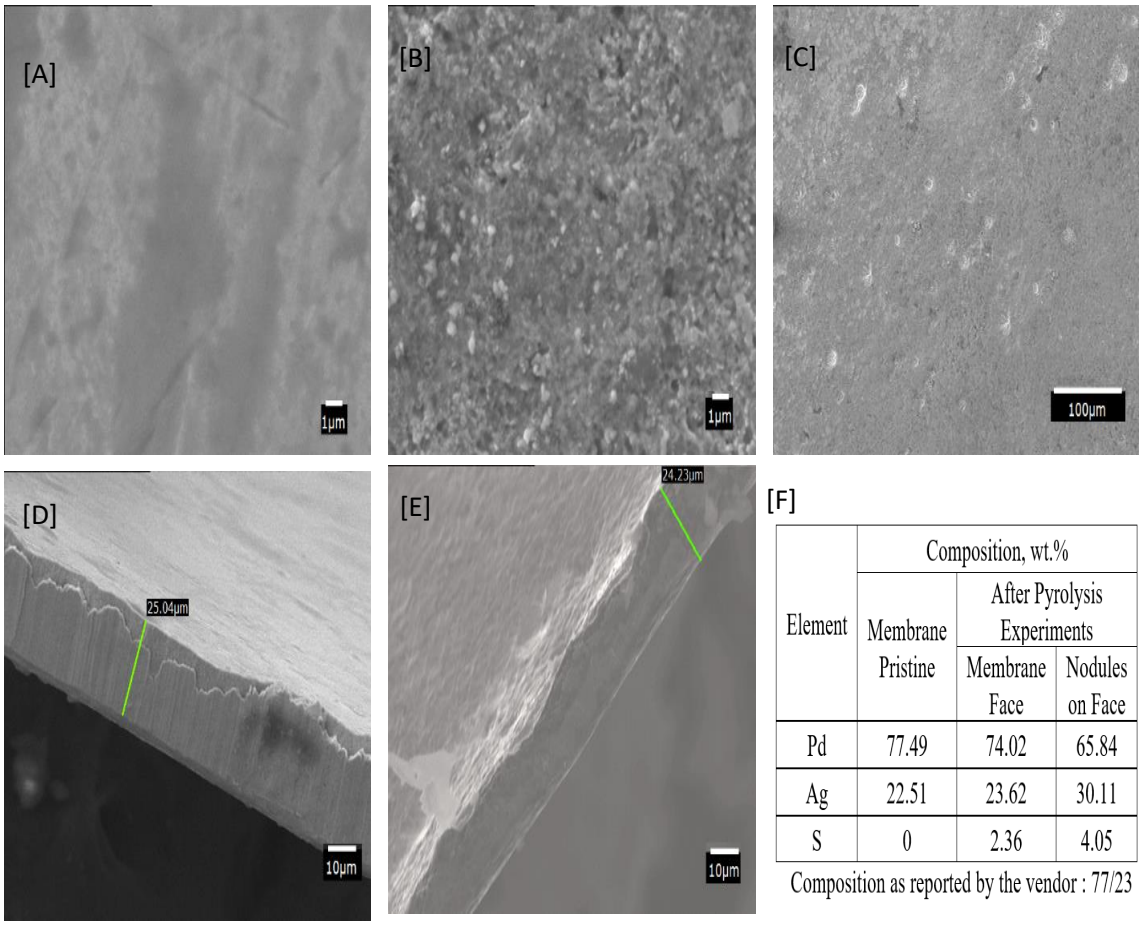

[F]

Element	Composition, wt.%		
	Membrane Pristine	After Pyrolysis Experiments	
		Membrane Face	Nodules on Face
Pd	77.49	74.02	65.84
Ag	22.51	23.62	30.11
S	0	2.36	4.05

Composition as reported by the vendor : 77/23

Figure 6.10: SEM surface morphology [A-C] and cross section [D, E] as well as EDAX analysis of the Pd_{77} Ag_{23} membrane before and after pyrolysis experiments.

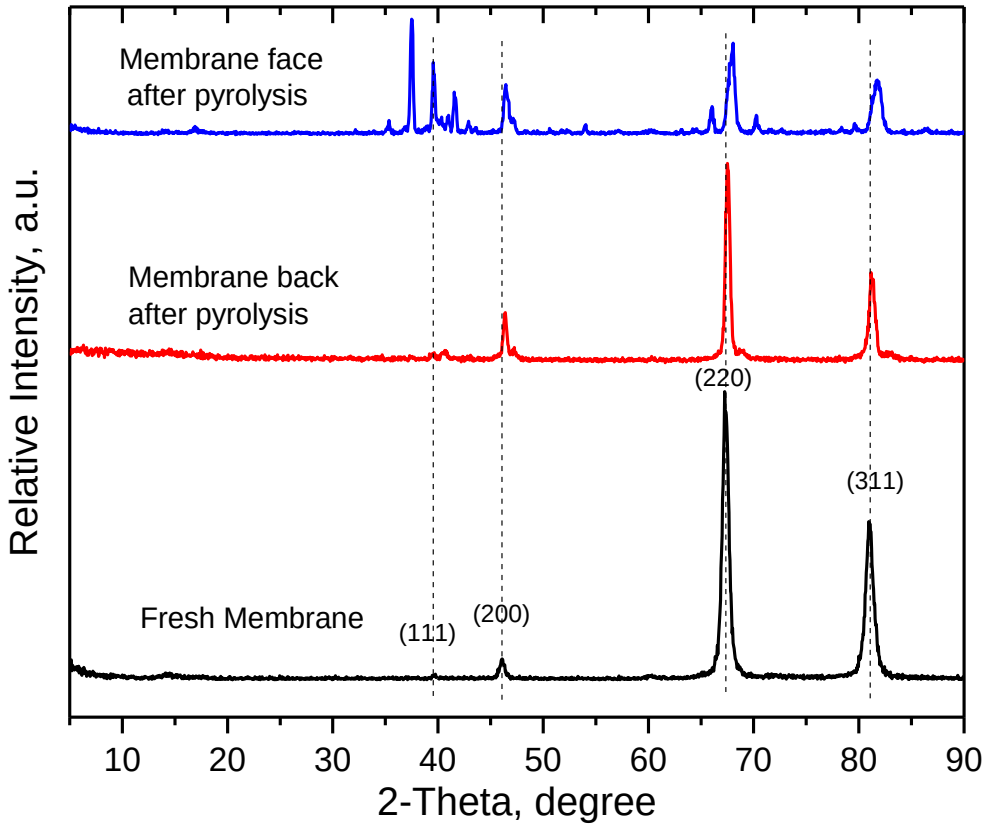

Figure 6.11: XRD patterns of the pristine Pd_{77} Ag_{23} membrane and the membrane (face and back) after pyrolysis.

Figure 6.11 shows the XRD patterns obtained for the pristine $Pd_{77}Ag_{23}$ film and the film after pyrolysis experiments. The XRD pattern for the Pd_{77} Ag_{23} alloy membrane shows diffraction peaks of all the major lattice planes of low Miller *indices* of the alloy's face-centered cubic structure (Mundschau et al., 2006; Peters et al., 2013). The XRD

pattern for the permeate side of the $Pd_{77}Ag_{23}$ membrane shows no structural significant changes or sulfide formation, only small shoulder peaks are observed at the (200), (220), and (311) diffraction peaks. Additional diffraction peaks are observed on the feed side of the membrane suggesting the formation of sulfides (a palladium–silver- sulfide phase). This phase has previously been identified as $Ag_5Pd_{10}S_5$ (Mundschau et al., 2006; Peters et al., 2013). It seems therefore reasonable to assume that the small decrease in the Pd/Ag ratio noticed by EDAX analysis is attributed to the formation of an $Ag_5Pd_{10}S_5$ phase (Mundschau et al., 2006; Peters et al., 2016). Obviously, the sulfur content does not correspond exactly to the $Ag_5Pd_{10}S_5$ phase stoichiometry. This can be explained by a dilution effect by the grains which do not contain sulfur, as previously detected in the SEM-EDAX analysis.

The H_2 permeability of the $Pd_{77}Ag_{23}$ as received membrane films is $5.3x10^{-9}$ mol/ (m^2 s $Pa^{0.5}$) obtained applying a feed gas mixture of 90% H_2 in N_2. A sharp reduction in the permeability was noticed in the first (0.3 g sample) and the second (0.4 g sample) pyrolysis experiments to about 1.6 $x10^{-10}$ and 1.4 $x10^{-10}$ mol/(m^2.s.$Pa^{0.5}$) respectively. In dense Pd-based membranes, molecular hydrogen must be dissociated on the feed-side membrane surface, to allow transport of atomic hydrogen through the bulk membrane and subsequent recombinative desorption at the low pressure, permeate surface (Mundschau et al., 2006). In consideration with the membrane thickness (25 μm), this may still indicate that the bulk diffusion is the rate-limiting step for H_2 permeation (Flanagan and Wang,

2010; Hurlbert and Konecny, 1961). However, the transport mechanism for hydrogen through a dense metal membrane can be described using the solution-diffusion model, where the permeability is expressed as the product of diffusivity and solubility of hydrogen in the dense metal membrane (Al-Mufachi et al., 2015). This sharp reduction in the permeability based on the characteristics of the membrane after pyrolysis experiments can be attributed basically to sulfide films formed on the membrane and detected using SEM and XRD. These sulfide films were found one order-of-magnitude less permeable to hydrogen than pure Pd (O'Brien et al., 2011), which could explain the gradual decrease in H_2 permeability.

It should be mentioned that H_2S in the H_2 feed gas inhibits H_2 transport by a secondary mechanism that may involve blocking of H_2 dissociation sites (O'Brien et al., 2011). Previous reports showed that Pd–Ag-based alloy membranes exhibit a sharp decrease in H_2 flux with around 85–95% compared to the H_2 flux obtained in the absence of only 20 ppm H_2S (Peters et al., 2016, 2013). It is also important to mention that surface segregation effects of Ag to the feed side could decrease the H_2 permeability because Ag has lower H_2 solubility than Pd (Lai and Lind, 2015). The main driving force for hydrogen permeation is the difference in hydrogen partial pressure between the feed side and permeate side of the membrane. Once, this driving force decreases due to hydrogen coming out of the membrane and or less hydrogen produced from biochar pyrolysis, the hydrogen permeance will decrease as noticed after ~ two hours of pyrolysis.

6.4 Conclusions

As hypothesized, the pyrolysis of HTL biochar from *Galdieria sulphuraria* at 500 ˚C ,1 atm for 24 h in a fixed bed reactor produces 5.93 wt.% gas, 46.68 wt.% oil/water and 44.67 wt.% solid residue, with the gaseous product containing 45.70 mol % H_2, 44.05 mol % CH_4 and 10.25 mol % of CO. This study also confirms that the involvement of a hydrogen-selective metal membrane in the reactor during the pyrolysis of HTL biochar results in recovery of hydrogen in the permeate stream (~twice the hydrogen remaining in the reactor or retentate stream) and further facilitates the decomposition process. The retentate stream shows reduced CO and CO_2 as well as increased CH_4 content compared to pyrolysis conditions with no membrane. This work suggests the need for developing membrane reactors for biomass pyrolysis with a continuous feed of solid or liquid low-lipid algae and hydrogen-permeable membranes with improved sulfur tolerance.

6.5 References

Al-Mufachi, N.A., Rees, N. V, Steinberger-Wilkens, R., 2015. Hydrogen selective membranes: A review of palladium-based dense metal membranes. Renew. Sustain. Energy Rev. 47, 540–551.

Antoniazzi, A.B., Haasz, A.A., Stangeby, P.C., 1989. The effect of adsorbed carbon and sulphur on hydrogen permeation through palladium. J. Nucl. Mater. 162, 1065–1070.

Bird, M.I., Wurster, C.M., de Paula Silva, P.H., Bass, A.M., De Nys, R., 2011. Algal biochar–production and properties. Bioresour. Technol. 102, 1886–1891.

Bird, M.I., Wurster, C.M., de Paula Silva, P.H., Paul, N.A., De Nys, R., 2012. Algal biochar: effects and applications. Gcb Bioenergy 4, 61–69.

Bordoloi, N., Goswami, R., Kumar, M., Kataki, R., 2017. Biosorption of Co (II) from aqueous solution using algal biochar: kinetics and isotherm studies. Bioresour. Technol. 244, 1465–1469.

Brennan, L., Owende, P., 2010. Biofuels from microalgae—a review of technologies for production, processing, and extractions of biofuels and co-products. Renew. Sustain. energy Rev. 14, 557–577.

Chen, Y., Wu, Y., Hua, D., Li, C., Harold, M.P., Wang, J., Yang, M., 2015. Thermochemical conversion of low-lipid microalgae for the production of liquid

fuels: challenges and opportunities. RSC Adv. 5, 18673–18701.

Cheng, F., Cui, Z., Chen, L., Jarvis, J., Paz, N., Schaub, T., Nirmalakhandan, N., Brewer, C.E., 2017. Hydrothermal liquefaction of high-and low-lipid algae: Bio-crude oil chemistry. Appl. Energy 206, 278–292.

Cheng, F., Cui, Z., Mallick, K., Nirmalakhandan, N., Brewer, C.E., 2018. Hydrothermal liquefaction of high-and low-lipid algae: Mass and energy balances. Bioresour. Technol. 258, 158–167.

Cole, A.J., Paul, N.A., De Nys, R., Roberts, D.A., 2017. Good for sewage treatment and good for agriculture: Algal based compost and biochar. J. Environ. Manage. 200, 105–113.

Daiyan, R., Lu, X., Ng, Y.H., Amal, R., 2017. Liquid Hydrocarbon Production from CO2: Recent Development in Metal-Based Electrocatalysis. ChemSusChem 10, 4342–4358.

Dandamudi, K.P.R., Muhammed Luboowa, K., Laideson, M., Murdock, T., Seger, M., McGowen, J., Lammers, P.J., Deng, S., 2020a. Hydrothermal liquefaction of Cyanidioschyzon merolae and Salicornia bigelovii Torr.: The interaction effect on product distribution and chemistry. Fuel 277, 118146. https://doi.org/https://doi.org/10.1016/j.fuel.2020.118146

Dandamudi, K.P.R., Muhammed Luboowa, K., Laideson, M., Murdock, T., Seger, M.,

McGowen, J., Lammers, P.J., Deng, S., 2020b. Hydrothermal Liquefaction of Cyanidioschyzon merolae and Salicornia bigelovii Torr.: The interaction effect on product distribution and chemistry. Fuel 277. https://doi.org/10.1016/j.fuel.2020.118146

Dandamudi, K.P.R., Muppaneni, T., Markovski, J.S., Lammers, P., Deng, S., 2019. Hydrothermal liquefaction of green microalga Kirchneriella sp. under sub- and super-critical water conditions. Biomass and Bioenergy 120. https://doi.org/10.1016/j.biombioe.2018.11.021

Dandamudi, K.P.R., Muppaneni, T., Sudasinghe, N., Schaub, T., Holguin, F.O., Lammers, P.J., Deng, S., 2017. Co-liquefaction of mixed culture microalgal strains under sub-critical water conditions. Bioresour. Technol. 236. https://doi.org/10.1016/j.biortech.2017.03.165

Elsherif, M., Manan, Z.A., Kamsah, M.Z., 2015. State-of-the-art of hydrogen management in refinery and industrial process plants. J. Nat. Gas Sci. Eng. 24, 346–356.

Flanagan, T.B., Wang, D., 2010. Exponents for the pressure dependence of hydrogen permeation through Pd and Pd− Ag alloy membranes. J. Phys. Chem. C 114, 14482–14488.

Guo, Y., Yeh, T., Song, W., Xu, D., Wang, S., 2015. A review of bio-oil production from

hydrothermal liquefaction of algae. Renew. Sustain. Energy Rev. 48, 776–790.

Hurlbert, R.C., Konecny, J.O., 1961. Diffusion of hydrogen through palladium. J. Chem. Phys. 34, 655–658.

Johansson, C.L., Paul, N.A., de Nys, R., Roberts, D.A., 2016. Simultaneous biosorption of selenium, arsenic and molybdenum with modified algal-based biochars. J. Environ. Manage. 165, 117–123.

Kikuchi, E., 2000. Membrane reactor application to hydrogen production. Catal. Today 56, 97–101.

Kulprathipanja, A., Alptekin, G.O., Falconer, J.L., Way, J.D., 2005. Pd and Pd–Cu membranes: inhibition of H2 permeation by H2S. J. Memb. Sci. 254, 49–62.

Kumar, A., Ergas, S., Yuan, X., Sahu, A., Zhang, Q., Dewulf, J., Malcata, F.X., Van Langenhove, H., 2010. Enhanced CO2 fixation and biofuel production via microalgae: recent developments and future directions. Trends Biotechnol. 28, 371–380.

Lai, T., Lind, M.L., 2015. Heat treatment driven surface segregation in Pd77Ag23 membranes and the effect on hydrogen permeability. Int. J. Hydrogen Energy 40, 373–382.

Li, Z., Savage, P.E., 2013. Feedstocks for fuels and chemicals from algae: treatment of crude bio-oil over HZSM-5. Algal Res. 2, 154–163.

Liu, Z., Zhang, F.-S., 2009. Removal of lead from water using biochars prepared from hydrothermal liquefaction of biomass. J. Hazard. Mater. 167, 933–939.

Maliutina, K., Tahmasebi, A., Yu, J., 2018. Pressurized entrained-flow pyrolysis of microalgae: Enhanced production of hydrogen and nitrogen-containing compounds. Bioresour. Technol. 256, 160–169.

Maliutina, K., Tahmasebi, A., Yu, J., Saltykov, S.N., 2017. Comparative study on flash pyrolysis characteristics of microalgal and lignocellulosic biomass in entrained-flow reactor. Energy Convers. Manag. 151, 426–438.

Mundschau, M. V, Xie, X., Evenson IV, C.R., Sammells, A.F., 2006. Dense inorganic membranes for production of hydrogen from methane and coal with carbon dioxide sequestration. Catal. Today 118, 12–23.

Muppaneni, T., Reddy, H.K., Selvaratnam, T., Dandamudi, K.P.R., Dungan, B., Nirmalakhandan, N., Schaub, T., Omar Holguin, F., Voorhies, W., Lammers, P., Deng, S., 2017. Hydrothermal liquefaction of Cyanidioschyzon merolae and the influence of catalysts on products. Bioresour. Technol. 223. https://doi.org/10.1016/j.biortech.2016.10.022

O'Brien, C.P., Gellman, A.J., Morreale, B.D., Miller, J.B., 2011. The hydrogen permeability of Pd4S. J. Memb. Sci. 371, 263–267.

Ockwig, N.W., Nenoff, T.M., 2007. Membranes for hydrogen separation. Chem. Rev.

107, 4078–4110.

Paglieri, S.N., Way, J.D., 2002. Innovations in palladium membrane research. Sep. Purif. Methods 31, 1–169.

Park, J.-N., McFarland, E.W., 2009. A highly dispersed Pd–Mg/SiO2 catalyst active for methanation of CO2. J. Catal. 266, 92–97.

Patil, P.D., Dandamudi, K.P.R., Wang, J., Deng, Q., Deng, S., 2018. Extraction of bio-oils from algae with supercritical carbon dioxide and co-solvents. J. Supercrit. Fluids 135, 60–68. https://doi.org/https://doi.org/10.1016/j.supflu.2017.12.019

Peters, T.A., Kaleta, T., Stange, M., Bredesen, R., 2013. Development of ternary Pd–Ag–TM alloy membranes with improved sulphur tolerance. J. Memb. Sci. 429, 448–458.

Peters, T.A., Stange, M., Veenstra, P., Nijmeijer, A., Bredesen, R., 2016. The performance of Pd–Ag alloy membrane films under exposure to trace amounts of H2S. J. Memb. Sci. 499, 105–115.

Salimi, P., Askari, K., Norouzi, O., Kamali, S., 2019a. Improving the electrochemical performance of carbon anodes derived from marine biomass by using ionic-liquid-based hybrid electrolyte for LIBs. J. Electron. Mater. 48, 951–963.

Salimi, P., Norouzi, O., Pourhoseini, S.E.M., Bartocci, P., Tavasoli, A., Di Maria, F., Pirbazari, S.M., Bidini, G., Fantozzi, F., 2019b. Magnetic biochar obtained through catalytic pyrolysis of macroalgae: A promising anode material for Li-ion batteries.

Renew. Energy 140, 704–714.

Son, E.-B., Poo, K.-M., Chang, J.-S., Chae, K.-J., 2018. Heavy metal removal from aqueous solutions using engineered magnetic biochars derived from waste marine macro-algal biomass. Sci. Total Environ. 615, 161–168.

Staffell, I., Scamman, D., Abad, A.V., Balcombe, P., Dodds, P.E., Ekins, P., Shah, N., Ward, K.R., 2019. The role of hydrogen and fuel cells in the global energy system. Energy Environ. Sci. 12, 463–491.

Taghavi, S., Norouzi, O., Tavasoli, A., Di Maria, F., Signoretto, M., Menegazzo, F., Di Michele, A., 2018. Catalytic conversion of Venice lagoon brown marine algae for producing hydrogen-rich gas and valuable biochemical using algal biochar and Ni/SBA-15 catalyst. Int. J. Hydrogen Energy 43, 19918–19929.

Thangalazhy-Gopakumar, S., Adhikari, S., Chattanathan, S.A., Gupta, R.B., 2012. Catalytic pyrolysis of green algae for hydrocarbon production using H+ ZSM-5 catalyst. Bioresour. Technol. 118, 150–157.

Toplin, J.A., Norris, T.B., Lehr, C.R., McDermott, T.R., Castenholz, R.W., 2008. Biogeographic and phylogenetic diversity of thermoacidophilic cyanidiales in Yellowstone National Park, Japan, and New Zealand. Appl. Environ. Microbiol. 74, 2822–2833.

Uemiya, S., Matsuda, T., Kikuchi, E., 1991. Hydrogen permeable palladium-silver alloy

membrane supported on porous ceramics. J. Memb. Sci. 56, 315–325.

Uemiya, S., Sato, N., Ando, H., Matsuda, T., Kikuchi, E., 1990. Steam reforming of methane in a hydrogen-permeable membrane reactor. Appl. Catal. 67, 223–230.

Wang, J., Krishna, R., Yang, J., Dandamudi, K.P.R., Deng, S., 2015. Nitrogen-doped porous carbons for highly selective CO<inf>2</inf> capture from flue gases and natural gas upgrading. Mater. Today Commun. 4. https://doi.org/10.1016/j.mtcomm.2015.06.009

Xiong, S., Lian, Y., Xie, H., Liu, B., 2019. Hydrogenation of CO2 to methanol over Cu/ZnCr catalyst. Fuel 256, 115975.

Yu, G., Zhang, Y., Schideman, L., Funk, T., Wang, Z., 2011. Distributions of carbon and nitrogen in the products from hydrothermal liquefaction of low-lipid microalgae. Energy Environ. Sci. 4, 4587–4595.

Yu, K.L., Lau, B.F., Show, P.L., Ong, H.C., Ling, T.C., Chen, W.-H., Ng, E.P., Chang, J.-S., 2017. Recent developments on algal biochar production and characterization. Bioresour. Technol. 246, 2–11.

Zheng, H., Guo, W., Li, S., Chen, Y., Wu, Q., Feng, X., Yin, R., Ho, S.-H., Ren, N., Chang, J.-S., 2017. Adsorption of p-nitrophenols (PNP) on microalgal biochar: analysis of high adsorption capacity and mechanism. Bioresour. Technol. 244, 1456–1464.

CHAPTER 7: CONCLUSIONS AND RECOMMENDATION FOR FUTURE WORK

In general, this dissertation work discussed the HTL conversion efficiencies of a wide variety of bio-based feedstocks such as microalgae, Salicornia bigelovii torr., and swine manure. This work identified the influence of various reaction conditions such as temperature, solid loading, residence time, input pressure on the HTL conversion efficiencies of biomass. Among all the reaction parameters, the temperature played a key role in the yield of products. Apart from individual liquefaction, biomass was also co-liquefied to investigate the influence of the synergistic effect. The latter part involved in investigated the physicochemical characteristics of products to recommend the utilization of products in multiple industries. These findings strengthened the feasibility of HTL process optimization, by-product development, improving the value chain, sustainability, and viability of HTL technology commercialization.

7.1 Hydrothermal Liquefaction of Microalgae Under Sub- and Super-Critical Water Conditions

HTL product yields depend on the processing conditions such as reaction temperature, residence time, and solid loading. In this study, the effect of pressure does not seem to have a significant influence on the biocrude oil yield. Three different microalgae (*Kirchneriella sp.*, *Micractinium sp.*, *Galdieria sp.*) were hydrothermally liquefied, and the influence of process parameters on the yield of product fractions was investigated. The process parameters were optimized based on the biocrude oil yield. The maximum biocrude

oil yield of 45.5% was obtained at 300 °C, 9 MPa, 10% solid loading, and for a residence time of 30 min. *Micractinium sp.* and *Galdieria sp.* have reported maximum biocrude oil yield (27.95 wt.% and 37.51 wt.%, respectively) at 350 °C. HTL conditions also reduced the oxygen content and led to the formation of energy-dense biocrude oil. The increase in temperature above 300 °C have led to super critical gasification and decreased the biocrude oil yield. The HHV of the HTL products biocrude and biochar were estimated to be 37.52 and 23.48 MJ kg^{-1} at the highest biocrude yield conditions. The energy recovery of products at the highest biocrude yield conditions were calculated to be 94.90%. The analysis of water-phase compounds identified a considerable concentration of nutrients such as organic carbon, ammoniacal nitrogen, phosphates, and dissolved carbohydrates. Elements such as phosphorous, sodium, magnesium, and potassium were also detected in both biomass and HTL products. Hypothesis #3 was tested based on the analysis of results from the upgrading of algae biocrude oil. The results suggest that all three catalysts employed were effective in decreasing the heteroatom content in the upgraded biocrude oil. The decrease in heteroatom content partially validates the hypothesis being tested and the additional experimental plan is discussed in the future work section.

Based on the conclusions from the previous upgrading experiments it is concluded that one specific catalyst material was effective in deoxygenation and the others were effective in decreasing the TAN values. This gives a scope where a mixture of these catalysts exhibits higher performance with respect to deoxygenation and denitrogenation of algal

biocrude than one specific catalyst, implying that upgrading using catalyst mixtures containing two or more components could be a productive avenue for additional research on the upgrading of algal biocrude. The further section describes about the future work planned.

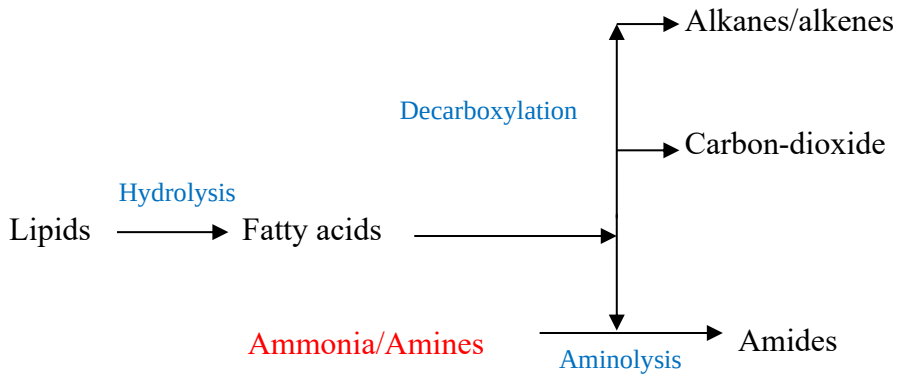

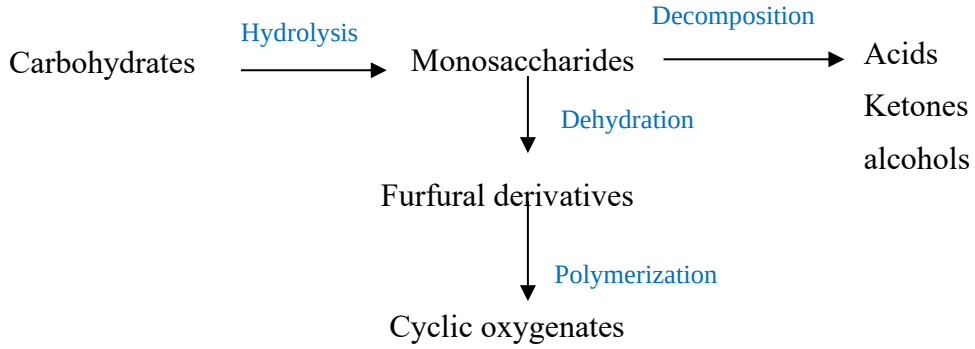

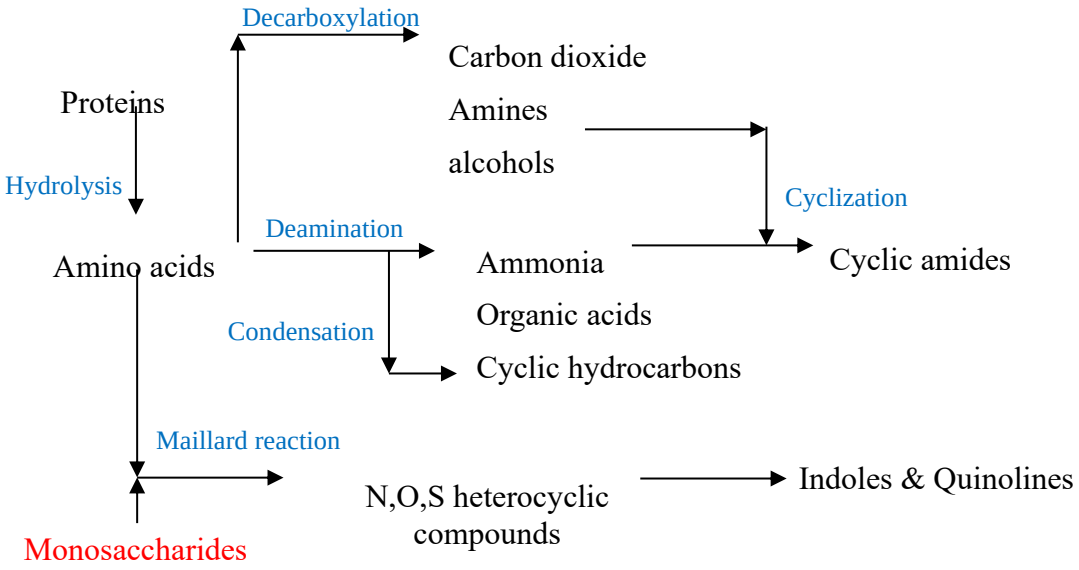

Fig 7.1: Possible reaction pathways based on the characterization by GC-MS chemical composition

7.2 Hydrothermal Liquefaction of Cyanidioschyzon Merolae with Salicornia Bigelovii Torr. and Swine Manure: The Synergistic Effect on Product Distribution and Chemistry

This study concluded that the yield of HTL biocrude oil strongly depends on the composition and the organic contents of the biomass feedstock. The maximum direct HTL biocrude yield of 7.65 wt. % and 34.63 wt. % was obtained at 300 °C, 10 wt. % solid loading, and 30 min of reaction time for *Salicornia bigelovii Torr*. and *C. merolae* biomass, respectively. Co-liquefaction of both biomasses increased the biocrude oil yield suggesting a positive synergistic effect. The maximum yield (32.95 wt. %) of biocrude oil was

obtained at 80-20 mass ratio of CM-SL at 300 °C and 30 minutes, which suggests that *Salicornia bigelovii Torr*. can be used as viable biomass feedstock in co-liquefaction with algae to produce renewable biofuels. The HTL products (biocrude, biochar) had higher energy content (HHV) than that of the original biomass, suggesting energy densification during the HTL process. The HHV of the biocrude oil produced from HTL of SL biomass was measured to be 28.29 MJ/kg, while that of CM biomass was around 32.5 MJ/kg. The co-liquefaction has led to the positive synergistic effect and maximum energy recovery (88.55 %) compared to individual liquefaction conditions. HTL water phase analysis showed the presence of water-soluble nutrients, which can be recycled to re-grow algae. The biomass, biocrude, and biochar were analyzed by ICP-OES for heavy metals, and the biochar contained the highest concentration of metals accumulated in the product phase. The GC-MS showed the presence of similar compounds in the co-liquefied oils compared to that of individual HTL oils. While HTL seems to be an effective technique, it should still address the limitations and challenges for the scalability of the current research such as feedstock preparation, continuous year-round supply of feedstock, scale-up of HTL units, nutrient recycle, by-product handling and commercialization, and process integration.

7.3 Physicochemical Characterization of Hydrothermally Produced Biochars from *Cyanidioschyzon Merolae* and Swine Manure

This study presents a comprehensive physicochemical and surface characterization of biochar obtained from the individual and co-liquefaction of microalgae *Cyanidioschyzon merolae* and swine manure acquired from a pig farm in Mount Olive, North Carolina. While due to the presence of heavy metals and the lower higher heating value (HHV), biochar may not qualify as fuel, biochar's applications may present new opportunities to enhance sustainability in the construction industry. Specifically, our study outcome shows that due to the presence of diverse surface functional groups, the high volatile matter, and the abundance of redox moieties on the surface of biochar, the biochar made from algae and swine manure has a great potential for use as a free-radical scavenger in asphalt roads and roofing shingles. Hydrothermal liquefaction of algae and swine manure blend at 330 °C yielded biochars in the range of 4.5-33.2 wt. % and biocrude in the range of 31.5-6.27 wt. %. The biochars from the individual liquefaction and those from the co-liquefaction exhibited a similar thermal degradation behavior under the presence of nitrogen (N_2), with 100-0 CM-SM biochar having the highest volatile content (59.27 %). The elemental and ultimate analysis of the co-liquefied biochars found that 80-20 CM-SM has a carbon content of 29.97 wt. % and the highest HHV of 10.87 MJ/kg compared with other scenarios. In the case of blended feedstocks, the O/C and H/C are indicative of demethanation. HTL biochar has a surface area of up to 5.8 m^2/g and is considered as a mesoporous substance (50nm > pores > 2nm). Among nutrients, P, Mg, and K were found to be dominant in all studied biochar. The functional group analysis using FT-IR revealed

the presence of oxygen-containing groups, alkenes, diimides, azides, and ketenes, cyclic amides, and carbohydrate derivatives. XRD analysis showed the presence of quartz (SiO_2), graphitic carbon, and hexagonal $AlPO_4$ with trace amounts of $CaCO_3$, and $Ca_2P_2O_7$.

7.4 Applications of biochar

The optimum utilization of HTL by-products improves the economics of the process and makes biofuels viable. The section elaborates the conclusions from the study of biochar to be:

1. Leached for nutrients and using the leachate to cultivate microalgae
2. Pyrolyzed to produce hydrogen using a selective membrane reactor

The research findings from the first study from the leaching of nutrients from biochar conclude that 32.54 % of the phosphorus may be recovered as phosphates; and 61 % of the nitrogen as ammoniacal nitrogen at a pH of 2.5 in 7 days of leaching experiments. It can be concluded that *G. sulphuraria* can be cultivated successfully in media leached from the HTL biochar without any inhibitions.

The research findings from the second study of pyrolyzing biochar to produce hydrogen using a selective membrane reactor conclude that the pyrolysis of HTL biochar from *Galdieria sulphuraria* at 500 ˚C ,1 atm for 24 h in a fixed bed reactor produces 5.93 wt. % gas, 46.68 wt. % oil/water and 44.67 wt. % solid residue, with the gaseous product containing 45.70 mol % H_2, 44.05 mol % CH_4 and 10.25 mol % of CO. This study also

confirms that the involvement of a hydrogen-selective metal membrane in the reactor during the pyrolysis of HTL biochar results in recovery of hydrogen in the permeate stream (~twice the hydrogen remaining in the reactor or retentate stream) and further facilitates the decomposition process. The retentate stream shows reduced CO and CO_2 as well as increased CH_4 content compared to pyrolysis conditions with no membrane.

7.5 Recommendations

In this dissertation, we studied the HTL of three different kinds of bio-based feedstocks and their following product applications. The first kind of feedstock include microalgae such as *Kirchneriella sp.*, *Micractinium sp.*, *Galdieria sp.* The second and third kind included Salicornia bigelovii Torr. and Swine manure. Based on the findings of this study, the following recommendations can be made:

1. Investigation of a variety of biomasses that can be grown via crop-rotation strategies to maximize annual biomass productivity.
2. HTL processing of these biomasses produces a gaseous phase, which needs to be analyzed for high-energy dense gases such as hydrogen, carbon monoxide, methane, and other light hydrocarbon gases.
3. The biocrude oil produced form individual liquefaction can be used as the feedstock in the two-component heterogenous catalyst mixture screening study.

4. During the co-liquefaction, positive synergy was observed between microalgae with Salicornia and swine manure. The positive synergy can also be verified using heterogeneous catalysts to treat the high-ash content of both the salt-tolerant biomass and swine manure.
5. The positive synergy suggests that at a specific biomass ratio (80/20 algae: other biomass, this study) the extent of synergy was highest. This can be verified by the investigation of reaction mechanisms using model compounds of proteins and lipids. The future study of manning reaction with model compounds needs to be evaluated.
6. The physicochemical characterization has concluded that biochar contains a variety of surface functional groups. Future study is recommended to determine the applications and dosage quantities of biochar into the asphalt and construction industry for protection against ultra-violet ray damage and moisture susceptibility.
7. This study used the biochar produced from *Galdieria sulphuraria* (GS) to leach the nutrients. It is recommended that future studies evaluate different algae biochar to see any inhibitory effects during algal cultivation. The effect of the addition of biochar into the algae cultivation
8. This study used biochar to produce hydrogen using a membrane reactor via pyrolysis. Future study is recommended to use different kinds of membranes and/or biochar to test the membrane reliability towards sulphur in the biochar. It is also

recommended to investigate less expensive membrane options as using platinum and palladium was not economical considering membrane deactivation and poisoning.

9. Considering the significant positive economic and sustainable impacts of biomasses and HTL, a complete life-cycle assessment of the HTL process with these applications is recommended.
10. Considering the true versatility of HTL conversion technology, the potential application of products needs to be .investigated. The biocrude oil blended with different recycled asphalts need to be investigated for moisture retention and UV susceptibility. The role of heteroatoms (N, S, O) of the biocrude oil in the blending performance needs to be evaluated.

REFERENCES

Administration, [USEIA] U S Energy Information, 2018. Annual Energy Outlook 2018 with projections to 2050.

Ahmad, A.L., Yasin, N.H.M., Derek, C.J.C., Lim, J.K., 2011. Microalgae as a sustainable energy source for biodiesel production: a review. Renew. Sustain. Energy Rev. 15, 584–593.

Akhtar, J., Amin, N.A.S., 2011. A review on process conditions for optimum bio-oil yield in hydrothermal liquefaction of biomass. Renew. Sustain. Energy Rev. 15, 1615–1624.

Alaswad, A., Dassisti, M., Prescott, T., Olabi, A.G., 2015. Technologies and developments of third generation biofuel production. Renew. Sustain. Energy Rev. 51, 1446–1460.

Anastasakis, K., Ross, A.B., 2011. Hydrothermal liquefaction of the brown macro-alga Laminaria Saccharina: Effect of reaction conditions on product distribution and composition. Bioresour. Technol. 102, 4876–4883.

ATAG, 2009. Beginners Guide to Aviation Biofuels.

Aysu, T., Demirbaş, A., Bengü, A.Ş., Küçük, M.M., 2015. Evaluation of Eremurus spectabilis for production of bio-oils with supercritical solvents. Process Saf. Environ. Prot. 94, 339–349.

Barba, F.J., Grimi, N., Vorobiev, E., 2015. New approaches for the use of non-conventional cell disruption technologies to extract potential food additives and nutraceuticals from microalgae. Food Eng. Rev. 7, 45–62.

Barry, A., Wolfe, A., English, C., Ruddick, C., Lambert, D., 2016. National algal biofuels technology review. US Dep. Energy, Off. Energy Effic. Renew. Energy, Bioenergy Technol. Off.

Barzagli, F., Mani, F., 2019. The increased anthropogenic gas emissions in the atmosphere and the rising of the Earth's temperature: are there actions to mitigate the global warming? Substantia 3, 101–111.

Brennan, L., Mostaert, A., Murphy, C., Owende, P., 2012. Phytochemicals from algae. Biorefinery Co-Products Phytochem. Prim. Metab. Value-Added Biomass Process. 199–240.

Chauton, M.S., Reitan, K.I., Norsker, N.H., Tveterås, R., Kleivdal, H.T., 2015. A techno-

economic analysis of industrial production of marine microalgae as a source of EPA and DHA-rich raw material for aquafeed: research challenges and possibilities. Aquaculture 436, 95–103.

Chèze, B., Gastineau, P., Chevallier, J., 2011. Forecasting world and regional aviation jet fuel demands to the mid-term (2025). Energy Policy 39, 5147–5158.

Chiaramonti, D., Prussi, M., Buffi, M., Rizzo, A.M., Pari, L., 2017. Review and experimental study on pyrolysis and hydrothermal liquefaction of microalgae for biofuel production. Appl. Energy 185, 963–972.

Chisti, Y., 2007. Biodiesel from microalgae. Biotechnol. Adv. 25, 294–306.

Christensen, E., Sudasinghe, N., Dandamudi, K.P.R., Sebag, R., Schaub, T., Laurens, L.M.L., 2015. Rapid Analysis of Microalgal Triacylglycerols with Direct-Infusion Mass Spectrometry. Energy and Fuels 29. https://doi.org/10.1021/acs.energyfuels.5b01205

Conti, J., Holtberg, P., Diefenderfer, J., LaRose, A., Turnure, J.T., Westfall, L., 2016. International energy outlook 2016 with projections to 2040. USDOE Energy Information Administration (EIA), Washington, DC (United States ….

Creutzig, F., Breyer, C., Hilaire, J., Minx, J., Peters, G.P., Socolow, R., 2019. The mutual dependence of negative emission technologies and energy systems. Energy Environ. Sci. 12, 1805–1817.

Demirbas, A., 2009. Political, economic and environmental impacts of biofuels: A review. Appl. Energy 86, S108–S117.

Elliott, D.C., 2016. Review of recent reports on process technology for thermochemical conversion of whole algae to liquid fuels. Algal Res. 13, 255–263.

Elliott, D.C., Biller, P., Ross, A.B., Schmidt, A.J., Jones, S.B., 2015. Hydrothermal liquefaction of biomass: developments from batch to continuous process. Bioresour. Technol. 178, 147–156.

Fukuda, H., Kondo, A., Noda, H., 2001. Biodiesel fuel production by transesterification of oils. J. Biosci. Bioeng. 92, 405–416.

Gnansounou, E., Dauriat, A., Villegas, J., Panichelli, L., 2009. Life cycle assessment of biofuels: energy and greenhouse gas balances. Bioresour. Technol. 100, 4919–4930.

Guo, Y., Yeh, T., Song, W., Xu, D., Wang, S., 2015. A review of bio-oil production from hydrothermal liquefaction of algae. Renew. Sustain. Energy Rev. 48, 776–790.

Hansen, J., Sato, M., Ruedy, R., Lo, K., Lea, D.W., Medina-Elizade, M., 2006. Global temperature change. Proc. Natl. Acad. Sci. 103, 14288–14293.

Hileman, J.I., Stratton, R.W., 2014. Alternative jet fuel feasibility. Transp. Policy 34, 52–62.

Hoffert, M.I., Caldeira, K., Benford, G., Criswell, D.R., Green, C., Herzog, H., Jain, A.K., Kheshgi, H.S., Lackner, K.S., Lewis, J.S., 2002. Advanced technology paths to global climate stability: energy for a greenhouse planet. Science (80-.). 298, 981–987.

Karl, T.R., Trenberth, K.E., 2003. Modern global climate change. Science (80-.). 302, 1719–1723.

Kröger, M., Müller-Langer, F., 2012. Review on possible algal-biofuel production processes. Biofuels 3, 333–349.

Lardon, L., Hélias, A., Sialve, B., Steyer, J.-P., Bernard, O., 2009. Life-cycle assessment of biodiesel production from microalgae.

Lelieveld, J., Klingmüller, K., Pozzer, A., Burnett, R.T., Haines, A., Ramanathan, V., 2019. Effects of fossil fuel and total anthropogenic emission removal on public health and climate. Proc. Natl. Acad. Sci. 116, 7192–7197.

Lowrey, J., Brooks, M.S., McGinn, P.J., 2015. Heterotrophic and mixotrophic cultivation of microalgae for biodiesel production in agricultural wastewaters and associated challenges—a critical review. J. Appl. Phycol. 27, 1485–1498.

Ma, F., Hanna, M.A., 1999. Biodiesel production: a review. Bioresour. Technol. 70, 1–15.

Mata, T.M., Martins, A.A., Caetano, N.S., 2010. Microalgae for biodiesel production and other applications: a review. Renew. Sustain. energy Rev. 14, 217–232.

McKendry, P., 2002. Energy production from biomass (part 2): conversion technologies. Bioresour. Technol. 83, 47–54.

Meher, L.C., Sagar, D.V., Naik, S.N., 2006. Technical aspects of biodiesel production by transesterification—a review. Renew. Sustain. energy Rev. 10, 248–268.

Mercure, J.-F., Pollitt, H., Viñuales, J.E., Edwards, N.R., Holden, P.B., Chewpreecha, U., Salas, P., Sognnaes, I., Lam, A., Knobloch, F., 2018. Macroeconomic impact of stranded fossil fuel assets. Nat. Clim. Chang. 8, 588–593.

Mohan, D., Pittman Jr, C.U., Steele, P.H., 2006. Pyrolysis of wood/biomass for bio-oil: a critical review. Energy & fuels 20, 848–889.

Naik, S.N., Goud, V. V, Rout, P.K., Dalai, A.K., 2010. Production of first and second generation biofuels: a comprehensive review. Renew. Sustain. energy Rev. 14, 578–597.

Onwudili, J.A., Lea-Langton, A.R., Ross, A.B., Williams, P.T., 2013. Catalytic hydrothermal gasification of algae for hydrogen production: composition of reaction products and potential for nutrient recycling. Bioresour. Technol. 127, 72–80.

Park, K.-C., Ihm, S.-K., 2000. Comparison of Pt/zeolite catalysts for n-hexadecane hydroisomerization. Appl. Catal. A Gen. 203, 201–209.

Patel, M., Zhang, X., Kumar, A., 2016. Techno-economic and life cycle assessment on lignocellulosic biomass thermochemical conversion technologies: A review. Renew. Sustain. Energy Rev. 53, 1486–1499.

Patil, P.D., Reddy, H., Muppaneni, T., Deng, S., 2017. Biodiesel fuel production from algal lipids using supercritical methyl acetate (glycerin-free) technology. Fuel 195, 201–207.

Peterson, A.A., Vogel, F., Lachance, R.P., Fröling, M., Antal Jr, M.J., Tester, J.W., 2008. Thermochemical biofuel production in hydrothermal media: a review of sub-and supercritical water technologies. Energy Environ. Sci. 1, 32–65.

Ponnusamy, S., Reddy, H.K., Muppaneni, T., Downes, C.M., Deng, S., 2014. Life cycle assessment of biodiesel production from algal bio-crude oils extracted under subcritical water conditions. Bioresour. Technol. 170, 454–461.

Reddy, H.K., Muppaneni, T., Sun, Y., Li, Y., Ponnusamy, S., Patil, P.D., Dailey, P., Schaub, T., Holguin, F.O., Dungan, B., Cooke, P., Lammers, P., Voorhies, W., Lu, X., Deng, S., 2014. Subcritical water extraction of lipids from wet algae for biodiesel production. Fuel 133, 73–81. https://doi.org/https://doi.org/10.1016/j.fuel.2014.04.081

Rodolfi, L., Chini Zittelli, G., Bassi, N., Padovani, G., Biondi, N., Bonini, G., Tredici, M.R., 2009. Microalgae for oil: Strain selection, induction of lipid synthesis and outdoor mass cultivation in a low-cost photobioreactor. Biotechnol. Bioeng. 102, 100–112.

Sarmah, S.B., Kalita, P., Garg, A., Niu, X., Zhang, X.-W., Peng, X., Bhattacharjee, D., 2019. A review of state of health estimation of energy storage systems: challenges and possible solutions for futuristic applications of Li-Ion battery packs in electric vehicles. J. Electrochem. Energy Convers. Storage 16.

Selvaratnam, T., Pegallapati, A.K., Reddy, H., Kanapathipillai, N., Nirmalakhandan, N., Deng, S., Lammers, P.J., 2015a. Algal biofuels from urban wastewaters: Maximizing biomass yield using nutrients recycled from hydrothermal processing of biomass. Bioresour. Technol. 182, 232–238.

Selvaratnam, T., Reddy, H., Muppaneni, T., Holguin, F.O., Nirmalakhandan, N.,

Lammers, P.J., Deng, S., 2015b. Optimizing energy yields from nutrient recycling using sequential hydrothermal liquefaction with Galdieria sulphuraria. Algal Res. 12, 74–79.

Shonnard, D.R., Williams, L., Kalnes, T.N., 2010. Camelina-derived jet fuel and diesel: Sustainable advanced biofuels. Environ. Prog. Sustain. Energy 29, 382–392.

Singh, A., Olsen, S.I., 2011. A critical review of biochemical conversion, sustainability and life cycle assessment of algal biofuels. Appl. Energy 88, 3548–3555.

Spolaore, P., Joannis-Cassan, C., Duran, E., Isambert, A., 2006. Commercial applications of microalgae. J. Biosci. Bioeng. 101, 87–96.

Statistics, I.E.A., 2011. CO2 emissions from fuel combustion-highlights. IEA, Paris http//www. iea. org/co2highlights/co2highlights. pdf. Cited July.

Tian, C., Li, B., Liu, Z., Zhang, Y., Lu, H., 2014. Hydrothermal liquefaction for algal biorefinery: a critical review. Renew. Sustain. Energy Rev. 38, 933–950.

Toor, S.S., Reddy, H., Deng, S., Hoffmann, J., Spangsmark, D., Madsen, L.B., Holm-Nielsen, J.B., Rosendahl, L.A., 2013. Hydrothermal liquefaction of Spirulina and Nannochloropsis salina under subcritical and supercritical water conditions. Bioresour. Technol. 131, 413–419.

Toor, S.S., Rosendahl, L., Rudolf, A., 2011. Hydrothermal liquefaction of biomass: a review of subcritical water technologies. Energy 36, 2328–2342.

U.S. EIA, U.S. Energy Information Administration (EIA), 2019. Annual Energy Outlook 2019 with projections to 2050. Annu. Energy Outlook 2019 with Proj. to 2050. https://doi.org/DOE/EIA-0383(2012) U.S.

Valdez, P.J., Nelson, M.C., Wang, H.Y., Lin, X.N., Savage, P.E., 2012. Hydrothermal liquefaction of Nannochloropsis sp.: Systematic study of process variables and analysis of the product fractions. Biomass and Bioenergy 46, 317–331.

Verma, M., Godbout, S., Brar, S.K., Solomatnikova, O., Lemay, S.P., Larouche, J.P., 2012. Biofuels production from biomass by thermochemical conversion technologies. Int. J. Chem. Eng. 2012.

Wang, Z., Adhikari, S., Valdez, P., Shakya, R., 2015. Upgrading of hydrothermal liquefaction biocrude from algae grown in municipal wastewater, in: 2015 ASABE Annual International Meeting. American Society of Agricultural and Biological Engineers, p. 1.

White, A.W., Shilo, M., 1975. Heterotrophic growth of the filamentous blue-green alga Plectonema boryanum. Arch. Microbiol. 102, 123–127.

Wigley, T.M.L., Raper, S.C.B., 2001. Interpretation of high projections for global-mean warming. Science (80-.). 293, 451–454.

Winwood, R.J., 2013. Recent developments in the commercial production of DHA and EPA rich oils from micro-algae. Ocl 20, D604.

Zhou, D., Zhang, L., Zhang, S., Fu, H., Chen, J., 2010. Hydrothermal liquefaction of macroalgae Enteromorpha prolifera to bio-oil. Energy & Fuels 24, 4054–4061.

Anastasakis, K., Ross, A.B., 2011. Hydrothermal liquefaction of the brown macro-alga Laminaria Saccharina: Effect of reaction conditions on product distribution and composition. Bioresour. Technol. 102, 4876–4883.

Biller, P., Ross, A.B., Skill, S.C., Lea-Langton, A., Balasundaram, B., Hall, C., Riley, R., Llewellyn, C.A., 2012. Nutrient recycling of aqueous phase for microalgae cultivation from the hydrothermal liquefaction process. Algal Res. 1, 70–76.

Borowitzka, M.A., 2013. High-value products from microalgae—their development and commercialisation. J. Appl. Phycol. 25, 743–756.

Browne, F.X., 1990. Stormwater management, Standard Handbook of Environmental Engineering, RA Corbitt.

Chakraborty, M., Miao, C., McDonald, A., Chen, S., 2012. Concomitant extraction of bio-oil and value added polysaccharides from Chlorella sorokiniana using a unique sequential hydrothermal extraction technology. Fuel 95, 63–70.

Chemists, A. of O.A., Horwitz, W., 1975. Official methods of analysis. Association of Official Analytical Chemists Washington, DC.

Chen, W.-T., Zhang, Y., Zhang, J., Yu, G., Schideman, L.C., Zhang, P., Minarick, M., 2014. Hydrothermal liquefaction of mixed-culture algal biomass from wastewater treatment system into bio-crude oil. Bioresour. Technol. 152, 130–139.

Dandamudi, K.P.R., Muppaneni, T., Markovski, J.S., Lammers, P., Deng, S., 2019. Hydrothermal liquefaction of green microalga Kirchneriella sp. under sub- and super-critical water conditions. Biomass and Bioenergy 120. https://doi.org/10.1016/j.biombioe.2018.11.021

Doucha, J., Lívanský, K., 2012. Production of high-density Chlorella culture grown in fermenters. J. Appl. Phycol. 24, 35–43.

Duan, P., Savage, P.E., 2011. Upgrading of crude algal bio-oil in supercritical water. Bioresour. Technol. 102, 1899–1906.

Eboibi, B.E.-O., Lewis, D.M., Ashman, P.J., Chinnasamy, S., 2014. Hydrothermal liquefaction of microalgae for biocrude production: Improving the biocrude

properties with vacuum distillation. Bioresour. Technol. 174, 212–221.

Eustance, E.O., 2011. Biofuel potential, nitrogen utilization, and growth rates of two green algae isolated from a wastewater treatment facility.

Gai, C., Liu, Z., Han, G., Peng, N., Fan, A., 2015a. Combustion behavior and kinetics of low-lipid microalgae via thermogravimetric analysis. Bioresour. Technol. 181, 148–154.

Gai, C., Zhang, Y., Chen, W.-T., Zhang, P., Dong, Y., 2015b. An investigation of reaction pathways of hydrothermal liquefaction using Chlorella pyrenoidosa and Spirulina platensis. Energy Convers. Manag. 96, 330–339.

Huang, C., Zeng, G., Huang, D., Lai, C., Xu, P., Zhang, C., Cheng, M., Wan, J., Hu, L., Zhang, Y., 2017. Effect of Phanerochaete chrysosporium inoculation on bacterial community and metal stabilization in lead-contaminated agricultural waste composting. Bioresour. Technol. 243, 294–303.

Jarvis, J.M., Sudasinghe, N.M., Albrecht, K.O., Schmidt, A.J., Hallen, R.T., Anderson, D.B., Billing, J.M., Schaub, T.M., 2016. Impact of iron porphyrin complexes when hydroprocessing algal HTL biocrude. Fuel 182, 411–418.

Jazrawi, C., Biller, P., Ross, A.B., Montoya, A., Maschmeyer, T., Haynes, B.S., 2013. Pilot plant testing of continuous hydrothermal liquefaction of microalgae. Algal Res. 2, 268–277.

Jena, U., Vaidyanathan, N., Chinnasamy, S., Das, K.C., 2011. Evaluation of microalgae cultivation using recovered aqueous co-product from thermochemical liquefaction of algal biomass. Bioresour. Technol. 102, 3380–3387.

Jin, M., Oh, Y.-K., Chang, Y.K., Choi, M., 2017. Optimum utilization of biochemical components in Chlorella sp. KR1 via subcritical hydrothermal liquefaction. ACS Sustain. Chem. Eng. 5, 7240–7248.

Laurens, L.M.L., 2016. Summative Mass Analysis of Algal Biomass-Integration of Analytical Procedures: Laboratory Analytical Procedure (LAP). National Renewable Energy Lab.(NREL), Golden, CO (United States).

Lombardi, A.T., Vieira, A.A.H., Sartori, L.A., 2002. Mucilaginous capsule adsorption and intracellular uptake of copper by Kirchneriella aperta (Chlorococcales). J. Phycol. 38, 332–337.

Lourenço, S.O., Barbarino, E., Lavín, P.L., Lanfer Marquez, U.M., Aidar, E., 2004. Distribution of intracellular nitrogen in marine microalgae: calculation of new nitrogen-to-protein conversion factors. Eur. J. Phycol. 39, 17–32.

Lourenço, S.O., Barbarino, E., Marquez, U.M.L., Aidar, E., 1998. Distribution of intracellular nitrogen in marine microalgae: basis for the calculation of specific nitrogen-to-protein conversion factors. J. Phycol. 34, 798–811.

Mendes, A., Reis, A., Vasconcelos, R., Guerra, P., da Silva, T.L., 2009. Crypthecodinium cohnii with emphasis on DHA production: a review. J. Appl. Phycol. 21, 199–214.

Milledge, J.J., 2012. Microalgae-commercial potential for fuel, food and feed. Food Sci. Technol. 26, 28–30.

Moore, J.C., DeVries, J.W., Lipp, M., Griffiths, J.C., Abernethy, D.R., 2010. Total protein methods and their potential utility to reduce the risk of food protein adulteration. Compr. Rev. Food Sci. Food Saf. 9, 330–357.

Muppaneni, T., Reddy, H.K., Selvaratnam, T., Dandamudi, K.P.R., Dungan, B., Nirmalakhandan, N., Schaub, T., Omar Holguin, F., Voorhies, W., Lammers, P., Deng, S., 2017. Hydrothermal liquefaction of Cyanidioschyzon merolae and the influence of catalysts on products. Bioresour. Technol. 223. https://doi.org/10.1016/j.biortech.2016.10.022

Pachauri, R.K., Allen, M.R., Barros, V.R., Broome, J., Cramer, W., Christ, R., Church, J.A., Clarke, L., Dahe, Q., Dasgupta, P., 2014. Climate change 2014: synthesis report. Contribution of Working Groups I, II and III to the fifth assessment report of the Intergovernmental Panel on Climate Change. Ipcc.

Patil, P.D., Dandamudi, K.P.R., Wang, J., Deng, Q., Deng, S., 2018. Extraction of bio-oils from algae with supercritical carbon dioxide and co-solvents. J. Supercrit. Fluids 135, 60–68. https://doi.org/https://doi.org/10.1016/j.supflu.2017.12.019

Saeed, A., Iqbal, M., Sahibzada, K.I., Parvez, S., 2012. Evaluation of the biosequestering potential of microalga kirchneriella contorta in the removal of hexavalent chromium from aqueous solution: Batch and continuous flow fixed-bed column bioreactor studies. Pak J Bot 44, 989–998.

Schenk, P.M., Thomas-Hall, S.R., Stephens, E., Marx, U.C., Mussgnug, J.H., Posten, C., Kruse, O., Hankamer, B., 2008. Second generation biofuels: high-efficiency microalgae for biodiesel production. Bioenergy Res. 1, 20–43.

Selvaratnam, T., Pegallapati, A.K., Montelya, F., Rodriguez, G., Nirmalakhandan, N., Van Voorhies, W., Lammers, P.J., 2014. Evaluation of a thermo-tolerant acidophilic alga, Galdieria sulphuraria, for nutrient removal from urban wastewaters. Bioresour. Technol. 156, 395–399.

Selvaratnam, T., Pegallapati, A.K., Reddy, H., Kanapathipillai, N., Nirmalakhandan, N., Deng, S., Lammers, P.J., 2015a. Algal biofuels from urban wastewaters:

Maximizing biomass yield using nutrients recycled from hydrothermal processing of biomass. Bioresour. Technol. 182, 232–238.

Selvaratnam, T., Reddy, H., Muppaneni, T., Holguin, F.O., Nirmalakhandan, N., Lammers, P.J., Deng, S., 2015b. Optimizing energy yields from nutrient recycling using sequential hydrothermal liquefaction with Galdieria sulphuraria. Algal Res. 12, 74–79.

Song, M., Pei, H., Hu, W., Ma, G., 2013. Evaluation of the potential of 10 microalgal strains for biodiesel production. Bioresour. Technol. 141, 245–251.

Sudasinghe, N., Dungan, B., Lammers, P., Albrecht, K., Elliott, D., Hallen, R., Schaub, T., 2014. High resolution FT-ICR mass spectral analysis of bio-oil and residual water soluble organics produced by hydrothermal liquefaction of the marine microalga Nannochloropsis salina. Fuel 119, 47–56.

Toor, S.S., Reddy, H., Deng, S., Hoffmann, J., Spangsmark, D., Madsen, L.B., Holm-Nielsen, J.B., Rosendahl, L.A., 2013. Hydrothermal liquefaction of Spirulina and Nannochloropsis salina under subcritical and supercritical water conditions. Bioresour. Technol. 131, 413–419.

Toor, S.S., Rosendahl, L., Rudolf, A., 2011. Hydrothermal liquefaction of biomass: a review of subcritical water technologies. Energy 36, 2328–2342.

Toplin, J.A., Norris, T.B., Lehr, C.R., McDermott, T.R., Castenholz, R.W., 2008. Biogeographic and phylogenetic diversity of thermoacidophilic cyanidiales in Yellowstone National Park, Japan, and New Zealand. Appl. Environ. Microbiol. 74, 2822–2833.

Valdez, P.J., Nelson, M.C., Wang, H.Y., Lin, X.N., Savage, P.E., 2012. Hydrothermal liquefaction of Nannochloropsis sp.: Systematic study of process variables and analysis of the product fractions. Biomass and Bioenergy 46, 317–331.

Van Wychen, S., Laurens, L.M.L., 2016. Determination of total carbohydrates in algal biomass: laboratory analytical procedure (LAP). National Renewable Energy Lab.(NREL), Golden, CO (United States).

Van Wychen, S., Ramirez, K., Laurens, L.M.L., 2016. Determination of total lipids as fatty acid methyl esters (FAME) by in situ transesterification: laboratory analytical procedure (LAP). National Renewable Energy Lab.(NREL), Golden, CO (United States).

Wang, J., Krishna, R., Yang, J., Dandamudi, K.P.R., Deng, S., 2015. Nitrogen-doped porous carbons for highly selective CO<inf>2</inf> capture from flue gases and natural gas upgrading. Mater. Today Commun. 4.

https://doi.org/10.1016/j.mtcomm.2015.06.009

Wang, J., Peng, X., Chen, X., Ma, X., 2019. Co-liquefaction of low-lipid microalgae and starch-rich biomass waste: The interaction effect on product distribution and composition. J. Anal. Appl. Pyrolysis 139, 250–257.

Wang, Z., Adhikari, S., Valdez, P., Shakya, R., 2015. Upgrading of hydrothermal liquefaction biocrude from algae grown in municipal wastewater, in: 2015 ASABE Annual International Meeting. American Society of Agricultural and Biological Engineers, p. 1.

Yang, W., Li, X., Li, Z., Tong, C., Feng, L., 2015. Understanding low-lipid algae hydrothermal liquefaction characteristics and pathways through hydrothermal liquefaction of algal major components: Crude polysaccharides, crude proteins and their binary mixtures. Bioresour. Technol. 196, 99–108.

Laminaria saccharina: effect of reaction conditions on product distribution and composition. Bioresour. Technol. 102, 4876–4883.

Aresta, M., Dibenedetto, A., Carone, M., Colonna, T., Fragale, C., 2005. Production of biodiesel from macroalgae by supercritical CO 2 extraction and thermochemical liquefaction. Environ. Chem. Lett. 3, 136–139.

Azar, C., Lindgren, K., Obersteiner, M., Riahi, K., van Vuuren, D.P., den Elzen, K.M.G.J., Möllersten, K., Larson, E.D., 2010. The feasibility of low CO 2 concentration targets and the role of bio-energy with carbon capture and storage (BECCS). Clim. Change 100, 195–202.

Balat, M., 2008. Mechanisms of thermochemical biomass conversion processes. Part 1: reactions of pyrolysis. Energy Sources, Part A 30, 620–635.

Barreiro, D.L., Prins, W., Ronsse, F., Brilman, W., 2013. Hydrothermal liquefaction (HTL) of microalgae for biofuel production: state of the art review and future prospects. Biomass and Bioenergy 53, 113–127.

Beal, C.M., Archibald, I., Huntley, M.E., Greene, C.H., Johnson, Z.I., 2018. Integrating algae with bioenergy carbon capture and storage (ABECCS) increases sustainability. Earth's Futur. 6, 524–542.

Biller, P., Ross, A.B., Skill, S.C., Lea-Langton, A., Balasundaram, B., Hall, C., Riley, R., Llewellyn, C.A., 2012. Nutrient recycling of aqueous phase for microalgae cultivation from the hydrothermal liquefaction process. Algal Res. 1, 70–76.

Brown, T.M., Duan, P., Savage, P.E., 2010. Hydrothermal liquefaction and gasification of Nannochloropsis sp. Energy & Fuels 24, 3639–3646.

Bui, H.H., Tran, K.Q., Chen, W.H., 2015. Pyrolysis of microalgae residues - A Kinetic study. Bioresour. Technol. https://doi.org/10.1016/j.biortech.2015.08.069

Bui, M., Adjiman, C.S., Bardow, A., Anthony, E.J., Boston, A., Brown, S., Fennell, P.S., Fuss, S., Galindo, A., Hackett, L.A., 2018. Carbon capture and storage (CCS): the way forward. Energy Environ. Sci. 11, 1062–1176.

Cantero-Tubilla, B., Cantero, D.A., Martinez, C.M., Tester, J.W., Walker, L.P., Posmanik, R., 2018. Characterization of the solid products from hydrothermal liquefaction of waste feedstocks from food and agricultural industries. J. Supercrit. Fluids. https://doi.org/10.1016/j.supflu.2017.07.009

Carrier, M., Loppinet-Serani, A., Denux, D., Lasnier, J.M., Ham-Pichavant, F., Cansell, F., Aymonier, C., 2011. Thermogravimetric analysis as a new method to determine the lignocellulosic composition of biomass. Biomass and Bioenergy. https://doi.org/10.1016/j.biombioe.2010.08.067

Chakraborty, M., Miao, C., McDonald, A., Chen, S., 2012. Concomitant extraction of bio-oil and value added polysaccharides from Chlorella sorokiniana using a unique sequential hydrothermal extraction technology. Fuel 95, 63–70.

Chen, W.T., Zhang, Y., Zhang, J., Schideman, L., Yu, G., Zhang, P., Minarick, M., 2014. Co-liquefaction of swine manure and mixed-culture algal biomass from a wastewater treatment system to produce bio-crude oil. Appl. Energy. https://doi.org/10.1016/j.apenergy.2014.04.068

Cho, H.-S., Oh, Y.-K., Park, S.-C., Lee, J.-W., Park, J.-Y., 2013. Effects of enzymatic hydrolysis on lipid extraction from Chlorella vulgaris. Renew. Energy 54, 156–160. https://doi.org/https://doi.org/10.1016/j.renene.2012.08.031

D3172-07a, A., 2013. Standard Practice for Proximate Analysis of Coal and Coke.

Dandamudi, K.P.R., Muppaneni, T., Markovski, J.S., Lammers, P., Deng, S., 2019. Hydrothermal liquefaction of green microalga Kirchneriella sp. under sub-and super-critical water conditions. Biomass and bioenergy 120, 224–228.

Dandamudi, K.P.R., Muppaneni, T., Sudasinghe, N., Schaub, T., Holguin, F.O., Lammers, P.J., Deng, S., 2017. Co-liquefaction of mixed culture microalgal strains under sub-critical water conditions. Bioresour. Technol. 236. https://doi.org/10.1016/j.biortech.2017.03.165

Dimitriadis, A., Bezergianni, S., 2017. Hydrothermal liquefaction of various biomass and waste feedstocks for biocrude production: A state of the art review. Renew. Sustain. Energy Rev. 68, 113–125.

Garcia Alba, L., Torri, C., Samorì, C., van der Spek, J., Fabbri, D., Kersten, S.R.A.,

Brilman, D.W.F., 2011. Hydrothermal treatment (HTT) of microalgae: evaluation of the process as conversion method in an algae biorefinery concept. Energy & fuels 26, 642–657.

Glenn, E., Miyamoto, S., Moore, D., Brown, J.J., Thompson, T.L., Brown, P., 1997. Water requirements for cultivatingSalicornia bigeloviiTorr. with seawater on sand in a coastal desert environment. J. Arid Environ. 36, 711–730.

Glenn, E.P., Brown, J.J., Blumwald, E., 1999. Salt tolerance and crop potential of halophytes. CRC. Crit. Rev. Plant Sci. 18, 227–255.

Glenn, E.P., O'LEARY, J.W., Watson, M.C., Thompson, T.L., Kuehl, R.O., 1991. Salicornia bigelovii Torr.: an oilseed halophyte for seawater irrigation. Science (80-.). 251, 1065–1067.

Gude, V.G., Patil, P., Martinez-Guerra, E., Deng, S., Nirmalakhandan, N., 2013. Microwave energy potential for biodiesel production. Sustain. Chem. Process. 1, 5.

Henkanatte-Gedera, S.M., Selvaratnam, T., Karbakhshravari, M., Myint, M., Nirmalakhandan, N., Van Voorhies, W., Lammers, P.J., 2017. Removal of dissolved organic carbon and nutrients from urban wastewaters by Galdieria sulphuraria: laboratory to field scale demonstration. Algal Res. 24, 450–456.

Jarvis, J.M., Sudasinghe, N.M., Albrecht, K.O., Schmidt, A.J., Hallen, R.T., Anderson, D.B., Billing, J.M., Schaub, T.M., 2016. Impact of iron porphyrin complexes when hydroprocessing algal HTL biocrude. Fuel 182, 411–418. https://doi.org/https://doi.org/10.1016/j.fuel.2016.05.107

Jena, U., Vaidyanathan, N., Chinnasamy, S., Das, K.C., 2011. Evaluation of microalgae cultivation using recovered aqueous co-product from thermochemical liquefaction of algal biomass. Bioresour. Technol. 102, 3380–3387.

Jiang, J., Savage, P.E., 2017. Influence of process conditions and interventions on metals content in biocrude from hydrothermal liquefaction of microalgae. Algal Res. 26, 131–134.

Jin, B., Duan, P., Xu, Y., Wang, F., Fan, Y., 2013. Co-liquefaction of micro- and macroalgae in subcritical water. Bioresour. Technol. https://doi.org/10.1016/j.biortech.2013.09.045

Kruse, A., Bernolle, P., Dahmen, N., Dinjus, E., Maniam, P., 2010. Hydrothermal gasification of biomass: consecutive reactions to long-living intermediates. Energy Environ. Sci. 3, 136–143.

Marcilla, A., Gómez-Siurana, A., Gomis, C., Chápuli, E., Catalá, M.C., Valdés, F.J., 2009. Characterization of microalgal species through TGA/FTIR analysis:

Application to nannochloropsis sp. Thermochim. Acta 484, 41–47.

McKechnie, M.T., Thompson, D.G., 1987. Method for desalting crude oil.

Miao, C., Chakraborty, M., Chen, S., 2012. Impact of reaction conditions on the simultaneous production of polysaccharides and bio-oil from heterotrophically grown Chlorella sorokiniana by a unique sequential hydrothermal liquefaction process. Bioresour. Technol. 110, 617–627.

Minowa, T., Inoue, S., Hanaoka, T., MATSUMURA, Y., 2004. Hydrothermal reaction of glucose and glycine as model compounds of biomass. J. Japan Inst. Energy 83, 794–798.

Minowa, T., Sawayama, S., 1999. A novel microalgal system for energy production with nitrogen cycling. Fuel 78, 1213–1215.

Miranda, R., Bustos-Martinez, D., Blanco, C.S., Villarreal, M.H.G., Cantú, M.E.R., 2009. Pyrolysis of sweet orange (Citrus sinensis) dry peel. J. Anal. Appl. Pyrolysis. https://doi.org/10.1016/j.jaap.2009.06.001

Muppaneni, T., Reddy, H.K., Selvaratnam, T., Dandamudi, K.P.R., Dungan, B., Nirmalakhandan, N., Schaub, T., Omar Holguin, F., Voorhies, W., Lammers, P., Deng, S., 2017. Hydrothermal liquefaction of Cyanidioschyzon merolae and the influence of catalysts on products. Bioresour. Technol. 223. https://doi.org/10.1016/j.biortech.2016.10.022

Peng, W., Wu, Q., Tu, P., Zhao, N., 2001. Pyrolytic characteristics of microalgae as renewable energy source determined by thermogravimetric analysis. Bioresour. Technol. https://doi.org/10.1016/S0960-8524(01)00072-4

Pourzolfaghar, H., Abnisa, F., Daud, W.M.A.W., Aroua, M.K., 2016. A review of the enzymatic hydroesterification process for biodiesel production. Renew. Sustain. Energy Rev. 61, 245–257. https://doi.org/https://doi.org/10.1016/j.rser.2016.03.048

Reddy, H.K., Muppaneni, T., Ponnusamy, S., Sudasinghe, N., Pegallapati, A., Selvaratnam, T., Seger, M., Dungan, B., Nirmalakhandan, N., Schaub, T., 2016. Temperature effect on hydrothermal liquefaction of Nannochloropsis gaditana and Chlorella sp. Appl. Energy 165, 943–951.

Reddy, H.K., Muppaneni, T., Sun, Y., Li, Y., Ponnusamy, S., Patil, P.D., Dailey, P., Schaub, T., Holguin, F.O., Dungan, B., Cooke, P., Lammers, P., Voorhies, W., Lu, X., Deng, S., 2014. Subcritical water extraction of lipids from wet algae for biodiesel production. Fuel 133, 73–81. https://doi.org/https://doi.org/10.1016/j.fuel.2014.04.081

Ross, A.B., Biller, P., Kubacki, M.L., Li, H., Lea-Langton, A., Jones, J.M., 2010.

Hydrothermal processing of microalgae using alkali and organic acids. Fuel 89, 2234–2243.

Sanchez-Silva, L., López-González, D., Villaseñor, J., Sánchez, P., Valverde, J.L., 2012. Thermogravimetric–mass spectrometric analysis of lignocellulosic and marine biomass pyrolysis. Bioresour. Technol. 109, 163–172.

Savage, P.E., Hestekin, J.A., 2013. A perspective on algae, the environment, and energy. Environ. Prog. Sustain. Energy 32, 877–883.

Selvaratnam, T., Reddy, H., Muppaneni, T., Holguin, F.O., Nirmalakhandan, N., Lammers, P.J., Deng, S., 2015. Optimizing energy yields from nutrient recycling using sequential hydrothermal liquefaction with Galdieria sulphuraria. Algal Res. 12, 74–79.

Singh, R., Prakash, A., Dhiman, S.K., Balagurumurthy, B., Arora, A.K., Puri, S.K., Bhaskar, T., 2014. Hydrothermal conversion of lignin to substituted phenols and aromatic ethers. Bioresour. Technol. 165, 319–322.

Sudasinghe, N., Cort, J.R., Hallen, R., Olarte, M., Schmidt, A., Schaub, T., 2014a. Hydrothermal liquefaction oil and hydrotreated product from pine feedstock characterized by heteronuclear two-dimensional NMR spectroscopy and FT-ICR mass spectrometry. Fuel 137, 60–69.

Sudasinghe, N., Dungan, B., Lammers, P., Albrecht, K., Elliott, D., Hallen, R., Schaub, T., 2014b. High resolution FT-ICR mass spectral analysis of bio-oil and residual water soluble organics produced by hydrothermal liquefaction of the marine microalga Nannochloropsis salina. Fuel 119, 47–56.

Templeton, D.W., Laurens, L.M.L., 2015. Nitrogen-to-protein conversion factors revisited for applications of microalgal biomass conversion to food, feed and fuel. Algal Res. 11, 359–367.

Tian, C., Li, B., Liu, Z., Zhang, Y., Lu, H., 2014. Hydrothermal liquefaction for algal biorefinery: A critical review. Renew. Sustain. Energy Rev. 38, 933–950. https://doi.org/https://doi.org/10.1016/j.rser.2014.07.030

Valdez, P.J., Dickinson, J.G., Savage, P.E., 2011. Characterization of product fractions from hydrothermal liquefaction of Nannochloropsis sp. and the influence of solvents. Energy & Fuels 25, 3235–3243.

Ventura, Y., Sagi, M., 2013. Halophyte crop cultivation: the case for Salicornia and Sarcocornia. Environ. Exp. Bot. 92, 144–153.

Wahidin, S., Idris, A., Shaleh, S.R.M., 2014. Rapid biodiesel production using wet microalgae via microwave irradiation. Energy Convers. Manag. 84, 227–233.

https://doi.org/https://doi.org/10.1016/j.enconman.2014.04.034

Wang, J., Krishna, R., Yang, J., Dandamudi, K.P.R., Deng, S., 2015. Nitrogen-doped porous carbons for highly selective CO 2 capture from flue gases and natural gas upgrading. Mater. Today Commun. 4, 156–165.

Wang, J., Peng, X., Chen, X., Ma, X., 2019. Co-liquefaction of low-lipid microalgae and starch-rich biomass waste: The interaction effect on product distribution and composition. J. Anal. Appl. Pyrolysis 139, 250–257.

Yang, C., Li, R., Zhang, B., Qiu, Q., Wang, B., Yang, H., Ding, Y., Wang, C., 2019. Pyrolysis of microalgae: A critical review. Fuel Process. Technol. https://doi.org/10.1016/j.fuproc.2018.12.012

Zhang, B., Chen, J., He, Z., Chen, H., Kandasamy, S., 2019. Hydrothermal liquefaction of fresh lemon-peel: Parameter optimisation and product chemistry. Renew. Energy 143, 512–519.

Zhou, D., Zhang, L., Zhang, S., Fu, H., Chen, J., 2010. Hydrothermal liquefaction of macroalgae Enteromorpha prolifera to bio-oil. Energy & Fuels 24, 4054–4061.

Bartoli, M., Giorcelli, M., Jagdale, P., Rovere, M., Tagliaferro, A., 2020. A review of non-soil biochar applications. Materials (Basel). 13, 261.

Baxter, L.L., Miles, T.R., Miles Jr, T.R., Jenkins, B.M., Milne, T., Dayton, D., Bryers, R.W., Oden, L.L., 1998. The behavior of inorganic material in biomass-fired power boilers: field and laboratory experiences. Fuel Process. Technol. 54, 47–78.

Brum, M.C., Capitaneo, J.L., Oliveira, J.F., 2010. Removal of hexavalent chromium from water by adsorption onto surfactant modified montmorillonite. Miner. Eng. 23, 270–272.

Cantero-Tubilla, B., Cantero, D.A., Martinez, C.M., Tester, J.W., Walker, L.P., Posmanik, R., 2018. Characterization of the solid products from hydrothermal liquefaction of waste feedstocks from food and agricultural industries. J. Supercrit. Fluids. https://doi.org/10.1016/j.supflu.2017.07.009

Cantrell, K.B., Hunt, P.G., Uchimiya, M., Novak, J.M., Ro, K.S., 2012. Impact of pyrolysis temperature and manure source on physicochemical characteristics of biochar. Bioresour. Technol. 107, 419–428.

Cao, X., Harris, W., 2010. Properties of dairy-manure-derived biochar pertinent to its potential use in remediation. Bioresour. Technol. 101, 5222–5228.

Cheng, F., Cui, Z., Chen, L., Jarvis, J., Paz, N., Schaub, T., Nirmalakhandan, N., Brewer, C.E., 2017. Hydrothermal liquefaction of high-and low-lipid algae: Bio-crude oil

chemistry. Appl. Energy 206, 278–292.

Chisti, Y., 2007. Biodiesel from microalgae. Biotechnol. Adv. 25, 294–306.

Christensen, E., Sudasinghe, N., Dandamudi, K.P.R., Sebag, R., Schaub, T., Laurens, L.M.L., 2015. Rapid Analysis of Microalgal Triacylglycerols with Direct-Infusion Mass Spectrometry. Energy and Fuels 29. https://doi.org/10.1021/acs.energyfuels.5b01205

Coats, A.W., Redfern, J.P., 1963. Thermogravimetric analysis. A review. Analyst 88, 906–924.

Cuthbertson, D., Berardi, U., Briens, C., Berruti, F., 2019. Biochar from residual biomass as a concrete filler for improved thermal and acoustic properties. Biomass and Bioenergy 120, 77–83.

Dandamudi, K.P.R., Muhammed Luboowa, K., Laideson, M., Murdock, T., Seger, M., McGowen, J., Lammers, P.J., Deng, S., 2020. Hydrothermal Liquefaction of Cyanidioschyzon merolae and Salicornia bigelovii Torr.: The interaction effect on product distribution and chemistry. Fuel 277. https://doi.org/10.1016/j.fuel.2020.118146

Dandamudi, K.P.R., Muppaneni, T., Markovski, J.S., Lammers, P., Deng, S., 2019. Hydrothermal liquefaction of green microalga Kirchneriella sp. under sub-and super-critical water conditions. Biomass and bioenergy 120, 224–228.

Dandamudi, K.P.R., Muppaneni, T., Sudasinghe, N., Schaub, T., Holguin, F.O., Lammers, P.J., Deng, S., 2017. Co-liquefaction of mixed culture microalgal strains under sub-critical water conditions. Bioresour. Technol. 236. https://doi.org/10.1016/j.biortech.2017.03.165

Dixit, A., Gupta, S., Dai Pang, S., Kua, H.W., 2019. Waste Valorisation using biochar for cement replacement and internal curing in ultra-high performance concrete. J. Clean. Prod. 238, 117876.

Downie, A., Crosky, A., Munroe, P., 2009. Physical properties of biochar. Biochar Environ. Manag. Sci. Technol. 1.

Fan, W., Bryant, L., Srisupan, M., Trembly, J., 2018a. An assessment of hydrothermal treatment of dairy waste as a tool for a sustainable phosphorus supply chain in comparison with commercial phosphatic fertilizers. Clean Technol. Environ. Policy 20, 1467–1478.

Fan, W., Srisupan, M., Bryant, L., Trembly, J.P., 2018b. Utilization of fly ash as pH adjustment for efficient immobilization and reutilization of nutrients from swine manure using hydrothermal treatment. Waste Manag. 79, 709–716.

Fini, E.H., 2019. Preparation and uses of bio-adhesives.

Fini, E.H., Høgsaa, B., Christiansen, J.D.C., Sanporean, C.-G., Jensen, E.A., Mousavi, M., Pahlavan, F., 2017. Multiscale investigation of a bioresidue as a novel intercalant for sodium montmorillonite. J. Phys. Chem. C 121, 1794–1802.

Fini, E.H., Kalberer, E.W., Shahbazi, A., Basti, M., You, Z., Ozer, H., Aurangzeb, Q., 2011. Chemical characterization of biobinder from swine manure: Sustainable modifier for asphalt binder. J. Mater. Civ. Eng. 23, 1506–1513.

Gupta, S., Kua, H.W., 2017. Factors determining the potential of biochar as a carbon capturing and sequestering construction material: critical review. J. Mater. Civ. Eng. 29, 4017086.

Gupta, S., Kua, H.W., Low, C.Y., 2018. Use of biochar as carbon sequestering additive in cement mortar. Cem. Concr. Compos. 87, 110–129.

Høgsaa, B., Fini, E.H., Christiansen, J. de C., Hung, A., Mousavi, M., Jensen, E.A., Pahlavan, F., Pedersen, T.H., Sanporean, C.-G., 2018. A novel bioresidue to compatibilize sodium montmorillonite and linear low density polyethylene. Ind. Eng. Chem. Res. 57, 1213–1224.

Hu, X., Song, J., Wang, H., Zhang, W., Wang, B., Lyu, W., Wang, Q., Liu, P., Chen, L., Xing, J., 2019. Adsorption of Cr (VI) and Cu (II) from aqueous solutions by biochar derived from Chaenomeles sinensis seed. Water Sci. Technol. 80, 2260–2272.

Hung, A., Fini, E.H., 2020. Surface Morphology and Chemical Mapping of UV-Aged Thin Films of Bitumen. ACS Sustain. Chem. Eng. 8, 11764–11771.

Hung, A.M., Kazembeyki, M., Hoover, C.G., Fini, E.H., 2019. Evolution of Morphological and Nanomechanical Properties of Bitumen Thin Films as a Result of Compositional Changes Due to Ultraviolet Radiation. ACS Sustain. Chem. Eng. 7, 18005–18014.

Ibrahim, A.F.M., Dandamudi, K.P.R., Deng, S., Lin, J.Y.S., 2020. Pyrolysis of hydrothermal liquefaction algal biochar for hydrogen production in a membrane reactor. Fuel 265, 116935. https://doi.org/https://doi.org/10.1016/j.fuel.2019.116935

Jin, B., Duan, P., Xu, Y., Wang, F., Fan, Y., 2013. Co-liquefaction of micro- and macroalgae in subcritical water. Bioresour. Technol. https://doi.org/10.1016/j.biortech.2013.09.045

Khiari, Z., Alka, K., Kelloway, S., Mason, B., Savidov, N., 2020. Integration of Biochar Filtration into Aquaponics: Effects on Particle Size Distribution and Turbidity Removal. Agric. Water Manag. 229, 105874.

Lehmann, J., Joseph, S., 2015. Biochar for environmental management: an introduction, in: Biochar for Environmental Management. Routledge, pp. 33–46.

Leng, L., Yuan, X., Huang, H., Wang, H., Wu, Z., Fu, L., Peng, X., Chen, X., Zeng, G., 2015. Characterization and application of bio-chars from liquefaction of microalgae, lignocellulosic biomass and sewage sludge. Fuel Process. Technol. 129, 8–14.

Liang, Y., Cao, X., Zhao, L., Xu, X., Harris, W., 2014. Phosphorus release from dairy manure, the manure-derived biochar, and their amended soil: Effects of phosphorus nature and soil property. J. Environ. Qual. 43, 1504–1509.

Liu, W.-J., Jiang, H., Yu, H.-Q., 2019. Emerging applications of biochar-based materials for energy storage and conversion. Energy Environ. Sci. 12, 1751–1779.

Liu, W.-J., Jiang, H., Yu, H.-Q., 2015. Development of biochar-based functional materials: toward a sustainable platform carbon material. Chem. Rev. 115, 12251–12285.

Liu, Z., Quek, A., Hoekman, S.K., Balasubramanian, R., 2013. Production of solid biochar fuel from waste biomass by hydrothermal carbonization. Fuel 103, 943–949.

Lozano, E.M., Pedersen, T.H., Rosendahl, L.A., 2020. Integration of hydrothermal liquefaction and carbon capture and storage for the production of advanced liquid biofuels with negative CO2 emissions. Appl. Energy 279, 115753.

Masto, R.E., Kumar, S., Rout, T.K., Sarkar, P., George, J., Ram, L.C., 2013. Biochar from water hyacinth (Eichornia crassipes) and its impact on soil biological activity. Catena 111, 64–71.

Meng, J., Wang, L., Liu, X., Wu, J., Brookes, P.C., Xu, J., 2013. Physicochemical properties of biochar produced from aerobically composted swine manure and its potential use as an environmental amendment. Bioresour. Technol. 142, 641–646.

Miranda, R., Bustos-Martinez, D., Blanco, C.S., Villarreal, M.H.G., Cantú, M.E.R., 2009. Pyrolysis of sweet orange (Citrus sinensis) dry peel. J. Anal. Appl. Pyrolysis. https://doi.org/10.1016/j.jaap.2009.06.001

Mohanty, P., Nanda, S., Pant, K.K., Naik, S., Kozinski, J.A., Dalai, A.K., 2013. Evaluation of the physiochemical development of biochars obtained from pyrolysis of wheat straw, timothy grass and pinewood: effects of heating rate. J. Anal. Appl. Pyrolysis 104, 485–493.

Muppaneni, T., Reddy, H.K., Patil, P.D., Dailey, P., Aday, C., Deng, S., 2012. Ethanolysis of camelina oil under supercritical condition with hexane as a co-solvent. Appl. Energy 94, 84–88.

Muppaneni, T., Reddy, H.K., Selvaratnam, T., Dandamudi, K.P.R., Dungan, B., Nirmalakhandan, N., Schaub, T., Omar Holguin, F., Voorhies, W., Lammers, P., Deng, S., 2017. Hydrothermal liquefaction of Cyanidioschyzon merolae and the influence of catalysts on products. Bioresour. Technol. 223. https://doi.org/10.1016/j.biortech.2016.10.022

Naik, S., Goud, V. V, Rout, P.K., Jacobson, K., Dalai, A.K., 2010. Characterization of Canadian biomass for alternative renewable biofuel. Renew. energy 35, 1624–1631.

Nam, H., Choi, J., Capareda, S.C., 2016. Comparative study of vacuum and fractional distillation using pyrolytic microalgae (Nannochloropsis oculata) bio-oil. Algal Res. 17, 87–96.

Nosaka, T., Lankone, R., Westerhoff, P., Herckes, P., 2020. Flame retardant performance of carbonaceous nanomaterials on polyester fabric. Polym. Test. 106497.

Oancea, I., Bujoreanu, C., Budescu, M., Benchea, M., Grădinaru, C.M., 2018. Considerations on sound absorption coefficient of sustainable concrete with different waste replacements. J. Clean. Prod. 203, 301–312.

Ofori-Boadu, A.N., Abrokwah, R.Y., Gbewonyo, S., Fini, E., 2018. Effect of swine-waste bio-char on the water absorption characteristics of cement pastes. Int. J. Build. Pathol. Adapt.

Pahlavan, F., Rajib, A., Deng, S., Lammers, P., Fini, E.H., 2020. Investigation of Balanced Feedstocks of Lipids and Proteins To Synthesize Highly Effective Rejuvenators for Oxidized Asphalt. ACS Sustain. Chem. Eng.

Patil, P.D., Dandamudi, K.P.R., Wang, J., Deng, Q., Deng, S., 2018. Extraction of bio-oils from algae with supercritical carbon dioxide and co-solvents. J. Supercrit. Fluids 135, 60–68. https://doi.org/https://doi.org/10.1016/j.supflu.2017.12.019

Peng, W., Wu, Q., Tu, P., Zhao, N., 2001. Pyrolytic characteristics of microalgae as renewable energy source determined by thermogravimetric analysis. Bioresour. Technol. https://doi.org/10.1016/S0960-8524(01)00072-4

Phillips, L.N., Kappagantula, K.S., Trembly, J.P., 2019. Mechanical performance of thermoplastic composites using bituminous coal as filler: Study of a potentially sustainable end-use application for Appalachian coal. Polym. Compos. 40, 591–599.

Ponnusamy, V.K., Nagappan, S., Bhosale, R.R., Lay, C.-H., Nguyen, D.D., Pugazhendhi, A., Woong, C.S., Kumar, G., 2020. Review on sustainable production of biochar through hydrothermal liquefaction: Physico-chemical properties and applications. Bioresour. Technol. 123414.

Qambrani, N.A., Rahman, M.M., Won, S., Shim, S., Ra, C., 2017. Biochar properties and

eco-friendly applications for climate change mitigation, waste management, and wastewater treatment: A review. Renew. Sustain. Energy Rev. 79, 255–273.

Radis Steinmetz, R.L., Kunz, A., Dressler, V.L., de Moraes Flores, É.M., Figueiredo Martins, A., 2009. Study of metal distribution in raw and screened swine manure. CLEAN–Soil, Air, Water 37, 239–244.

Rahman, M.Z., Edvinsson, T., Kwong, P., 2020. Biochar for Electrochemical Applications. Curr. Opin. Green Sustain. Chem.

Rajib, A., Fini, E.H., 2020. Inherently Functionalized Carbon from Lipid and Protein-Rich Biomass to Reduce Ultraviolet-Induced Damages in Bituminous Materials. ACS Omega. https://doi.org/10.1021/acsomega.0c03514

Reddy Karnati, S., Høgsaa, B., Zhang, L., Fini, E.H., 2020. Developing carbon nanoparticles with tunable morphology and surface chemistry for use in construction. Constr. Build. Mater. 262, 120780. https://doi.org/https://doi.org/10.1016/j.conbuildmat.2020.120780

Rengaraj, S., Yeon, K.-H., Moon, S.-H., 2001. Removal of chromium from water and wastewater by ion exchange resins. J. Hazard. Mater. 87, 273–287.

Ross, A.B., Biller, P., Kubacki, M.L., Li, H., Lea-Langton, A., Jones, J.M., 2010. Hydrothermal processing of microalgae using alkali and organic acids. Fuel 89, 2234–2243.

Savage, P.E., Hestekin, J.A., 2013. A perspective on algae, the environment, and energy. Environ. Prog. Sustain. Energy 32, 877–883.

Sudasinghe, N., Cort, J.R., Hallen, R., Olarte, M., Schmidt, A., Schaub, T., 2014. Hydrothermal liquefaction oil and hydrotreated product from pine feedstock characterized by heteronuclear two-dimensional NMR spectroscopy and FT-ICR mass spectrometry. Fuel 137, 60–69.

Sues, A., Juraščík, M., Ptasinski, K., 2010. Exergetic evaluation of 5 biowastes-to-biofuels routes via gasification. Energy 35, 996–1007.

Suresh, S., Kante, K., Fini, E.H., Bandosz, T.J., 2019. Combination of alkalinity and porosity enhances formaldehyde adsorption on pig manure-derived composite adsorbents. Microporous Mesoporous Mater. 286, 155–162.

Thompson, K.A., Shimabuku, K.K., Kearns, J.P., Knappe, D.R.U., Summers, R.S., Cook, S.M., 2016. Environmental comparison of biochar and activated carbon for tertiary wastewater treatment. Environ. Sci. Technol. 50, 11253–11262.

Toor, S.S., Reddy, H., Deng, S., Hoffmann, J., Spangsmark, D., Madsen, L.B., Holm-

Nielsen, J.B., Rosendahl, L.A., 2013. Hydrothermal liquefaction of Spirulina and Nannochloropsis salina under subcritical and supercritical water conditions. Bioresour. Technol. 131, 413–419.

Toor, S.S., Rosendahl, L., Rudolf, A., 2011. Hydrothermal liquefaction of biomass: a review of subcritical water technologies. Energy 36, 2328–2342.

Tsai, W.-T., Liu, S.-C., Chen, H.-R., Chang, Y.-M., Tsai, Y.-L., 2012. Textural and chemical properties of swine-manure-derived biochar pertinent to its potential use as a soil amendment. Chemosphere 89, 198–203.

Vardon, D.R., Sharma, B.K., Scott, J., Yu, G., Wang, Z., Schideman, L., Zhang, Y., Strathmann, T.J., 2011. Chemical properties of biocrude oil from the hydrothermal liquefaction of Spirulina algae, swine manure, and digested anaerobic sludge. Bioresour. Technol. 102, 8295–8303.

Verheijen, F., Jeffery, S., Bastos, A.C., Van der Velde, M., Diafas, I., 2010. Biochar application to soils. A Crit. Sci. Rev. Eff. soil Prop. Process. Funct. EUR 24099, 162.

Wallace, R., Suresh, S., Fini, E.H., Bandosz, T.J., 2017. Efficient Air Desulfurization Catalysts Derived from Pig Manure Liquefaction Char. C—Journal Carbon Res. 3, 37.

Walters, R., Begum, S.A., Fini, E.H., Abu-Lebdeh, T.M., 2015. Investigating bio-char as flow modifier and water treatment agent for sustainable pavement design. Am. J. Eng. Appl. Sci. 8, 138–146.

Wang, J., Krishna, R., Yang, J., Dandamudi, K.P.R., Deng, S., 2015. Nitrogen-doped porous carbons for highly selective CO<inf>2</inf> capture from flue gases and natural gas upgrading. Mater. Today Commun. 4. https://doi.org/10.1016/j.mtcomm.2015.06.009

Wang, J., Peng, X., Chen, X., Ma, X., 2019. Co-liquefaction of low-lipid microalgae and starch-rich biomass waste: The interaction effect on product distribution and composition. J. Anal. Appl. Pyrolysis 139, 250–257.

Wang, L., Chen, L., Tsang, D.C.W., Guo, B., Yang, J., Shen, Z., Hou, D., Ok, Y.S., Poon, C.S., 2020. Biochar as green additives in cement-based composites with carbon dioxide curing. J. Clean. Prod. 258, 120678.

Waqas, M., Aburiazaiza, A.S., Miandad, R., Rehan, M., Barakat, M.A., Nizami, A.S., 2018. Development of biochar as fuel and catalyst in energy recovery technologies. J. Clean. Prod. 188, 477–488.

Wiedemeier, D.B., Abiven, S., Hockaday, W.C., Keiluweit, M., Kleber, M., Masiello,

C.A., McBeath, A. V, Nico, P.S., Pyle, L.A., Schneider, M.P.W., 2015. Aromaticity and degree of aromatic condensation of char. Org. Geochem. 78, 135–143.

Zhang, B., Chen, J., He, Z., Chen, H., Kandasamy, S., 2019. Hydrothermal liquefaction of fresh lemon-peel: Parameter optimisation and product chemistry. Renew. Energy 143, 512–519.

Alba, L.G., Torri, C., Fabbri, D., Kersten, S.R.A., Brilman, D.W.F.W., 2013. Microalgae growth on the aqueous phase from hydrothermal liquefaction of the same microalgae. Chem. Eng. J. 228, 214–223.

Andersen, R.A., 2005. Algal culturing techniques. Elsevier.

Aysu, T., Demirbaş, A., Bengü, A.Ş., Küçük, M.M., 2015. Evaluation of Eremurus spectabilis for production of bio-oils with supercritical solvents. Process Saf. Environ. Prot. 94, 339–349.

Barreiro, D.L., Prins, W., Ronsse, F., Brilman, W., 2013. Hydrothermal liquefaction (HTL) of microalgae for biofuel production: state of the art review and future prospects. Biomass and Bioenergy 53, 113–127.

Beal, C.M., Archibald, I., Huntley, M.E., Greene, C.H., Johnson, Z.I., 2018. Integrating algae with bioenergy carbon capture and storage (ABECCS) increases sustainability. Earth's Futur. 6, 524–542.

Bouwman, L., Goldewijk, K.K., Van Der Hoek, K.W., Beusen, A.H.W., Van Vuuren, D.P., Willems, J., Rufino, M.C., Stehfest, E., 2013. Exploring global changes in nitrogen and phosphorus cycles in agriculture induced by livestock production over the 1900–2050 period. Proc. Natl. Acad. Sci. 110, 20882–20887.

Bridgwater, A. V, 2012. Review of fast pyrolysis of biomass and product upgrading. Biomass and bioenergy 38, 68–94.

Chisti, Y., 2007. Biodiesel from microalgae. Biotechnol. Adv. 25, 294–306.

Cisse, L., Mrabet, T., 2004. World phosphate production: overview and prospects. Phosphorus Res. Bull. 15, 21–25.

Collard, F.-X., Blin, J., 2014. A review on pyrolysis of biomass constituents: Mechanisms and composition of the products obtained from the conversion of cellulose, hemicelluloses and lignin. Renew. Sustain. Energy Rev. 38, 594–608.

Dandamudi, K.P.R., Muhammed Luboowa, K., Laideson, M., Murdock, T., Seger, M., McGowen, J., Lammers, P.J., Deng, S., 2020. Hydrothermal liquefaction of Cyanidioschyzon merolae and Salicornia bigelovii Torr.: The interaction effect on product distribution and chemistry. Fuel 277.

https://doi.org/10.1016/j.fuel.2020.118146

Dandamudi, K.P.R., Muppaneni, T., Markovski, J.S., Lammers, P., Deng, S., 2019. Hydrothermal liquefaction of green microalga Kirchneriella sp. under sub-and super-critical water conditions. Biomass and bioenergy 120, 224–228.

Dandamudi, K.P.R., Muppaneni, T., Sudasinghe, N., Schaub, T., Holguin, F.O., Lammers, P.J., Deng, S., 2017. Co-liquefaction of mixed culture microalgal strains under sub-critical water conditions. Bioresour. Technol. 236. https://doi.org/10.1016/j.biortech.2017.03.165

Demirbas, A., 2009. Political, economic and environmental impacts of biofuels: A review. Appl. Energy 86, S108–S117.

Gai, C., Liu, Z., Han, G., Peng, N., Fan, A., 2015. Combustion behavior and kinetics of low-lipid microalgae via thermogravimetric analysis. Bioresour. Technol. 181, 148–154.

Godwin, C.M., Hietala, D.C., Lashaway, A.R., Narwani, A., Savage, P.E., Cardinale, B.J., 2017. Algal polycultures enhance coproduct recycling from hydrothermal liquefaction. Bioresour. Technol. 224, 630–638.

Gross, J.D., Matsuo, H., Fletcher, M., Sachs, A.B., Wagner, G., 2001. Interactions of the eukaryotic translation initiation factor eIF4E, in: Cold Spring Harbor Symposia on Quantitative Biology. Cold Spring Harbor Laboratory Press, pp. 397–402.

He, S., Zhao, M., Wang, J., Cheng, Z., Yan, B., Chen, G., 2020. Hydrothermal liquefaction of low-lipid algae Nannochloropsis sp. and Sargassum sp.: Effect of feedstock composition and temperature. Sci. Total Environ. 712, 135677.

Ibrahim, A.F.M., Dandamudi, K.P.R., Deng, S., Lin, J.Y.S., 2020. Pyrolysis of hydrothermal liquefaction algal biochar for hydrogen production in a membrane reactor. Fuel 265, 116935. https://doi.org/https://doi.org/10.1016/j.fuel.2019.116935

Ikenaga, N., Ueda, C., Matsui, T., Ohtsuki, M., Suzuki, T., 2001. Co-liquefaction of micro algae with coal using coal liquefaction catalysts. Energy and Fuels. https://doi.org/10.1021/ef000129u

Jiang, L., Liang, B., Xue, Q., Yin, C., 2016. Characterization of phosphorus leaching from phosphate waste rock in the Xiangxi River watershed, Three Gorges Reservoir, China. Chemosphere 150, 130–138.

Karbakhshravari, M., Abeysiriwardana-Arachchige, I.S.A., Henkanatte-Gedera, S.M., Cheng, F., Papelis, C., Brewer, C.E., Nirmalakhandan, N., 2020. Recovery of struvite from hydrothermally processed algal biomass cultivated in urban wastewaters. Resour. Conserv. Recycl. 163, 105089.

Kruse, A., Dinjus, E., 2007. Hot compressed water as reaction medium and reactant: properties and synthesis reactions. J. Supercrit. Fluids 39, 362–380.

Lammers, P.J., Huesemann, M., Boeing, W., Anderson, D.B., Arnold, R.G., Bai, X., Bhole, M., Brhanavan, Y., Brown, L., Brown, J., 2017. Review of the cultivation program within the National Alliance for Advanced Biofuels and Bioproducts. Algal Res. 22, 166–186.

Muppaneni, T., Reddy, H.K., Selvaratnam, T., Dandamudi, K.P.R., Dungan, B., Nirmalakhandan, N., Schaub, T., Omar Holguin, F., Voorhies, W., Lammers, P., Deng, S., 2017. Hydrothermal liquefaction of Cyanidioschyzon merolae and the influence of catalysts on products. Bioresour. Technol. 223. https://doi.org/10.1016/j.biortech.2016.10.022

Patil, P.D., Dandamudi, K.P.R., Wang, J., Deng, Q., Deng, S., 2018. Extraction of bio-oils from algae with supercritical carbon dioxide and co-solvents. J. Supercrit. Fluids 135, 60–68. https://doi.org/https://doi.org/10.1016/j.supflu.2017.12.019

Reddy, H.K., Muppaneni, T., Sun, Y., Li, Y., Ponnusamy, S., Patil, P.D., Dailey, P., Schaub, T., Holguin, F.O., Dungan, B., Cooke, P., Lammers, P., Voorhies, W., Lu, X., Deng, S., 2014. Subcritical water extraction of lipids from wet algae for biodiesel production. Fuel 133, 73–81. https://doi.org/https://doi.org/10.1016/j.fuel.2014.04.081

Samieadel, A., Rajib, A.I., Dandamudi, K.P.R., Deng, S., Fini, E.H., 2020. Improving recycled asphalt using sustainable hybrid rejuvenators with enhanced intercalation into oxidized asphaltenes nanoaggregates. Constr. Build. Mater. 262, 120090.

Selvaratnam, T., Pegallapati, A.K., Montelya, F., Rodriguez, G., Nirmalakhandan, N., Van Voorhies, W., Lammers, P.J., 2014. Evaluation of a thermo-tolerant acidophilic alga, Galdieria sulphuraria, for nutrient removal from urban wastewaters. Bioresour. Technol. 156, 395–399.

Selvaratnam, T., Pegallapati, A.K., Reddy, H., Kanapathipillai, N., Nirmalakhandan, N., Deng, S., Lammers, P.J., 2015a. Algal biofuels from urban wastewaters: Maximizing biomass yield using nutrients recycled from hydrothermal processing of biomass. Bioresour. Technol. 182, 232–238.

Selvaratnam, T., Reddy, H., Muppaneni, T., Holguin, F.O., Nirmalakhandan, N., Lammers, P.J., Deng, S., 2015b. Optimizing energy yields from nutrient recycling using sequential hydrothermal liquefaction with Galdieria sulphuraria. Algal Res. 12, 74–79.

Son, E.-B., Poo, K.-M., Chang, J.-S., Chae, K.-J., 2018. Heavy metal removal from aqueous solutions using engineered magnetic biochars derived from waste marine

macro-algal biomass. Sci. Total Environ. 615, 161–168.

Toor, S.S., Reddy, H., Deng, S., Hoffmann, J., Spangsmark, D., Madsen, L.B., Holm-Nielsen, J.B., Rosendahl, L.A., 2013. Hydrothermal liquefaction of Spirulina and Nannochloropsis salina under subcritical and supercritical water conditions. Bioresour. Technol. 131, 413–419.

U.S. EIA, U.S. Energy Information Administration (EIA), 2019. Annual Energy Outlook 2019 with projections to 2050. Annu. Energy Outlook 2019 with Proj. to 2050. https://doi.org/DOE/EIA-0383(2012) U.S.

Wang, J., Krishna, R., Yang, J., Dandamudi, K.P.R., Deng, S., 2015. Nitrogen-doped porous carbons for highly selective CO<inf>2</inf> capture from flue gases and natural gas upgrading. Mater. Today Commun. 4. https://doi.org/10.1016/j.mtcomm.2015.06.009

Wang, J., Peng, X., Chen, X., Ma, X., 2019. Co-liquefaction of low-lipid microalgae and starch-rich biomass waste: The interaction effect on product distribution and composition. J. Anal. Appl. Pyrolysis 139, 250–257.

Xu, D., Lin, G., Guo, S., Wang, S., Guo, Y., Jing, Z., 2018. Catalytic hydrothermal liquefaction of algae and upgrading of biocrude: a critical review. Renew. Sustain. Energy Rev. 97, 103–118.

Xu, D., Savage, P.E., 2017. Effect of temperature, water loading, and Ru/C catalyst on water-insoluble and water-soluble biocrude fractions from hydrothermal liquefaction of algae. Bioresour. Technol. 239, 1–6.

Yang, C.-M., Lee, C.-G., Won, J.-I., 2017. Improvement of Bio-crude Oil Yield and Phosphorus Content by Hydrothermal Liquefaction Using Microalgae. Chem. Eng. Technol. 40, 2188–2196.

Zhan, L., Jiang, L., Zhang, Y., Gao, B., Xu, Z., 2020. Reduction, detoxification and recycling of solid waste by hydrothermal technology: A review. Chem. Eng. J. 124651.

Al-Mufachi, N.A., Rees, N. V, Steinberger-Wilkens, R., 2015. Hydrogen selective membranes: A review of palladium-based dense metal membranes. Renew. Sustain. Energy Rev. 47, 540–551.

Antoniazzi, A.B., Haasz, A.A., Stangeby, P.C., 1989. The effect of adsorbed carbon and sulphur on hydrogen permeation through palladium. J. Nucl. Mater. 162, 1065–1070.

Bird, M.I., Wurster, C.M., de Paula Silva, P.H., Bass, A.M., De Nys, R., 2011. Algal biochar–production and properties. Bioresour. Technol. 102, 1886–1891.

Bird, M.I., Wurster, C.M., de Paula Silva, P.H., Paul, N.A., De Nys, R., 2012. Algal biochar: effects and applications. Gcb Bioenergy 4, 61–69.

Bordoloi, N., Goswami, R., Kumar, M., Kataki, R., 2017. Biosorption of Co (II) from aqueous solution using algal biochar: kinetics and isotherm studies. Bioresour. Technol. 244, 1465–1469.

Brennan, L., Owende, P., 2010. Biofuels from microalgae—a review of technologies for production, processing, and extractions of biofuels and co-products. Renew. Sustain. energy Rev. 14, 557–577.

Chen, Y., Wu, Y., Hua, D., Li, C., Harold, M.P., Wang, J., Yang, M., 2015. Thermochemical conversion of low-lipid microalgae for the production of liquid fuels: challenges and opportunities. RSC Adv. 5, 18673–18701.

Cheng, F., Cui, Z., Chen, L., Jarvis, J., Paz, N., Schaub, T., Nirmalakhandan, N., Brewer, C.E., 2017. Hydrothermal liquefaction of high-and low-lipid algae: Bio-crude oil chemistry. Appl. Energy 206, 278–292.

Cheng, F., Cui, Z., Mallick, K., Nirmalakhandan, N., Brewer, C.E., 2018. Hydrothermal liquefaction of high-and low-lipid algae: Mass and energy balances. Bioresour. Technol. 258, 158–167.

Cole, A.J., Paul, N.A., De Nys, R., Roberts, D.A., 2017. Good for sewage treatment and good for agriculture: Algal based compost and biochar. J. Environ. Manage. 200, 105–113.

Daiyan, R., Lu, X., Ng, Y.H., Amal, R., 2017. Liquid Hydrocarbon Production from CO2: Recent Development in Metal-Based Electrocatalysis. ChemSusChem 10, 4342–4358.

Dandamudi, K.P.R., Muhammed Luboowa, K., Laideson, M., Murdock, T., Seger, M., McGowen, J., Lammers, P.J., Deng, S., 2020a. Hydrothermal liquefaction of Cyanidioschyzon merolae and Salicornia bigelovii Torr.: The interaction effect on product distribution and chemistry. Fuel 277, 118146. https://doi.org/https://doi.org/10.1016/j.fuel.2020.118146

Dandamudi, K.P.R., Muhammed Luboowa, K., Laideson, M., Murdock, T., Seger, M., McGowen, J., Lammers, P.J., Deng, S., 2020b. Hydrothermal Liquefaction of Cyanidioschyzon merolae and Salicornia bigelovii Torr.: The interaction effect on product distribution and chemistry. Fuel 277. https://doi.org/10.1016/j.fuel.2020.118146

Dandamudi, K.P.R., Muppaneni, T., Markovski, J.S., Lammers, P., Deng, S., 2019. Hydrothermal liquefaction of green microalga Kirchneriella sp. under sub- and

super-critical water conditions. Biomass and Bioenergy 120. https://doi.org/10.1016/j.biombioe.2018.11.021

Dandamudi, K.P.R., Muppaneni, T., Sudasinghe, N., Schaub, T., Holguin, F.O., Lammers, P.J., Deng, S., 2017. Co-liquefaction of mixed culture microalgal strains under sub-critical water conditions. Bioresour. Technol. 236. https://doi.org/10.1016/j.biortech.2017.03.165

Elsherif, M., Manan, Z.A., Kamsah, M.Z., 2015. State-of-the-art of hydrogen management in refinery and industrial process plants. J. Nat. Gas Sci. Eng. 24, 346–356.

Flanagan, T.B., Wang, D., 2010. Exponents for the pressure dependence of hydrogen permeation through Pd and Pd− Ag alloy membranes. J. Phys. Chem. C 114, 14482–14488.

Guo, Y., Yeh, T., Song, W., Xu, D., Wang, S., 2015. A review of bio-oil production from hydrothermal liquefaction of algae. Renew. Sustain. Energy Rev. 48, 776–790.

Hurlbert, R.C., Konecny, J.O., 1961. Diffusion of hydrogen through palladium. J. Chem. Phys. 34, 655–658.

Johansson, C.L., Paul, N.A., de Nys, R., Roberts, D.A., 2016. Simultaneous biosorption of selenium, arsenic and molybdenum with modified algal-based biochars. J. Environ. Manage. 165, 117–123.

Kikuchi, E., 2000. Membrane reactor application to hydrogen production. Catal. Today 56, 97–101.

Kulprathipanja, A., Alptekin, G.O., Falconer, J.L., Way, J.D., 2005. Pd and Pd–Cu membranes: inhibition of H2 permeation by H2S. J. Memb. Sci. 254, 49–62.

Kumar, A., Ergas, S., Yuan, X., Sahu, A., Zhang, Q., Dewulf, J., Malcata, F.X., Van Langenhove, H., 2010. Enhanced CO2 fixation and biofuel production via microalgae: recent developments and future directions. Trends Biotechnol. 28, 371–380.

Lai, T., Lind, M.L., 2015. Heat treatment driven surface segregation in Pd77Ag23 membranes and the effect on hydrogen permeability. Int. J. Hydrogen Energy 40, 373–382.

Li, Z., Savage, P.E., 2013. Feedstocks for fuels and chemicals from algae: treatment of crude bio-oil over HZSM-5. Algal Res. 2, 154–163.

Liu, Z., Zhang, F.-S., 2009. Removal of lead from water using biochars prepared from hydrothermal liquefaction of biomass. J. Hazard. Mater. 167, 933–939.

Maliutina, K., Tahmasebi, A., Yu, J., 2018. Pressurized entrained-flow pyrolysis of microalgae: Enhanced production of hydrogen and nitrogen-containing compounds. Bioresour. Technol. 256, 160–169.

Maliutina, K., Tahmasebi, A., Yu, J., Saltykov, S.N., 2017. Comparative study on flash pyrolysis characteristics of microalgal and lignocellulosic biomass in entrained-flow reactor. Energy Convers. Manag. 151, 426–438.

Mundschau, M. V, Xie, X., Evenson IV, C.R., Sammells, A.F., 2006. Dense inorganic membranes for production of hydrogen from methane and coal with carbon dioxide sequestration. Catal. Today 118, 12–23.

Muppaneni, T., Reddy, H.K., Selvaratnam, T., Dandamudi, K.P.R., Dungan, B., Nirmalakhandan, N., Schaub, T., Omar Holguin, F., Voorhies, W., Lammers, P., Deng, S., 2017. Hydrothermal liquefaction of Cyanidioschyzon merolae and the influence of catalysts on products. Bioresour. Technol. 223. https://doi.org/10.1016/j.biortech.2016.10.022

O'Brien, C.P., Gellman, A.J., Morreale, B.D., Miller, J.B., 2011. The hydrogen permeability of Pd4S. J. Memb. Sci. 371, 263–267.

Ockwig, N.W., Nenoff, T.M., 2007. Membranes for hydrogen separation. Chem. Rev. 107, 4078–4110.

Paglieri, S.N., Way, J.D., 2002. Innovations in palladium membrane research. Sep. Purif. Methods 31, 1–169.

Park, J.-N., McFarland, E.W., 2009. A highly dispersed Pd–Mg/SiO2 catalyst active for methanation of CO2. J. Catal. 266, 92–97.

Patil, P.D., Dandamudi, K.P.R., Wang, J., Deng, Q., Deng, S., 2018. Extraction of bio-oils from algae with supercritical carbon dioxide and co-solvents. J. Supercrit. Fluids 135, 60–68. https://doi.org/https://doi.org/10.1016/j.supflu.2017.12.019

Peters, T.A., Kaleta, T., Stange, M., Bredesen, R., 2013. Development of ternary Pd–Ag–TM alloy membranes with improved sulphur tolerance. J. Memb. Sci. 429, 448–458.

Peters, T.A., Stange, M., Veenstra, P., Nijmeijer, A., Bredesen, R., 2016. The performance of Pd–Ag alloy membrane films under exposure to trace amounts of H2S. J. Memb. Sci. 499, 105–115.

Salimi, P., Askari, K., Norouzi, O., Kamali, S., 2019a. Improving the electrochemical performance of carbon anodes derived from marine biomass by using ionic-liquid-based hybrid electrolyte for LIBs. J. Electron. Mater. 48, 951–963.

Salimi, P., Norouzi, O., Pourhoseini, S.E.M., Bartocci, P., Tavasoli, A., Di Maria, F.,

Pirbazari, S.M., Bidini, G., Fantozzi, F., 2019b. Magnetic biochar obtained through catalytic pyrolysis of macroalgae: A promising anode material for Li-ion batteries. Renew. Energy 140, 704–714.

Son, E.-B., Poo, K.-M., Chang, J.-S., Chae, K.-J., 2018. Heavy metal removal from aqueous solutions using engineered magnetic biochars derived from waste marine macro-algal biomass. Sci. Total Environ. 615, 161–168.

Staffell, I., Scamman, D., Abad, A.V., Balcombe, P., Dodds, P.E., Ekins, P., Shah, N., Ward, K.R., 2019. The role of hydrogen and fuel cells in the global energy system. Energy Environ. Sci. 12, 463–491.

Taghavi, S., Norouzi, O., Tavasoli, A., Di Maria, F., Signoretto, M., Menegazzo, F., Di Michele, A., 2018. Catalytic conversion of Venice lagoon brown marine algae for producing hydrogen-rich gas and valuable biochemical using algal biochar and Ni/SBA-15 catalyst. Int. J. Hydrogen Energy 43, 19918–19929.

Thangalazhy-Gopakumar, S., Adhikari, S., Chattanathan, S.A., Gupta, R.B., 2012. Catalytic pyrolysis of green algae for hydrocarbon production using H+ ZSM-5 catalyst. Bioresour. Technol. 118, 150–157.

Toplin, J.A., Norris, T.B., Lehr, C.R., McDermott, T.R., Castenholz, R.W., 2008. Biogeographic and phylogenetic diversity of thermoacidophilic cyanidiales in Yellowstone National Park, Japan, and New Zealand. Appl. Environ. Microbiol. 74, 2822–2833.

Uemiya, S., Matsuda, T., Kikuchi, E., 1991. Hydrogen permeable palladium-silver alloy membrane supported on porous ceramics. J. Memb. Sci. 56, 315–325.

Uemiya, S., Sato, N., Ando, H., Matsuda, T., Kikuchi, E., 1990. Steam reforming of methane in a hydrogen-permeable membrane reactor. Appl. Catal. 67, 223–230.

Wang, J., Krishna, R., Yang, J., Dandamudi, K.P.R., Deng, S., 2015. Nitrogen-doped porous carbons for highly selective CO<inf>2</inf> capture from flue gases and natural gas upgrading. Mater. Today Commun. 4. https://doi.org/10.1016/j.mtcomm.2015.06.009

Xiong, S., Lian, Y., Xie, H., Liu, B., 2019. Hydrogenation of CO2 to methanol over Cu/ZnCr catalyst. Fuel 256, 115975.

Yu, G., Zhang, Y., Schideman, L., Funk, T., Wang, Z., 2011. Distributions of carbon and nitrogen in the products from hydrothermal liquefaction of low-lipid microalgae. Energy Environ. Sci. 4, 4587–4595.

Yu, K.L., Lau, B.F., Show, P.L., Ong, H.C., Ling, T.C., Chen, W.-H., Ng, E.P., Chang, J.-S., 2017. Recent developments on algal biochar production and characterization.

Bioresour. Technol. 246, 2–11.

Zheng, H., Guo, W., Li, S., Chen, Y., Wu, Q., Feng, X., Yin, R., Ho, S.-H., Ren, N., Chang, J.-S., 2017. Adsorption of p-nitrophenols (PNP) on microalgal biochar: analysis of high adsorption capacity and mechanism. Bioresour. Technol. 244, 1456–1464.

APPENDIX A

Appendix A describes the additional information mentioned in chapter 3

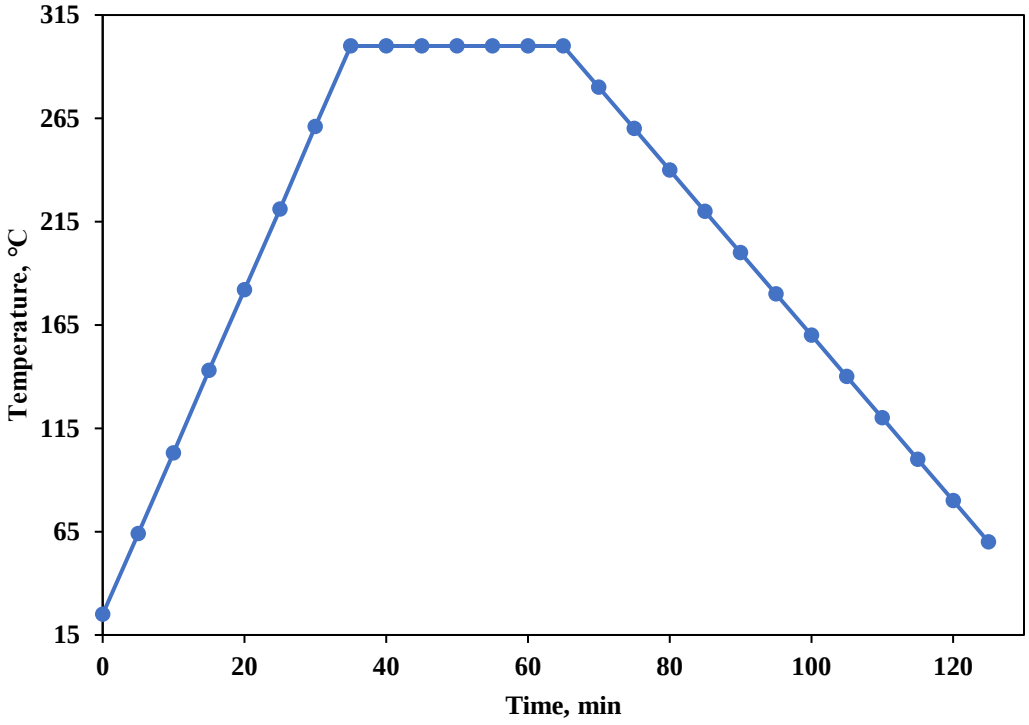

Figure A-1: Heating and cooling profile of the reactor @ 300 °C, 30 min residence time, and 10 wt. % solid loading.

Digestion procedure for ICP-OES analysis

The samples were divided into two sets; set 1: biomass, biocrude oils, and set 2: Biochar samples. Each set consisted of a blank and a QC to test the validity of the final results.

Set 1 Digestion procedure:

1. Approximately 100 mg of the samples were weighed and added to the Teflon microwave digestion vessels.
2. 10 ml of concentrated Nitric acid was added to each vessel and let to react in the hood for 30 min.
3. Following the reaction, the vessels were sealed and digested using a CEM Microwave Digester. The following settings were used for the digestion: 1600 W @80 %, 10 min ramp with 20 min holding time at 180 °C.
4. Post digestion, the samples were let to cool down and examined to see for any residues.
5. If there are no residues, 1 ml of hydrogen peroxide is added to each vessel and let to react overnight.
6. The samples are running through step 3 to complete the digestion step.
7. Post cooling, the samples are diluted with 2 % nitric acid (1 part of sample: 10 part of 2% nitric acid) before running on the ICP-OES instrument.

Set 2 Digestion procedure:

1. Approximately 100 mg of the samples were weighed and added to the Teflon microwave digestion vessels.
2. 5 ml of concentrated sulphuric acid was added to each vessel and let to react in the hood for 30 min.

3. 5 ml of concentrated Nitric acid was added to each vessel and let to react in the hood for 30 min.
4. Following the reactions, the vessels were sealed and digested using a CEM Microwave Digester. The following settings were used for the digestion: 1600 W @80 %, 15 min ramp with 15 min holding time at 170 °C.
5. Post digestion, the samples were let to cool down and examined to see for any residues.
6. Since residues were present, the vessels were added with 2 ml of hydrofluoric acid and allowed to react for 30 min in the hood.
7. Following the reactions, the vessels were sealed and digested using a CEM Microwave Digester. The following settings were used for the digestion: 1600 W @80 %, 15 min ramp with 15 min holding time at 200 °C.
8. Post digestion, the samples were let to cool down and examined to see for any residues.
9. The vessels were added with 10 ml of 4.5 % boric acid to facilitate the neutralization of excess Hydrofluoric acid. The mixtures were let to react for 30 min in the hood.
10. Following the reactions, the vessels were sealed and digested using a CEM Microwave Digester. The following settings were used for the digestion: 800 W @100 %, 20 min ramp with 10 min holding time at 160 °C.
11. The vessels were vented after they reach room temperature.

12. The samples were filtered through a 0.45 µm polypropylene filter.
13. The filtered sample was diluted with five parts of 2 % nitric acid before running on ICP-OES.

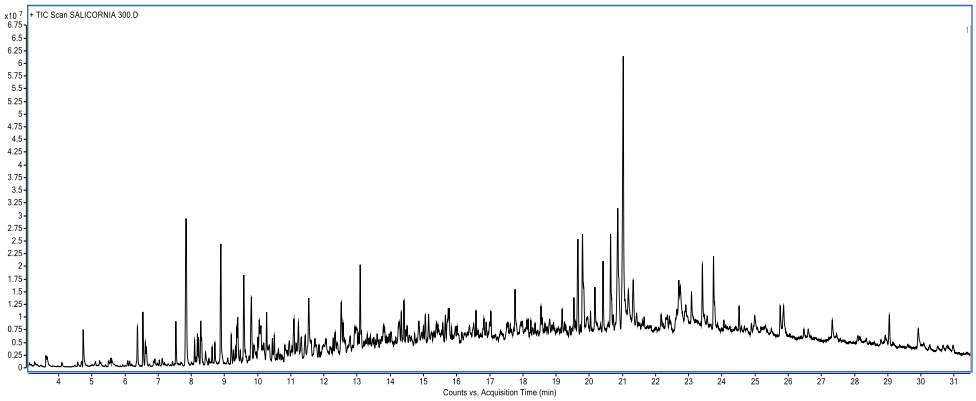

Figure A-2: GC-MS chromatogram of the SL biocrude oil produced @ 300 °C, 30 min residence time, and 10 wt. % solid loading.

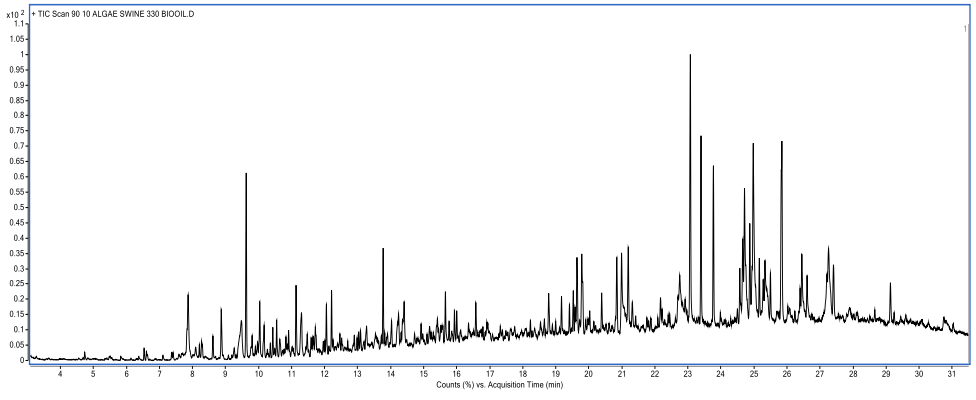

Figure A-3: GC-MS chromatogram of the CM biocrude oil produced @ 300 °C, 30 min residence time, and 10 wt. % solid loading.

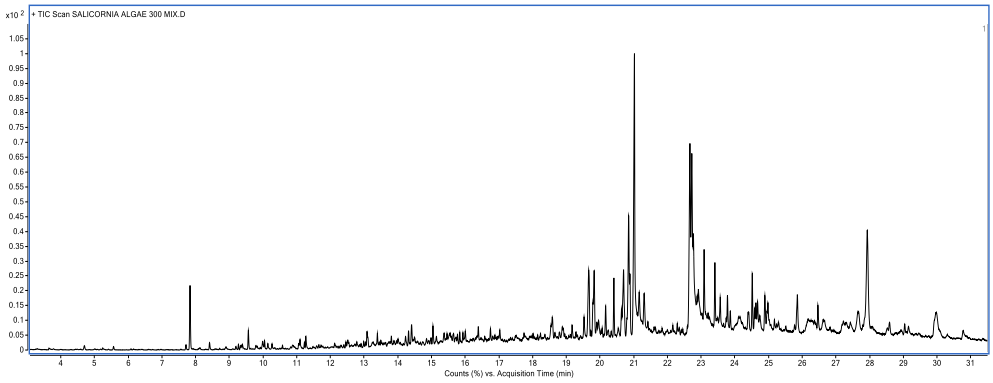

Figure A-4: GC-MS chromatogram of the CS* biocrude oil produced @ 300 °C, 30 min residence time, and 10 wt. % solid loading.

APPENDIX B

Appendix B describes the additional information mentioned in chapter 6

TGA characteristics of used biomass and HTL biochar samples.

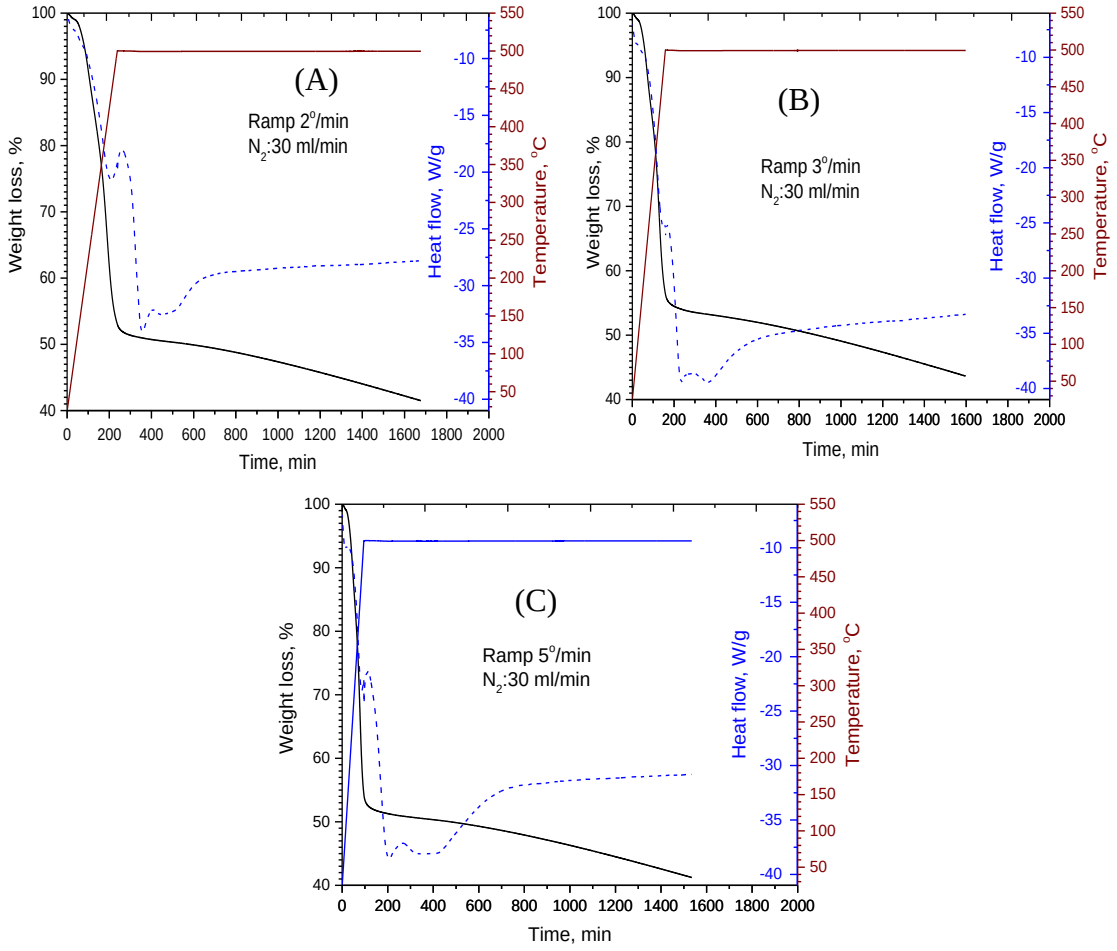

Figure B-1: The weight loss of a biochar sample heated to 500 °C for 24 has a function of time at different ramping rates of: A)2, B) 3, and C) 5 °/min

Graphite Ring Thermal Properties

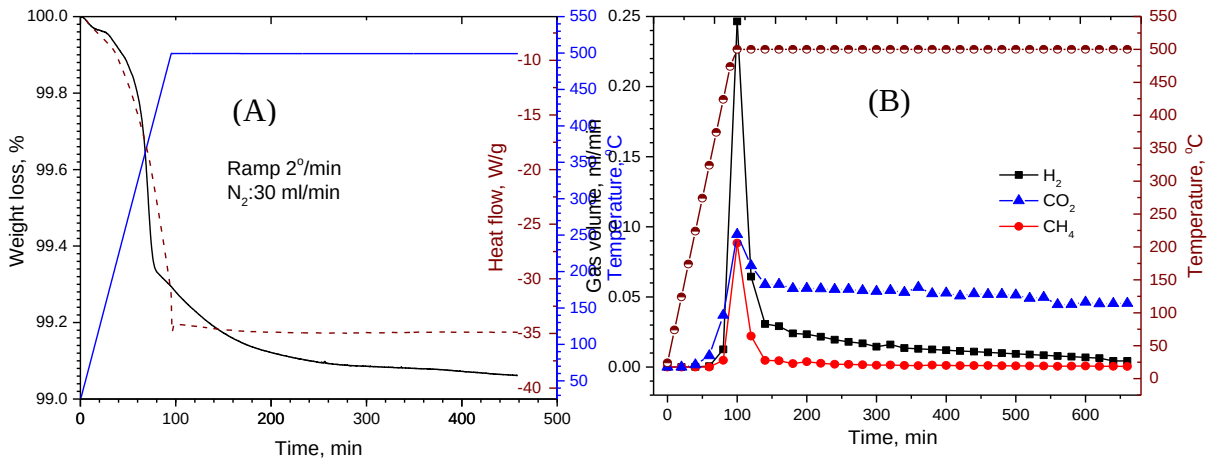

Figure B-2: Thermal Properties of used graphite O-rings: A) weight loss as a function of temperature in nitrogen atmosphere and B) gas composition as a function of pyrolysis time in a fixed bed reactor (no biochar sample).

The graphite O-ring shows a weight loss of 0.94 % when heated in nitrogen stream to 500 ^{o}C and kept at this temperature for 6 hrs. As a result, when heating the reactor with no sample, H_2, CH_4, and CO_2 gases were identified. H_2, CH_4 go to minimal after 10 h of heating at 500 ^{o}C, while CO_2 was almost constant, probably due to ppm level of oxygen in the used industrial nitrogen. The total weight of graphite O-rings used in the reactor to seal it is about 4.8 g.

EDAX Characteristics of the Membrane

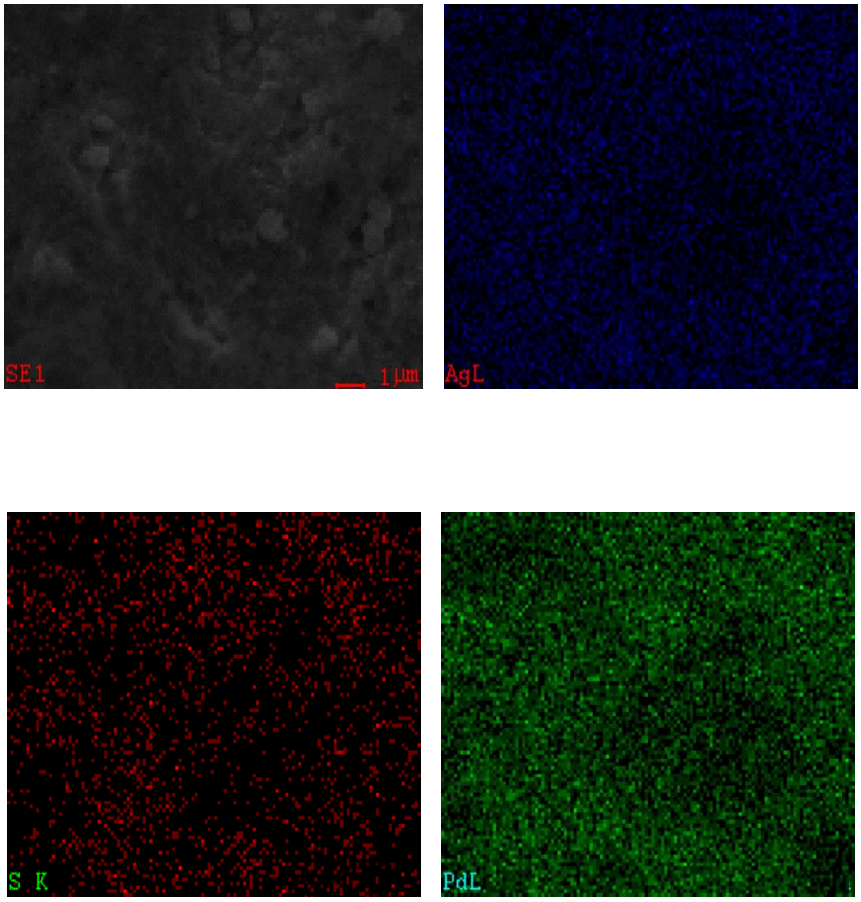

Figure B-3: EDAX map scan for the Pd_{77} Ag_{23} membrane surface after pyolysis.

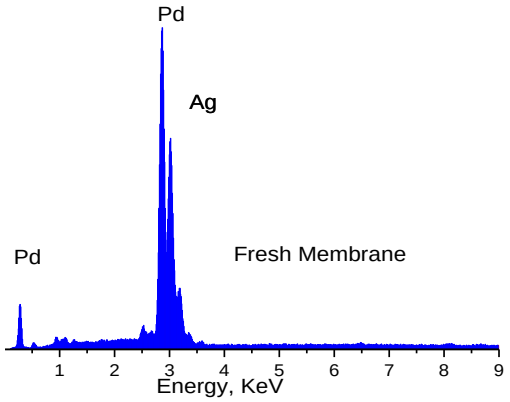

Element	Composition, wt.%		
	Membrane Pristine	After Pyrolysis Experiments	
		Membrane Face	Nodules on Face
Pd	77.49	74.02	65.84
Ag	22.51	23.62	30.11
S	0	2.36	4.05

Composition as reported by the vendor : 77/23

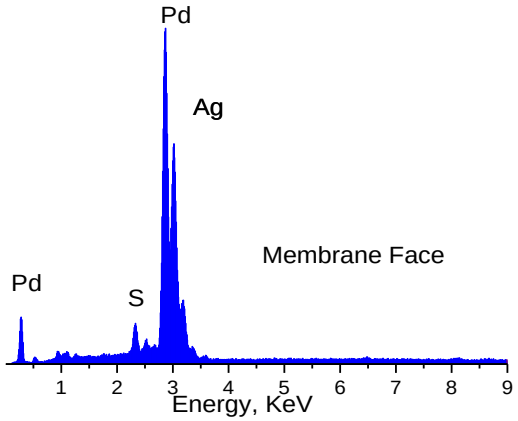

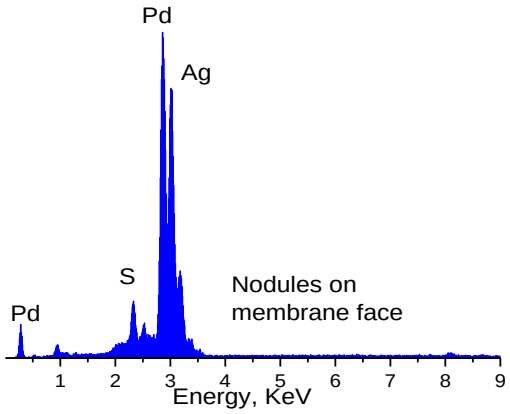

Figure B-4: EDAX Characteristics of the Pd_{77} Ag_{23} membrane before and after pyrolysis experiments .

APPENDIX C

The following chapters are a modified version of the published journal articles, manuscripts under review or will be submitted:

Chapter 2

Dandamudi, K.P.R., Muppaneni, T., Markovski, J.S., Lammers, P., Deng, S., 2019. Hydrothermal liquefaction of green microalga Kirchneriella sp. under sub-and super-critical water conditions. Biomass and bioenergy 120, 224–228.

Chapter 3

Dandamudi, K.P.R., Muhammed Luboowa, K., Laideson, M., Murdock, T., Seger, M., McGowen, J., Lammers, P.J., Deng, S., 2020. Hydrothermal liquefaction of Cyanidioschyzon merolae and Salicornia bigelovii Torr.: The interaction effect on product distribution and chemistry. Fuel 277.

Chapter 4

Dandamudi, K.P.R., Murdock, T., Lammers, P. J., Deng, S., and Fini, E.H., 2020. Hydrothermally produced biochar: A viable product to enhance biomass value and biofuel sustainability (under review: Resources, Conservation, & Recycling)

Chapter 6

Ibrahim, A.F.M., Dandamudi, K.P.R., Deng, S., Lin, J.Y.S., 2020. Pyrolysis of hydrothermal liquefaction algal biochar for hydrogen production in a membrane reactor. Fuel 265, 116935.

Chapter 5 will be modified as a manuscript to be submitted for a journal publication.

LIST OF PATENTS

1. Biochar Additives for Bituminous Composites (Provisional) – United States Patent Office-63/062,032 filed on August 06, 2020.

LIST OF PEER REVIEWED PUBLICATIONS

1. Samieadel, A., Rajib, A. I., Dandamudi, K. P. R., Deng, S., & Fini, E. H. (2020). Improving recycled asphalt using sustainable hybrid rejuvenators with enhanced intercalation into oxidized asphaltenes nanoaggregates. Construction and Building Materials, 262, 120090.
2. Dandamudi, K. P. R., Luboowa, K. M., Laideson, M., Murdock, T., Seger, M., McGowen, J., & Deng, S. (2020). Hydrothermal liquefaction of Cyanidioschyzon merolae and Salicornia bigelovii Torr.: The interaction effect on product distribution and chemistry. Fuel, 277, 118146.
3. Ibrahim, A. F., Dandamudi, K. P. R., Deng, S., & Lin, Y. S. (2020). Pyrolysis of hydrothermal liquefaction algal biochar for hydrogen production in a membrane reactor. Fuel, 265, 116935.
4. Dandamudi, K. P. R., Muppaneni, T., Markovski, J. S., Lammers, P., & Deng, S. (2019). Hydrothermal liquefaction of green microalga Kirchneriella sp. under sub-and super-critical water conditions. Biomass and bioenergy, 120, 224-228.
5. Patil, P. D., Dandamudi, K. P. R., Wang, J., Deng, Q., & Deng, S. (2018). Extraction of bio-oils from algae with supercritical carbon dioxide and co-solvents. The Journal of Supercritical Fluids, 135, 60-68.
6. Dandamudi, K. P. R., Muppaneni, T., Sudasinghe, N., Schaub, T., Holguin, F. O., Lammers, P. J., & Deng, S. (2017). Co-liquefaction of mixed culture microalgal

strains under sub-critical water conditions. Bioresource technology, 236, 129-137.

7. Muppaneni, T., Reddy, H. K., Selvaratnam, T., Dandamudi, K. P. R., Dungan, B., Nirmalakhandan, N., & Deng, S. (2017). Hydrothermal liquefaction of Cyanidioschyzon merolae and the influence of catalysts on products. Bioresource technology, 223, 91-97.
8. Wang, J., Krishna, R., Yang, J., Dandamudi, K. P. R., & Deng, S. (2015). Nitrogen-doped porous carbons for highly selective CO2 capture from flue gases and natural gas upgrading. Materials Today Communications, 4, 156-165.
9. Christensen, E., Sudasinghe, N., Dandamudi, K. P. R., Sebag, R., Schaub, T., & Laurens, L. M. (2015). Rapid analysis of microalgal triacylglycerols with direct-infusion mass spectrometry. Energy & Fuels, 29(10), 6443-6449.
10. Dandamudi, K. P. R., Murdock, T., Deng, S., & Elham H. F. "Physicochemical Characterization of Hydrothermally Produced Biochars Obtained from Cyanidioschyzon merolae and Swine Manure. (under review- Journal of Resources, Conservation, and Recycling).
11. Dandamudi, K. P. R., Liu, Y., Wei, Y., Liu, W., Dai, L., Deng, S. "Synthesis and characterization of waste plastics with ionic liquids into fuel by hydrothermal liquefaction" (under preparation).

12. Liu, Y., Dandamudi, K. P. R., Fini, E., Deng, S. “Thermal decomposition of scrap rubber tires using sub- and super critical solvents” (under preparation).
13. Murdock, T., Dandamudi, K. P. R., Fini, E., Deng, S. “Production of renewable fuel from microalgae and swine manure by sub-critical water extraction” (under preparation).
14. Dandamudi, K. P. R., Mathew, M., Selvaratnam, T., Muppaneni, T., Lammers, P. J., & Deng, S. “Recycle of Nitrogen and Phosphorus in Hydrothermal Liquefaction Biochar from Galdieria sulphuraria to Regrow Microalgae” (under preparation).

LIST OF CONFERENCE PROCEEDINGS

1. Dandamudi, Kodanda Phani Raj ; Murdock, Tessa ; Lammers, Peter J. ; Deng Shuguang. “Heterogenous Catalysts role in the upgrading of liquid, intermediate biocrudes produced from hydrothermal liquefaction” 2020 Spring Meeting & 16th Global Congress on Process Safety, Houston, 2020.
2. Samieadel, Alireza; Amirul Islam, Rajib; Dandamudi, Kodanda Phani Raj; Daniel, Oldham; Shuguang, Deng; and Elham H., Fini. “Optimizing the Efficiency of Bio-Rejuvenators Using A Balanced Feedstock” Transportation Research Board 2020 Annual Meeting, Washington, D.C., 2020.
3. Dandamudi, Kodanda Phani Raj; Tessa, Murdock; Peter J., Lammers; Shuguang, Deng. “Effect of Process Parameters and Heterogeneous Catalysts on the Upgrading of Micro-Algal Bio-Crude Oil” 2019 AIChE Annual Meeting, Orlando, FL, U.S.A.
4. Murdock, Tessa; Dandamudi, Kodanda Phani Raj; Peter J., Lammers; Shuguang, Deng. “Hydrothermal Liquefaction of Micro-Algae to Produce Liquid Biofuels” 2019 AIChE Annual Meeting, Orlando, FL, U.S.A.
5. Dandamudi, Kodanda Phani Raj; Tessa, Murdock; Peter J., Lammers; Shuguang, Deng. *“*Effect of Heterogeneous Catalysts on Upgrading Quality of Bio-Crude Under Sub- and Super-Critical Water Conditions*”* 2018 AIChE Annual Meeting, Pittsburgh, PA, U.S.A.

6. Dandamudi, Kodanda Phani Raj; Tapaswy, Muppaneni; Mark, Seger; Peter J., Lammers; Shuguang, Deng. “Effect of process parameters on upgrading of biocrude oil produced by hydrothermal liquefaction of microalgae” The 8th International Conference on Algal Biomass, Biofuels and Bioproducts (2018), Seattle, WA, U.S.A.
7. Dandamudi, Kodanda Phani Raj; Connor, Copp; Mark, Seger; Peter J., Lammers; Shuguang, Deng. “Hydrothermal Liquefaction of Microalgae and Co-Product Development” 2017 AIChE Annual Meeting, Minneapolis, MN, U.S.A.
8. Dandamudi, Kodanda Phani Raj; Tapaswy, Muppaneni; Melvin, Mathew; Peter J., Lammers; Shuguang, Deng. “Hydrothermal liquefaction of microalgae and quantitative characterization of products” The 7th International Conference on Algal Biomass, Biofuels, and Bioproducts (2017), Miami, FL, U.S.A.
9. Dandamudi, Kodanda Phani Raj, Tapaswy, Muppaneni; Melvin, Mathew; Peter J., Lammers; Shuguang, Deng, “Effect of Process Parameters and Extractive Solvents on Hydrothermal Liquefaction of Microalgae” 2016 AIChE Annual Meeting, San Francisco, CA, U.S.A.
10. Dandamudi, Kodanda Phani Raj, Tapaswy, Muppaneni; Darrius J., Norris; Nilusha, Sudasinghe; Schaub, Tanner; F. Omar, Holguin; Shuguang, Deng. “Co-liquefaction of mixed culture microalgal strains under sub-critical water conditions” 2015 AIChE Annual Meeting, Salt Lake City, UT, U.S.A.

11. Sapkota, Rishi; Miguel, Garcia; Dandamudi, Kodanda Phani Raj; Tanner, Schaub; and Jeffrey, Arterburn. "Fluorescent triazaborolopyridinium dyes for cross metathesis labeling". 249th American Chemical Society National Meeting & Exposition, 2015, Denver, CO, U.S.A.

BIOGRAPHICAL SKETCH

Kodanda Phani Raj Dandamudi was born and brought up in Guntur (the chilly capital of Asia) and Vijayawada, Andhra Pradesh, India. He received his elementary education from Bhashyam Public school and secondary education from Nirmala High School (Vijayawada). He received his higher secondary education from Sri Chaitanya college of education, Guntur. He received his Bachelor of Technology in Chemical Engineering from R.V.R. & J.C. College of Engineering in May 2013. He received his Master of Science Degree in Chemical and Materials Engineering from New Mexico State University, Las Cruces, NM in December 2015. He started his Ph.D. work in 2016 at Arizona State University under the supervision of Dr. Shuguang Deng. His research focuses on the production of liquid renewable fuels from the thermochemical conversion of bio-based feedstocks. During his graduate studies, Kodanda Phani Raj Dandamudi has authored and co-authored 10 technical articles in prestigious journals of Bioresource Technology, Fuel, Biomass and bioenergy, Resources, Conservation and Recycling, Energy & Fuels, Materials Today Communications, Supercritical Fluids, Construction and Building Materials. He has also presented as the main author at American Institute of Chemical Engineers Annual Meetings (2015-2019) and the International Conference on Algal Biomass, Biofuels, and Bioproducts (2017-2019), and American Chemical Society National Meeting & Exposition. During his Ph.D. studies at ASU, he received Engineering Graduate Fellowship (Spring 2020) from the Ira A. Fulton Schools of Engineering and University Graduate Fellowship (Spring 2019) from the Graduate College at Arizona State University. He is also a recipient of Graduate Research and Support Program Grant (Spring 2018), Conference Travel Grant (May 2016, June 2017, September 2018), Outstanding Committee Member-Engineering Committee from the Graduate & Professional Student Association, Arizona State University. During his Ph. D. studies he has served as an Assembly Member (2016-2018) representing Ira A. Fulton Schools of Engineering in the Graduate & Professional Student Association, Arizona State University. He was also appointed as the Director of Outreach -Tempe and Polytechnic campuses in the Graduate & Professional Student Association (2017-2019). He has also served as the President of the Polytechnic Sustainable Gardening Club at Arizona State University.